

COMBINED ANALYSIS OF COUPLED ENERGY NETWORKS



A thesis submitted to Cardiff University

in candidature for the degree of

Doctor of Philosophy

by

Muditha Abeysekera

Institute of Energy, Cardiff School of Engineering

Cardiff University, 2016

ACKNOWLEDGEMENTS

I would like to express my sincere gratitude to Professor Jianzhong Wu and Professor Nick Jenkins for their steady support, encouragement and guidance during my candidacy. Thank you very much for giving me this opportunity and spending your valuable time to make me a better researcher and a person.

I would like to thank Mr. Joel Cardinal, the Head of Energy and Sustainability and his team at the University of Warwick for their keen interest in my work and providing access to data that enriched the research work.

I would like to acknowledge the EPSRC for their financial support through the HubNET and Top and Tail projects and Cardiff University for its unwavering support.

My sincere gratitude goes to all members of the Energy Infrastructure research group and the CIREGS group at Cardiff University (both past and present) for the engaging discussions and suggestions regarding my research work.

A special thank you goes to my friends Fernando Alvarez Martinez and Samuel Bray for sharing the PhD journey with me through thick and thin.

I would like to thank my parents and family for their love, support and understanding throughout my candidacy.

A special thank you goes to my wife Amodika Sumithraarachchi for her love, patience and understanding in what was a very challenging four years. It would not have been possible without your support. Thank you.

DECLARATION

ABSTRACT

Energy supply systems such as the electricity, natural gas, district heating and cooling networks are typically designed and operated independently of each other. The increasing use of technologies such as combined heat and power units, gas turbines, heat pumps and recently, power to gas systems are increasing the links between energy systems introducing technical and economic interactions. There is a significant interest from academics, industry and policy makers in different parts of the world to identify and realise the opportunities of integrating energy networks while avoiding any undesirable impacts.

Analysis of the interdependencies between different energy systems requires powerful software models and analysis tools. However, there are no commercial tools available to date. The aim of this research is to develop a model for the combined steady state simulation and operation planning of integrated energy supply systems. As part of this thesis, three key components of the model were developed i.e.,

- a) Optimal power dispatch of an integrated energy system: A real case study was used to demonstrate the economic benefits of considering the interactions between different energy systems in their design and operation planning.
- b) Simultaneous steady state analysis of coupled energy networks: An example of a coupled electricity, gas, district heating and district cooling network system was used to illustrate the formulation of equations and the iterative solution method. A case study was carried out to demonstrate the application of the method for integrated energy network analysis.
- c) Steady state analysis of gas networks with the distributed injection of alternative gases: A case study was carried out to demonstrate the impact of alternative gas injections on the pressure delivery and gas quality in the network.

Table of Contents

<i>List of figures</i>	viii
<i>List of tables</i>	x
<i>Publications</i>	xii
<i>Nomenclature</i>	xiii
Chapter 1: Introduction	
1.1 Energy vectors.....	1
1.2 Integrated energy systems.....	2
1.3 Challenges in integrating energy supply systems	6
1.4 Research objectives	6
1.5 Summary of the work and achievements	8
Chapter 2: A review of the benefits and analysis methods of integrated energy systems	
2.1 Introduction	10
2.2 Benefits of integrating energy systems	10
2.2.1 Carbon emissions reduction by increasing whole system energy efficiency.....	10
2.2.2 Increase the generation and utilisation of renewable energy.....	14
2.2.3 Reduce capital expenditure	16
2.2.4 Cost effective provision of flexibility in the electrical power system	21
2.2.5 Opportunities for business innovation	24
2.2.6 Increase reliability of the electrical power system	25
2.3 Review of analysis methods used in integrated energy systems	26
2.3.1 Integrated energy system modelling and simulation	27
2.3.2 Operation and control of the integrated energy system.....	29
2.3.3 Energy performance assessment.....	37
2.3.4 Design and expansion planning	38
2.3.5 Reliability analysis	41
2.3.6 Modelling tools	42
2.4 Summary of challenges and research gaps.....	43
2.4.1 Challenges	43
2.4.2 Research gaps	45

Chapter 3: Optimal power dispatch in integrated energy systems	
3.1 Introduction	48
3.2 System description.....	49
3.3 System modelling.....	50
3.4 Optimization problem.....	52
3.4.1 Marginal cost of energy	54
3.5 Case study data	55
3.6 Results and discussion	58
3.6.1 Case study results	58
3.6.2 Analysis for the complete range of electricity and heat demand combinations..	64
3.6.3 Conclusions	72
3.7 Chapter summary.....	75
Chapter 4: Simultaneous power flow analysis of coupled multi-energy networks	
4.1 Introduction	77
4.2 Problem description.....	79
4.3 Formulation of equations for steady state analysis.....	81
4.3.1 Modelling energy flows in network branches.....	82
4.3.2 Modelling of coupling component power flows.....	86
4.3.3 Formulating network equations	87
4.3.4 Combined set of equations for simultaneous network analysis.....	99
4.4 Solution method	101
4.4.1 Newton-Raphson method.....	102
4.4.2 Solution method for combined analysis of integrated networks	103
4.5 Chapter summary.....	110
Chapter 5: Case study of simultaneous power flow analysis	
5.1 Case study description	111
5.2 Results and discussion	115
5.2.1 Converged parameters	115
5.2.2 Energy supply and conversions.....	121
5.2.3 Energy distribution losses	123
5.2.4 Convergence characteristics	124
5.3 Chapter summary.....	126

Chapter 6: Gas network analysis with distributed injection of alternative gases	
6.1 Introduction	128
6.2 Gas interchangeability and the impact of alternative gases in the gas grid	130
6.3 Problem description.....	131
6.4 Methodology.....	131
6.4.1 Modelling gas demands	131
6.4.2 Modelling steady state gas flow in pipes.....	133
6.4.3 Formulating equations for pipe network analysis	134
6.4.4 Solution method	136
6.5 Case study	140
6.6 Results.....	143
6.6.1 Case 1 simulation results – Baseline	143
6.6.2 Case 2 & 3 simulation results – Impact of an alternative gas mixture	144
6.6.3 Case 4 & 5 simulation results – Impact of distributed injection of an alternative gas.....	147
6.7 Discussion.....	150
6.8 Chapter Summary	151
Chapter 7: Conclusions and future work	
7.1 Conclusions of the work.....	152
7.1.1 Review of the benefits, analysis methods, research gaps and challenges in integrated energy systems research	152
7.1.2 Optimal power dispatch in integrated energy systems	153
7.1.3 Simultaneous steady state analysis of coupled energy systems	155
7.1.4 Gas network analysis with distributed injection of alternative gas types	155
7.2 Contributions of the thesis	156
7.3 Future work.....	157
References	
Appendix A: Landscape of research activities in integrated energy systems.....	168
Appendix B: Steady state analysis of coupled energy networks	177
Appendix C: Gas network analysis with distributed injection of alternative gases.....	210

List of figures

Figure 1-1: Possible interactions between different energy carrier systems	4
Figure 1-2: Schematic of the proposed modelling environment for integrated energy networks analysis	7
Figure 2-1: Benefits of integrating energy systems	10
Figure 2-2: Example of energy and carbon emissions saving through cogeneration of electricity and heat.....	11
Figure 2-3: Schematic of the integrated energy supply system at University of Warwick....	13
Figure 2-4: Schematic of an integrated electricity and hydrogen energy system for increasing the installed capacity of a renewable plant.....	14
Figure 2-5: The potential for increased renewable energy capture and converting otherwise curtailed energy to hydrogen	15
Figure 2-6: Schematic of a power to gas energy storage system	18
Figure 2-7: A schematic of the 'power to gas' concept for sharing energy transport capacity	21
Figure 2-8: Variation in electricity load and renewable generation	22
Figure 2-9: Schematic of multiple integrated energy systems connected to electricity and gas grids.....	23
Figure 2-10: Example of an energy hub that contains a transformer, a microturbine, a heat exchanger, a furnace, an absorption chiller, a battery and a hot water storage.....	30
Figure 2-11: System setup of three interconnected energy hubs	32
Figure 2-12: Illustration of centralized and distributed control architecture.....	33
Figure 3-1: Simplified configuration of the integrated energy supply system at the University of Warwick	50
Figure 3-2: Schematic of the integrated energy supply system with power flows marked ..	51
Figure 3-3: Aggregated hourly electricity and heat demand	56
Figure 3-4: Frequency of occurrence of a particular combination of electricity and heat demand.....	56
Figure 3-5: Optimal power dispatch results in Case 1	58
Figure 3-6: Optimal power dispatch results in Case 2	60
Figure 3-7: Optimal power dispatch results in Case 3	61
Figure 3-8: Optimal power dispatch results in Case 4	63
Figure 3-9: Optimal power dispatch results for the range of electricity and heat demands	65
Figure 3-10: Optimal power dispatch results of the absorption chiller and electric chiller. .	67
Figure 3-11: Marginal cost of electricity	68
Figure 3-12: Marginal cost of heat.....	69
Figure 3-13: Marginal cost of cooling	71
Figure 3-14: Segmented diagram of load frequency	73
Figure 4-1: Example of an integrated electricity, gas, district heating and district cooling network system	79
Figure 4-2 : Electricity distribution line model.....	82
Figure 4-3: Gas pipe model	83
Figure 4-4: Thermal network branch model and single insulated pipe cross section.	84

Figure 4-5: Coupling component model	86
Figure 4-6: Illustration of an electricity network node	87
Figure 4-7: Illustration of natural gas network node	90
Figure 4-8: Illustration of a thermal network node	93
Figure 4-9: A simple meshed network illustrating independent loops.....	96
Figure 4-10: Flow chart for the method of solving the equations.....	109
Figure 5-1: Case study network schematic	111
Figure 5-2: Voltage variation for the case scenarios.....	115
Figure 5-3: Variation of gas pressure at natural gas network nodes.....	116
Figure 5-4: District heating network branch mass flow rates.....	118
Figure 5-5: District heating network node temperature	118
Figure 5-6: Power supply, demand and conversions at coupling components	121
Figure 5-7: Distribution line losses.....	124
Figure 5-8: Iterations information	125
Figure 6-1: Algorithm for establishing a node analysis sequence	137
Figure 6-2: Flow chart for the Method	139
Figure 6-3: Case study network	140
Figure 6-4: Case study network with distributed injection of alternative gases at node 12	141
Figure 6-5: Gas flow pattern in case 1	143
Figure 6-6: Pressure gradient plot from Node 1 to Node 11 -Case studies 2 and 3	145
Figure 6-7: Pressure profile plot for case 4 and case 5	148
Figure 6-8: Unmet energy demand at gas nodes in case studies 4 and 5	149
Figure 7-1: Proposed modelling environment for integrated energy systems analysis	157
Figure B-1: Schematic of the example system	177
Figure B-2: Load flow analysis results as seen in IPSA’s graphical user interface.....	205
Figure B-3: Load flow analysis results as seen in SINICAL’s graphical user interface	206
Figure C-1: Schematic of the example gas network.....	210

List of tables

Table 1-1: Different types of energy vectors and their characteristics	3
Table 1-2: Integration of energy systems using network coupling technologies	5
Table 2-1: Research questions in the analysis of integrated energy systems	27
Table 2-2: An overview of models and software tools used for integrated energy system analysis.....	43
Table 3-1: Technical specifications of the energy hub units.....	55
Table 3-2: Case studies	57
Table 3-3: Fuel prices	57
Table 3-4: Strategy for utilising energy conversion units and external grid imports	73
Table 3-5: Marginal costs and potential improvements to the energy system.....	73
Table 4-1: Widely used methods and software tools for steady state analysis of energy networks	78
Table 4-2: Electricity network node types	90
Table 4-3: Node types in gas networks.....	92
Table 4-4: Node types in thermal networks	99
Table 5-1: Coupling component data.....	112
Table 5-2: Energy demand data for case study.....	113
Table 5-3: Case study scenarios	115
Table 5-4: District cooling network results	120
Table 5-5: Convergence characteristics	124
Table 6-1: Summary of the problem.....	131
Table 6-2: Gas demand data	141
Table 6-3: Case studies	142
Table 6-4: Molar fractions of gases in mixtures used for case studies.....	142
Table 6-5: Steady state simulation results for case 1	143
Table 6-6: Results for Case 2 and 3 simulations	144
Table 6-7: Energy available at nodes in cases 2 & 3 - method A	146
Table 6-8: Simulation results for case study 4	147
Table 6-9: Simulation results for case study 5	148
Table B-1: Coupling component data	178
Table B-2: Node data for energy networks.....	178
Table B-3: Energy network parameters	179
Table B-4: Iterations information.....	202
Table B-5: Electricity network results validation using IPSA.....	205
Table B-6: Gas network results validation using SINCAL	206
Table B-7: District heating network results validation using Bentley sisHyd.....	207

Table B-8: District cooling network results validation using Bentley sisHyd	208
Table B-9: Energy network parameters	209
Table C-1: Gas demand data	210
Table C-2: Pipe data for example gas network	211
Table C-3: Molar fractions of gases in mixtures used for case studies.....	211

Publications

- **ABEYSEKERA, M.**, WU, J. & JENKINS, N. 2016. Integrated energy systems: An overview of benefits, analysis methods, research gaps and opportunities. *HubNET position paper series*. Available at <<http://www.hubnet.org.uk/filebyid/791/InteEnergySystems.pdf>> [Accessed 10th September 2016]
- **ABEYSEKERA, M.** & WU, J. 2015. Method for Simultaneous Power Flow Analysis in Coupled Multi-vector Energy Networks. *Energy Procedia*, 75, 1165-1171.
- **ABEYSEKERA, M.**, WU, J., JENKINS, N. & REES, M. 2016. Steady state analysis of gas networks with distributed injection of alternative gas. *Applied Energy*, 164, 991-1002.
- **ABEYSEKERA, M.**, REES, M. & WU, J. 2014. Simulation and Analysis of Low Pressure Gas Networks with Decentralized Fuel Injection. *Energy Procedia*, 61, 402-406.

Nomenclature

Abbreviations

AC	Alternating current or Absorption chiller
CHP	Combined heat and power
DHN	District heating network
DCN	District cooling network
EC	Electric chiller
EPSRC	Engineering and Physical Sciences Research Council, UK
ETH	Swiss Federal Institute of Technology, Zurich (German : Eidgenössische Technische Hochschule)
GB	Gas Boiler
GCV	Gross Calorific Value
Re	Reynolds number
SG	Specific gravity
TN	Thermal network
UK	United Kingdom
UoW	University of Warwick
WI	Wobbe Index

Capital letters (Latin)

A	Branch-nodal incidence matrix
B	Branch-loop incidence matrix
C	Cost amount or Coupling component
D	Pipe insulation outer Diameter
E	Energy Quantity
I	Electricity network node current injection (Matrix form)
K	Pipe constant
L	Lagrange function or pipe length or distribution line losses
M	Molar mass of gas component
\dot{M}	Mass flow to/from local connections
N	Number of gas components in the gas mixture
P	Active power (Matrix form)
Q	Thermal energy supply or reactive power

R	Gas constant
S	Apparent power (Matrix form) or pipe flow direction coefficient or relative density of gas
T	Temperature
V	Voltage (Matrix form)
\dot{V}	Gas volume flow rate
Y	Bus admittance matrix
Z	Gas compressibility factor

Simple letters (Latin)

b	Electrical circuit shunt susceptance
c_p	Specific heat capacity of water
d	Pipe internal diameter
i	Electrical current flow in a branch
l	Length
m	The gas flow exponent (gas networks)
\dot{m}	Mass flow rate in branch
n	Number of elements
p	Real power
pr	pressure
q	Reactive power
r	Electrical circuit series resistance
s	Apparent power injection at a bus
v	Electrical voltage at a bus bar
y	Series admittance of an electrical circuit
z	Electrical circuit impedance

Greek letters

δ	Voltage angle
ε	Pipe roughness
η	Efficiency of energy conversion
θ	Angle of admittance element
λ	Lagrange variables/pipe friction factor

ρ	Water density
τ	Transformer tap ratio
χ	Radial heat transmission coefficient
ψ	Gas flow function

Subscripts

amb	Ambient
avg	Average
bus	Electrical bus bar
cool	Cooling
d	Demand
e	Electricity
g	Generation
grid	Grid supply
heat	Heating
n	Standard conditions
out	Outlet of the heat substation
pipe	Heat/gas network pipe
ret	Return water line in thermal network
s	Supply source
sched	Scheduled
sup	Supply water line in thermal network

Superscripts

C	Cooling network
E	Electricity network
G	Gas network
H	Heating network
T	Thermal network
t	Transpose of matrix

Chapter 1: Introduction

More than half of the global population now lives in urban areas, a proportion that is expected to reach around 70% by 2050 (UNDESA, 2015). Modern cities require large quantities of energy to support various socio-economic activities such as mobility, space heating and cooling in buildings, lighting, electric power for appliances, industrial and commercial activities and communication.

According to recent statistics (UN-Habitat, 2011; IEA, 2008), cities are responsible for more than two-thirds of the global energy consumption and account for over 70% of greenhouse gas emissions. Consequently, increasing the performance of energy supply systems in urban areas is an important consideration in the transition to a low carbon economy.

1.1 Energy vectors

Primary energy resources such as solar and wind energy are converted to more usable and dense forms (e.g. electricity, hydrogen) that are conveniently transported and re-converted at points of demand. These are referred to as energy vectors or energy carriers.

Electricity is a good example of an energy vector obtained by converting or changing the natural form of an energy source. It is produced using a number of primary energy sources (e.g. oil, nuclear, solar, wind energy) and transmitted through a network of lines and cables to where it is consumed. Many natural energy sources and their refined forms can also be considered as energy vectors when they allow storage, transportation and ease of conversion to a usable form (e.g. natural gas, coal, biodiesel).

The main energy vectors in use are shown in Table 1-1. It also shows the most common method of transporting the different energy vectors. The different forms of energy supply infrastructure are designed and operated to source, manage and deliver each type of

energy vector efficiently and cost-effectively from the source to its point of use. This study focuses on the energy systems that supply electricity, gas, hot and chilled water.

1.2 Integrated energy systems

Modern cities can have several forms of physical infrastructure that distribute different energy vectors for supporting urban energy services. For example, the majority of towns and cities in the UK have electricity and gas networks for supplying electricity and natural gas to customer premises. District heating and district cooling networks are also being built to utilise local energy resources that would otherwise be wasted. District heating and district cooling networks are particularly well suited for urban developments with a high density of heat and/or cooling demand. The delivery of Hydrogen through a pipeline grid has also gained significant interest in the recent years (NaturalHy, 2008) primarily due to its potential as an environment friendly transport fuel.

The option of using different energy vectors for supplying energy services provides flexibility in design and an opportunity to utilize different forms of energy available in the local area. For example, an urban development may opt to use a district heating network with centralized heat sources (e.g. waste heat from an incineration plant) or individual gas boilers installed in the buildings and supplied by the local gas grid.

Table 1-1: Different types of energy vectors and their characteristics (Orechchini, 2012)

Energy vector	Description	Method of transport
Naturally occurring energy vectors		
Coal	A combustible solid extracted from the ground using a process of mining.	Road , railways, sea
Natural gas/ Shale gas	A hydrocarbon gas mixture consisting primarily of methane. It is found in deep underground rock formations and extracted from a process of drilling.	As liquefied natural gas (LNG) using tankers, gas pipelines
Energy vectors from refined/processed energy sources		
Petroleum derivatives (e.g. gasoline/ diesel)	A fossil fuel liquid found in geological formation beneath the earth's surface and extracted through drilling. It is refined to various types of fuels in a distillation process.	Road , sea, pipelines
Synthetic fuels (e.g. biodiesel, syngas, biogas)	Liquid and gaseous energy vectors obtained from the processing of biomass or fossil fuels.	Road, gas or liquid pipelines
Derived Energy vectors		
Electricity	A flow of electric charge through a conducting material. It is generated using different methods such as electro-mechanical generators (driven by heat engines or kinetic energy of flowing water and wind), photovoltaics and electrochemical batteries.	Transported using a cable or overhead line network operating at different voltage levels.
Hydrogen gas	A colourless, highly flammable gas which is found in the atmosphere at trace levels. Production is mainly from steam reforming of natural gas and the electrolysis of water.	Road , Gas pipelines
Hot/chilled water	Hot/chilled water can transport and store energy in the form of thermal energy. The distance of transport can vary from within a single apartment complex up to entire districts in the case of district heating/cooling.	Hot/chilled water pipe line network

Traditionally, in many countries, the different elements of energy supply infrastructure i.e. electricity, gas, district heating and district cooling networks have been developed and operated independently of each other. However, these are increasingly being interconnected through technologies such as combined heat and power, heat pumps and power to gas systems (see Figure 1-1). The integration of energy supply systems is expected to have an impact on the design and technical and economic operation of energy systems.

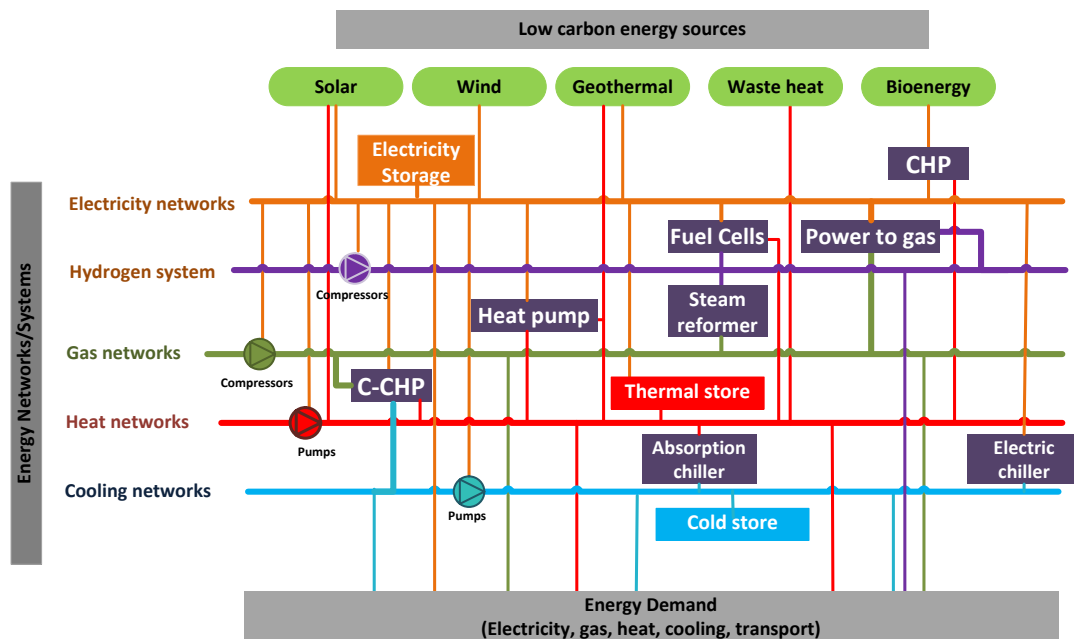


Figure 1-1: Possible interactions between different energy carrier systems

Figure 1-1 shows the different types of energy supply systems and low carbon energy sources that may be utilized in urban areas and the possible interactions between them. Electricity, natural gas, hydrogen, district heating and district cooling supply systems are shown using coloured line segments and the network coupling components are shown using purple coloured boxes. Different energy systems interact through energy conversion units and network support technologies. For example, a gas turbine is an energy conversion technology and a gas compressor (fuelled by electricity) supports the control of gas network operation. These units interconnect the electricity and natural gas energy supply

systems introducing technical and economic interdependencies. Table 1-2 shows the network coupling units and the mode of interaction between energy networks. In the table a '+' denotes energy supplied to the network, 'o' denotes energy being consumed and the letter 'M' denotes network control.

Table 1-2: Integration of energy systems using network coupling technologies

Note: '+' refers to energy supplied; 'o' refers to energy consumed; 'M' refers to network control support

Network coupling technology		Gas Fired C-CHP	Gas fired CHP	Heat pump	Fuel Cell	Power to Gas	Steam reform	Absorption chiller	Electric chiller	Electric Compressor	Pump
Electricity network		+	+	o	+	o			o	o	o
Hydrogen system					o	+	+			M	
Natural gas network		o	O			+	o			M	
Heat network		+	+	+	+			o			M
Cooling network		+						+	+		M

The integration of energy systems provides an additional degree of freedom for the overall energy system design and operation. For example, the electricity supply system can use energy from the natural gas network to generate electricity by using gas fired power generation technologies (e.g. combined cycle gas turbine units). At the same time, it introduces inter-dependence where the electrical power system relies on the natural gas supply system to balance its supply and demand.

A number of the potential benefits of integrating different energy networks are discussed in detail in Chapter 2, which can be summarised as:

- Reduction in carbon emissions by increasing whole system energy efficiency
- Increased generation and utilisation of renewable energy

- Reduction/delay of capital expenditure
- Provision of cost effective of flexibility in the electrical power system
- New opportunities for business innovation
- Increased reliability of the electrical power systems

1.3 Challenges in integrating energy supply systems

Some of the key challenges of integrating different energy supply systems are as follows.

- Integration introduces complicated interactions and interdependencies between energy systems (technical, economic and markets) that are not well understood
- Design and operation planning of energy supply needs to consider the interactions and interdependencies between different energy systems, to which there are no commercial tools available
- The fragmented institutional and market structures of different energy systems is a barrier to realise the benefits of integrating energy systems.
- Integration of multiple energy vector systems would result in a more complex energy system to manage and operate. The interdependencies between different energy systems and the ICT infrastructure that facilitates interoperability would require powerful software models and analysis tools. It is argued that if not managed properly the integration of multiple energy systems can result in an energy supply system that is more susceptible to cascaded failures affecting reliability of supply.

1.4 Research objectives

The aim of this research is to develop methods and modelling tools for the steady state simulation and operation planning of integrated energy supply systems.

Figure 1-2 shows the overall ambition and the components developed as part of this work.

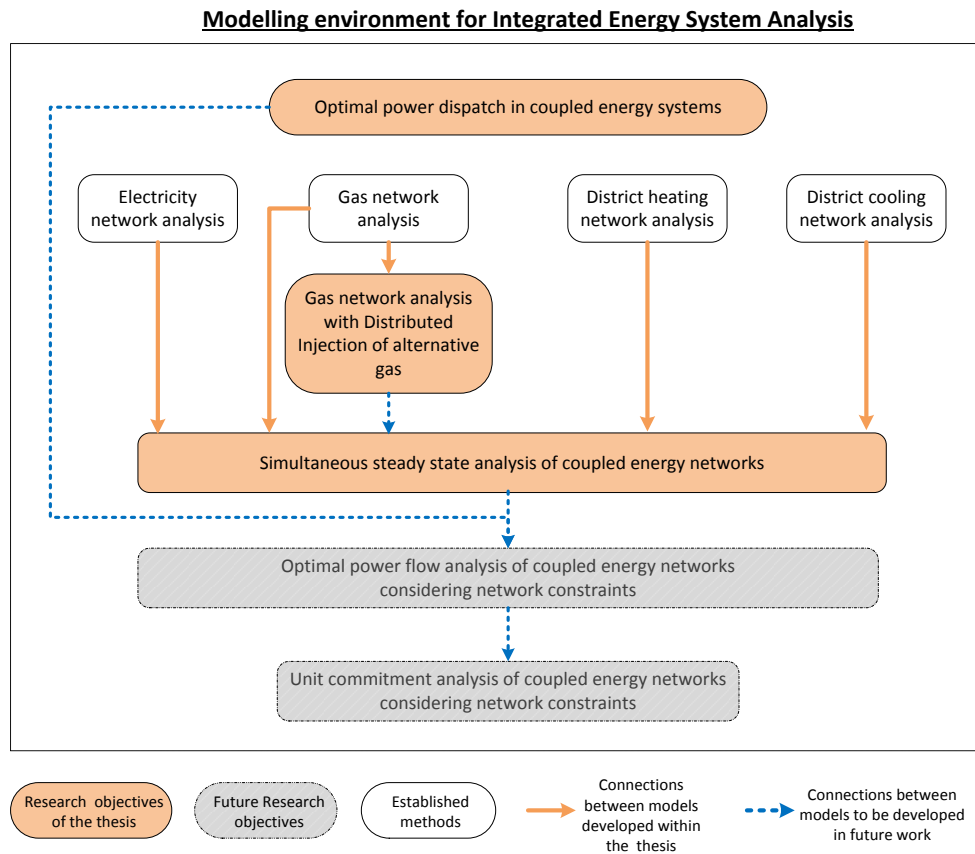


Figure 1-2: Schematic of the proposed modelling environment for integrated energy networks analysis

Traditionally, modelling, simulation and operation analysis of energy networks are carried out for each energy carrier system independently. There are well established methods for the analysis of electricity, gas and thermal energy networks. These methods are to be extended to develop a new set of modelling tools for the simultaneous steady state simulation and operation planning of integrated energy supply systems.

The research objectives considered in this thesis are,

- To analyse the optimal power dispatch problem in an integrated energy supply system
- To develop a method for the simultaneous steady state analysis of an integrated electricity, gas, district heating and district cooling network system

- To develop a method for the steady state analysis in gas networks with distributed injection of alternative gases

These would enable the development of a model for optimal power flow and unit commitment analysis considering supply network constraints. This is explored further in section 7.3 on future work.

1.5 Summary of the work and achievements

The work carried out and the main achievements are summarised below.

1. A review of the literature on potential benefits and methods for analysing integrated energy systems was undertaken. The findings are presented in Chapter 2 of the thesis. The current landscape of research activities is presented in Appendix A:. The findings were published in a position paper available at (HubNET, 2016).
2. A method for optimal power dispatch analysis in an integrated energy supply system was investigated. The mathematical formulation of the optimisation problem is based on the energy hub modelling concept developed in (Geidl, 2008). Real data from the energy supply system at the University of Warwick was used as a case study. Simulations were carried out to analyse the optimal power dispatch for different load scenarios representing seasonal demand variations. An optimal power dispatch strategy and recommendations for potential improvements of the energy supply system were discussed.
3. A method for the steady state simulation and analysis of a coupled electricity, gas, district heating and district cooling network system was developed (Abeysekera and Wu, 2015). This research work extends the work undertaken in (Liu, 2013). The physical energy flow equations for the different networks are formulated taking into account the network interactions. The set of equations are solved

simultaneously using the Newton-Raphson method. The mathematical model was implemented in MATLAB. An example case study is used to illustrate and discuss the advantages and disadvantages of the proposed method. This work is presented in Chapter 4 and Chapter 5.

4. A method was developed for steady state simulation and analysis of gas networks taking into account distributed injection of alternative gas types (Abeysekera et al., 2016b). It quantifies the impact of injecting gases such as hydrogen on gas pressure, flows and gas composition in the distribution grid. A case study in which hydrogen and bio-methane was injected in a low pressure gas distribution grid was simulated and the results are discussed. This work is presented in Chapter 6.

Chapter 7 summarises the conclusions of the research work and opportunities for future research in this area.

Chapter 2: A review of the benefits and analysis methods of integrated energy systems

2.1 Introduction

This chapter reviews the potential techno-economic benefits and the state of the art in the analysis methods used in the planning, design, operation and control of integrated energy systems. It concludes with a summary of the challenges and research gaps identified.

The energy supply networks (and their integration) considered in this thesis are limited to electricity, natural gas, district heating, district cooling and hydrogen.

2.2 Benefits of integrating energy systems

Figure 2.1 shows the potential benefits of integrating energy systems identified from a review of the literature.

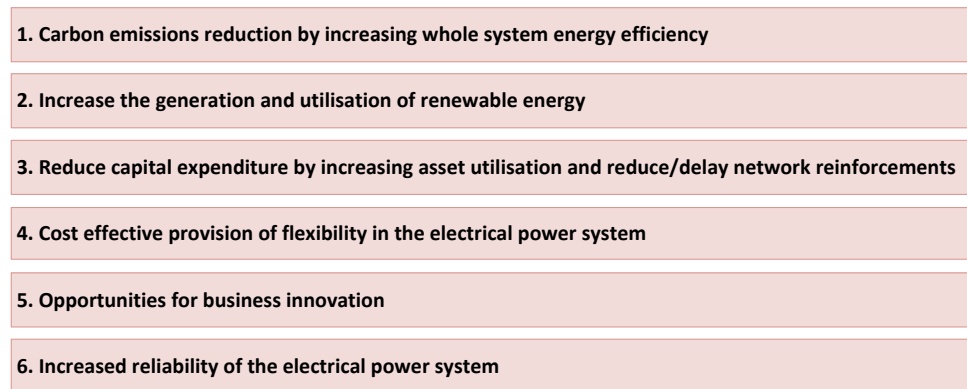


Figure 2-1: Benefits of integrating energy systems

2.2.1 Carbon emissions reduction by increasing whole system energy efficiency

A primary driver for the integration of different energy carrier networks is to be able to reduce emissions (and increase energy efficiency) through,

- a) co-generation of electricity and heat

- b) optimising (in terms of carbon emission and/or costs) the operation of the overall energy system.

2.2.1.1 Increasing energy efficiency through co-generation

Combined heat and power (CHP) or co-generation systems are widely recognised to have a high potential for improving energy and exergy¹ efficiency compared to the separate production of energy carriers (Horlock, 1987). Figure 2.2 shows an example of energy and carbon emissions savings when supplying a specified electricity and heat demand through a co-generation system compared to the separate production of electricity in a thermal power plant and heat in a gas fired boiler.

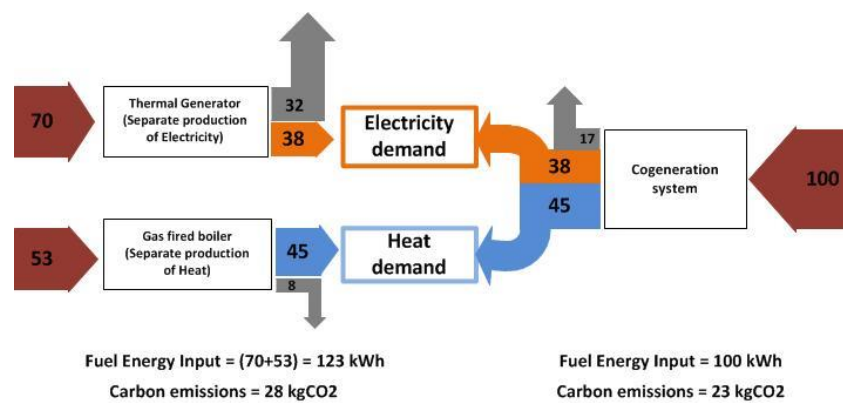


Figure 2-2: Example of energy and carbon emissions saving through cogeneration of electricity and heat (natural gas is assumed as the fuel input in all systems).

Note: A carbon intensity of 0.23 kgCO₂/kWh for natural gas is assumed; electrical efficiency of thermal generator = 55%; thermal efficiency of gas fired boiler = 85%; electrical efficiency of CHP = 38%; thermal efficiency of CHP = 45% (Horlock, 1987))

In thermal power plants for separate electricity generation, a large fraction of the fuel energy is released to the natural environment, mainly through the flue gas and condenser cooling systems (45% in the example above of a CCGT unit). Co-generation systems capture a large part of the otherwise wasted energy in order to supply a local industrial/commercial heat load, or to be used as hot water for district heating. The above example shows 19%

¹ Exergy is a thermodynamic concept used to characterize the quality of different energy flows. For example, it gauges that the quality of energy in 1kJ of electricity is greater than 1kJ of energy in a waste heat stream (at low temperature).

less fuel energy (compared to separate production) is required by a co-generation system to meet the same electricity and heat loads. In the example, the same percentage reduction of emissions (19%) is achieved.

The co-generation concept is extended as tri-generation or multi-generation according to a number of different energy vectors produced from a single source of fuel. For example, combined cooling, heat and power systems (CCHP) use the heat recovered from electricity generation to supply a heat load and also drive an absorption chiller² for cooling. A number of research studies have shown the potential for increasing the energy efficiency of supplying electricity, heat and cooling loads by using CCHP plants (Chicco and Mancarella, 2009, Rezaie and Rosen, 2012).

In many situations the development of multi-generation systems is hindered by the absence of a suitable load (or market) for some of the different energy products. Multi-energy networks allow the creation of markets by aggregating various energy demands scattered over a wide geographical area. Access to a reliable multi-energy load improves the financial viability and thereby supports the increased uptake of co-generation systems.

2.2.1.2 Increasing overall energy system efficiency through integrated operation strategies

An integrated system of multi-energy supply networks can use multiple paths to deliver different forms of energy.

For example, Figure 2.3 illustrates a simplified schematic of the energy supply system at the University of Warwick which comprises electricity, district heating and district cooling networks interconnected through gas fired CHP units, gas fired heat only boilers, electric chillers and heat driven absorption chillers.

² An absorption chiller is a device that uses heat energy to drive the refrigeration cycle for cooling supply.

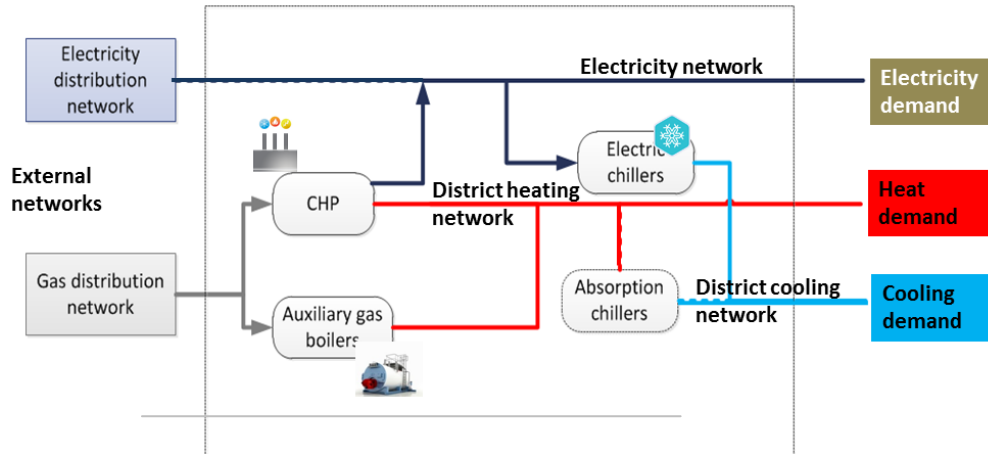


Figure 2-3: Schematic of the integrated energy supply system at University of Warwick

The multiple supply paths to deliver the different forms of energy to the loads are,

- electricity load - through importing electricity from the external grid or from the gas fired CHP generation
- heat load – through the gas fired CHP generation or gas fired heat only boilers
- cooling load – through electric compression chillers or heat driven absorption chillers (connected to the district heating network)

Carbon emissions depend on the amount of electricity and gas consumed from the external grids and the carbon intensity of grid electricity at the time of use. The amount of electricity and gas required from external grids depends on the efficiencies of conversion between different energy carriers. Due to the variations of the carbon intensity of grid electricity and the time-varying nature of different energy loads, multiple supply paths provide an opportunity to optimise the operation of the energy system with an objective to reduce carbon emissions. Optimal operation can be encouraged by suitable market instruments (e.g. a carbon tax) that encourages a system wide approach to reduce carbon emissions.

2.2.2 Increase the generation and utilisation of renewable energy

Progress in developing renewable generation systems is hindered by the lack of cost-effective energy storage capacity and the technical constraints of the existing electricity network (DECC, 2012a). For example, an increase in renewable generation connections may violate the voltage and thermal limits of the electrical network and its components. As a result, when providing a connection, electricity distribution network operators (DNO's) often put forward conditions in the form of:

- a) limiting the capacity of generation that can be connected
- b) contracts that allow tripping/curtailment of the renewable plant in case of network congestion
- c) charging any reinforcement costs of the network to the developer of renewable plant

These conditions are discouraging for a developer who wishes to maximize the economic potential of the investment. They also limit renewable energy generation from sites with the best resource.

There is a potential to increase the generation and utilisation of renewable energy by integrating the electricity network with other energy carriers (Niemi et al., 2012). For example consider the simple schematic of an integrated electricity and hydrogen energy system shown in Figure 2.4.

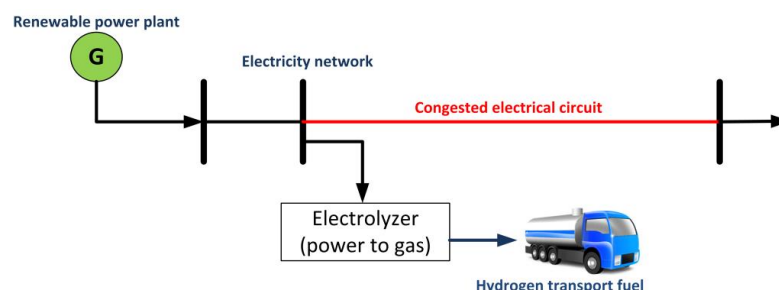


Figure 2-4: Schematic of an integrated electricity and hydrogen energy system for increasing the installed capacity of a renewable plant

Figure 2.4 shows a renewable generator and an electrolyser³ connected to a constrained part of the electrical grid. The electrolyser can be operated to avoid or reduce violations of the grid constraint. For example the power flow through the congested circuit can be regulated by adjusting the electricity consumption of the electrolyser. The hydrogen generated is then stored and reconverted to electrical energy or used to supply an alternative use directly (e.g. for transport). This arrangement allows a renewable power plant rated above the grid connection capacity to be installed and thereby captures a larger amount of renewable energy over the year (see Figure 2.5).

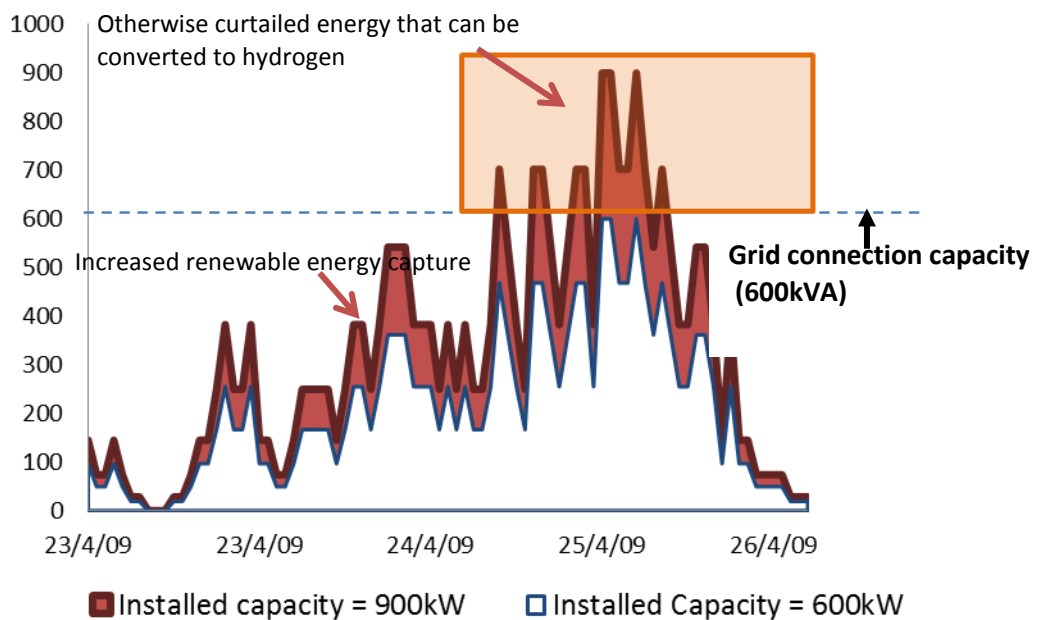


Figure 2-5: The potential for increased renewable energy capture and converting otherwise curtailed energy to hydrogen (Wind data from 23/04/09 to 26/04/09 at a site in mid-Wales)

Figure 2.5 shows a 4-day simulation of the electrical power generated by two different wind turbine installations at a site in mid-Wales. Assuming the DNO specified export capacity at the grid connection point is 600kVA, the maximum capacity of wind turbines in a typical installation is 600kW_p. If no other barriers exist (e.g. space, environmental etc.), a

³ An electrolyser produces hydrogen and oxygen from electrical current and a pure water supply through an electrochemical process.

larger capacity of wind turbines (900kW_p in the example) allows more renewable electricity to be generated (red shaded area in Figure 2.5). The 900kW_p installation exceeds the grid connection capacity several times during the 4 day period. The excess energy is then converted to a secondary energy vector (hydrogen) and utilised. This allows the electrical grid to absorb a larger quantity of renewable energy while adding an economic value to the energy that would otherwise be curtailed.

A number of research studies have investigated the potential to increase renewable generation by integrating energy systems. The use of electrically heated thermal storage is common in Denmark (Meibom et al., 2013) and electrolyzers are being trialled in a number of demonstration projects across Europe (Gahleitner, 2013). The opportunities for converting excess renewable electricity to a different energy vector only exist due to the present high cost of electrical energy storage at grid scale. The financial attractiveness of using thermal demand and/or electrolyzers for congestion management has yet to be demonstrated as, depending on the costs of equipment and fuel, it may remain more cost-effective to constrain the renewable generation.

2.2.3 Reduce capital expenditure

Integration of energy systems can provide additional energy supply capacity (e.g. electricity distribution capacity, energy storage capacity). Investments in upgrading energy infrastructure can be reduced or deferred by

- a) increasing utilization of existing assets
- b) reducing/delaying network reinforcement.

2.2.3.1 Increasing asset utilization

Asset utilization in energy systems is increased by delivering a larger quantity of energy during their functional life time. The economic advantages of increased asset utilization are:

- a) the cost to own equipment is distributed across a larger number of units of energy
- b) the payback period of investing in those assets will reduce, which reduces the investment risk

This can be achieved in integrated energy systems through,

- i. sharing energy storage: accessing low cost energy storage available in different energy systems
- ii. sharing power generation assets: co-generation of energy vectors
- iii. sharing energy transport assets: Shifting energy demand between different energy carrier networks

I. Sharing energy storage

Periods with excess renewable energy are expected to grow as the UK continues to invest simultaneously in (inflexible) nuclear power generation and intermittent renewables such as wind and solar generation (Strbac et al., 2012). As a result the value of energy storage is expected to increase. However, to date, the cost of grid scale electricity storage is significantly higher than that at which mass deployment can occur⁴. Therefore, it remains more cost-effective to curtail renewable generation when electricity supply exceeds demand (Qadrdan et al., 2015).

On the other hand, energy storage in chemical (natural gas, hydrogen) and thermal energy systems are well developed technologies and relatively inexpensive. Through integration of

⁴ Pumped hydro is the only economic form of storing grid scale amounts of excess electricity to date [3]

energy systems, electricity networks can access the energy storage capacity available in other already built energy systems (Vandewalle et al., 2012b). Many developed countries have an established gas grid and have access to its large energy storage capacity. For example GB's natural gas network has a large energy storage capacity due to its line pack mechanism⁵ and its existing gas storage facilities.

As shown in Figure 2.6, the excess electricity from renewables can be converted to hydrogen and/or synthetic methane and injected in the natural gas grid for storage (termed power to gas) (Grond et al., 2013). Existing gas fired power generators allow the reconversion of gaseous energy to electricity, allowing the renewable energy to be time-shifted. Alternatively, hydrogen and/or synthetic methane can be used as a CO₂ neutral fuel to substitute natural gas in the gas grid and reduce reliance on fuel imports (ITMPower, 2013).

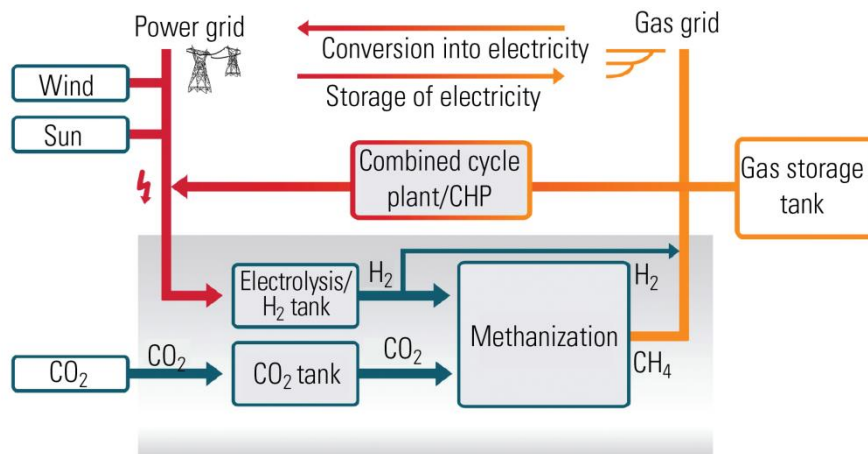


Figure 2-6: Schematic of a power to gas energy storage system (Patel, 2012)

Using spare capacity in the gas network for electricity storage is a potentially attractive solution to the problem of storing excess renewable energy. Germany is pioneering the development of power to gas energy storage systems through several demonstration and

⁵ Line packing is the process of compressing a larger quantity of gas into a pipeline using an increase in pressure

commercial projects (Patel, 2012). The main drawback of this type of storage solution is the relatively low round trip efficiency⁶ (around 35% for power to gas systems compared to above 90% for battery storage) (Rastetter, 2013).

II. Sharing generation assets

Generation assets can be shared between different energy systems through co-generation of electricity and useful heat. In the case of tri-generation, the co-generation system can be shared by electricity, heat and cooling systems.

For example an opportunity exists to use co-generation assets to provide balancing capacity to multiple energy systems. At present, they are designed with the aim of supplying a specific heat load. The electricity generated is used to offset grid imports and any excess is exported to the grid. Due to their relatively small capacity as individual units (less than 10MW) and their primary role in heat load supply, CHP plants are typically not considered reliable sources of electrical power to provide energy to the grid when needed. However, with the use of thermal storage, aggregators⁷ and co-ordinated controls, CHP plants can potentially provide balancing services to the electrical grid when required. This can be achieved by, decoupling the time of heat generation from heat demand (using heat storage) and engaging CHP plants in the electricity capacity market actively (Kitapbayev et al., 2014).

III. Increase utilisation of network assets

The utilisation of network assets can be increased by shifting complementary loads between energy carrier networks. For example, the annual space heating and cooling

⁶ Round-trip efficiency is the amount of energy available when an energy storage system is discharged as a fraction of the energy used for charging. It is a measure of inefficiency of the energy storage system.

⁷ In order to meet the minimum volume requirements of providing balancing services to the electricity system operator, smaller sites may be aggregated together with other sites

demand profiles (particularly in northern climates) display a complementary seasonal variation (Frederiksen and Werner, 2013). The assets designed for the supply of heat or cooling demand alone are then underutilized. This is a particular challenge when considering the large scale investment required in developing district heating/cooling networks.

Network utilization can be increased by combining complementary demand profiles of space heating and cooling to be supplied through a single energy carrier network. This can be achieved by shifting the space cooling load to a district heating network by using absorption chillers (see Figure 2.3). The use of absorption chillers will increase the district heating network load during summer periods (when space heating demand is low). This would increase the average annual energy flow through heat network assets and improve its economic viability for investment.

2.2.3.2 Reduce/delay electricity network reinforcements

In several parts of GB, the electricity transmission and distribution system is congested due to power flows reaching network design capacities. For example, on occasion, wind generation in Scotland needs to be constrained (Qadrdan et al., 2015). The development of renewable generation and the electrification of heating and transport⁸ (increasing network load) requires reinforcement of the congested areas of the network to allow increased power flows through its circuits.

Integrating the constrained parts of the electricity system with other established energy systems provide an opportunity to manage congestion and an alternative means of transporting electricity. For example, Figure 2.7 is a simple schematic of a potential 'power

⁸ It is expected that the level of electricity consumption will increase due to the expected electrification of heat and transport demand

to gas' arrangement to manage congestion in the electricity circuit and increase energy transport capacity in this route.

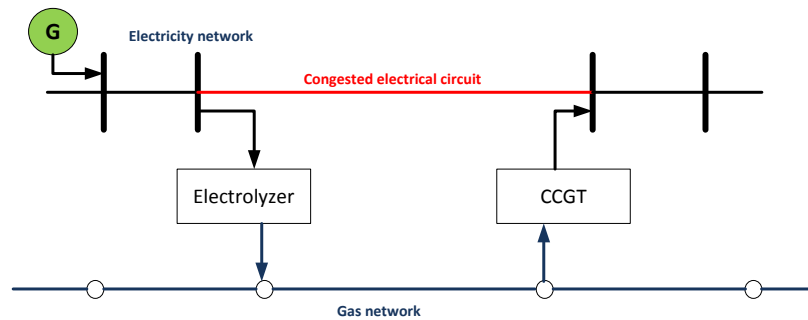


Figure 2-7: A schematic of the 'power to gas' concept for sharing energy transport capacity

During periods when the electrical circuit is congested the electrolyser absorbs the excess power and produce hydrogen or synthetic methane. The hydrogen or synthetic methane can then be injected in the gas grid to be transported and reconverted to electricity through gas fired power generation. This allows the electricity power flow to bypass the congested circuit. The main drawback in the above solution is again the low round trip efficiency as discussed in section 2.2. Several studies have investigated the feasibility of using the GB natural gas infrastructure for storage and transport of electricity in a future high wind scenario (Qardran et al., 2015, Clegg and Mancarella, 2015).

2.2.4 Cost effective provision of flexibility in the electrical power system

The flexibility of a power system is reflected in its ability to maintain electricity supplies of the required quality in the event of sudden and large variations of generation or demand. For example, to manage generation and demand variations in the short term, quick response generation plants are needed while for longer term variations the ability to store a large quantity of energy is required.

Flexibility is required increasingly in electricity networks due to the stochastic nature of renewable power that creates discrepancies between generation and demand. Figure 2.8 shows the variation in net electrical load which is defined as the difference between total electricity demand and wind power generation. This difference needs to be supplied using dispatchable plant. A large share of wind generation in the electrical power system causes the following to occur.

- Steeper ramping up and down of the net load will lead to higher rates of increase or decrease in dispatchable power generation.
- During periods of high wind power generation, the dispatchable generators need to turn down their output to low levels but remain available to ramp up quickly when required.
- The net load profile displays peak demands which are short in duration. This results in less operating hours for dispatchable plant, affecting cost recovery.

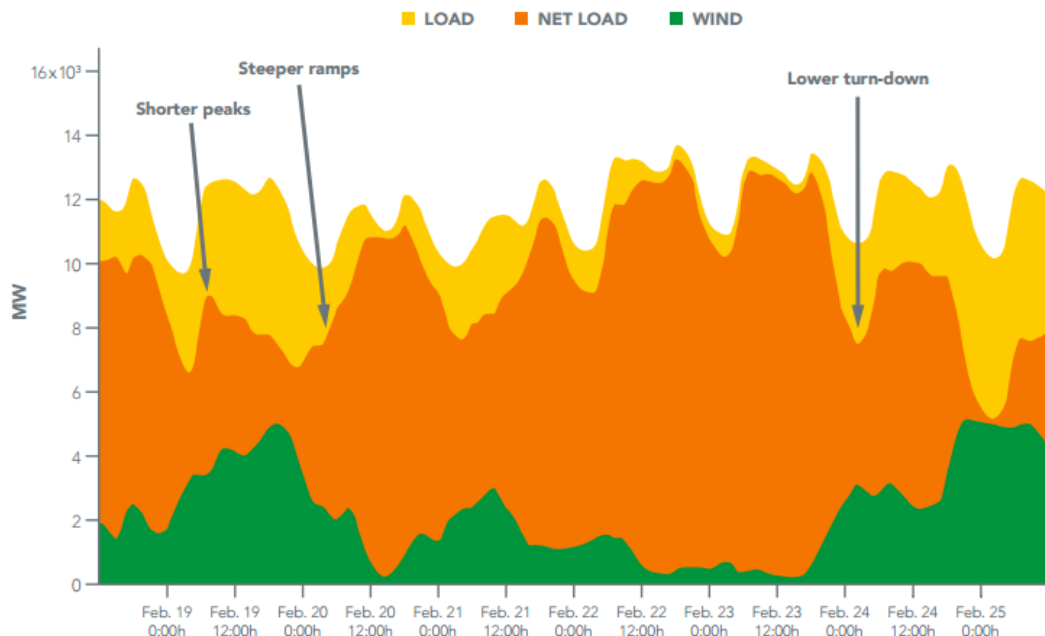


Figure 2-8: Variation in electricity load and renewable generation

Note: Example from utility in the western U.S. (21st Century Power Partnership, 2014)

Integration with other energy systems can provide flexibility to the electrical power system by,

- shifting electrical load between different energy systems
- providing access to a large pool of smaller sized quick response generation plant

The following example is used to illustrate flexibility provision in the electrical power system through integrated energy systems. Figure 2.9 shows multiple, integrated energy systems connected to the main electricity and gas grids. In each sub-system, the electrical load is supplied through the import of electricity from the main grid and/or generation from the local gas fired CHP. The heating load is met through a heat network supplied by the CHP coupled with a heat storage system. The cooling load is met through a chilled water network supplied from electricity driven chillers and/or heat driven absorption chillers coupled with a cold storage system.

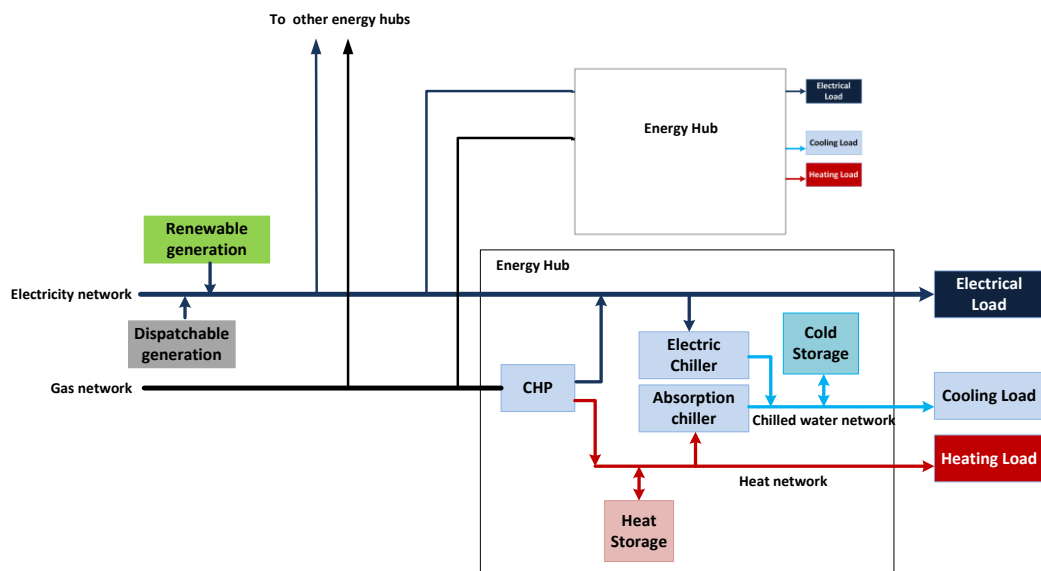


Figure 2-9: Schematic of multiple integrated energy systems connected to electricity and gas grids

In the event of a sudden increase in renewable generation coinciding with a low electricity load (steep ramp down in net load), the gas fired CHP unit reduces its generation output to balance the electrical power system. At the same time electric chillers are switched on (if switched off) to increase load. The heat and cold storage units allow the CHP unit and chiller operation to be decoupled from time of demand. Similarly, during a sudden loss of power generation in the main grid (steep ramp up in net load) the small scale gas fired CHP units increase generation rapidly. Simultaneously, the cooling load is shifted to the heat driven absorption chillers so reducing electrical load. On both these occasions, provision of flexibility to the electrical power system is achieved without any supply disruption to the final consumer.

The development of these flexibility services depend on an adequate communication and control infrastructure which for such small scale units may be expensive. The role of aggregators will be important to manage and provide a sufficiently sized response to the power system operator.

2.2.5 Opportunities for business innovation

Integration of energy systems creates new opportunities for partnerships between traditionally separate energy businesses. For example, the integration between electricity and hydrogen energy systems through power to gas systems could facilitate partnerships between the electricity and transport sectors and the uptake of hydrogen vehicles (Rastetter, 2013, Cipriani et al., 2013). Integration of systems would enable better co-ordination and planning of technical and commercial processes. For example, a fleet of hydrogen vehicles could plan its re-fuelling strategy in a way that complements power system operation. Potentially, this would lead to an overall cost reduction in power generation and supply. A large number of demonstration and commercial projects are investigating the business opportunities in integrating energy systems processes.

Integration of energy supply systems creates new opportunities for businesses to diversify products and services in the energy sector. Diversification of products/services provides an additional income or lowering the average cost for a firm to produce two or more products. For example, consider a conventional CHP plant that is heat driven. Through better coordinated control combined with heat storage, the CHP plant can actively participate in electricity load/demand balancing (Cardell, 2007). This would provide an additional revenue stream for the CHP owner and flexibility for the power system operator.

Integration of energy systems can also assist developing new markets in the energy sector. For example, the market for hydrogen can benefit from the numerous opportunities for hydrogen generation and consumption in an integrated energy system (Rastetter, 2013). New business models and innovative processes can be introduced to take advantage of the emerging markets. This would potentially increase market competition across different energy sectors bringing value to the final consumer.

2.2.6 Increase reliability of the electrical power system

Typically, energy supply systems are built with a certain level of redundancy (both generation and transport) to ensure reliable supply of energy. The interconnection of different energy systems makes it possible to supply a load from several different paths. For example, gas fired power generation establishes a connection between the electricity and gas network and when managed properly can improve the reliability and availability of electricity supply. However, the loads from the electrical network will migrate to the gas network, resulting in a more intensively used gas network. Reliability considerations in integrated energy systems were investigated in (Koeppel, 2007).

Another method to increase reliability is to enable parts of the electrical system to operate in islanded mode during faults in the main grid. These sections of the network are able to

increase the penetration of renewable resources and improve reliability through distributed local control when connected to the main grid or in an intentional islanded mode during supply interruptions. Multi-energy microgrids are gaining research interest due to the number of ways they offer to balance multi energy supply and demand (Kyriakarakos et al., 2011, Kyriakarakos et al., 2013).

However, increased interdependency between energy systems can create a system that is more susceptible to cascaded failures (Rinaldi et al., 2001). Detailed modelling and analysis is required to identify the advantages and disadvantages of certain interconnections between networks.

2.3 Review of analysis methods used in integrated energy systems

The literature on the analysis of integrated energy systems can be categorised as the following types:

- a) coupled energy network modelling and simulation
- b) operation planning and control (e.g. optimization, demand response)
- c) techno-economic and environmental performance analysis
- d) design and expansion planning
- e) reliability analysis

Table 2-1, provides examples of research questions in each of the areas of study.

Table 2-1: Research questions in the analysis of integrated energy systems

Problem type		Example research questions
Network modelling and simulation		What is the steady state and dynamic behaviour of an integrated energy system under different operating conditions?
OPERATION & CONTROL	Operation optimization	What is the optimal way to operate integrated energy systems to meet a particular objective of the overall energy system (e.g. cost minimization, CO ₂ minimization)?
	Control	How can the optimal control of integrated energy systems be achieved?
	Real time demand response and ancillary services provision	What are the potential opportunities to participate in real-time demand response and ancillary service markets through integrating energy systems?
	Interdependencies (Synergies/Conflicts)	What are the operational interdependencies that may occur from the integration of energy systems?
Performance analysis		What is the energy, economic and emissions performance of an integrated energy system?
DESIGN	Green field design	What is the most cost effective structure and sizing of the system components to meet the multi-energy demand?
	Expansion planning	What is the optimal way to invest in the expansion of energy infrastructure considering the future multi-energy demands?
Reliability of supply		What is the expected reliability of supply in the event of a failure in an integrated energy system?

2.3.1 Integrated energy system modelling and simulation

Traditionally, the modelling of energy networks and simulation is carried out for each energy carrier system independently. To understand the interactions between various energy systems and to design effective control strategies, integration of the different

models of each energy system and simulations performed as a combined system are required.

Integrated energy network modelling and simulation studies can be undertaken to investigate the steady-state and/or dynamic behaviour of the combined system.

2.3.1.1 Steady state modelling and simulation of coupled energy systems

Steady state modelling is undertaken to analyse the system when it is in a state of equilibrium (i.e. the operational parameters do not vary with time). For example, when the volume flow rate of gas through a gas pipe or electrical power flow through a circuit is in steady state, the properties of gas flow (pressure) and electricity (voltage magnitude and angle) do not change with time.

Several studies have investigated the integrated modelling and simulation of the electrical network coupled with other energy systems in steady-state. Integrated modelling and analysis of coupled electricity and gas networks in steady state was investigated in (Martinez-Mares and Fuerte-Esquivel, 2012) . Combined modelling and analysis of coupled electricity and heat networks with CHP units and heat pumps was studied in (Liu, 2013). The simultaneous analysis of coupled electricity, gas and heat networks was investigated in (Abeysekera and Wu, 2015, Liu and Mancarella, 2015).

2.3.1.2 Dynamic modelling and simulation of coupled energy systems

The steady state assumption neglects the significant distinction to be made in the dynamic behaviour of coupling components and different energy carrier types. For example, gas and thermal energy systems have much slower travelling speeds of energy and a larger storage capacity within the transport infrastructure compared to electricity. Dynamic models are important to understand the interactions between different systems and to characterise

the propagation of transients from one system to another during normal and abnormal operation.

The integrated modelling and simulation of coupled energy systems considering their transient characteristics is an underdeveloped area of research. Pioneering work was carried out in (Xu et al., 2015a) where dynamic models of coupling components (microturbines and electricity/heat storage) and energy carriers were used to analyse the interactions between electricity and natural gas networks in a microgrid.

2.3.2 Operation and control of the integrated energy system

Similar to network modelling and simulation, operation analyses are normally carried out independently for each energy carrier system. Increasing interactions and interdependencies between different energy systems require new methods of analyses to ensure reliable and efficient operation of the integrated energy system. The different types of operation analyses undertaken in integrated energy systems literature can be categorised as,

- a) operation scheduling/optimization
- b) control of integrated energy systems
- c) flexibility provision (real time demand response and ancillary services)
- d) interdependencies analyses

2.3.2.1 Operation scheduling/optimization

Operation scheduling practices, planning timeframes and modelling tools used for operation optimization vary in different energy systems. For example, the electricity sector uses a half hour balancing period while the gas transmission system typically uses a 24 hour balancing period (Nationalgrid, 2008).

A number of studies examine the extension of traditional concepts used in the electrical power system to the operation scheduling of interconnected energy systems, such as,

- i. Economic dispatch
- ii. Optimal power flow analysis
- iii. Unit commitment

I. Economic dispatch in integrated energy systems

A method for optimal power generation and energy conversion in a coupled multi-energy carrier system that uses the energy hub concept (see Figure 2.10) was introduced in (Geidl and Andersson, 2008). It is a modification of the classical economic dispatch method in electrical power systems (Wood et al., 2014) to account for the different energy demands (i.e. electricity, gas, heat and cooling) and energy conversion between different energy carrier systems. The method is widely used in research related to the operation and design optimization and control of integrated energy systems (Geidl and Andersson, 2006, Xu et al., 2015c).

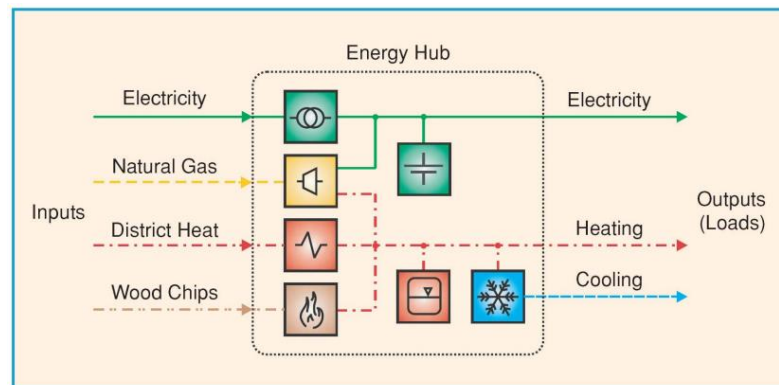


Figure 2-10: Example of an energy hub that contains a transformer, a microturbine, a heat exchanger, a furnace, an absorption chiller, a battery and a hot water storage (Geidl, 2007)

II. Unit commitment in integrated energy systems

The unit commitment problem in electrical power systems is to obtain the optimal start up and shut down schedule for electricity generation plant to satisfy the forecasted demand profile considering cost and constraints such as ramp rates and part load efficiencies (Wood et al., 2014). In integrated energy systems context it refers to the optimal start-up and shut down of each plant component to supply multi-energy demand. The role of energy storage is an important consideration for unit commitment in integrated energy systems.

A framework for the unit commitment problem that uses the energy hub concept was proposed in (Ramirez-Elizondo and Paap, 2009). The electricity and heat storage scheduling was investigated as a part of the unit commitment problem in (Ramirez-Elizondo et al., 2010). A comparison of using an energy or exergy based approach for unit commitment was undertaken in (Ramirez-Elizondo et al., 2013).

III. Optimal power flow in integrated energy systems

In electrical power system studies, the optimal power flow considers the generation dispatch that satisfies the constraints of the transmission system (e.g. operational voltage range, thermal limits of circuits and transformers) while minimising costs (Wood et al., 2014). It combines the economic dispatch calculation with the steady state power flow equations and solves them simultaneously. Optimal power flow in an integrated energy system considers the supply of multi-energy demands using multiple energy sources and energy conversion units while complying with transmission system constraints in each energy carrier system (see Figure 2.11).

The optimal power flow of coupled electricity and natural gas systems was investigated in (Seungwon et al., 2003). The mathematical model of this problem is an optimization

problem where the objective function is to find operational set points of the different components that minimize the electricity and gas system operation cost and does not violate the electricity and gas transmission system constraints. A method for optimal power flow computation in coupled electricity, gas and heat systems was developed in (Geidl and Andersson, 2007).

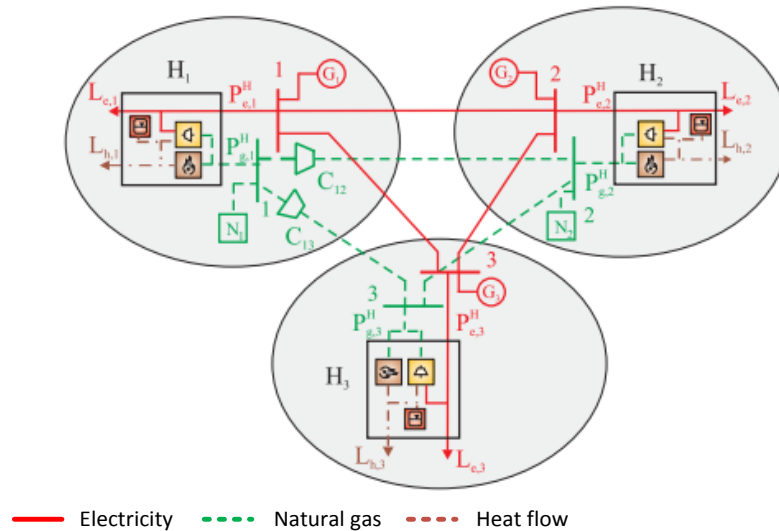


Figure 2-11: System setup of three interconnected energy hubs (Arnold et al., 2010)

Multi time period optimal power flow investigates operation planning for a specified time horizon. Due to the slow travel speeds and inherent storage characteristics in gas and thermal energy systems it is important to account for the dynamic behaviour of these energy systems in multi time period operation planning. A method for optimal power flow and scheduling of combined electricity and natural gas systems with a transient model for natural gas flow was investigated in (Liu et al., 2011). Numerical examples were used to compare the solutions for steady-state and transient models of natural gas transmission systems. A multi-time period optimal power flow model was developed for the combined GB electricity and gas networks in (Chaudry et al., 2008) and (Clegg and Mancarella, 2014).

2.3.2.2 Control of integrated energy systems

The control of integrated energy systems can be categorised into centralized or distributed architectures.

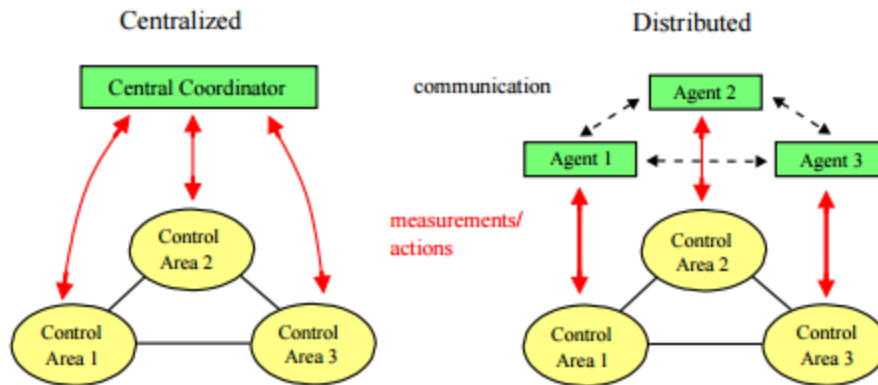


Figure 2-12: Illustration of centralized and distributed control architecture

Note: The solid arrows refer to communication of measurements/control actions between the physical system and the control unit(s). Information exchange between control units is indicated by dashed arrows.

I. Centralized control

A centralized controller measures variables in the multiple energy networks and determine actions for all actuators in the integrated energy system. In a centralized controller (see Figure 2.12) the optimization and control problems are solved by a single control agent.

A centralized controller that uses a model predictive approach to control (MPC) integrated energy systems was investigated in (Arnold et al., 2009). The controller determines actions for each energy hub that gives the best performance based on steady state behaviour of the transmission system, the dynamics of storage devices and the load and price predictions.

A hierarchical centralized control for an integrated energy microgrid was proposed in (Xu et al., 2015b). The controller incorporates transient characteristics of natural gas flow and the

dynamics of energy converters. In order to accommodate the dynamic characteristics of different systems the controller was decomposed into three sub-layers: slow, medium and fast. The control of actuators during fluctuations of renewable power, start-up of an air-conditioner and a microturbine, demand response and energy storage saturation was investigated. The study was extended to the control of an integrated community energy system in (Xu et al., 2015c).

A strategy for the real time control of a coupled electricity and heat system was proposed in (Velez et al., 2011). The control strategy has a hierarchical, centralized architecture and aims to maintain the electricity system frequency at 50Hz and the temperature of district heating water supply at 100°C. A scheduling framework was also presented in (Ramírez-Elizondo and Paap, 2015) where optimization is carried out for a period of 24 hours and the real-time control strategy compensates for the mismatches between the scheduled load and the real load by means of control actions.

II. Distributed control

Even though a centralized control architecture may give the best overall performance, practical and computational difficulties restrict it from being applied in practice. Distributed control architectures decompose the overall optimization and control problem in to sub-problems that are solved using part-models of the system. However, a local control action to be taken depends on the actions of the surrounding controllers and needs to be managed in a coordinated way (see Figure 2.12)

A distributed control system for integrated electricity and natural gas systems was proposed in (Arnold et al., 2008b). A system consisting of several interconnected energy hubs was controlled by their respective control agents. In (Arnold et al., 2010) the study

was extended to investigate a distributed MPC scheme and the dynamics of storage devices in natural gas systems.

Mean-variance portfolio theory and distributed control applied to a system of energy hubs interconnecting electricity and natural gas systems was investigated in (Arnold et al., 2008a).

2.3.2.3 Analysis of the potential to provide flexibility to the electrical power system

A framework to assess real-time demand response provision from the integration of energy systems was investigated in (Mancarella and Chicco, 2013b). The concept of ‘electricity shifting potential’ was introduced as an indicator of the possible reduction of electricity flowing from the external grid to the integrated energy system (without interrupting user’s load). Demand response profitability maps were also introduced to visualize the benefits of electrical load shifting in the presence of incentives.

In (Kitapbayev et al., 2014, Kitapbayev et al., 2013) a method for the optimal control of thermal storage coupled to CHP units in the presence of uncertain market prices and the value of thermal storage as a demand response enabler was investigated.

The work on dynamic response provision in (Mancarella and Chicco, 2013b) was extended to analyse and quantify the benefits of providing ancillary services to the electricity network operator in (Mancarella and Chicco, 2013a). The concept of ‘ancillary services profitability maps’ were introduced to visualize how internal energy shifting potential in integrated energy systems can provide value through the provision of ancillary services.

2.3.2.4 Interdependency analysis

The operational interdependencies investigated in literature can be categorised as between the following energy systems,

- i. electricity and gas
- ii. electricity and heat
- iii. electricity, gas and heat

I. Operational interdependencies between electricity and gas systems

Today, the interdependencies between electricity and gas systems are primarily due to the increasing number of gas fired power generation units (e.g. CCGT). The impact of natural gas prices on electricity generation scheduling and the impact of natural gas infrastructure constraints on the operation of electrical power systems were investigated in (Shahidehpour et al., 2005). The impact of wind variability on the GB gas and electricity supply was investigated in (Qadrdan et al., 2010) using a combined electricity and gas network OPF model. In (Qadrdan et al., 2014), novel operating strategies were recommended for the combined electricity and gas network in GB considering the uncertainty in wind power forecasts. Several studies have also investigated the impact of small scale gas fired power generation and electric vehicles on combined electric and gas distribution networks (Acha et al., 2010, Acha and Hernandez-Aramburo, 2008).

Power to gas or the conversion of electricity to hydrogen (subsequently to synthetic methane if required) and using the gas infrastructure for the storage and transport of energy has gained significant interest in the recent years. A number of studies (Qadrdan et al., 2015, Clegg and Mancarella, 2015) have investigated the interdependencies introduced by power-to-gas units on the combined electricity and gas network operation in GB.

II. Operational interdependencies between electricity and district heating systems

The interdependencies between electricity and heating systems primarily occur at district/community level and are due to

- combined production of electricity and heat in cogeneration systems
- use of thermal storage to increase CHP flexibility and ancillary services provision
- use of electric heating technologies (e.g. electric boilers) coupled with heating systems and thermal storage to provide demand response

The operation and planning of co-generation considering the interactions between electricity and heat systems has been investigated extensively (Salgado and Pedrero, 2008). The potential interactions between electricity and heating systems due to the provision of demand response have been examined in (Houwing et al., 2011, Arteconi et al., 2012)

III. Interdependencies between electricity, gas and district heating systems

Combined heat and power units couple electricity, gas and district heating infrastructure. In (Liu and Mancarella, 2015), Sankey diagrams were used to illustrate the energy flows through the electricity, gas and district heating systems under several scenarios of CHP and heat pump penetration. The study also investigated the impact of different technologies on the steady state operational parameters of each network. The impact on district heating and natural gas grids when aiming towards electricity grid decarbonisation were investigated in (Kusch et al., 2012, Vandewalle et al., 2012a).

2.3.3 Energy performance assessment

The main approaches used in literature to assess the energy and environmental performance of integrated energy systems can be categorised as energy or exergy based. Energy performance indicators (e.g. energy efficiency, primary energy saving) are commonly used in the overall performance assessment of integrated energy systems

(Mancarella, 2012). The performance is typically assessed compared to a benchmark system which, in most studies, is the separate production of each energy-carrier in reference production technologies.

Exergy performance indicators (e.g. exergetic efficiency, exergy destruction) which account for variations in the quality of different energy carriers have also been used for performance analysis in integrated energy systems (Krause et al., 2010, Bagdanavicius et al., 2012, Ramirez-Elizondo et al., 2013). An assessment of different community energy supply systems (CHP using natural gas or biomass gasification) using energy based and exergy based approaches was undertaken in (Bagdanavicius et al., 2012). A comparison of using energy and exergy indicators in promoting cogeneration was investigated in (Nesheim and Ertesvåg, 2007) and the conflicts were highlighted. Exergy based approaches are widely used in thermal engineering research, however its application to real world engineering and power systems is limited.

A review of methods and performance criteria used to assess the energy and environmental performance of integrated energy systems was carried out in (Mancarella, 2014).

2.3.4 Design and expansion planning

The problem of the design and expansion planning of integrated energy systems is to identify the optimal combination of energy supply, conversion and storage technologies as well as the network infrastructure required to meet the estimated energy demand and its future evolution. New analyses argue that integrated design and expansion planning of multi-energy systems is beneficial compared to the independent development practiced today (Saldarriaga et al., 2013).

Literature on the design of integrated energy systems can be categorised as using deterministic or probabilistic methods of analyses.

2.3.4.1 Deterministic models

Deterministic methods are used when variables that affect the investment are assumed to be known with a degree of certainty. Traditionally, the discounted cash flow method using NPV (net present value), IRR (internal rate of return) and payback time indicators are used to assess the profitability of an investment. The design of CHP coupled district heating systems using the NPV and IRR indicator for their economic assessment was investigated in (Horlock, 1987).

A method for expansion planning of an integrated electricity and gas system at the distribution level that has a high penetration of gas fired power generators was investigated in (Saldarriaga et al., 2013). The study claims lower investment costs compared to methods that consider expansion of each energy system independently. A method for the expansion planning of combined gas and electricity networks at the transmission level was investigated in (Chaudry et al., 2014). The model was used to analyse the GB gas and electricity system expansion for several scenarios of the low carbon transition.

The design of multi-energy supply infrastructure for new build schemes with carbon emissions constraints was investigated in (Rees et al., 2014). The objective of the study was to find the optimal mix of on-site and building level energy supply technologies that meets the energy service demand and targets of greenhouse gas emissions at a minimum cost to the developer.

A method for identifying the optimal coupling between networks in an integrated energy system that includes electricity, natural gas and district heating infrastructure was investigated in (Geidl and Andersson, 2006).

2.3.4.2 Probabilistic models

Stochastic (or probabilistic) models are being used in design studies due to the uncertainties in the energy sector introduced by energy markets (e.g. natural gas price) and large volumes of intermittent generation. A method for computing probabilistic NPV and IRR indicators for cogeneration planning under uncertainty using Monte Carlo simulations was investigated in (Carpaneto et al., 2011a, Carpaneto et al., 2011b).

A method for valuing investments in multi-energy conversion, storage and demand side management under uncertainty was examined in (Kienzle and Andersson, 2011). The potential to provide demand side management to uncertain and volatile market prices was valued together with the efficiency gains of integrating energy systems. The study was extended for location dependent valuation of energy hubs with storage in (Kienzle and Andersson, 2010).

A method for assessing the optimal design of integrated energy systems considering its potential for providing demand response and ancillary services was investigated in (Kitapbayev et al., 2013). The proposed approach uses real options valuation methods⁹ as used in finance to capture long term uncertainties and investment flexibility (defer or accelerate investments).

The mean-variance portfolio theory was used to investigate the different solutions for the design of integrated energy systems in (Favre-Perrod et al., 2010).

⁹ Real options theory captures the value from exercising the option that is investing in the plant at a later stage and in a modular basis. Classical engineering economics assume the investment is carried out at the beginning of the analysis window, with no room for postponing the investment. On the other hand, in the presence of uncertainty there may be value in waiting.

2.3.5 Reliability analysis

Assessing the reliability of the electrical power system is a mature field. However, limited work has been carried out investigating the reliability of other energy carrier systems (Helseth and Holen, 2006). A methodology for reliability analysis of the natural gas system based on the method used in electrical systems has been investigated in (Helseth and Holen, 2006). An assessment of the European natural gas system reliability was undertaken in (Olanrewaju et al., 2015).

The reliability analysis of combined electricity and natural gas systems has gained significant interest due to the increasing number of CCGTs in electrical power systems. Modelling of the natural gas system suitable for electrical power system reliability studies was proposed in (Munoz et al., 2003). A method for reliability analysis of the combined electricity and gas network was investigated in (Chaudry et al., 2013). A case study demonstrated the reliability analysis of GB's integrated gas and electricity network given uncertainty in wind variability, gas supply availability and outages to network assets.

A framework for reliability analysis in integrated energy systems, based on the energy hub modelling concept was developed in (Koeppel, 2007, Koeppel and Andersson, 2009). The model computes expected reliability of supply and Expected Energy Not Supplied (EENS). The model is used for systems with and without energy storage devices. The study claims that interconnections between different energy carriers are beneficial particularly for reducing 'expected energy not supplied' in all energy carrier systems¹⁰.

¹⁰ This is true for integrated electricity, natural gas and district heating systems as long as the ratings of the loads and installed components are similar

2.3.6 Modelling tools

A number of modelling tools are available to analyse different aspects of integrated energy systems. Reviews of the models and software tools available were undertaken in several studies as outlined below,

- A review of modelling approaches and software tools available for the analyses of district-scale interactions in energy systems was undertaken in (Allegrini et al., 2015).
- A review of urban energy system models was carried out in (Keirstead et al., 2012). The models and tools were grouped according to their use in technology design, building design, urban climate, systems design and policy assessment.
- A review of software tools available for analysing the integration of renewable energy into various energy systems was undertaken in (Connolly et al., 2010). The study reviewed 37 tools in collaboration with the tool developers or recommended points of contact.
- A review and survey of available tools for planning and analysis of community energy systems was undertaken in (Mendes et al., 2011).

An overview of some of the commonly used modelling tools collated from the review studies is shown below (Mancarella, 2013).

Table 2-2: An overview of models and software tools used for integrated energy system analysis

	Network studies	Operation	Design	Time Resolution /Horizon	Accessibility	Link
EnergyPLAN	No	Yes	No	Hourly/ Annual	Free	http://www.energyplan.eu/
RET Screen	No	No	Yes	Monthly/up to 50 years	Free	http://www.retscreen.net/
H2RES	No	Yes	No	Hourly/ Annual	Internal research	http://h2res.fsb.hr/index.html
DER-CAM	No	Yes	Yes	Variable	Internal research and collaborations	https://building-microgrid.lbl.gov/projects/der-cam
eTransport	Yes	Yes	Yes	Hourly/ Lifetime	Internal research	(Bakken et al., 2007)
SynCity	Yes	No	Yes	-	Internal research	(Kierstead et al.)

2.4 Summary of challenges and research gaps

Realisation of the potential benefits of integrating energy systems faces significant challenges. Some of the key challenges and research gaps are highlighted below.

2.4.1 Challenges

1. The fragmented institutional and market structures of different energy sectors

In the UK in particular, the energy supply systems, their markets and regulatory frameworks have traditionally been separated depending on the type of energy carrier. For example the markets and regulatory frameworks for electricity, natural gas and fuel oils are independent. The restructuring and privatisation of the energy supply businesses resulted in a fragmented institutional framework of individual energy systems where no single party was responsible for the seamless technical functioning and performance enhancement of the overall system. In a report by the IET (IET, 2014), the challenges faced by the electricity

sector due to the multi-party institutional structure were highlighted. It is recognized that the effective decarbonisation of energy relies on a whole systems approach.

The existing detached institutional and market structure is a barrier to realising the benefits of integrating energy systems. The potential benefits need to be shared between multiple stakeholders that operate in independent markets. For example, the value of a CHP system is shared between the electricity and heat sector (low cost heat supply).

The success of integrated energy systems in Denmark (Meibom et al., 2013) and Sweden can in part be attributed to the role of municipal utilities that own and operate multiple energy carrier systems and are responsible for the entire local energy system.

2. The increased complexity of the overall energy system

Integration of multiple energy systems would result in a more complex energy system to manage and operate. The interdependencies between different energy systems and the ICT infrastructure that facilitates interoperability are complicated and require powerful models and software tools to analyse. It is argued that the integration of multiple energy systems can result in an energy supply system that is more susceptible to cascaded failures affecting reliability of supply.

3. Multidisciplinary nature of research and development in integrated energy systems

The integration of energy systems requires co-ordination and collaboration between traditionally detached stakeholders in the energy sector. Research and project development would be multi-disciplinary by nature and requires knowledge of the dissimilar technical, economic and market arrangements.

2.4.2 Research gaps

A number of research gaps in integrated energy systems research identified by a review of the literature and a stakeholder workshop held as part of the EPSRC HubNET project (HubNET, 2015) are highlighted below. The minutes of the stakeholder meeting held at Imperial College, London are available at (Abeysekera et al., 2016a).

1. Methods and tools for modelling and simulation of integrated energy systems need to be developed

Although there are an increasing number of studies investigating the integrated energy systems, the modelling and simulation of integrated energy systems is still an underdeveloped area of research. In particular studies should extend beyond single node and steady state energy flow regime to modelling dynamic behaviour of coupled energy networks and systems. Validation of models with actual data is required to build confidence in the simulations. This is essential for the design of integrated control algorithms and operation strategies to realise the benefits of synergies between networks.

2. Methods and software tools for integrated design, operation, expansion planning and reliability analysis need to be developed

There is a need for methods and tools to aid the co-ordinated design, operation and expansion planning of integrated energy systems. The models/tools need to consider interactions between different energy systems at different scales (community, district, regional, national, European) in sufficient detail. Otherwise there is a potential risk of conflicting results when the system boundary is altered.

3. Standard test networks to perform case studies and validate models are required

There is a need of standard test networks (similar to IEEE standard electricity networks) for natural gas, district heating and district cooling systems. The current practice is to develop case study networks or use data from an actual system for research purposes. This creates a challenge to compare and validate results from different research studies and hinders progress.

4. Assessment criteria for the quantification of interdependencies and the overall performance of the integrated energy system are required

The overall techno-economic performance and interdependencies between coupled energy systems need to be quantified. The independent energy systems have established their own performance assessment methods and evaluation criteria. There is a gap in literature of relevant indicators and assessment methods to characterize the overall performance and interdependencies between energy systems.

5. Quantitative evidence of the benefits of integrating energy systems needs to be demonstrated

There is a need to quantify the multi-party benefits of co-ordinated design, operation and planning of the coupled energy system. Models and software tools will be required to analyse this complex energy system.

6. New opportunities for business innovation needs to be investigated

New business models that aggregate the multiple benefits of integrating energy systems need to be investigated. A comprehensive value proposition that can be realised within the current regulatory and market framework needs to be presented.

7. Demonstration projects are required to show evidence of the practical application and validation of research

Real projects that demonstrate the interoperability of integrated energy networks are required to validate the application of theoretical results.

8. Market design, policy drivers and regulation that promotes integration of energy systems needs to be investigated

There is a clear need for innovation in market design to promote co-ordination between multi-energy systems and realise the potential benefits. Similarly, policy instruments and regulation that can promote the realisation of benefits of energy system integration need to be investigated.

Chapter 3: Optimal power dispatch in integrated energy systems

This chapter presents the method of mathematical formulation and analysis of optimal power dispatch in an integrated energy supply system. The integrated energy supply system at the University of Warwick was used as a case study. Simulations were carried out to analyse the optimal power dispatch for different load scenarios representing the seasonal demand variations in the case system.

3.1 Introduction

Numerous techniques are used in electrical power system optimization. ‘Economic dispatch’ is one such method that computes the optimal power output of a number of electricity generation plants that are available to meet the system demand at the lowest possible cost. Mathematical methods for economic dispatch are well established. A detailed description of the mathematical formulation of the economic dispatch problem and solution methods in electrical power systems is presented in (Wood et al., 2014). A similar approach is adopted in district heating system optimization to compute the optimal heat output in a number of available heat generation plants to meet the system heat load (Eriksson, 1994).

The increasing use of combined heat and power units and other technologies that couple different energy networks are expected to have an impact on both the technical and economic operation of energy systems. The availability of different energy carriers and the use of energy conversion units provide flexibility to meet the different energy demands through multiple routes. For example, the heat demand can be supplied by converting electricity using a heat pump or heat from a combined heat and power unit. Therefore, the

technique of economic dispatch applied to an integrated energy system is important in whole energy system optimization.

A number of recent studies have investigated methods for the optimal power dispatch in an integrated energy system with multiple energy carriers. These were discussed in section 2.2 in Chapter 2. In particular the ‘Vision of Future Energy Networks’ project at ETH, Zurich (Favre-Perrod et al., 2005) carried out pioneering work in developing the mathematical framework for formulating the economic dispatch problem in an energy system with multiple energy carriers and energy conversions.

Nonetheless, to the authors’ best knowledge, none of the previous studies have applied these methods to analyse optimal power dispatch in a real integrated energy system. This is due to the challenges in accessing real energy demand data and the lack of incentives for whole system optimisation under current regulatory frameworks.

This chapter presents the analysis of optimal power dispatch and energy conversions in a real integrated energy supply system in the UK i.e. the energy supply system at University of Warwick (UoW) estates. The mathematical formulation of the optimization problem is presented. Real energy demand data is used to develop case studies for the analysis. The mathematical problem is solved using the optimisation toolbox available in MATLAB software. The results of the case studies are analysed.

3.2 System description

Figure 3.1 shows the simplified configuration of the integrated energy supply system at UoW studied in this chapter.

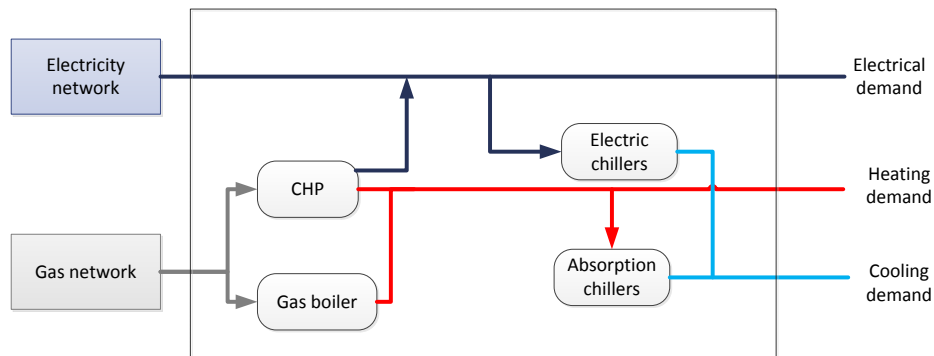


Figure 3-1: Simplified configuration of the integrated energy supply system at the University of Warwick

The on-site integrated energy system is connected to an electricity network and a gas supply network. The energy demands being served are an electricity demand, a heating demand and a cooling demand. The energy conversion units in the energy hub are,

- A combined heat and power generation (CHP) unit – consumes gas from the external gas grid and generates electricity and heat.
- A gas boiler system – consumes gas from the external gas grid and generates heat
- An electric chiller – consumes electricity from the CHP unit and/or the external electricity network and generates cooling
- An absorption chiller - consumes heat from the CHP unit and/or the gas boiler unit and generates cooling

3.3 System modelling

Figure 3-1 is reproduced as Figure 3-2 with labels on the different power flows for modelling. The modelling is based on the concept of energy hubs introduced in (Geidl and Andersson, 2008). It comprises of a system of energy conversion units that convert energy to different forms. As shown in Figure 3-2 the energy hub connects demands to energy supply networks.

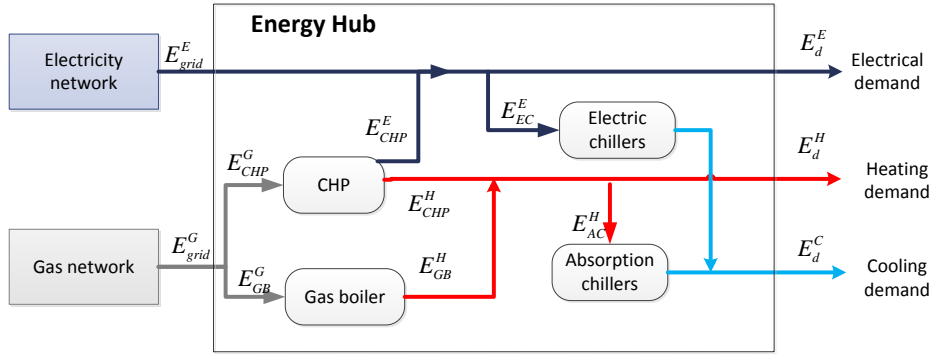


Figure 3-2: Schematic of the integrated energy supply system with power flows marked

The conversion of energy at a network coupling unit C from one energy type to another (e.g. α to β) is characterized by an efficiency ($\eta_C^{\alpha/\beta}$) given by,

$$E_C^\beta = \eta_C^{\alpha/\beta} \times E_C^\alpha \quad (3.1)$$

where,

- E_C^α - power input to coupling unit C of energy carrier type α ;
- E_C^β - power output from coupling unit C of energy carrier type β ;

The converter efficiencies are assumed as a constant. The energy conversions at the units in the energy hub shown in Figure 3-1 is expressed as,

$$\begin{aligned} \text{At the CHP unit; } E_{CHP}^E &= \eta_{CHP}^{G/E} \times E_{CHP}^G \\ E_{CHP}^H &= \eta_{CHP}^{G/H} \times E_{CHP}^G \\ \text{At the GB unit; } E_{GB}^H &= \eta_{GB}^{G/H} \times E_{GB}^G \\ \text{At the AC unit; } E_{AC}^C &= \eta_{AC}^{H/C} \times E_{AC}^H \\ \text{At the EC unit; } E_{EC}^C &= \eta_{EC}^{E/C} \times E_{EC}^E \end{aligned} \quad (3.2)$$

The balance of energy supply and demand is expressed as,

$$\begin{aligned} \text{Electricity demand; } E_d^E &= E_{grid}^E + E_{CHP}^E - E_{EC}^E \\ \text{Heating demand; } E_d^H &= E_{CHP}^H + E_{GB}^H - E_{AC}^H \\ \text{Cooling demand; } E_d^C &= E_{EC}^C + E_{AC}^C \end{aligned} \quad (3.3)$$

where,

- E_d^α - power demand of energy carrier type α , where α is electricity (E), heat (H) or cooling (C)
- E_{grid}^E - electrical power input to the hub from the electricity network

Substituting from (3.2) the set of equations (3.3) is expressed in matrix form as,

$$\begin{bmatrix} E_d^E \\ E_d^H \\ E_d^C \end{bmatrix} = \begin{bmatrix} 1 & \eta_{CHP}^{G/E} & 0 & -1 & 0 \\ 0 & \eta_{CHP}^{G/H} & \eta_{GB}^{G/H} & 0 & -1 \\ 0 & 0 & 0 & 1 & 1 \end{bmatrix} \begin{bmatrix} E_{grid}^E \\ E_{CHP}^G \\ E_{GB}^G \\ E_{EC}^E \\ E_{AC}^H \end{bmatrix} \quad (3.4)$$

3.4 Optimization problem

The optimization problem is to find the least cost method to meet the energy demands using the energy hub and the external energy supply networks. The objective function is expressed as,

$$\begin{aligned} \text{minimize } C &= (C_{grid}^E \times E_{grid}^E) + (C_{grid}^G \times E_{grid}^G) \\ C &= (C_{grid}^E \times E_{grid}^E) + (C_{grid}^G \times (E_{CHP}^G + E_{GB}^G)) \end{aligned} \quad (3.5)$$

where,

- C - total system cost [£]
- C_{grid}^α - the cost of consuming energy carrier type α , where α is electricity (E) or gas (G) [£/kW $^\alpha$]

The energy balance equations formulated in (3.4) are a set of constraints to be satisfied by the optimal solution.

The technical power supply limitations of the energy supply networks and the network coupling units i.e. minimum and maximum power supply capacities introduce another set of constraints to be satisfied.

The optimization problem is summarised as,

$$\text{minimize } C = (C_{grid}^E \times E_{grid}^E) + (C_{grid}^G \times (E_{CHP}^G + E_{GB}^G))$$

subject to;

$$\begin{bmatrix} E_d^E \\ E_d^H \\ E_d^C \end{bmatrix} = \begin{bmatrix} 1 & \eta_{CHP}^{G/E} & 0 & -1 & 0 \\ 0 & \eta_{CHP}^{G/H} & \eta_{GB}^{G/H} & 0 & -1 \\ 0 & 0 & 0 & 1 & 1 \end{bmatrix} \begin{bmatrix} E_{grid}^E \\ E_{CHP}^G \\ E_{GB}^G \\ E_{EC}^E \\ E_{AC}^H \end{bmatrix} \quad (3.6)$$

$$(E_{grid}^E)_{\min} \leq E_{grid}^E \leq (E_{grid}^E)_{\max}$$

$$(E_{CHP}^G)_{\min} \leq E_{CHP}^G \leq (E_{CHP}^G)_{\max}$$

$$(E_{GB}^G)_{\min} \leq E_{GB}^G \leq (E_{GB}^G)_{\max}$$

$$(E_{EC}^E)_{\min} \leq E_{EC}^E \leq (E_{EC}^E)_{\max}$$

$$(E_{AC}^H)_{\min} \leq E_{AC}^H \leq (E_{AC}^H)_{\max}$$

The mathematical problem is a nonlinear programming problem solved using the optimization toolbox in MATLAB software (in particular the MATLAB function *fmincon* is used). The solution computes the optimum values for all variables in X given by,

$$X = \begin{bmatrix} E_{grid}^E \\ E_{CHP}^G \\ E_{GB}^G \\ E_{EC}^E \\ E_{AC}^H \end{bmatrix} \quad (3.7)$$

3.4.1 Marginal cost of energy

Marginal cost of energy is defined as the change in system cost if the output of energy increased by a single unit. In electrical power systems marginal costs are used to compare different electricity generation sources and develop a merit order for dispatch of power supply units (Wood et al., 2014).

In the case of an integrated energy system with different energy types the marginal cost is defined for each type of energy delivered. For example, in the study of the system in Figure 3-1 the marginal cost of electricity, heating and cooling is calculated individually.

The marginal costs for each energy type at the energy hub output are obtained when solving the optimization problem. These are given by the Lagrange variables of the optimization problem (Geidl and Andersson, 2008). The method of solving the optimisation problem using the Lagrange method is described in detail in (Wood et al., 2014).

In summary the Lagrange function (L) for the constrained optimization problem¹¹ considered in (3.6) is expressed as,

$$L = \left[\left(C_{grid}^E \times E_{grid}^E \right) + \left(C_{grid}^G \times \left(E_{CHP}^G + E_{GB}^G \right) \right) \right] + \dots$$

$$+ \left[\lambda^E \quad \lambda^H \quad \lambda^C \right] \left\{ \begin{array}{l} \left[\begin{array}{l} E_d^E \\ E_d^H \\ E_d^C \end{array} \right] - \left[\begin{array}{ccccc} 1 & \eta_{CHP}^{G/E} & 0 & -1 & 0 \\ 0 & \eta_{CHP}^{G/H} & \eta_{GB}^{G/H} & 0 & -1 \\ 0 & 0 & 0 & 1 & 1 \end{array} \right] \left[\begin{array}{l} E_{grid}^E \\ E_{CHP}^G \\ E_{GB}^G \\ E_{EC}^E \\ E_{AC}^H \end{array} \right] \end{array} \right\} \quad (3.8)$$

where,

- λ^α - Lagrange variables representing the marginal cost of energy type α

¹¹ Only the equality constraint is shown here

MATLAB's *fmincon* function computes the optimum values for all variables (eqn. (3.7)) and the Lagrange variables λ^E , λ^H and λ^C .

3.5 Case study data

The technical specifications and the monitored energy demands of the energy supply system at University of Warwick are used to develop the case studies. Technical specifications of the energy conversion units (see Figure 3-2) are presented in Table 3-1.

Table 3-1: Technical specifications of the energy hub units

Note: The minimum power output capacity for all units are assumed as zero.

Component	Maximum power output Capacity ¹² (E_C^α) _{max}	Energy conversion efficiency ($\eta_C^{\alpha/\beta}$)
CHP unit	9.2 MW _e	Electrical efficiency of CHP ($\eta_{CHP}^{G/E}$) = 0.35
	10.5 MW _{th,heat}	Thermal efficiency of CHP ($\eta_{CHP}^{G/H}$) = 0.4
Gas Boiler	19.7 MW _{th,heat}	Thermal efficiency of Gas Boiler ($\eta_{GB}^{G/H}$) = 0.9
Electric chiller	2 MW _{th,cool}	Coefficient of Performance of electric chiller ($\eta_{EC}^{E/C}$) = 3
Absorption chiller	1.2 MW _{th,cool}	Efficiency of absorption chiller ($\eta_{AC}^{H/C}$) = 0.7

The aggregated hourly electricity and heat demand variation from 1st of April 2013 to 31st of March 2014 is shown in Figure 3-3. The large seasonal variation of the heat demand and the relatively regular weekly oscillations of the electricity demand are observed.

¹² The actual energy system consists of multiple units of smaller capacity. A single unit of the total aggregated capacity is assumed for the case study.

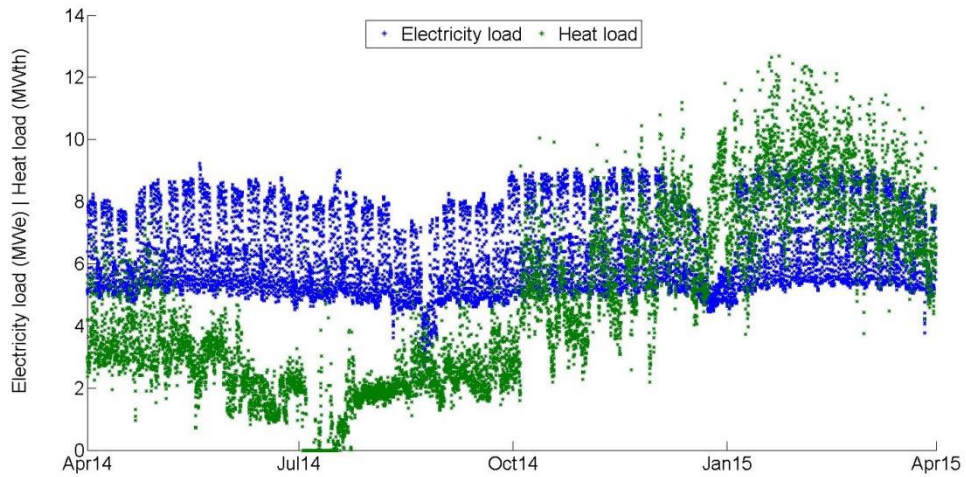


Figure 3-3: Aggregated hourly electricity and heat demand

The frequency of occurrence (no of hours) of a particular combination of electricity and heat demand is shown in Figure 3-4.

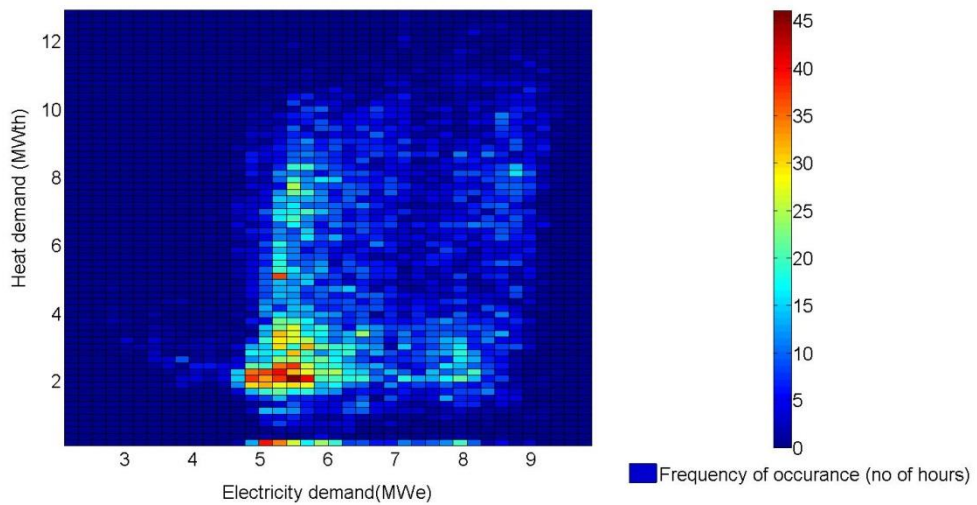


Figure 3-4: Frequency of occurrence of a particular combination of electricity and heat demand

Note: A granularity of 0.2 MW was chosen for clustering electricity and heat demands

Monitored cooling demand data was unavailable. Therefore, the cooling demand is deemed as a constant value of $1.2 \text{ MW}_{\text{th,cool}}$ for the study.

The electricity, heating and cooling demand shown in Table 3-2 are used as load scenarios to represent typical seasonal demand combinations of the energy system.

Case studies representing typical demand combinations in winter, summer, spring/autumn and an extreme winter are analysed in detail.

Table 3-2: Case studies

	Case 1	Case 2	Case 3	Case 4
Load scenario	Winter	Summer	Spring/Autumn	Winter-peak
Electricity demand	5.5 MW _e	5.5 MW _e	6 MW _e	9 MW _e
Heating demand	10 MW _{th,heat}	3 MW _{th,heat}	6 MW _{th,heat}	12 MW _{th,heat}
Cooling demand	1.2 MW _{th,cool}	1.2 MW _{th,cool}	1.2 MW _{th,cool}	1.2 MW _{th,cool}

The full range of electricity and heating demand combinations are also simulated and the results are discussed in section 3.6.2 .

The fuel prices for the study are as shown in Table 3-3. It is assumed that the export of electricity back to the grid **does not** provide an income¹³.

Table 3-3: Fuel prices

Fuel type	Price
Electricity	0.1 £/kWh _e
Gas	0.03 £/kWh _{gas}

¹³ This is a distinct feature of the energy system being studied where the institution does not have a power export agreement with an energy supplier and the local distribution network operator.

3.6 Results and discussion

3.6.1 Case study results

3.6.1.1 Case 1 results

In Case 1, the electricity demand is 5.5 MW_e , the heat demand is $10 \text{ MW}_{th,heat}$ and the cooling demand is $1.2 \text{ MW}_{th,cool}$. This load combination is typically observed in the winter period when the heating demand is relatively high. The results of optimal power dispatch are shown in Figure 3-5

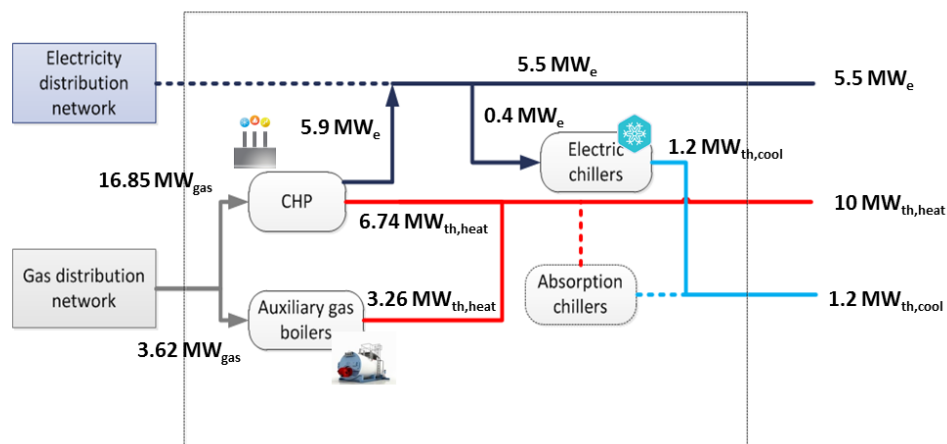


Figure 3-5: Optimal power dispatch results in Case 1

- **Electricity demand** is supplied using the CHP unit that generates 5.9 MW_e . There is no electricity imported from the external grid.
- **Heating demand** is supplied by the CHP unit that generates $6.74 \text{ MW}_{th,heat}$ and the gas boiler unit that generates $3.26 \text{ MW}_{th,heat}$.
- **The cooling demand** is supplied by the electric chillers that consume 0.4 MW_e . The absorption chiller is not used.

The marginal costs for the different energy outputs are shown below.

Marginal cost of electricity	0.047 £/kWh _e
Marginal cost of heat	0.033 £/kWh _{th,heat}
Marginal cost of cooling	0.016 £/kWh _{th,cool}

The marginal cost of electricity in Case 1 (i.e. 0.47 £/kWh_e) is lower than the cost of grid electricity imports. This is due to an additional unit of electricity being supplied by the CHP unit. Electricity supply using the CHP unit is cheaper due to the simultaneous production of heat which reduces overall system cost compared to using grid electricity imports and heat from the gas boiler.

The marginal cost of heat in Case 1 is the cost of supplying a unit of heat using only the gas boiler unit. An additional unit of heat needs to be supplied by the gas boiler unit as the CHP heat output is fixed by the electricity demand.

The optimisation chooses the electric chiller for cooling supply. It increases the electrical load in the system allowing additional power output from the CHP unit. The marginal cost of cooling is 1/3 of the marginal cost of electricity due to the coefficient of performance of the electric chiller unit.

3.6.1.2 Case 2 results

In case 2, the electricity demand is 5.5 MW_e, the heat demand is 3 MW_{th,heat} and the cooling demand is 1.2 MW_{th,cool}. This load combination is typically observed in the summer period when the heating demand is relatively low. The results of optimal power dispatch in the system are shown in Figure 3-6.

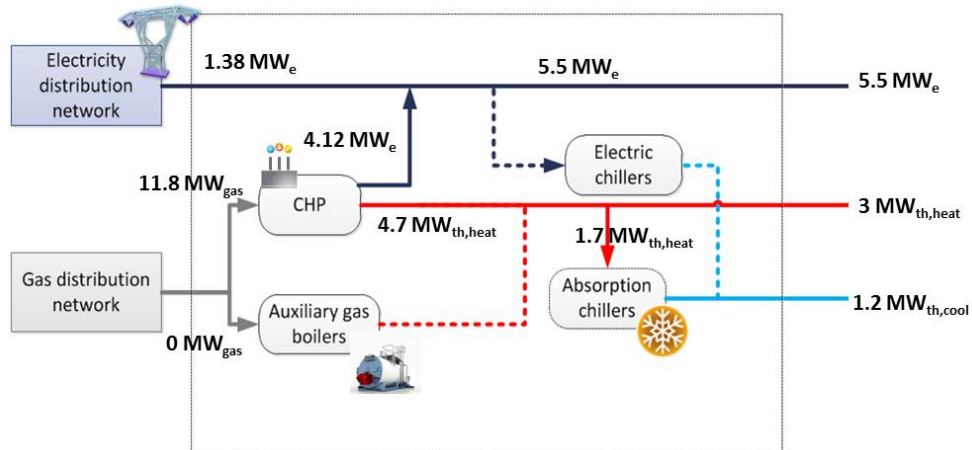


Figure 3-6: Optimal power dispatch results in Case 2

- **Electricity** is supplied using the CHP unit that generates 4.12 MW_e and 1.38 MW_e of electrical power that is imported from the external grid.
- **Heating** is supplied by the CHP unit that generates 4.7 MW_{th,heat}. The gas boiler unit is not used.
- **The cooling** is supplied by the absorption chillers consuming 1.7 MW_{th,heat}. The electric chiller is not used.

The marginal costs for the different energy outputs are shown below.

Marginal cost of electricity	0.1000 £/kWh _e
Marginal cost of heat	-0.0125 £/kWh _e
Marginal cost of cooling	-0.0179 £/kWh _e

The marginal cost of electricity in Case 2 is the cost of grid imported electricity. Any additional unit of electricity needs to be imported from the external grid as the output of the CHP unit is fixed by the heat demand and there being no incentive to export excess electricity.

The marginal cost of heat in Case 2 is $-0.0125 \text{ £/kWh}_{\text{th,heat}}$. The negative value implies that an additional unit of heat demand will **reduce** the overall system operation cost. Any additional unit of heat is supplied by the CHP unit. The increase in heat demand allows the CHP unit to increase its heat output while simultaneously generating electricity. This reduces the grid electricity imports which in turn reduce the overall system cost. It also explains the use of the absorption chiller for cooling supply, whereby the system heat load is increased allowing additional power output from the CHP unit.

The marginal cost of cooling in Case 2 is also a negative value. The cooling demand translates to an additional heat demand when it is supplied from the absorption chiller. In this circumstance, an additional unit of cooling and hence heat demand allows more electricity generation from the CHP unit and hence **reduces** the overall system operation cost.

3.6.1.3 Case 3 results

In Case 3, the electricity demand is 6 MW_e , the heat demand is 6 MW_{th} and the cooling demand is $1.2 \text{ MW}_{\text{th}}$. This load combination is typically observed in the autumn and spring period of operation. The results of optimal power dispatch in the system are shown in Figure 3-7.

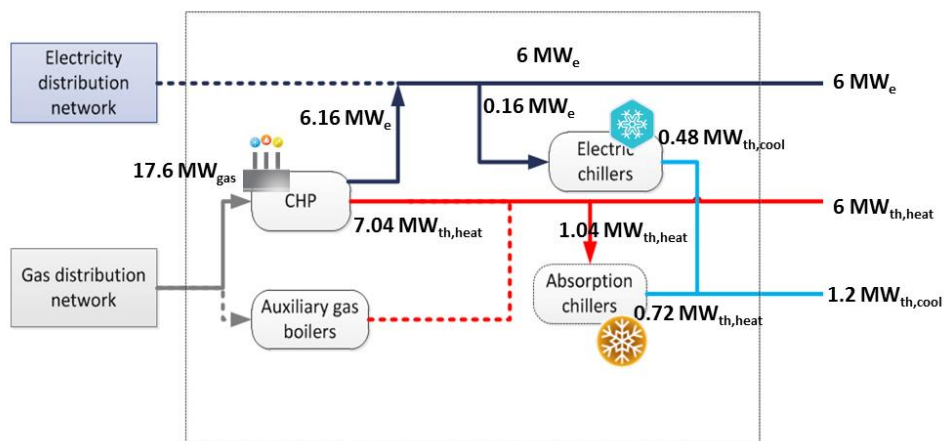


Figure 3-7: Optimal power dispatch results in Case 3

- **Electricity** is supplied using the CHP unit that generates 6.16 MW_e. There is no electricity imported from the external grid.
- **Heating** is supplied by the CHP unit that generates 7.04 MW_{th,heat}. The gas boiler unit is not used.
- **Cooling** is supplied using both the absorption chiller and the electric chiller providing 0.72 MW_{th,cool} and 0.48 MW_{th,cool}.

The marginal costs for the different energy outputs are shown below.

Marginal cost of electricity	0.0670 £/kWh _e
Marginal cost of heat	0.0158 £/kWh _{th,heat}
Marginal cost of cooling	0.0230 £/kWh _{th,cool}

The CHP output is not limited by either the electricity or heat demand.

The marginal cost of electricity is higher than in Case 1 (0.047 £/kWh_e) and lower than the cost of grid imported electricity (0.1 £/kWh_e). Any additional unit of electricity is supplied by the CHP unit similar to Case 1. However, the marginal cost of electricity is higher than in Case 1 due to the comparatively low marginal cost of heat in this Case.

The marginal cost of heat is +0.0158 £/kWh_e. It is lower than the cost of supplying heat from the gas boiler unit (0.033 £/kWh_e). This is due to an additional unit of heat being supplied by the CHP unit similar to Case 2. However, the cost is higher than in Case 2 due to the relatively low marginal cost of electricity in this Case.

The marginal cost of cooling is +0.023 £/kWh_{th,cool}. The electric chiller is used to supply the additional unit of cooling using the CHP unit's electricity output. Therefore the cost is 1/3 of the marginal cost of electricity. It is higher than in Case 1 due to the corresponding higher marginal cost of electricity in this Case.

3.6.1.4 Case 4 results

In Case 4, the electricity demand is 9 MW_e , the heat demand is 12 MW_{th} and the cooling demand is $1.2 \text{ MW}_{th,cool}$. This load combination is typically observed in a peak winter period when a high electricity demand and heat demand coincide. The results of optimal power dispatch in the system are shown in Figure 3-8.

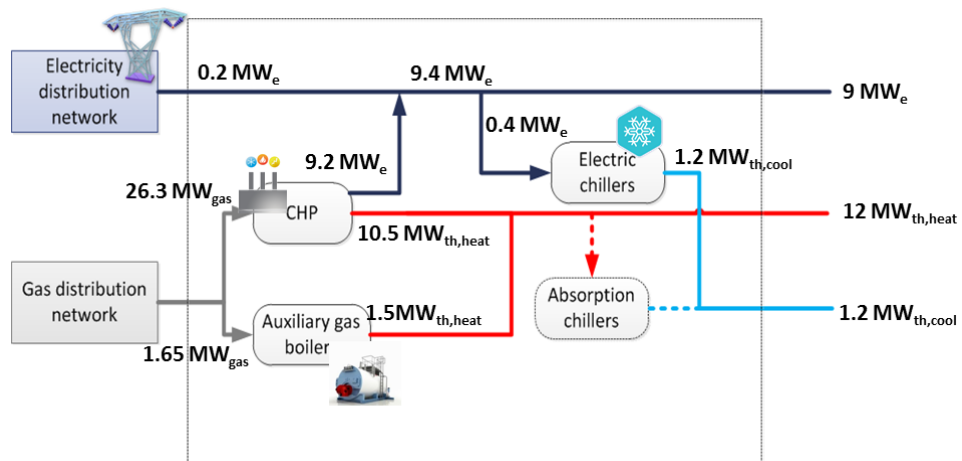


Figure 3-8: Optimal power dispatch results in Case 4

- **Electricity** is supplied using the CHP unit that generates its rated electrical power output of 9.2 MW_e and in addition 0.2 MW_e of electrical power is imported from the external grid.
- **Heating** is supplied by the CHP unit that generates its rated heat output of $10.5 \text{ MW}_{th,heat}$ and in addition the gas boiler unit that generates $1.5 \text{ MW}_{th,heat}$.
- **Cooling** is supplied using the electric chillers that consume 0.4 MW_e . The absorption chiller is not used.

The marginal costs for the different energy outputs are shown below.

Marginal cost of electricity	0.100 £/kWh_e
Marginal cost of heat	$0.033 \text{ £/kWh}_{th,heat}$
Marginal cost of cooling	$0.033 \text{ £/kWh}_{th,cool}$

The marginal cost of electricity in Case 4 is the cost of grid imported electricity. Any additional unit of electricity needs to be imported from the external grid as the CHP unit is operating at its rated capacity.

The marginal cost of heat is the cost of heat supplied from the gas boiler unit. Any additional unit of heat needs to be supplied from the gas boiler as the CHP unit is at its rated thermal capacity.

The marginal cost of cooling is 0.033 £/kWh_{th,cool}. This is the highest marginal cost of cooling observed in the case studies. An additional unit of cooling demand is supplied from the electric chiller using grid imported electricity. This is cost-effective compared to using the absorption chiller with heat generated by the gas boiler.

3.6.2 Analysis for the complete range of electricity and heat demand combinations

Simulations were carried out to calculate the optimal power dispatch for the complete range of electricity and heat demand combinations. This allows the optimal power dispatch for the range of energy demand combinations to be studied and any conditions that are different to the case studies analysed. The cooling demand was held constant at 1.2MW_{th,cool}.

3.6.2.1 Electricity and heating supply

Figure 3-9 shows the optimal power dispatch results of grid electricity imports (in kW_e), the gas consumption in the CHP and the gas boiler (in kW_g) for the complete range of electricity and heat demand combinations.

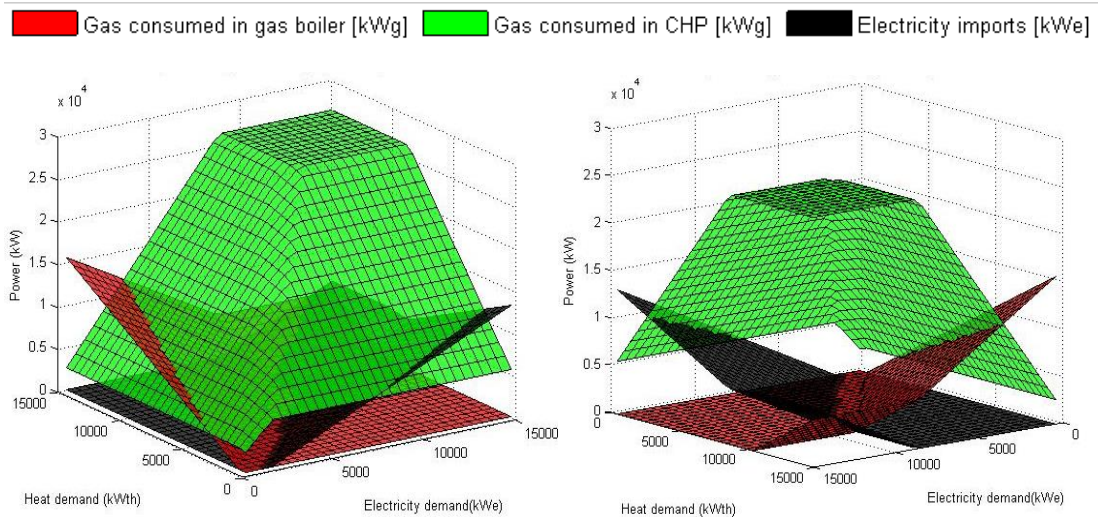


Figure 3-9: Optimal power dispatch results for the range of electricity and heat demands
Note: The figure on the right is the same 3D figure rotated by 180°; the vertical axis shows power in kW of electricity imports and gas consumed in either the gas boiler or CHP unit

- **CHP:** The green colour surface shows the gas consumption in the CHP unit for different combinations of electricity and heat demand. The two inclined surface sections show a linear increase in gas consumption with the increase of electricity and heat demand. The horizontal surface section at high electricity and heat demand combinations show that the CHP unit has reached its rated capacity.
- **Gas boiler:** The red colour surface shows the gas consumption in the gas boiler unit for different combinations of electricity and heat demand. The horizontal surface section at zero power level shows the demand combinations in which the gas boiler is not used for heat supply. This is when the CHP power output is fixed by the heat demand as discussed in section 3.6.1.2 . The inclined red colour surface section (see left hand figure in Figure 3-9) shows a linear increase in gas consumption of the gas boiler with increasing heat demand. This is when the CHP power output is fixed by the electricity demand as discussed in section 3.6.1.1 . The figure also shows the increase in utilisation of the gas boiler when both the electricity and

heat demands are high and the CHP has reached its rated capacity (see right hand side figure).

- **Electricity import:** The black colour surface in Figure 3-9 show the external electricity imports for different combinations of electricity and heat demand. The horizontal surface section at zero power level shows the demand combinations where there is no electricity imported from the external grid. This is when the CHP power output is fixed by the electricity demand as discussed in section 3.6.1.1 . The inclined black colour surface section (see left hand figure in Figure 3-9) shows a linear increase in grid electricity imports with increasing electricity demand. This is when the CHP power output is fixed by the heat demand as discussed in section 3.6.1.2 . The figure also shows the increase in electricity imports when the electricity and heat demands are high and the CHP unit has reached its rated capacity (see right hand side figure).

Therefore, the CHP unit plays a central role in supplying electricity and heat to the integrated energy supply system. The analysis shows that the gas boiler and electricity imports are only considered when either the CHP unit is fixed or when it's reached full capacity. The adequate sizing of the CHP unit could provide significant savings in operational cost.

3.6.2.2 Cooling supply

Figure 3-10 shows the optimal power dispatch results of the electricity consumed in the electric chiller (in kW_e) and the heat consumed in the absorption chiller (in $\text{kW}_{\text{th,heat}}$). The cooling demand was held constant at $1.2 \text{ MW}_{\text{th,cool}}$. The figure is used to examine when the optimal dispatch chooses the electric chiller or the absorption chiller or a combination of both for cooling supply.

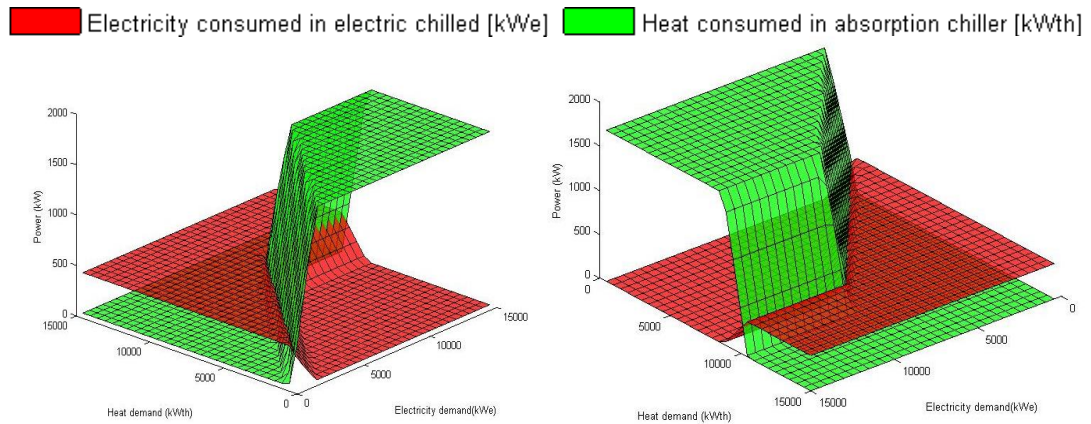


Figure 3-10: Optimal power dispatch results of the absorption chiller and electric chiller.
Note: The figure on the right is the same 3D figure rotated by 180°; the vertical axis shows power in kW of electricity consumed by electric chiller and heat consumed by absorption chiller

- The area where the horizontal green surface is above the red surface shows the demand combinations when the absorption chiller alone is used for cooling supply. This is when the CHP electrical power output is fixed by the heat demand as discussed in 3.6.1.2 . Utilising the absorption chiller transfers the cooling demand to heat and allows the output from the CHP unit to be increased.
- The area where the horizontal red surface is above the green surface shows the demand combinations when the electric chiller alone is used for cooling supply. This is when the CHP power output is fixed by the electricity demand as discussed in 3.6.1.1 and when the CHP unit has reached its rated capacity as discussed in 3.6.1.4 . In that situation, transferring the cooling demand to electricity allows increasing the output from the CHP unit (when it hasn't reached full capacity).
- The area where the red and green surfaces are inclined and intersect each other shows the demand combinations when both the electric chiller and the absorption chiller are used for cooling supply. This is similar to the case discussed in 3.6.1.3 where the CHP unit alone supplies power for the electricity, heat and cooling demands.

The electric chiller and the absorption chiller provide flexibility to the operation of the integrated energy supply system. By transferring the cooling demand between electricity and heat it increases the utilisation of the CHP unit. Increasing the utilisation of the CHP unit reduces overall system operational costs.

3.6.2.3 Marginal cost of electricity supply

Figure 3-11 shows the variation of the marginal cost of electricity for the range of electricity and heat demand combinations in the case system.

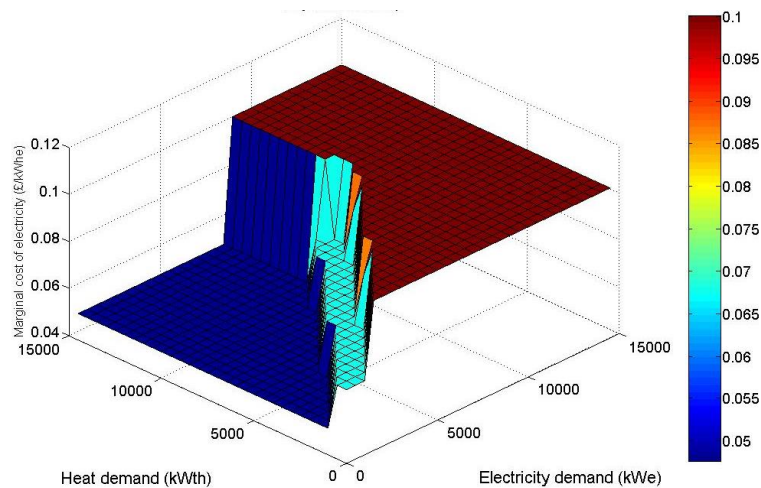


Figure 3-11: Marginal cost of electricity

- The dark blue colour area shows the combinations of electricity and heat demands where the marginal cost of electricity is 0.047 €/kWh_e. This is when the CHP power output is fixed by the electricity demand as discussed in section 3.6.1.1. An additional unit of electricity is supplied by increasing the CHP unit power output.
- The light blue colour area shows the marginal cost of electricity at ~0.067 €/kWh_e. This is similar to the case discussed in section 3.6.1.3 where again any additional unit of electricity is supplied by increasing the CHP unit power output. The marginal cost is higher than in the dark blue area due to the corresponding low marginal cost of heat.

- The red colour area shows the combinations of electricity and heat demands where the marginal cost of electricity is 0.1 £/kWh_e. This is when the CHP power output is fixed by the heat demand as discussed in 3.6.1.2 and when the CHP unit has reached its rated capacity as discussed in section 3.6.1.4 . Any additional unit of electricity is supplied by external grid imports.

The low marginal cost of electricity in the dark blue and light blue colour areas is typically observed in winter periods when the CHP electrical power output supplies the electricity demand. In this situation, it is beneficial to consider opportunities to increase the CHP output and export excess electricity to generate an additional income.

3.6.2.4 Marginal cost of heat supply

Figure 3-12 shows the variation of marginal cost of heat for the range of electricity and heat demand combinations in the case system.

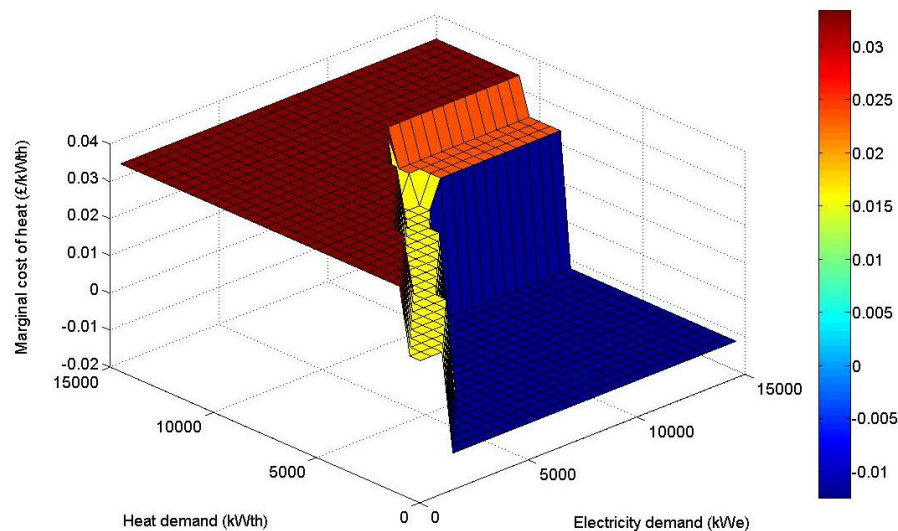


Figure 3-12: Marginal cost of heat

- The dark blue colour area shows the combinations of electricity and heat demands where the marginal cost of heat is a negative value (-0.0125 £/kWh_{th,heat}). This is when the CHP power output is fixed by the limited heat demand as discussed in

section 3.6.1.2 . An additional unit of electricity is supplied by increasing the CHP unit power output.

- The yellow and orange colour areas show the marginal cost of heat is a positive value at $\sim 0.02 \text{ £/kWh}_{\text{th,heat}}$. This is similar to the case discussed in section 3.6.1.3 . An additional unit of heat is supplied by increasing the CHP unit power output.
- The red colour area shows the combinations of electricity and heat demands where the marginal cost of heat is $0.033 \text{ £/kWh}_{\text{th,heat}}$. This is when the CHP power output is fixed by the electricity demand as discussed in 3.6.1.1 and when the CHP unit has reached its rated capacity as discussed in section 3.6.1.4 . Any additional unit of heat is supplied by the gas boiler.

The negative marginal cost of heat in the dark blue area suggests that extra heat demand in this situation would reduce the total system cost. This is typically observed during the summer periods when the CHP power output is fixed by the low heat demand. In this situation it is beneficial to consider opportunities to connect with neighbouring heat networks or the use of heat storage in order to allow increasing the heat output of the CHP unit.

3.6.2.5 Marginal cost of cooling supply

Figure 3-13 shows the variation of marginal cost of cooling for the range of electricity and heat demand combinations in the case system.

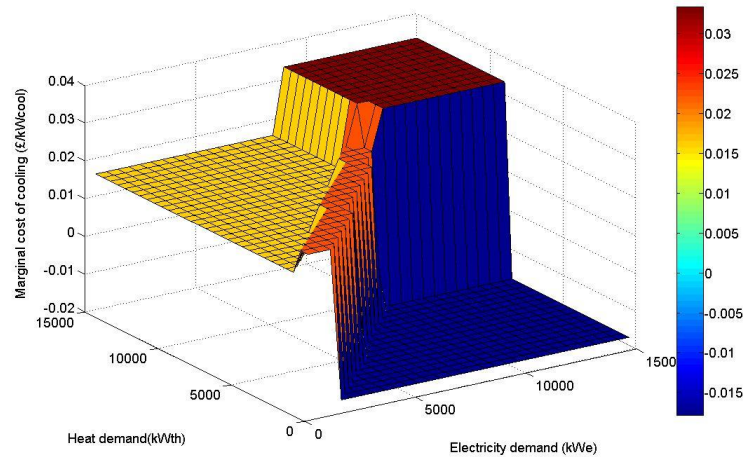


Figure 3-13: Marginal cost of cooling

- The dark blue colour area shows the combinations of electricity and heat demands where the marginal cost of cooling is a negative value ($-0.0179 \text{ £/kWh}_{\text{th,cool}}$). This is when the CHP power output is fixed by the low heat and cooling demand as discussed in section 3.6.1.2 . An additional unit of cooling is supplied by the absorption chiller unit driven by the CHP units' heat output.
- The yellow colour area shows the combinations of electricity and heat demands where the marginal cost of cooling is $0.016 \text{ £/kWh}_{\text{th,cool}}$. This is when the CHP power output is fixed by the electricity demand as discussed in section 3.6.1.1 . An additional unit of cooling is supplied by the electric chiller unit driven by the CHP units' electricity output.
- The orange colour area shows the combinations of electricity and heat demands where the marginal cost of cooling is $0.023 \text{ £/kWh}_{\text{th,cool}}$. This is similar to the case discussed in section 3.6.1.3 where a combination of the electric chiller and absorption chiller driven by the CHP units' power output supplies the cooling demand.
- The red colour area shows the combinations of electricity and heat demands where the marginal cost of heat is $0.033 \text{ £/kWh}_{\text{th,heat}}$. This is when the CHP unit has

reached its rated capacity as discussed in section 3.6.1.4 . An additional unit of cooling is supplied by the electric chiller unit driven by grid imported electricity.

The negative marginal cost of cooling is typically observed during the summer periods when the CHP power output is fixed by the heat/cooling demand. In this situation it is beneficial to consider opportunities to connect additional cooling demands to the energy system (e.g. space cooling). Cold storage units would also provide flexibility to the CHP units' operation.

It is important to note that these investments need to be examined in detail using an investment analysis considering the costs of implementation and the time varying nature of the energy demands.

3.6.3 Conclusions

The optimal power dispatch analysis of the case study shows that operational cost savings are achieved by the strategic use of external grid supplies and energy conversion units of the integrated energy supply system.

The strategy for optimal power dispatch for different electricity and heat demand combinations is summarised using Figure 3-14 and Table 3-4. Note that the cooling demand is a constant $1.2 \text{ MW}_{\text{th,cool}}$ for all electricity and heat combinations. The diagram illustrating the frequency of occurrence (no of hours) of a particular combination of electricity and heat demand is reproduced in Figure 3-14. It is separated into four areas A, B, C and D according to the different strategies for optimal power dispatch at load combination within each segment. Table 3-4 shows the strategy for utilising the energy conversion units and external grid imports in each segment shown in Figure 3-14.

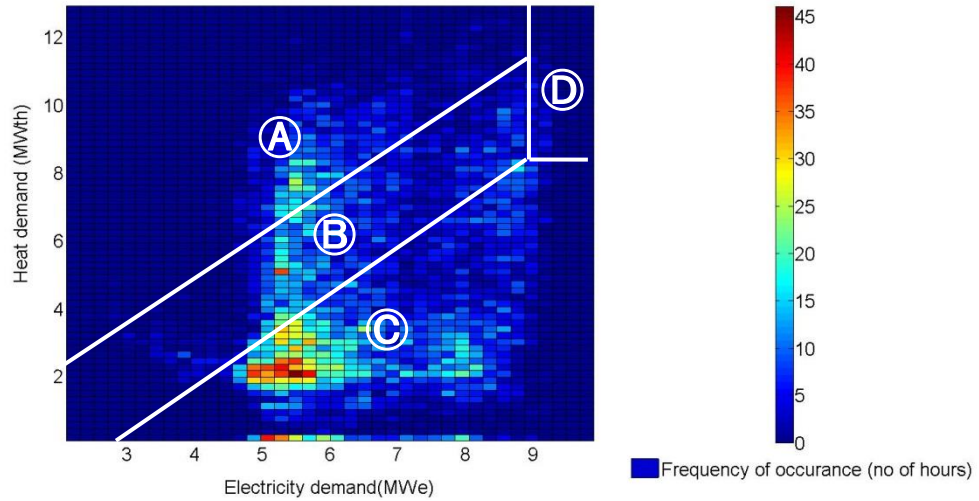


Figure 3-14: Segmented diagram of load frequency

Table 3-4: Strategy for utilising energy conversion units and external grid imports

Segment	Grid electricity imports	CHP	Gas Boiler	Electric Chiller	Absorption chiller
A	X	Electricity driven	Heat balancing	Cooling balancing	X
B	X	Yes	X	Yes	Yes
C	Electricity balancing	Heat driven	X	X	Cooling balancing
D	Electricity balancing	Rated capacity output	Heat balancing	Cooling balancing	X

Table 3-5: Marginal costs and potential improvements to the energy system

Segment	Marginal cost of electricity	Marginal cost of heat	Marginal cost of cooling	Potential improvements
	£/kWh _e	£/kWh _{th.heat}	£/kWh _{th.cool}	
A	0.047	0.033	0.016	Electricity export contract
B	0.067	0.0158	0.023	-
C	0.1	-0.0125	-0.0179	Increase heat/cooling demand, heat/cold storage
D	0.1	0.033	0.033	Peak demand shaving

- **Segment A:** This segment represents typical electricity and heat demand combinations in the winter period. The CHP unit is operated to meet the electricity load of the system. The electrical output of the CHP unit supplies energy to the electric chiller that provides the cooling. The CHP units' power output is limited by the electrical load of the system. The gas boiler is operated to balance the residue of heat demand. Considering the low marginal cost of electricity it would be beneficial to consider an electricity export contract to supply excess electricity to the grid and generate additional income. However, the frequency of occurrence of electricity and heat load combinations in this segment is low and therefore a detailed investment analysis is required.
- **Segment B:** This segment represents typical electricity and heat demand combinations in the autumn/spring period. The CHP unit is operated to meet electricity, heating and cooling demands simultaneously. External electricity imports and the gas boiler are not used for energy supply. The electric chiller and the absorption chiller collectively supply the cooling demand. The share of each is chosen to provide flexibility for the CHP unit operation.
- **Segment C:** This segment represents typical electricity and heat demand combinations in the summer period. The CHP unit is operated to meet the heat load of the system. This includes the absorption chiller load that meets the cooling demand. External electricity imports are required to meet the electricity demand. The electrical output of the CHP unit is limited by the heating load of the system. Considering the negative marginal cost of heat and cooling it is desirable to consider connections to neighbouring heating or cooling networks to increase summer heat demand or using heat or cold storage units to provide flexibility for the CHP unit operation. The frequency of occurrence of electricity and heat load

combinations in this segment is relatively high and the above investments could potentially have significant benefits for the overall system.

- **Segment D:** This segment represents typical electricity and heat demand combinations in a winter period with peak electricity and heat demands. The CHP unit is operated at its rated power output. External electricity imports are required to meet the electricity demand. Gas boilers are used to meet the heating demand. Electric chillers are used to supply the cooling demand.

The optimal power dispatch analysis shows that valuable insights to the design and operation of an energy supply system are realised through an integrated approach to energy systems analysis.

3.7 Chapter summary

A method for mathematical formulation and analysis of optimal power dispatch in an integrated energy supply system was presented. The energy supply system at the University of Warwick was used as a case study. Four load scenarios representing the seasonal demand variations were analysed in detail. Simulations were carried out to analyse the optimal power dispatch for the complete range of electricity and heat demand combinations in the case system.

It was shown that the CHP unit is a key component in the optimal design and operation of the integrated energy supply system. The use of the CHP unit was shown to be cost-effective compared to the use of grid imported electricity and a gas boiler for the supply of heat. The operation of the CHP unit output was fixed by either the on-site electricity or heat demand in different load combinations.

The cooling supply system in the case study, comprising of an electric chiller and an absorption chiller was a source of flexibility for the integrated energy supply system

operation. The electric chiller and the absorption chiller are used to facilitate the maximum utilisation of the CHP unit while meeting the cooling demand.

The marginal costs for the different energy outputs were analysed. The various opportunities to: export electricity back to the grid, connect to neighbouring heat networks, invest in heat and cold storage, or increase summer time cooling demand were discussed and identified as possibly beneficial to reduce the cost of operation. However these investments would require detailed investment analysis considering the time varying nature of energy demands and the costs of implementation and maintenance.

This study demonstrates the value of considering the overall energy system and the interactions between different energy systems in design and operation planning to achieve the most economic system design.

Chapter 4: Simultaneous power flow analysis of coupled multi-energy networks

This chapter presents a method developed for the simultaneous steady state power flow analysis of coupled multi energy networks. Description of the problem and the method of formulating equations for each energy carrier system are shown. A method of solving the set of non-linear equations is also presented. The method of formulating network equations and the solution method is illustrated using an example in Appendix B.1. The results are validated using commercial software.

4.1 Introduction

Steady state simulations are carried out to analyse the state of an energy distribution network assuming the operational parameters do not vary with time. For example, steady state simulations provide information on the voltage profile in electricity networks and the pressure profile in gas networks in a state of equilibrium.

Traditionally, steady state analyses are carried out for each energy distribution system independently. Analyses inform the design and operation planning of each energy system. Established methods and software tools are used for steady state simulations of individual energy networks as shown in Table 4-1.

The increasing interactions between different energy supply systems (Abeysekera and Wu, 2015)(Kroposki et al., 2012a) necessitate the analysis of interdependencies among energy networks. Although methods for analysing each network have been studied individually, only a few recent publications focus on a unified approach for the steady state analysis of integrated multi energy systems.

Table 4-1: Widely used methods and software tools for steady state analysis of energy networks

	Methods used	Software tools
Electricity network	Gauss-Seidel	IPSA ^a
	Newton-Raphson	NEPLAN ^b
	Decoupled	MatPower ^c
Natural gas network	Hardy cross	DNV GL Synergi Gas ^d
	Newton-nodal	SIEMENS-SINCAL ^e
	Newton-loop	
Thermal energy networks	Hardy cross	SIEMENS-SINCAL
	Newton	Bentley sisHyd ^f

Note- The methods and software tools highlighted in the table are independent.

Information on software tools available at the following web links.

a-<http://www.ipso-power.com/>

b-<http://www.neplan.ch/>

c-<http://www.pserc.cornell.edu/matpower/>

d-<https://www.dnvgi.com/services/synergi-gas-modules-3895>

e-www.siemens.com/download?DLA15_1843

f-ftp2.bentley.com/dist/collateral/docs/bentley_sishyd/bentley-sisHYD_product-data-sheet.pdf

The formulation of equations for the combined steady state analysis of electricity and natural gas systems was investigated in (Contreras and Fernández, 2012). The set of non-linear equations representing the natural gas and electricity systems was obtained based on nodal balance of gas and electricity flow and solved simultaneously using Newton's method. The combined analysis of electricity and district heating networks was investigated in (Liu, 2013). Two methods of solving the set of non-linear equations were compared based on their convergence characteristics. A method for steady state analysis of a coupled electricity, natural gas and district heating network system was investigated in (Liu and Mancarella, 2016, Shabanpour-Haghighi and Seifi, 2015). In both studies, the nodal balance of electricity and gas flows, hydraulic and thermal equations in district heating networks were solved iteratively in a single Jacobian matrix using the Newton-Raphson technique. Incorporating the thermal equations increases the dimensions of the Jacobian matrix. This problem is aggravated when considering large district heating networks and district cooling systems.

This chapter presents a unified approach to formulate the steady state power flow analysis of a coupled electricity, natural gas, district heating and district cooling system. Network equations are formulated for each individual energy carrier system considering the interactions with other energy networks. The set of equations are solved simultaneously using the Newton-Raphson method.

4.2 Problem description

Figure 4-1 shows an example system of integrated energy networks used to describe the problem being solved.

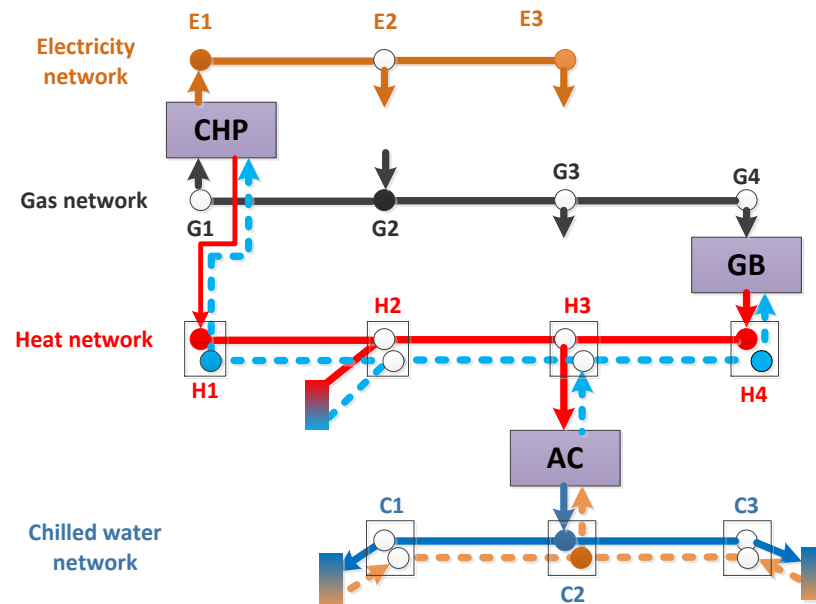


Figure 4-1: Example of an integrated electricity, gas, district heating and district cooling network system

Note- The filled circles represent supply nodes and the non-filled circles represent demand nodes. The dashed lines denote return lines in thermal energy supply networks.

The four different energy supply networks i.e. electricity, gas, district heating and district cooling shown in Figure 4-1 are coupled through,

- A CHP unit which consumes natural gas from gas node G1 and injects electrical power in electricity network node E1 and thermal power in heat node H1.

- b) A Gas boiler unit (GB) which consumes natural gas from gas node G4 and injects heat in node H4.
- c) An absorption chiller unit (AC) which consumes heat from the district heating network at heat node H3 and supplies cooling at cooling node C2.

The coupling introduces interdependencies between the states of different energy networks. For example in the system shown in Figure 4-1, the cooling demand and network characteristics (e.g. pipe length, diameters) of the district cooling system effects the heat demand at node H3. The heat demand and the district heating network characteristics impact the gas demand and the electricity injected in node E1 by the CHP unit which in turn affects the electricity and gas network operational states.

The problem of steady state analysis in an integrated energy network system is to formulate a combined set of equations to compute the steady state parameters in each network considering the energy exchanges introduced through network coupling.

The parameters to compute in the electricity network are the voltage magnitude ($|v|$) and the voltage angle (δ) at all bus bars. The voltages then allow the calculation of active and reactive power flows and losses in the electricity network.

The parameter to compute in the natural gas network is gas pressure (pr) at all gas network nodes. The nodal gas pressures allow the calculation of natural gas flow rates in gas pipes and thereby energy flows in each branch of the gas network.

Parameters to compute in district heating and district cooling networks are the mass flow rate in each branch (\dot{m}) and the temperature of water flow in the supply line (T_{sup}) and return line (T_{ret}) at all nodes. Branch mass flow rates and node temperatures allow the

calculation of thermal power flows, thermal losses, pressure drops and pumping power in thermal networks.

4.3 Formulation of equations for steady state analysis

Graphs are used as an efficient way to model and represent energy networks (Osiadacz, 1987). A graph consists of a set of nodes drawn as points and branches drawn as line segments connecting these points. The branches represent energy distribution circuits (e.g. electricity cables, gas pipes) and nodes represent their connections and the locations of energy supply and demands.

The following definitions and conventions are used in the mathematical formulations.

- Superscript letters are used to indicate energy network type. Electricity network is denoted by letter 'E', gas network by 'G', any thermal network by 'T', district heating by 'H' and district cooling networks by 'C'.
- Subscript letters indicate node, branch and coupling component numbers.
- A single lower case Latin letter/number (e.g. i, j) denotes node numbers.
- One or two letters/numbers written within parenthesis denotes a branch (e.g. (i) or (ij)). One letter/number within parenthesis denotes a branch identification number. Two lower case Latin letters within parenthesis denotes a branch and its designated direction of energy flow i.e. $node\ i \rightarrow node\ j$.
- Letter C with a subscript of a single Latin letter/number denotes coupling component numbers (e.g. C_i).
- The subscript g denotes power supply/generation, d denotes power demand, L denotes distribution line losses
- Bold letters are used to denote complex numbers.

4.3.1 Modelling energy flows in network branches

4.3.1.1 Electricity distribution lines

Short and medium length electricity distribution lines are modelled using the nominal π model as shown in Figure 4-2 (Grainger and Stevenson Jr, 1994).

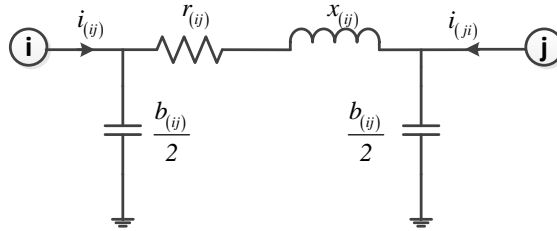


Figure 4-2 : Electricity distribution line model

Electricity distribution lines are represented by its series resistance $r_{(ij)}$, and reactance $x_{(ij)}$, as lumped parameters which gives a series impedance $z_{(ij)}$ and shunt susceptance for line charging $b_{(ij)}$, lumped at each end of the equivalent circuit. For low voltage circuits and short overhead lines the shunt capacitance $b_{(ij)}$ is omitted with little loss of accuracy.

The current injections from either ends of the branch, can be expressed in terms of the branch admittances and the respective terminal voltages v_i and v_j as,

$$\begin{bmatrix} i_{(ij)} \\ i_{(ji)} \end{bmatrix} = \begin{bmatrix} y_{(ij)} & -y_{(ij)} \\ -y_{(ij)} & y_{(ij)} \end{bmatrix} \begin{bmatrix} v_i \\ v_j \end{bmatrix} \quad (4.1)$$

where $y_{(ij)}$ - series admittance of the branch denoted by

$$y_{(ij)} = |y_{(ij)}| \angle \theta_{(ij)} = \frac{1}{z_{(ij)}} = \frac{1}{r_{(ij)} + j x_{(ij)}}$$

where $\theta_{(ij)}$ - the angle of $y_{(ij)}$ in polar form

4.3.1.2 Modelling natural gas flow in pipes

Figure 4-3 shows a gas pipe k starting at node i and ending at node j .

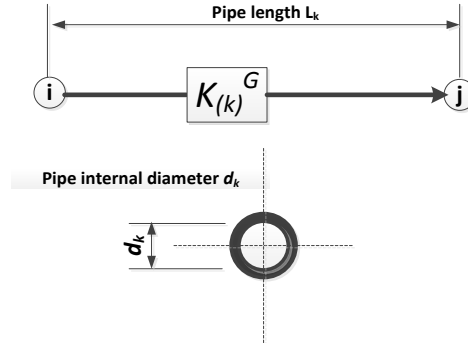


Figure 4-3: Gas pipe model

The relationship between natural gas flow rate and nodal gas pressure is expressed in general form as given in (Osiaacz, 1987) by,

$$\dot{V}_{(k)}^G = S_{(ij)}^G \left(S_{(ij)}^G \frac{(Pr_i^G - Pr_j^G)}{K_{(k)}^G} \right)^{\frac{1}{m^G}} \quad (4.2)$$

where,

- $\dot{V}_{(k)}^G$ - gas volume flow rate in pipe k at standard temperature and pressure conditions [m^3/hr];
- $Pr_i^G - \left\{ \begin{array}{l} pr_i^G [\text{mbar}] \text{ for low pressure networks } (0-100\text{mbar}) \\ (pr_i^G)^2 [\text{bar}^2] \text{ for medium pressure networks } (0.1-7\text{bar}) \end{array} \right\}$

where, pr_i^G - gas pressure at node i ;

- $K_{(k)}^G$ - pipe constant for natural gas flow in pipe k is given

$$\text{by, } \left\{ \begin{array}{l} K_{(k)}^G = 11.7 \times 10^3 \frac{L_{(k)}^G}{d_{(k)}^G{}^5} \text{ for low pressure networks } (0-100\text{mbar}) \\ K_{(k)}^G = 27.24 \frac{L_{(k)}^G}{d_{(k)}^G{}^{4.848}} \text{ for medium pressure networks } (0.1-7\text{bar}) \end{array} \right\};$$

- $L_{(k)}^G$ - pipe length [meters];
- $d_{(k)}^G$ - pipe internal diameter [mili meters];

- m^G -The flow exponent given by $\begin{cases} m^G = 2 & \text{for low pressure networks} \\ m^G = 1.848 & \text{for medium pressure networks} \end{cases}$;
- $S^G_{(ij)}$ -pipe flow direction coefficient given by $\begin{cases} S^G_{(ij)} = 1 & \text{if } Pr^G_i > Pr^G_j \\ S^G_{(ij)} = -1 & \text{if } Pr^G_i < Pr^G_j \end{cases}$

4.3.1.3 Modelling hot/cold water flows in pipes

Figure 4-3 shows a water supply and return line in a thermal energy supply network (TN) branch k , starting at node i and ending at node j .

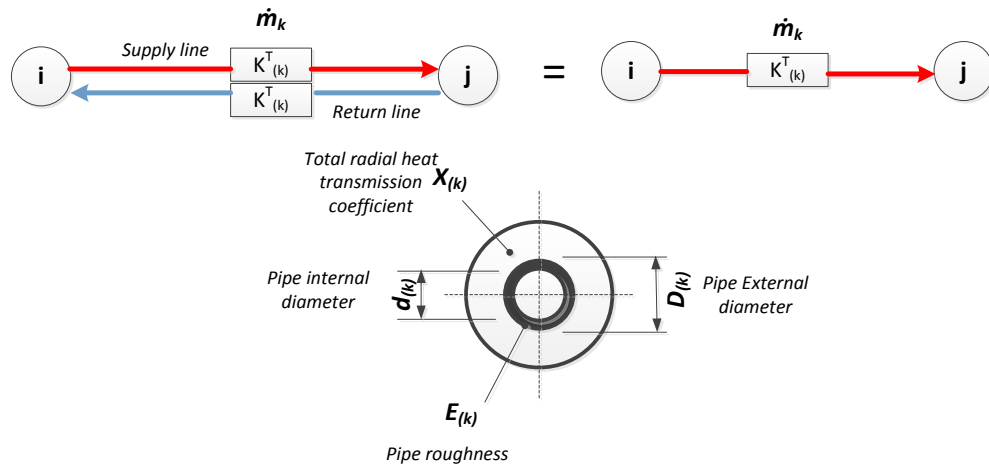


Figure 4-4: Thermal network branch model and single insulated pipe cross section.
Note- $\chi_{(k)}$ is the radial heat transmission coefficient with reference to the pipe external diameter.

It is assumed that the supply and return pipes are separate and insulated, the mass flow rate in the supply and return pipe are identical in quantity and opposite in direction (Frederiksen and Werner, 2013).

The relationship between mass flow rate, $\dot{m}^T_{(k)}$ and pressure drop in a circular pipe k is given by (Frederiksen and Werner, 2013)

$$\dot{m}^T_{(k)} = S^T_{(ij)} \left(S^T_{(ij)} \frac{(pr^T_i - pr^T_j)}{K^T_{(k)}} \right)^{1/2} \quad (4.3)$$

where,

- $S_{(ij)}^T$ - pipe flow direction coefficient given by $\begin{cases} S_{(ij)}^T = 1 & \text{if } pr_i^T > pr_j^T \\ S_{(ij)}^T = -1 & \text{if } pr_i^T < pr_j^T \end{cases}$
- pr_i^T - water pressure at node i [Pa];
- $K_{(k)}^T$ - pipe constant for water flow in pipe k given by $K_{(k)}^T = \left(\frac{8\lambda_{(k)}^T L_{(k)}^T}{(d_{(k)}^T)^5 \pi^2 \rho} \right)$
- $\lambda_{(k)}^T$ – friction factor
- ρ – water density [kg/m³].

The friction factor λ depends on the inner pipe roughness (ε) and the Reynolds number Re , a dimensionless parameter for flow velocity. The Moody diagram¹⁴ is used to approximate the friction factor for a particular pipe roughness and flow Reynolds number.

The radial heat loss/gain for a single insulated pipe k above ground $E_{L,(k)}^T$ is given by¹⁵ (Frederiksen and Werner, 2013),

$$\left(E_{L,(k)}^T \right) = \chi_{(k)}^T \pi D_{(k)}^T L_{(k)}^T \times (T_{avg,(k)}^T - T_{amb}) \quad (4.4)$$

where,

- $\chi_{(k)}^T$ -radial heat transmission coefficient of pipe with reference to the outer pipe surface [W/m².°C];
- $D_{(k)}^T$ - pipe external diameter [meters]
- $T_{avg,(k)}^T$ - average temperature of water in pipe k [°C]
- T_{amb} - ambient temperature [°C]

The radial heat loss/gain translates to a temperature change in the direction of water flow given by (Frederiksen and Werner, 2013)¹⁶,

¹⁴ The Moody diagram is a graph in non-dimensional form that relates the Darcy-Weisbach friction factor λ , Reynolds number Re , and relative roughness for fully developed flow in a circular pipe. It can be used for working out pressure drop or flow rate in a pipe.

¹⁵The heat loss is assumed small compared to the heat transferred through pipe. Otherwise, the temperature drop in the flow direction must be included in the calculation

$$(T_{start,(k)}^T - T_{end,(k)}^T) = - \frac{\pi \chi_{(k)}^T L_{(k)}^T D_{(k)}^T (T_{start,(k)}^T - T_{amb})}{\dot{m}_{(k)}^T c_p} \quad (4.5)$$

where,

- $T_{start,(k)}^T$ - temperature of water flow entering pipe k [$^{\circ}\text{C}$];
- $T_{end,(k)}^T$ - temperature of water flow leaving pipe k [$^{\circ}\text{C}$];
- c_p - specific heat capacity of water assumed as 4200 [J/kg. $^{\circ}\text{C}$].

4.3.2 Modelling of coupling component power flows

The energy exchanges between networks through a coupling component C_k are modelled as simple energy conversions across efficiency factors. The efficiency factors are assumed to be constant.

Figure 4-5 shows an illustration of a coupling component connected between node i in network type α and node j in network type β . Energy flows, $E_{C_k,i}^{\alpha}$ and $E_{C_k,j}^{\beta}$ are denoted as leaving C_k and coefficients $C_{C_k,i}^{\alpha}$ and $C_{C_k,j}^{\beta}$ are used to specify their true

direction. $C_{C_k,i}^{\alpha}$ is derived as

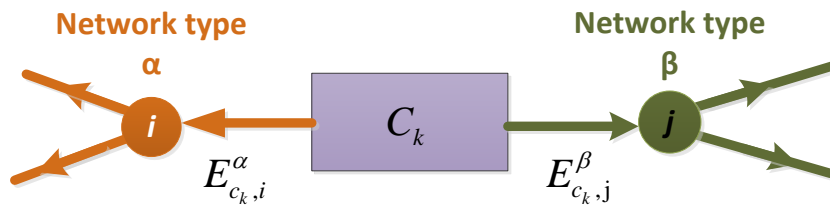
$$\begin{cases} C_{C_k,i}^{\alpha} = +1 & \text{if } C_k \text{ supplies power to node } i \\ C_{C_k,i}^{\alpha} = -1 & \text{if } C_k \text{ consumes power from node } i \\ C_{C_k,i}^{\alpha} = 0 & \text{if } C_k \text{ is not connected to node } i \end{cases}$$


Figure 4-5: Coupling component model

¹⁶ The formula neglects the temperature drop in its derivation as it is small compared to the temperature difference between supply pipe and the ambient temperature.

Assuming the coupling component (C_k) consumes energy carrier type α i.e. $C_{k,i}^\alpha = -I$ and generates β i.e. $C_{k,j}^\beta = +I$, the relationship between the rate of energy consumed and the rate of energy output of a coupling component (C_k) is expressed using an efficiency factor $\eta_{C_k}^{\alpha/\beta}$ as,

$$\eta_{C_k}^{\alpha/\beta} = \left| \frac{E_{C_k,j}^\beta}{E_{C_k,i}^\alpha} \right| \quad (4.6)$$

where,

- $E_{C_k,j}^\beta$ - rate of energy flow from C_k to node j in network type β ;
- $E_{C_k,i}^\alpha$ - rate of energy flow from C_k to node i in network type α ;
- $\eta_{C_k}^{\alpha/\beta}$ -energy conversion efficiency of C_k from network type α to β .

4.3.3 Formulating network equations

4.3.3.1 Formulating electricity network equations

Electrical power flowing in and out of an electricity network node is shown in Figure 4-6.

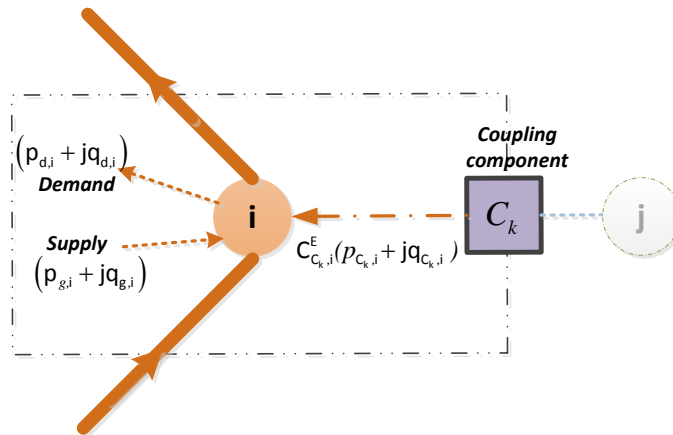


Figure 4-6: Illustration of an electricity network node

The electrical current injected (\mathbf{i}_i) at a node i is calculated using branch admittances and node voltages as (Grainger and Stevenson Jr, 1994),

$$\mathbf{i}_i = \sum_{n=1}^{n_{elec}} \mathbf{Y}_{i,n} \times \mathbf{v}_n \quad (4.7)$$

where,

- \mathbf{v}_n - complex voltage at node n
- $\mathbf{Y}_{i,n}$ - elements of the network admittance matrix (\mathbf{Y}_{bus}) derived as;

$$\begin{cases} \mathbf{Y}_{i,i} = \sum_j \mathbf{y}_{ij} & \text{Sum of all admittance elements connected to node } i \\ \mathbf{Y}_{i,j} = -\mathbf{y}_{ij} & \text{If } i \neq j \text{ and a circuit from node } i \text{ to node } j \text{ exist} \\ \mathbf{Y}_{i,j} = 0 & \text{If a circuit from node } i \text{ to node } j \text{ does not exist} \end{cases}$$

- n_{elec} - number of electricity network nodes

The apparent electrical power (\mathbf{s}_i) injected at a node i is calculated by the multiplication of the node voltage (\mathbf{v}_i), and the conjugate of the net electrical current (\mathbf{i}_i^*) (Grainger and Stevenson Jr, 1994) as,

$$\mathbf{s}_i = \mathbf{v}_i \cdot \mathbf{i}_i^* \quad (4.8)$$

By substituting for \mathbf{i}_i from equation (4.7)

$$\mathbf{s}_i = \mathbf{v}_i \left[\sum_{n=1}^{n_{elec}} \mathbf{Y}_{in} \times \mathbf{v}_n \right]^* \quad (4.9)$$

The apparent electrical power injected at node i is also given by,

$$\mathbf{s}_i = \mathbf{s}_{g,i}^E - \mathbf{s}_{d,i}^E + \mathbf{C}_{C_k,i}^E \left| \mathbf{s}_{C_k,i}^E \right| \quad (4.10)$$

Equating the real and imaginary components of (4.9) and (4.10),

Real power flow component is given by,

$$0 = p_{g,i}^E - p_{d,i}^E + C_{C_k,i}^E |p_{C_k,i}^E| - \text{real} \left[\mathbf{v}_i \sum_{n=1}^{n_{elec}} \mathbf{Y}_{in} \times \mathbf{v}_n \right] \quad (4.11)$$

Reactive power flow component is given by,

$$0 = q_{g,i}^E - q_{d,i}^E + C_{C_k,i}^E |q_{C_k,i}^E| - \text{imag} \left[\mathbf{v}_i \sum_{n=1}^{n_{elec}} \mathbf{Y}_{in} \times \mathbf{v}_n \right] \quad (4.12)$$

where,

- $p_{g,i}^E$ -local real (electrical) power supply at node i ;
- $p_{d,i}^E$ -local real power demand at node i ;
- $p_{C_k,i}^E$ - real power flow from/to node i due to coupling component C_k ;
- $C_{C_k,i}^E$ - coefficient denoting direction of $p_{C_k,i}^E$ derived as

$$\begin{cases} C_{C_k,i}^a = +1 & \text{if } C_k \text{ supplies power to node } i \\ C_{C_k,i}^a = -1 & \text{if } C_k \text{ consumes power from node } i \\ C_{C_k,i}^a = 0 & \text{if } C_k \text{ is not connected to node } i \end{cases}$$
- *real* - the real component of the complex term within brackets;
- $q_{g,i}^E$ -local reactive power supply at node i ;
- $q_{d,i}^E$ -local reactive power demand at node i ;
- $q_{C_k,i}^E$ - reactive power flow from/to node i due to coupling component C_k ;
- *imag* -the imaginary component of the complex term within brackets;

The specified inputs, state parameters to be computed and the equations to be formulated at electricity network nodes are shown in Table 4-2.

Table 4-2: Electricity network node types

Node type	Description	Specified inputs	State variables to compute	Equations formulated
Slack	Typically the connection point to the bulk power supply/large electricity generation plant that is considered the marginal source of supply. It acts as the reference node to calculate voltage variation across the network.	Voltage magnitude (v_i) Voltage angle (δ_i)	-	-
PV	Typically connects to an electricity generation plant with voltage control capability at the node of connection	Real power injections $(p_{g,i}^E, p_{d,i}^E)$ Voltage magnitude (v_i)	Voltage angle (δ_i)	Real power balance Eqn. (4.11)
PQ	Typically a node connected to an electrical load or a generation plant with specified real and reactive power generation.	Real power injections $p_{g,i}^E, p_{d,i}^E$ Reactive power injections $q_{g,i}^E, q_{d,i}^E$	Voltage magnitude (v_i) Voltage angle (δ_i)	Real power balance Eqn.(4.11) & Reactive power balance Eqn. (4.12)

4.3.3.2 Formulating gas network equations

Natural gas flows entering and leaving a gas network node are shown in Figure 4-7.

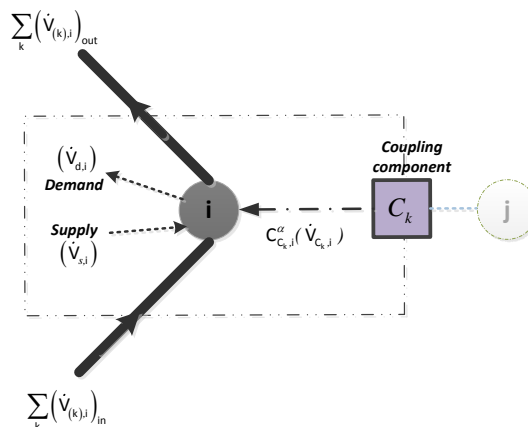


Figure 4-7: Illustration of natural gas network node

Gas volume at standard temperature and pressure conditions (i.e. constant density) is used to formulate the equations for mass conservation of natural gas flows at a node.

The net gas demand at a node i (\dot{V}_i^G) is expressed as,

$$\dot{V}_i^G = \sum_{k=1}^{n_{gas\ pipe}} A_{i,k}^G \times \dot{V}_{(k)}^G \quad (4.13)$$

where,

- $n_{gas\ pipe}$ -number of gas pipes
- $A_{i,k}^G$ - elements of the gas network branch-nodal incidence matrix (A^G) derived as,
$$A_{i,k}^G = \begin{cases} -1 & \text{if } V_k \text{ is leaving node } i \\ +1 & \text{if } V_k \text{ is entering node } i \\ 0 & \text{if branch } k \text{ is not connected to node } i \end{cases} ;$$
- $\dot{V}_{(k)}^G$ - gas flow rate in gas pipe k as given by equation (4.2);

The gas supply/demand at node i due to an energy exchange at a network coupling is calculated as,

$$\dot{V}_{C_k,i}^G = \frac{(E_{C_k,i}^G)}{GCV} \times 3600 \quad (4.14)$$

where,

- $\dot{V}_{C_k,i}^G$ - Natural gas supply/demand at node i due to coupling component C_k
 $[m^3 / hr]$;
- $E_{C_k,i}^G$ - Energy supply/demand rate at node i due to coupling component C_k
 $[kW^G]$
- GCV -Gross Calorific Value of Natural gas $[kJ / m^3]$

The balance of gas flows at a node i in natural gas networks is expressed as,

$$0 = \dot{V}_{s,i}^G - \dot{V}_{d,i}^G + C_{c_k,i}^G \left| \dot{V}_{c_k,i}^G \right| + \dot{V}_i^G \quad (4.15)$$

where,

- $\dot{V}_{s,i}^G$ -Local natural gas supply at node i $[m^3 / hr]$
- $\dot{V}_{d,i}^G$ -Local natural gas demand at node i $[m^3 / hr]$
- $C_{c_k,i}^G$ - coefficient denoting direction of $\dot{V}_{c_k,i}^G$ as describe in equation (4.11) and (4.12)

By substituting from equation (4.14) and (4.13),

$$0 = \dot{V}_{s,i}^G - \dot{V}_{d,i}^G + C_{c_k,i}^G \left| \frac{(E_{C_k,i}^G)}{GCV} \times 3600 \right| + \sum_{k=1}^{n_{gas\ pipe}} A_{i,k}^G \times \dot{V}_k \quad (4.16)$$

By substituting for \dot{V}_k from equation (4.2),

$$0 = \dot{V}_{s,i}^G - \dot{V}_{d,i}^G + C_{c_k,i}^G \left| \frac{(E_{C_k,i}^G)}{GCV} \times 3600 \right| + \sum_{k=1}^{n_{gas\ pipe}} A_{i,k}^G \times S_{(ij)}^G \left(S_{(ij)}^G \frac{(Pr_i^G - Pr_j^G)}{K_{(k)}^G} \right)^{\frac{1}{m}} \quad (4.17)$$

For steady state analyses the nodes in a gas network are characterised as gas infeed nodes and gas load nodes. The node types, the specified inputs, the steady state variables to be computed and the equations formulated at gas network nodes are shown in Table 4-3.

Table 4-3: Node types in gas networks

Node type	Description	Specified inputs	State variables to compute	Equations formulated
Gas Infeed node	The connection points to the gas in-feeders	Gas pressure Reference (pr_i^G)	-	-
Gas load node	Gas load node where local supply and demands are specified	Gas supply and demands $\dot{V}_{s,i}^G, \dot{V}_{d,i}^G$	Gas pressure (pr_i^G)	Gas volume flow balance Eqn. (4.16)

4.3.3.3 Formulating thermal network equations

In thermal network analysis (TN) the mass flow and energy balance at nodes and loop pressure drops (explained below) are considered for formulating network equations. Only the supply line network is considered in formulating the pipe flow hydraulic equations. Both the supply and return line networks are considered in formulating the equations for computing nodal temperatures.

Water flows entering and leaving a thermal network node is shown in Figure 4-8. It should be noted that in reality a node connects to either a single supply unit, a demand substation or network branches only. Figure 4-8 shows the general representation used for formulating equations for network analysis. Upper case \dot{M} refers to mass flows to/from local connections of the node. Lower case \dot{m} refers to mass flows in network branches.

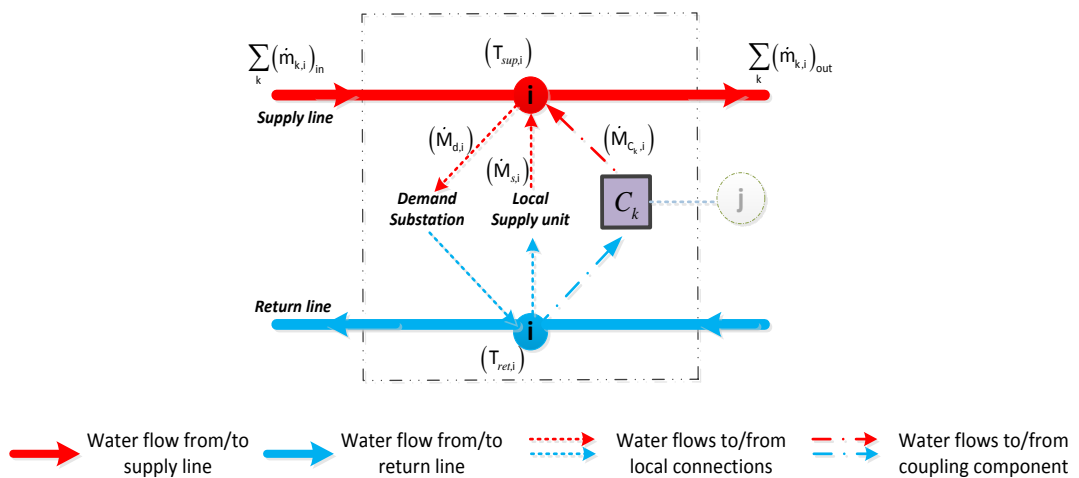


Figure 4-8: Illustration of a thermal network node

The mass flow supplied by a local thermal energy supply source connected at a node i is computed using the heat transfer equation as,

$$\dot{M}_{s,i}^T = \frac{\dot{Q}_{s,i}^T}{c_p \times (T_{s,i}^T - T_{ret,i}^T)} \quad (4.18)$$

where,

- $\dot{M}_{s,i}^T$ - Mass flow rate supplied by local supply unit [kg/s]
- $\dot{Q}_{s,i}^T$ - Thermal energy supply by local supply source at node i [kW_{th}]
- $T_{s,i}^T$ - Temperature of water supply by local supply source at node i [°C]. This is always specified for steady state analysis.
- $T_{ret,i}^T$ - Temperature of water at node i in the return network [°C]

The mass flow demanded by a local thermal load connected at node i is expressed as,

$$\dot{M}_{d,i}^T = \frac{\dot{Q}_{d,i}^T}{c_p \times (T_{sup,i}^T - T_{out,i}^T)} \quad (4.19)$$

where,

- $\dot{M}_{d,i}^T$ - Mass flow rate demanded by local substation unit [kg/s]
- $\dot{Q}_{d,i}^T$ - Thermal energy demand of local substation unit connected to node i [kW_{th}]
- $T_{sup,i}^T$ - Temperature of water at node i in the supply network [°C]
- $T_{out,i}^T$ - The temperature of water leaving the local demand substation unit [°C]. This is always specified for steady state analysis.

A network coupling connected to a thermal network node is categorised as a supply or demand unit (e.g. Gas boiler connected to a district heating network is a supply unit whereas an absorption chiller is a demand unit). At a supply unit the supply node temperature is specified and at a demand unit the temperature of water leaving the unit is

specified. The mass flow rate supplied or demanded by a network coupling $(\dot{M}_{C_k,i}^T)$ is calculated using equation (4.18) or equation (4.19).

The algebraic sum of mass flow from network branch connections at a node i (\dot{m}_i^T) is expressed as,

$$\dot{m}_i^T = \sum_{k=1}^{n_{pipe}^T} A_{i,k}^T \dot{m}_{(k)}^T \quad (4.20)$$

where,

- n_{pipe}^T - number of pipes;
- $A_{i,k}^T$ - elements of the thermal network branch-nodal incidence matrix (A^T)

$$\text{derived as, } A_{i,k}^T = \begin{cases} -1 & \text{if } \dot{m}_k \text{ is leaving node } i \\ +1 & \text{if } \dot{m}_k \text{ is entering node } i \\ 0 & \text{if branch } k \text{ is not connected to node } i \end{cases} ;$$

- $\dot{m}_{(k)}$ - mass flow rate in water pipe k as given by equation (4.3);

The mass flow balance of water at node i in a thermal network is given by,

$$0 = \dot{M}_{s,i}^T - \dot{M}_{d,i}^T + \left[C_{C_k,i}^T \left| \dot{M}_{C_k,i}^T \right. \right] + \sum_{k=1}^{n_{pipe}^T} A_{i,k}^T \dot{m}_{(k)}^T \quad (4.21)$$

where,

- $C_{C_k,i}^T$ - coefficient denoting direction of $\dot{M}_{C_k,i}^\beta$ as described in Equation (4.12)

Additional equations are required for the pipe flow hydraulic calculation in the case of meshed networks. Kirchoff's second law for meshed pipe network analysis states (Osiadacz, 1987) that the algebraic sum of pressure drops around any closed loop in the network is zero. Figure 4-9 shows independent network loops in a simple meshed network.

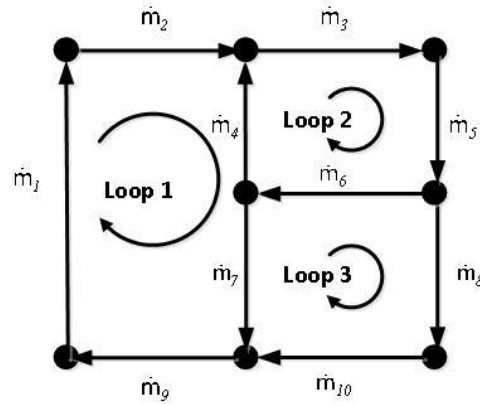


Figure 4-9: A simple meshed network illustrating independent loops

For any loop i in the thermal network, the loop equation can be written in general form as,

$$0 = \sum_{k=1}^{n_{pipe}^T} B_{i,k}^T (\Delta p r_{(k)}) \quad (4.22)$$

where,

- n_{pipe}^T - number of pipes in the thermal network;
- k - pipe number;
- $\Delta p r_{(k)}$ - pressure drop of water flow in pipe k given by equation (4.3);
- $B_{i,k}^T$ - elements of the thermal network branch-loop incidence matrix (B^T)

$$\text{expressed as, } B_{ik}^T = \begin{cases} +1; & \text{if } \dot{m}_{(k)} \text{ is the same direction as loop } i \\ -1; & \text{if } \dot{m}_{(k)} \text{ is flowing in the opposite direction as loop } i \\ 0; & \text{if branch } k \text{ is not connected to loop } i \end{cases} ;$$

Substituting for $\Delta p r_{(k)}$ from equation (4.3),

$$0 = \sum_{k=1}^{n_{pipe}^T} B_{ik}^T \left(K_{(k)} \dot{m}_{(k)} \left| \dot{m}_{(k)} \right| \right)^T \quad (4.23)$$

The water temperatures across the network is based on the supply temperatures at source units, temperature of water leaving thermal loads, heat gains/losses in each pipe and the mixing of water at nodes. Equation (4.5) is used to calculate temperature change in each pipe. In case of mixing of two or more water streams at nodes, the temperature of water

leaving node i (T_i) is calculated by considering the energy balance of water flows entering node i expressed as,

$$\left(\sum_k \dot{m}_{(k)} \right) T_i = \left(\sum_k \dot{m}_{(k)} T_{i,(k)} \right) \quad k \text{ -pipes with flow entering node } i \quad (4.24)$$

where,

- \dot{m}_k - mass flow rate in branch k where flow enters node i
- $T_{i,(k)}$ -temperature of water leaving pipe k and enters node i .

Therefore, temperature at a node i in the supply network ($T_{sup,i}$) is computed as¹⁷,

$$T_{sup,i} = \begin{cases} T_{s,i} & \text{if a local supply unit connected at node } i \\ \frac{\left(\sum_k \dot{m}_{(k)} (T_{i,(k)}) \right)}{\sum_k \dot{m}_{(k)}} & (k \in \text{flows entering node } i); \text{if no supply units at node } i \\ T_{s,C_k} & \text{if } C_k \text{ is a supply unit} \end{cases} \quad (4.25)$$

where,

- $T_{s,i}$ - Temperature of water supply by local supply source at node i [°C].
- T_{s,C_k} - Temperature of water supply by coupling component C_k (when C_k is a thermal energy supply source).

¹⁷ It is assumed that only one supply source i.e. either a local supply connection or a coupling component connects to a single node

The temperature at a node i in the return network ($T_{ret,i}$) is calculated as,

$$T_{ret,i} = \frac{\left(\sum_k \dot{m}_{(k)} T_{i,(k)} \right) + \dot{M}_{d,i} T_{out,i} + \dot{M}_{C_k,i} T_{out,C_k}}{\left(\sum_k \dot{m}_{(k)} \right) + \dot{M}_{d,i} + \dot{M}_{C_k,i}} \quad (4.26)$$

where,

- $\dot{M}_{d,i}$ - Mass flow rate demanded by local thermal load [kg/s]
- $T_{out,i}$ - The temperature of water leaving the local thermal demand unit [°C]
- $\dot{M}_{C_k,i}$ - Mass flow rate demanded by C_k (if C_k is a thermal load) [kg/s]
- T_{out,C_k} - Temperature of water leaving C_k [°C]

Equations (4.25) and (4.26) combined with equation (4.5) for temperature drop/gain in a thermal network pipe allows computing the temperature of water at all nodes in the supply and return network.

The nodes in a thermal energy distribution network are characterised according to the specified inputs and the state parameters to be computed at each node. The different node types, the specified inputs and the steady state variables to be computed are shown in Table 4-4. The steady state analysis computes the parameters detailed in Table 4-4 and the mass flow rate in each branch of the thermal network.

Table 4-4: Node types in thermal networks

Node type	Description	Specified inputs	State variables to compute	Equations formulated
Slack_T	A thermal energy supply plant that balances the energy demand and losses in the network	Supply line temperature $T_{s,i}$	Return line temperature $T_{ret,i}$	-
Supply_T	Thermal energy supply plant with a pre-specified thermal power supply and supply temperature.	Thermal power injected $\dot{Q}_{s,i}^T$ and Supply line temperature $T_{s,i}$	Return line temperature $T_{ret,i}$	Mass flow rate calculation Eqn.(4.18) Mass flow balance Eqn. (4.22) Temperature calculation Eqn(4.25),(4.26)
Demand_T	TN node which is either a connection to a demand substation or a connection between multiple branches.	Thermal demand $\dot{Q}_{d,i}^T$	Supply line temperature $T_{sup,i}$, Return line temperature $T_{ret,i}$	Mass flow rate calculation Eqn.(4.19) Mass flow balance Eqn. (4.22) Temperature calculation Eqn.(4.25),(4.26)

4.3.4 Combined set of equations for simultaneous network analysis

The set of non-linear equations to be solved for steady state analysis of coupled electricity, natural gas and thermal energy supply network systems is summarised as,

1. Equating real (electrical) power flow injections at all *PV* and *PQ* nodes in the electricity network (Eqn. (4.11)),

$$F_{I,i} = 0 = p_{g,i}^E - p_{d,i}^E + C_{C_k,i}^E |p_{C_k,i}^E| - real \left[\mathbf{v}_i \sum_{n=1}^{n_{dec}} \mathbf{Y}_{in} \times \mathbf{v}_n \right]$$

2. Equating reactive (electrical) power flow injections at all PQ nodes in the electricity network (Eqn. (4.12)),

$$F_{2,i} = 0 = q_{g,i}^E - q_{d,i}^E + C_{C_k,i}^E |q_{C_k,i}^E| - \text{imag} \left[\mathbf{v}_i \sum_{n=1}^{n_{elec}} \mathbf{Y}_{in} \times \mathbf{v}_n \right]$$

3. Gas volume flow balance at all *gas load* nodes in the gas network (Eqn. (4.17)),,

$$F_{3,i} = 0 = \dot{V}_{s,i}^G - \dot{V}_{d,i}^G + C_{C_k,i}^G \left| \frac{(E_{C_k,i}^G)}{GCV} \times 3600 \right| + \sum_{k=1}^{n_{gas_pipe}} A_{i,k}^G \times S_{ij} \left(S_{ij} \frac{(Pr_i - Pr_j)}{K_{(k)}^G} \right)^{\frac{1}{m}}$$

4. Thermal network mass flow balance at all *Supply_T* and *Demand_T* nodes (Eqn. (4.21)),

$$F_{4,i} = 0 = \dot{M}_{s,i}^T - \dot{M}_{d,i}^T + \left[C_{C_k,i}^T | \dot{M}_{C_k,i}^T | \right] + \sum_{k=1}^{n_{th_pipe}} A_{i,k}^T \dot{m}_{(k)}^T$$

where,

- $\dot{M}_{s,i}^T = \frac{\dot{Q}_{s,i}^T}{c_p \times (T_{s,i}^T - T_{ret,i}^T)}$

- $\dot{M}_{d,i}^T = \frac{\dot{Q}_{d,i}^T}{c_p \times (T_{sup,i}^T - T_{out,i}^T)}$

- $T_{sup,i} = \begin{cases} T_{s,i} & \text{if a local supply unit connected at node } i \\ \frac{\left(\sum_k \dot{m}_{(k)} (T_{i,(k)}) \right)}{\sum_k \dot{m}_{(k)}} & (k \in \text{flows entering node } i); \text{ if no supply units at node } i \\ T_{s,C_k} & \text{if } C_k \text{ is a supply unit} \end{cases}$

- $T_{ret,i} = \frac{\left(\sum_k \dot{m}_{(k)} T_{i,(k)} \right) + \dot{M}_{d,i} T_{out,i} + \dot{M}_{C_k,i} T_{out,C_k}}{\left(\sum_k \dot{m}_{(k)} \right) + \dot{M}_{d,i} + \dot{M}_{C_k,i}}$

5. At all independent loops in the thermal networks (Eqn. (4.23)),

$$F_{5,i} = 0 = \sum_{k=1}^{n_{th_pipe}} B_{ik}^T \left(K_{(k)} \dot{m}_{(k)} \mid \dot{m}_{(k)} \right)^T$$

For simulations the coupling components have either,

- a) Specified energy injection of the coupling unit ($E_{C_k,i}^\alpha$ or $E_{C_k,j}^\beta$). The corresponding energy injected in the coupled network is calculated using the efficiency of energy conversion.
- b) The coupling unit is connected at the slack node of an electricity or thermal energy network. The energy flow at the coupling unit ($E_{C_k,i}^\alpha$ and $E_{C_k,j}^\beta$) is a function of the state variables in the network being balanced and the efficiency of energy conversion.

The energy flow across a coupling component is calculated by,

$$E_{C_k,j}^\beta = \eta_{C_k}^{\alpha/\beta} E_{C_k,i}^\alpha$$

If connected to the slack node, the energy injection at the slack node is given by,

$$\left(E_{C_k,slack}^\alpha \right) = \left\{ \begin{array}{l} \text{real} \left\{ V_{slack} \left(\sum_{n=1}^{n_{max}} Y_{slack,n} V_n \right)^* \right\} \text{ if } \alpha \text{ is an electricity network} \\ \left[\sum_{j=1}^{n_{th_pipe}} a_{ij} \dot{m}_j \right]_{th} C_p \times (T_{s,slack} - T_{r,slack})_{th} \text{ if } \alpha \text{ is a thermal energy network} \end{array} \right\}$$

4.4 Solution method

The set of non-linear algebraic equations are solved to compute the set of steady state parameters in each network for a given network configuration and energy demands. The Newton-Raphson method is used to solve the set of non-linear algebraic equations.

4.4.1 Newton-Raphson method

The Newton-Raphson method for solving a non-linear algebraic equation is based on the Taylor series expansion of a function $f(x)$ about an operating point x_0 given by,

$$f(x) = f(x_0) + \left. \frac{\partial f}{\partial x} \right|_{x=x_0} (x - x_0) + \left. \frac{\partial^2 f}{\partial x^2} \right|_{x=x_0} (x - x_0)^2 + \dots \quad (4.27)$$

The higher order terms of $(x - x_0)$ in the equation are ignored by assuming the value of $(x - x_0)$ is small enough. Then solving the function $f(x) = 0$ reduces to finding a value for x , that satisfies the following,

$$0 = f(x_0) + \left[\left. \frac{\partial f}{\partial x} \right|_{x=x_0} \right] (x - x_0)$$

$$x = x_0 - \left[\left. \frac{\partial f}{\partial x} \right|_{x=x_0} \right]^{-1} f(x_0) \quad (4.28)$$

The Newton-Raphson method is an iterative method to find the best approximation for x by calculating a correction in each iteration. The new value for x to be used in the subsequent iteration is calculated using the following,

$$x^{i+1} = x^i - \left[\left. \frac{\partial f}{\partial x} \right|_{x=x^i} \right]^{-1} f(x^i) \quad (4.29)$$

where,

- i -iteration counter

The iterations are repeated until the value of the function $f(x^i)$ is less than a specified tolerance.

The Newton-Raphson method can be applied for solving a set of equations expressed as,

$$F(x) = \begin{cases} F_1(x_1, x_2, \dots, x_n) = 0 \\ F_2(x_1, x_2, \dots, x_n) = 0 \\ \vdots \\ F_n(x_1, x_2, \dots, x_n) = 0 \end{cases} \quad (4.30)$$

The correction to the vector of variables x in each iteration is calculated as,

$$\begin{bmatrix} x_1^{i+1} \\ x_2^{i+1} \\ \vdots \\ x_n^{i+1} \end{bmatrix} = \begin{bmatrix} x_1^i \\ x_2^i \\ \vdots \\ x_n^i \end{bmatrix} - [J^i]^{-1} \begin{bmatrix} F_1(x^i) \\ F_2(x^i) \\ \vdots \\ F_n(x^i) \end{bmatrix} \quad (4.31)$$

where the Jacobian matrix J is given by,

$$J = \begin{bmatrix} \frac{\partial F_1}{\partial x_1} & \frac{\partial F_1}{\partial x_2} & \dots & \frac{\partial F_1}{\partial x_n} \\ \frac{\partial F_2}{\partial x_1} & \frac{\partial F_2}{\partial x_2} & \dots & \frac{\partial F_2}{\partial x_n} \\ \vdots & \vdots & \ddots & \vdots \\ \frac{\partial F_n}{\partial x_1} & \frac{\partial F_n}{\partial x_2} & \dots & \frac{\partial F_n}{\partial x_n} \end{bmatrix} \quad (4.32)$$

4.4.2 Solution method for combined analysis of integrated networks

The steps of the iterative method to solve the equations in section 0 are as follows.

- Step 1: The first iteration uses a first estimate of the state parameters to calculate imbalances in network equations shown in section 4.3.4. The method for estimating initial values for state parameters is shown in the example calculation in Appendix B.1.

$$X^o = \begin{bmatrix} \delta^o \\ |V^o| \\ Pr^o \\ \dot{m}^o \end{bmatrix} \begin{array}{l} \text{Voltage angle vector} \\ \text{Voltage magnitude vector} \\ \text{Gas nodal pressure vector} \\ \text{Thermal networks branch mass flow rate vector} \end{array}$$

- Step 2: Calculate an initial estimate for the local mass flow rates $(\dot{M}_{s,i}^T, \dot{M}_{d,i}^T, \dot{M}_{C_k,i}^T)$ at all thermal network nodes using an estimate for the temperature difference between supply and return line at nodes

$$\begin{cases} \text{For district heating networks assume } \left| (T_{sup,i}^o - T_{ret,i}^o) \right|^H = 50^\circ C \\ \text{For district cooling networks assume } \left| (T_{sup,i}^o - T_{ret,i}^o) \right|^C = 10^\circ C \end{cases}$$

- Step 3: Calculate the imbalances of the electricity, natural gas and thermal network hydraulic equations for the initial estimate of steady state variables.

$$F(X^o) = \begin{bmatrix} F_1(X^o) \\ F_2(X^o) \\ F_3(X^o) \\ F_4(X^o) \\ F_5(X^o) \end{bmatrix} \begin{array}{l} \text{Real power imbalances} \\ \text{Reactive power imbalances} \\ \text{Gas flow imbalances} \\ \text{Thermal network/s flow imbalances} \\ \text{Thermal network/s loop pressure imbalances} \end{array}$$

- Step 4: Calculate elements of the Jacobian matrix given by,

$$J^o = \begin{bmatrix} \frac{\partial F_1}{\partial \delta} & \frac{\partial F_1}{\partial |V|} & \frac{\partial F_1}{\partial Pr} & \frac{\partial F_1}{\partial \dot{m}} \\ \frac{\partial F_2}{\partial \delta} & \frac{\partial F_2}{\partial |V|} & \frac{\partial F_2}{\partial Pr} & \frac{\partial F_2}{\partial \dot{m}} \\ \frac{\partial F_3}{\partial \delta} & \frac{\partial F_3}{\partial |V|} & \frac{\partial F_3}{\partial Pr} & \frac{\partial F_3}{\partial \dot{m}} \\ \frac{\partial F_4}{\partial \delta} & \frac{\partial F_4}{\partial |V|} & \frac{\partial F_4}{\partial Pr} & \frac{\partial F_4}{\partial \dot{m}} \\ \frac{\partial F_5}{\partial \delta} & \frac{\partial F_5}{\partial |V|} & \frac{\partial F_5}{\partial Pr} & \frac{\partial F_5}{\partial \dot{m}} \end{bmatrix}_{X=X^o}$$

$$J^0 = \begin{bmatrix} \frac{\partial F_{1,1}}{\partial \delta_1} & \dots & \frac{\partial F_{1,1}}{\partial \delta_{n_{elec}}} & \frac{\partial F_{1,1}}{\partial |\mathbf{V}_1|} & \dots & \frac{\partial F_{1,1}}{\partial |\mathbf{V}_{n_{elec}}|} & \frac{\partial F_{1,1}}{\partial Pr_1} & \dots & \frac{\partial F_{1,1}}{\partial Pr_{n_{gas}}} & \frac{\partial F_{1,1}}{\partial \dot{m}_1^T} & \dots & \frac{\partial F_{1,1}}{\partial \dot{m}_{n_{th}}^T} \\ \vdots & \ddots & \vdots & \vdots & \ddots & \vdots & \vdots & \ddots & \vdots & \vdots & \ddots & \vdots \\ \frac{\partial F_{1,n_{elec}}}{\partial \delta_1} & \dots & \frac{\partial F_{1,n_{elec}}}{\partial \delta_{n_{elec}}} & \frac{\partial F_{1,n_{elec}}}{\partial |\mathbf{V}_1|} & \dots & \frac{\partial F_{1,n_{elec}}}{\partial |\mathbf{V}_{n_{elec}}|} & \frac{\partial F_{1,n_{elec}}}{\partial Pr_1} & \dots & \frac{\partial F_{1,n_{elec}}}{\partial Pr_{n_{gas}}} & \frac{\partial F_{1,n_{elec}}}{\partial \dot{m}_1^T} & \dots & \frac{\partial F_{1,n_{elec}}}{\partial \dot{m}_{n_{th}}^T} \\ \hline \frac{\partial F_{2,1}}{\partial \delta_1} & \dots & \frac{\partial F_{2,1}}{\partial \delta_{n_{elec}}} & \frac{\partial F_{2,1}}{\partial |\mathbf{V}_1|} & \dots & \frac{\partial F_{2,1}}{\partial |\mathbf{V}_{n_{elec}}|} & \frac{\partial F_{2,1}}{\partial Pr_1} & \dots & \frac{\partial F_{2,1}}{\partial Pr_{n_{gas}}} & \frac{\partial F_{2,1}}{\partial \dot{m}_1^T} & \dots & \frac{\partial F_{2,1}}{\partial \dot{m}_{n_{th}}^T} \\ \vdots & \ddots & \vdots & \vdots & \ddots & \vdots & \vdots & \ddots & \vdots & \vdots & \ddots & \vdots \\ \frac{\partial F_{2,n_{elec}}}{\partial \delta_1} & \dots & \frac{\partial F_{2,n_{elec}}}{\partial \delta_{n_{elec}}} & \frac{\partial F_{2,n_{elec}}}{\partial |\mathbf{V}_1|} & \dots & \frac{\partial F_{2,n_{elec}}}{\partial |\mathbf{V}_{n_{elec}}|} & \frac{\partial F_{2,n_{elec}}}{\partial Pr_1} & \dots & \frac{\partial F_{2,n_{elec}}}{\partial Pr_{n_{gas}}} & \frac{\partial F_{2,n_{elec}}}{\partial \dot{m}_1^T} & \dots & \frac{\partial F_{2,n_{elec}}}{\partial \dot{m}_{n_{th}}^T} \\ \hline \frac{\partial F_{3,1}}{\partial \delta_1} & \dots & \frac{\partial F_{3,1}}{\partial \delta_{n_{elec}}} & \frac{\partial F_{3,1}}{\partial |\mathbf{V}_1|} & \dots & \frac{\partial F_{3,1}}{\partial |\mathbf{V}_{n_{elec}}|} & \frac{\partial F_{3,1}}{\partial Pr_1} & \dots & \frac{\partial F_{3,1}}{\partial Pr_{n_{gas}}} & \frac{\partial F_{3,1}}{\partial \dot{m}_1^T} & \dots & \frac{\partial F_{3,1}}{\partial \dot{m}_{n_{th}}^T} \\ \vdots & \ddots & \vdots & \vdots & \ddots & \vdots & \vdots & \ddots & \vdots & \vdots & \ddots & \vdots \\ \frac{\partial F_{3,n_{gas}}}{\partial \delta_1} & \dots & \frac{\partial F_{3,n_{gas}}}{\partial \delta_{n_{elec}}} & \frac{\partial F_{3,n_{gas}}}{\partial |\mathbf{V}_1|} & \dots & \frac{\partial F_{3,n_{gas}}}{\partial |\mathbf{V}_{n_{elec}}|} & \frac{\partial F_{3,n_{gas}}}{\partial Pr_1} & \dots & \frac{\partial F_{3,n_{gas}}}{\partial Pr_{n_{gas}}} & \frac{\partial F_{3,n_{gas}}}{\partial \dot{m}_1^T} & \dots & \frac{\partial F_{3,n_{gas}}}{\partial \dot{m}_{n_{th}}^T} \\ \hline \frac{\partial F_{4,1}}{\partial \delta_1} & \dots & \frac{\partial F_{4,1}}{\partial \delta_{n_{elec}}} & \frac{\partial F_{4,1}}{\partial |\mathbf{V}_1|} & \dots & \frac{\partial F_{4,1}}{\partial |\mathbf{V}_{n_{elec}}|} & \frac{\partial F_{4,1}}{\partial Pr_1} & \dots & \frac{\partial F_{4,1}}{\partial Pr_{n_{gas}}} & \frac{\partial F_{4,1}}{\partial \dot{m}_1^T} & \dots & \frac{\partial F_{4,1}}{\partial \dot{m}_{n_{th}}^T} \\ \vdots & \ddots & \vdots & \vdots & \ddots & \vdots & \vdots & \ddots & \vdots & \vdots & \ddots & \vdots \\ \frac{\partial F_{4,n_{th}}}{\partial \delta_1} & \dots & \frac{\partial F_{4,n_{th}}}{\partial \delta_{n_{elec}}} & \frac{\partial F_{4,n_{th}}}{\partial |\mathbf{V}_1|} & \dots & \frac{\partial F_{4,n_{th}}}{\partial |\mathbf{V}_{n_{elec}}|} & \frac{\partial F_{4,n_{th}}}{\partial Pr_1} & \dots & \frac{\partial F_{4,n_{th}}}{\partial Pr_{n_{gas}}} & \frac{\partial F_{4,n_{th}}}{\partial \dot{m}_1^T} & \dots & \frac{\partial F_{4,n_{th}}}{\partial \dot{m}_{n_{th}}^T} \\ \hline \frac{\partial F_{5,1}}{\partial \delta_1} & \dots & \frac{\partial F_{5,1}}{\partial \delta_{n_{elec}}} & \frac{\partial F_{5,1}}{\partial |\mathbf{V}_1|} & \dots & \frac{\partial F_{5,1}}{\partial |\mathbf{V}_{n_{elec}}|} & \frac{\partial F_{5,1}}{\partial Pr_1} & \dots & \frac{\partial F_{5,1}}{\partial Pr_{n_{gas}}} & \frac{\partial F_{5,1}}{\partial \dot{m}_1^T} & \dots & \frac{\partial F_{5,1}}{\partial \dot{m}_{n_{th}}^T} \\ \vdots & \ddots & \vdots & \vdots & \ddots & \vdots & \vdots & \ddots & \vdots & \vdots & \ddots & \vdots \\ \frac{\partial F_{5,n_{th,loop}}}{\partial \delta_1} & \dots & \frac{\partial F_{5,n_{th,loop}}}{\partial \delta_{n_{elec}}} & \frac{\partial F_{5,n_{th,loop}}}{\partial |\mathbf{V}_1|} & \dots & \frac{\partial F_{5,n_{th,loop}}}{\partial |\mathbf{V}_{n_{elec}}|} & \frac{\partial F_{5,n_{th,loop}}}{\partial Pr_1} & \dots & \frac{\partial F_{5,n_{th,loop}}}{\partial Pr_{n_{gas}}} & \frac{\partial F_{5,n_{th,loop}}}{\partial \dot{m}_1^T} & \dots & \frac{\partial F_{5,n_{th,loop}}}{\partial \dot{m}_{n_{th}}^T} \end{bmatrix}_{X=X^0}$$

where,

$$\circ \frac{\partial F_{1,i}}{\partial \delta_n} = \begin{cases} -(|\mathbf{v}_i \mathbf{Y}_{in} \mathbf{v}_n| \sin(\delta_i - \theta_{in} - \delta_n)) & \text{for } i \neq n \\ \left[\sum_{n=1}^{n_{elec}} |\mathbf{v}_i \mathbf{Y}_{in} \mathbf{v}_n| \sin(\delta_i - \theta_{in} - \delta_n) \right] & \text{for } i = n \end{cases}$$

$$\circ \frac{\partial F_{1,i}}{\partial |\mathbf{v}_n|} = \begin{cases} -(|\mathbf{v}_i \mathbf{Y}_{in}| \cos(\delta_i - \theta_{in} - \delta_n)) & \text{for } i \neq n \\ \left[\sum_{n=1}^{n_{elec}} |\mathbf{Y}_{in} \mathbf{v}_n| \cos(\delta_i - \theta_{in} - \delta_n) \right] & \text{for } i = n \end{cases}$$

$$\circ \frac{\partial F_1}{\partial Pr} = \text{zeros}; \text{ as real power imbalances do not depend on gas network variables.}$$

- $$\frac{\partial F_{1,i}}{\partial \dot{m}_{(n)}^T} = \frac{C_{C_k,i}^E}{baseMVA \times \eta_{C_k}^{T/E}} \left| A_{i,n}^T C_p \times (T_{sup,i}^T - T_{ret,i}^T) \right|$$
- for i = thermal network slack node*
- $$\frac{\partial F_{2,i}}{\partial \delta_n} = \begin{cases} (|\mathbf{v}_i \mathbf{Y}_{in} \mathbf{v}_n| \cos(\delta_i - \theta_{in} - \delta_n)) & \text{for } i \neq n \\ - \left[\sum_{n=1}^{n_{elec}} |\mathbf{v}_i \mathbf{Y}_{in} \mathbf{v}_n| \cos(\delta_i - \theta_{in} - \delta_n) \right] & \text{for } i = n \end{cases}$$
- $$\frac{\partial F_{2,i}}{\partial |\mathbf{v}_n|} = \begin{cases} - (|\mathbf{v}_i \mathbf{Y}_{in}| \sin(\delta_i - \theta_{in} - \delta_n)) & \text{for } i \neq n \\ - \left[\sum_{n=1}^{n_{elec}} |\mathbf{Y}_{in} \mathbf{v}_n| \sin(\delta_i - \theta_{in} - \delta_n) \right] & \text{for } i = n \end{cases}$$
- $\frac{\partial F_2}{\partial Pr} = \text{zeros}$; as reactive power imbalances do not depend on gas network variables.
- $\frac{\partial F_2}{\partial \dot{m}^T} = \text{zeros}$; as reactive power imbalances do not depend on thermal network variables.
- $$\frac{\partial F_{3,i}}{\partial \delta_n} = \frac{3600 \times C_{C_k,i}^G}{\eta_{C_k}^{G/E} GCV} (|\mathbf{v}_i \mathbf{Y}_{i,n} \mathbf{v}_n| \sin(\delta_i - \theta_{i,n} - \delta_n))$$
- for i = electricity network slack node*
- $$\frac{\partial F_{3,i}}{\partial |\mathbf{v}_n|} = \frac{3600 \times C_{C_k,i}^G}{\eta_{C_k}^{G/E} GCV} (|\mathbf{v}_{slack} \mathbf{Y}_{slack,n}| \cos(\delta_{slack} - \theta_{slack,n} - \delta_n))$$
- for i = electricity network slack node*
- $\frac{\partial F_3}{\partial Pr} = -A_1^G D (A_1^G)^t$

where,

- A_1^G -Reduced branch nodal incidence matrix for gas network
- $(A_1^G)^t$ - transpose of A_1^G
- $D = \text{diag} \left(\frac{1}{m} \frac{\dot{V}_{(k)}}{\Delta P_{(k)}} \right)$ for $k = 1, \dots, n_{gas\ pipe}$ -

$$\frac{\partial F_{3,i}}{\partial \dot{m}_{(n)}^T} = \frac{C_{C_k,i}^G \times A_{slack,n}^T \times c_p \times (T_{sup,slack}^T - T_{ret,slack}^T)}{\eta_{C_k}^{G/H} \times GCV}$$

for i = thermal network slack node

$$\frac{\partial F_4}{\partial \delta_n} = \frac{C_{C_k,i}^T}{\eta_{C_k}^{E/H} c_p \times (T_{sup,i}^T - T_{ret,i}^T)} \left(|v_{slack} Y_{slack,n} v_n| \sin(\delta_{slack} - \theta_{slack,n} - \delta_n) \right)$$

for i = electricity network slack node

$$\frac{\partial F_4}{\partial |v_n|} = \frac{C_{C_k,i}^T}{\eta_{C_k}^{E/H} c_p \times (T_{sup,i}^T - T_{ret,i}^T)} \left(|v_{slack} Y_{slack,n}| \cos(\delta_i - \theta_{in} - \delta_n) \right)$$

for i = electricity network slack node

$$\frac{\partial F_4}{\partial Pr} = \text{zeros}; \text{ as thermal network mass flow rates do not depend on gas network}$$

variables

$$\frac{\partial F_4}{\partial \dot{m}^H} = A_1^H$$

○ If there is a district cooling network balanced by a district heating network,

$$\frac{\partial F_{4,i}}{\partial \dot{m}_{(n)}^C} = \frac{C_{C_k,i}^H \times A_{slack,n}^C \times c_p \times (T_{sup,slack}^C - T_{ret,slack}^C)}{c_p \times \eta_{C_k}^{H/C} (T_{sup,i}^H - T_{ret,i}^H)}$$

for i = district cooling network slack node

$$\frac{\partial F_{5,i}}{\partial \delta_n} = \text{zeros}; \text{ as loop pressure drops do not depend on electricity network variables}$$

$$\frac{\partial F_{5,i}}{\partial |v_n|} = \text{zeros}; \text{ as loop pressure drops do not depend on electricity network}$$

variables

$$\frac{\partial F_{5,i}}{\partial Pr_n} = \text{zeros}; \text{ as loop pressure drops do not depend on gas network variables}$$

$$\frac{\partial F_{5,i}}{\partial \dot{m}_{(n)}^T} = 2B_{ik}^T \left(K_{(k)} \left| \dot{m}_{(k)} \right| \right)^T$$

- Step 5: Calculate the correction ΔX^o for the state parameters by solving,

$$\Delta X^o = -(J^o)^{-1} F(X^o)$$

$$\begin{bmatrix} \Delta \delta^o \\ \Delta |V|^o \\ \Delta Pr^o \\ \Delta \dot{m}^o \end{bmatrix} = -(J^k)^{-1} \begin{bmatrix} F_1(X^o) \\ F_2(X^o) \\ F_3(X^o) \\ F_4(X^o) \\ F_5(X^o) \end{bmatrix}$$

- Step 6: Apply the correction and determine the value of X for the next iteration

$$X^1 = X^o + \Delta X^o$$

$$\begin{bmatrix} \delta^1 \\ |V|^1 \\ Pr^1 \\ \dot{m}^1 \end{bmatrix} = \begin{bmatrix} \delta^o \\ |V|^o \\ Pr^o \\ \dot{m}^o \end{bmatrix} + \begin{bmatrix} \Delta \delta^o \\ \Delta |V|^o \\ \Delta Pr^o \\ \Delta \dot{m}^o \end{bmatrix}$$

- Step 7: Compute the supply line temperatures at thermal network nodes using the new branch flow rate estimates.
- Step 9: As described in step 2 re-calculate and the local mass flow rates at thermal network nodes using the updated figures for nodal temperatures.

Repeat the iterations from step 3 until the imbalances $F(X^k)$ and the change in local mass flow rates between iterations are less than a specified tolerance.

The flow chart of the solution method is shown in Figure 4-10 .

The method is applied for an example energy system of the structure presented in Figure 4-1. It is illustrated in Appendix B.1. The results of the simulation are validated using commercial software packages used for load flow analysis in individual energy networks.

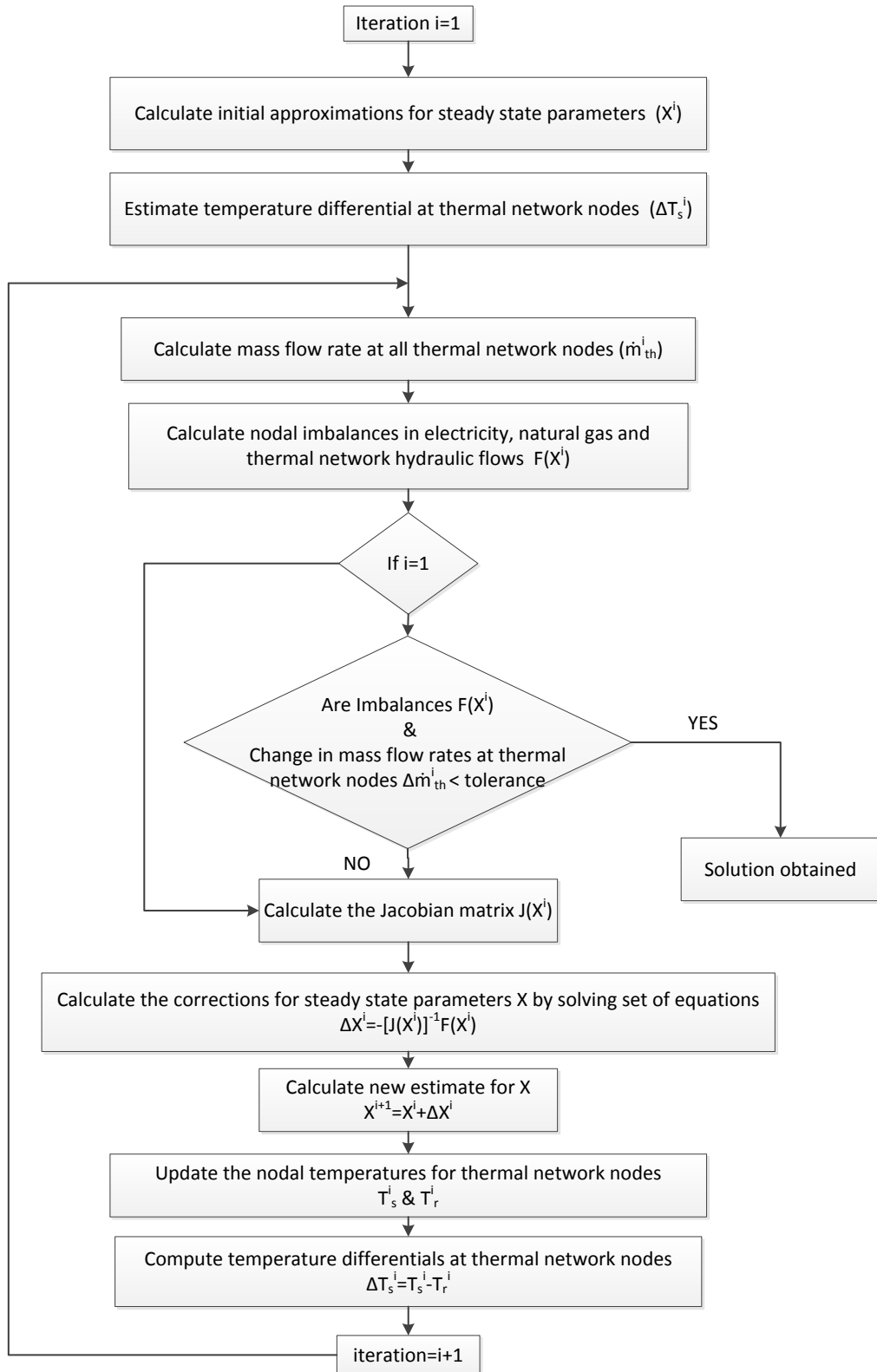


Figure 4-10: Flow chart for the method of solving the equations

4.5 Chapter summary

A method for the simultaneous steady state power flow analysis of coupled multi energy networks was developed. The problem of steady state analysis in a system of coupled energy networks was described using an example system. The modelling of network components and the method of formulating network equations for each energy carrier system was shown. A method for solving the set of equations was also developed. The set of equations of electricity, natural gas and thermal network pipeline hydraulics are solved simultaneously using the Newton-Raphson method with a correction for temperature at thermal network nodes computed separately in each iteration. The model was implemented in MATLAB software. An example is used to illustrate the formulation of network equations and the step by step solution method (available in Appendix B.1). The results were validated using commercial software packages used for load flow analysis in each energy network.

Chapter 5: Case study of simultaneous power flow analysis

This chapter presents a case study of simultaneous steady state analysis of a coupled energy network system. It is used to demonstrate the applications of the developed method for analysing interdependencies between coupled energy networks. Convergence characteristics of the solution method are also analysed.

5.1 Case study description

The schematic of the case study network system is shown in Figure 5-1. The network parameters for the case study are provided in the Appendix B.3.

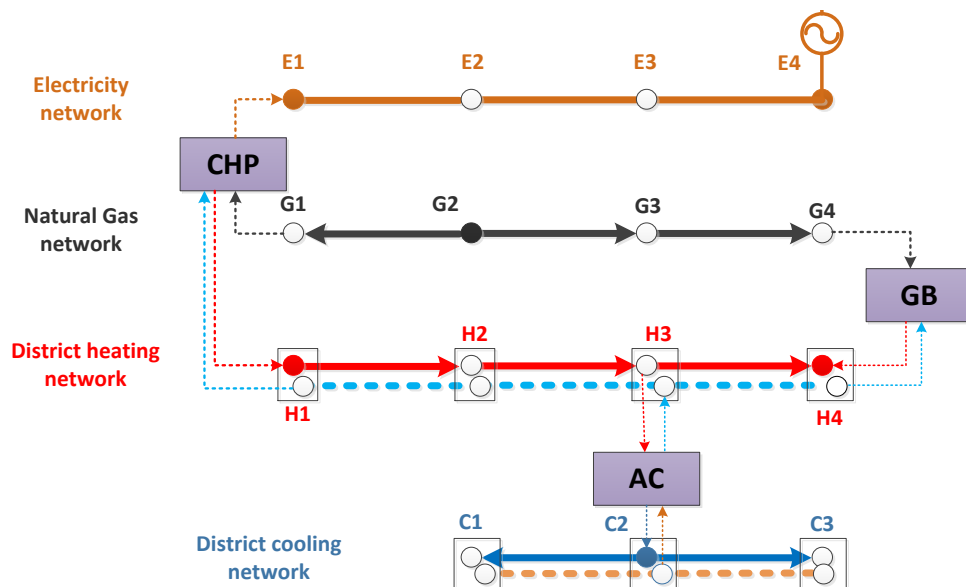


Figure 5-1: Case study network schematic

Note: Filled circles represent energy supply nodes and empty circles represent energy demand nodes

The energy supply sources for each network are described below.

- Electricity network – A CHP unit connected at node E1 and an external grid connection at node E4.
- Natural gas network – External grid connection at node G2.

- District heating network –CHP unit connected at node H1 and a gas boiler connected at node G4.
- District cooling network – Absorption chiller unit connected at node C2.

The energy conversion efficiencies of the coupling components are shown in Table 5-1.

Table 5-1: Coupling component data

Component Type	Conversion Efficiency
CHP	$\eta_{C_1}^{G/E} = 0.35$ $\eta_{C_1}^{G/H} = 0.4$
Gas Boiler (GB)	$\eta_{C_2}^{G/H} = 0.9$
Absorption Chiller	$\eta_{C_3}^{H/C} = 0.65$

The nodal energy demand data for the different networks are shown in Table 5-2.

The simulations are performed as detailed below.

- Reference case: The individual energy networks are simulated **without** the coupling components to establish a reference. The slack node in each network for the Reference case is,

	Slack node
Electricity network	E4
Gas network	G2
District heating network	H4
District cooling network	C2

In the Reference case all the other nodes are considered energy demand nodes.

Table 5-2: Energy demand data for case study

Electricity network nodal demand data		
Node	Local demand	
	$p_{d,i}^E$ [MW _e]	$q_{d,i}^E$ [MVar]
E1	0.8	0.1
E2	0.8	0.1
E3	0.8	0.25
E4	0.4	0.1
Natural gas network nodal demand data		
Node	Local demand	
	$\dot{V}_{d,i}^G$ [m3/hr]	
G1	200	
G2	50	
G3	100	
G4	180	
District heating network nodal demand data		
Node	Local demand	
	$\dot{Q}_{d,i}^H$ [kW _{th}]	
H1	400	
H2	1200	
H3	400	
H4	200	
District cooling network nodal demand data		
Node	Local demand	
	$\dot{Q}_{d,i}^H$ [kW _{th}]	
C1	400	
C2	0	
C3	400	

- **Case A:** The energy flows from network coupling components i.e. CHP unit, gas boiler (GB) and the absorption chiller (AB) **are connected** as shown in Figure 5-1.
 - The slack node for the electricity network is **changed** to E1. Therefore the CHP unit balances the electricity network load. Node E4 is changed to a PV type node. A fixed 0.5 MW_e of real electrical power is injected at node E4 and maintains the voltage magnitude at 1.0 p.u.

- The slack node for the gas network **remains the same** at node G2. The gas demand at node G1 depends on the CHP unit and the gas demand at node G4 depends on the GB unit.
- The slack node for the district heating network **remains the same** at node H4. Therefore the GB unit balances the district heating network load. The CHP unit injects thermal power in the district heating network and H1 is **changed** to an energy supply (*supply_T* type) node.
- The slack node for the district cooling network **remains the same** at node C2. The absorption chiller balances the district cooling network load.
- **Case B:** The following changes are applied to the network described in case A.
 - The slack node for the electricity network is **changed** to E4. Node E1 is **changed** to a PQ type node.
 - The gas network remains the same as case A.
 - The slack node for the district heating network is **changed** to node H1. Therefore the CHP unit balances the district heating network load. Node H4 is **changed** to an energy supply (*supply_T* type) node. The GB injects 0.5 MW_{th} of thermal power at node H4 at a supply temperature of 100°C.
 - The district cooling network remains the same as case A.
- **Case C:** The network is the same as Case B. The nodal energy demands of the different networks are varied using a demand factor defined as,

$$\text{Demand factor} = \frac{\text{Simulated Demand}}{\text{'Reference Case' Demand}}$$

The demand factors used for the different networks are shown in Table 5-3.

A summary of the case studies are shown in Table 5-3.

Table 5-3: Case study scenarios

	Description	Electricity network		Gas network	District Heating Network		District Cooling Network
		Slack bus	Demand factor	Demand factor	Slack node	Demand factor	Demand factor
Reference	No coupling units	E4	1	1	H4	1	1
Case A	CHP electricity driven	E1	1	1	H4	1	1
Case B	CHP heat driven	E4	1	1	H1	1	1
Case C	Varied demand	E4	0.5	1.25	H1	1.25	0.75

5.2 Results and discussion

5.2.1 Converged parameters

A. Electricity network

The variation of voltage magnitude and voltage angle at nodes in the electricity network is shown in Figure 5-2.

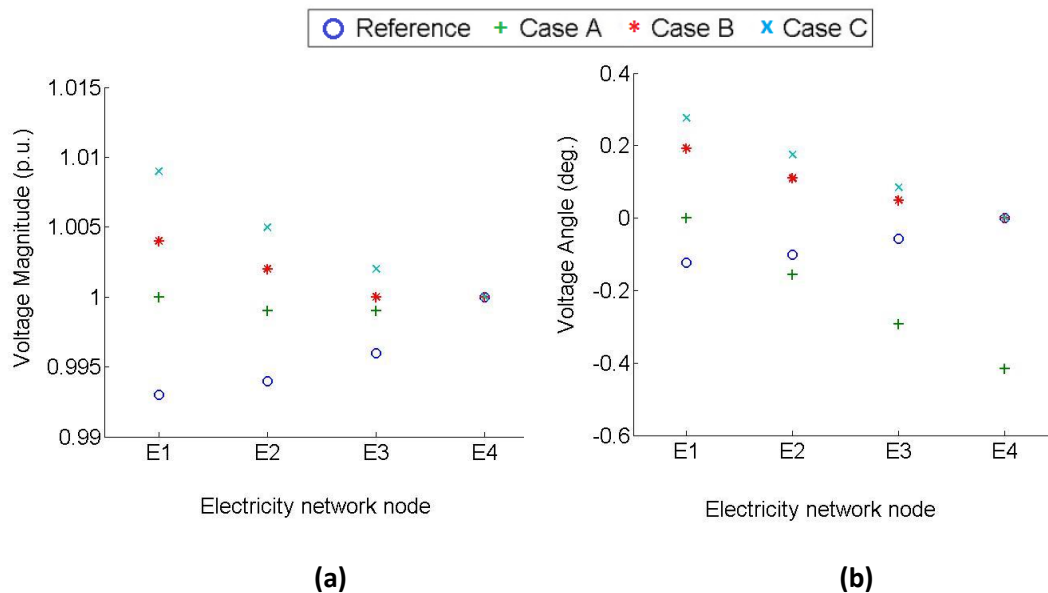


Figure 5-2: Voltage variation for the case scenarios a) voltage magnitude b) voltage angle

The gradient of the voltage magnitude and angle along the network for the Reference case shows the real and reactive power flows are from node E4 toward node E1.

In case A, node E1 is the slack node for the electricity network. The voltage magnitude at node E4 (a PV node) is maintained at 1.0 p.u. The voltage magnitude shows a flat profile, whereas the voltage angle shows a decline from node E1 to E4. Therefore the real power flow is predominantly from node E1 towards node E4.

In case B and case C, the CHP unit is connected to the slack node of the district heating network (node H4). Node E1 is specified as a PQ type node. The CHP unit injects electrical power at node E1 corresponding to the heat production required to balance the district heating network. The voltage magnitude and angle at nodes E1, E2 and E3 increase compared to the Reference case and case A. The voltage magnitude and angle show a decrease from node E1 to E4 similar to case A. This shows the impact of the CHP unit on network voltage levels in various operating modes and network configurations.

B. Natural gas network

The variation of gas pressure at nodes in the natural gas network is shown in Figure 5-3.

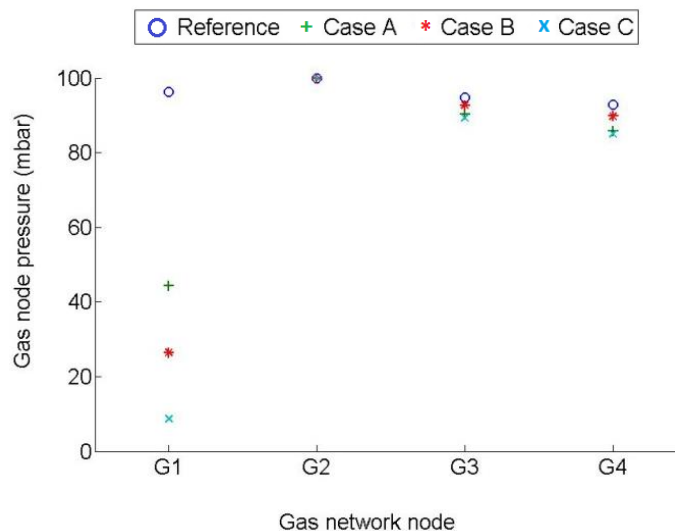


Figure 5-3: Variation of gas pressure at natural gas network nodes

The pressure at node G2 is held constant at 100mbar in all cases. The gas flows are from node $G2 \rightarrow G1$ and node $G2 \rightarrow G3 \rightarrow G4$. In the Reference case the pressure at node G1 is 96.3mbar. The pressure at node G4 is 92.9mbar.

In case A, the gas demand of the CHP unit reduces the pressure at node G1 to 44.4mbar. The pressure at node G4 drops to 85.8mbar due to the gas demand of the GB.

In case B, an increase in the CHP units' gas demand reduces the gas pressure at node G1 to 26.8mbar. The gas demand of the gas boiler is reduced compared to case A which results in an increase in nodal pressure at G4 to 89.8mbar.

In case C, the energy demand levels of the gas network and the district heating network are increased by 25%. This increases the gas demand of the CHP unit. The nodal gas pressure at G1 drops to 8.7mbar. The gas pressure at G4 drops to 85.0mbar.

The results show the impact of varying energy demands, the operation of the CHP unit and gas boiler on gas network pressure delivery.

C. District heating network

The branch mass flow rates in the district heating network for different case studies are shown in Figure 5-4. A negative flow represents a flow in the opposite direction to that shown in Figure 5-1.

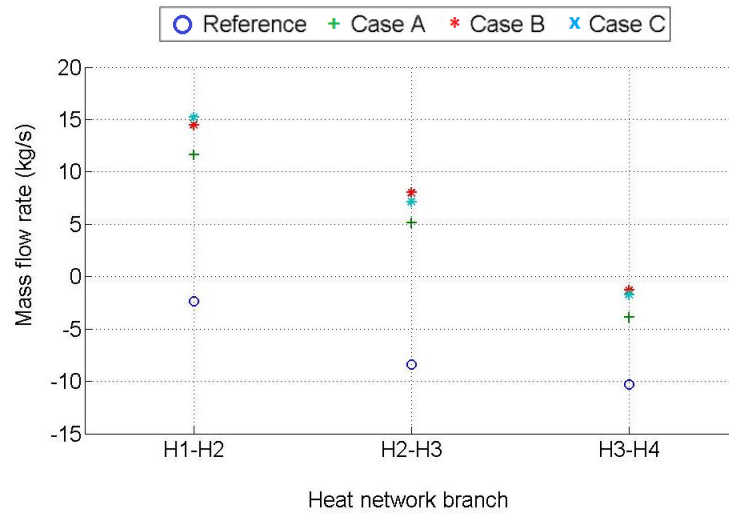


Figure 5-4: District heating network branch mass flow rates

The variations of supply and return line nodal temperatures are shown in Figure 5-5.

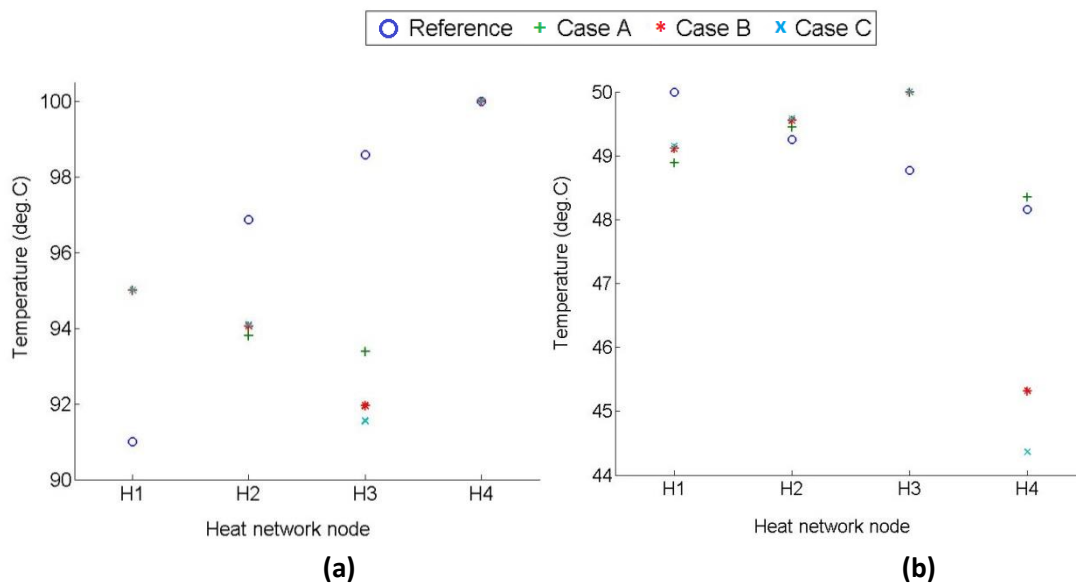


Figure 5-5: District heating network node temperature a) supply line b) return line

In the Reference case the slack node is H4. All mass flow rates are negative as the water flow directions in the supply network branches are from node $H4 \rightarrow H3 \rightarrow H2 \rightarrow H1$. The mass flow rate in branch H3-H4 is the largest (10.3 kg/s) as it carries the total energy to be delivered to node H3, H2 and H1. The supply line nodal temperatures decrease from node $H4 \rightarrow H1$. The highest and lowest supply line temperatures of 100°C and 91°C are at node H4 and node H1. The return line mass flows are from node $H1 \rightarrow H2 \rightarrow H3 \rightarrow H4$. The return

line nodal temperatures decrease from node H1→H4. The highest and lowest return line temperatures of 50°C and 48.2°C are at node H1 and node H4.

In case A, the CHP and GB units inject heat at node H1 and node H4. The heat injected by the CHP unit relates to the electricity network load. The absorption chiller consumes heat at node H3. The absorption chiller heat demand relates to the district cooling network load.

In case A, the slack node in the district heating network is H4. The gas boiler generates heat required to balance the heat demands, supplies and energy losses in the distribution lines.

The mass flow rate in branches H1-H2 and H2-H3 are positive as the direction of flow in the supply network **changes** to node H1→H2→H3. The mass flow rate in branch H3-H4 remains negative, but reduces in quantity (3.9kg/s). The supply line nodal temperature at node H1 and node H4 are maintained at 95°C and 100°C by the CHP and GB unit. The supply line temperature decreases from node H1→H3. The lowest supply line temperature is 93.4°C at node H3. The return line mass flows are from node H3→H2→H1 and from node H3→H4. The highest return line temperature of 50°C is at node H3. The return line temperature decreases in the directions H3→H2→H1 and H3→H4. The return line temperature at node H1 and H4 are 48.9°C and 48.4°C. The total heat demand in the district heating network is higher in case A compared to the Reference case due to the absorption chiller demand. The additional heat demand is supplied by an increase in total mass flow rate in the district heating network i.e. 15.5kg/s in case A compared to 10.3kg/s in the Reference case.

In case B the slack node in the district heating network is changed to H1. The CHP unit balances the district heating network, whereas the gas boiler injects 0.5 MW_{th} of thermal power at node H4. The direction of mass flows, supply and return line temperature gradients are the same as in case A. The total heat demand remains the same as in case A and therefore the total mass flow rate in the supply network is approximately the same i.e.

15.8kg/s. The mass flow rate through the CHP unit increases and that through the gas boiler unit decreases. A drop in the return line temperature at node H4 is observed due to the reduced mass flow rate in branch H3-H4.

In case C the nodal energy demands of the district heating network are increased by 25% and of the district cooling network are reduced by 25%. The direction of mass flows, supply and return line temperature gradients are the same as in case A and case B. The total mass flow entering the supply network increases to 16.9kg/s to accommodate the increase in heat demand.

D. District cooling network

The branch mass flow rates and the nodal temperatures in the district cooling network are shown in Table 5-4.

Table 5-4: District cooling network results

Branch number	Mass flow rate [kg/s]	
	Reference case/ Case A/Case B	Case C
C2-C1	13.76	10.35
C2-C3	13.76	10.35

Node number	Supply line temperature [°C]		Return line temperatures [°C]	
	Reference case/ Case A/Case B	Case C	Reference case/ Case A/Case B	Case C
C1	5.1	5.1	12	12
C2	5	5	11.98	11.98
C3	5.1	5.1	12	12

In the Reference case, case A and case B the characteristics of the district cooling network does not vary. The branch mass flow rates in C2-C1 and C2-C3 are 13.7kg/s as the network is symmetrical around node C2. The supply line temperature is maintained at 5°C at node C2 by the absorption chiller. The supply line temperature at node C1 and C3 increases to

5.1°C due to **heat gains** from the atmosphere (atmospheric temperature is 10°C). The return line temperature remains approximately the same in all nodes as the heat losses are very small.

In case C the cooling demands are reduced by 25%. Therefore the branch mass flow rates drop to 10.4kg/s. The nodal temperatures are the same as above.

5.2.2 Energy supply and conversions

The energy conversions at the coupling units, electricity imported from the external grid and total energy demands in the different networks are shown in Figure 5-6.

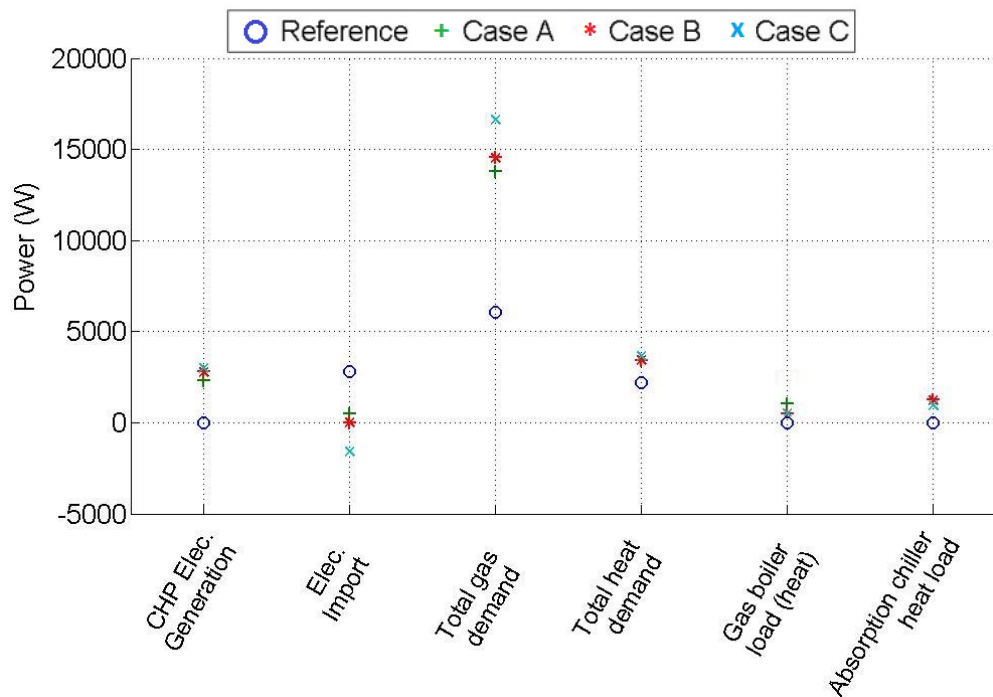


Figure 5-6: Power supply, demand and conversions at coupling components

In the Reference case the CHP unit, gas boiler and the absorption chiller is not considered.

The electricity demands are supplied by importing 2810kW_e at node E4. The total gas and

heat demands are 6042kW_g^{18} and 2200kW_{th} given by the summation of energy demands specified in Table 5-2.

In case A the CHP unit generates 2310kW_e whereas 500kW_e of electrical power is imported at node E4. The total gas demand increases to 13803kW_g due to the additional gas demands of the CHP unit and gas boiler. The total heat demand increases to 3436kW_{th} due to the absorption chiller heat demand. The gas boiler generates 1039kW_{th} of heat to balance the district heating network. The absorption chiller consumes 1236kW_{th} of heat from the district heating network.

In case B, the CHP unit generates 2790kW_e of electrical power. The slack node in the electricity network (node E4) imports 20kW_e to balance the electricity load. The gas demand increases to 14538kW_g due to the increased CHP generation. The total heat demand and the absorption chiller heat demand remains the same as in case A.

In case C, the CHP generation increases to supply the increased heat demand. At the same time the electricity demands are reduced by 50%. An excess electrical power of 1580kW_e is exported back to the grid at node E4. The total gas demand increases to 16645kW_g due to the increased CHP generation. The district cooling network demands are reduced by 25%. Therefore the absorption chiller heat demand reduces to 929kW_{th} . The district heating network nodal demands increase by 25%. However, due to the reduced absorption chiller heat demand the total heat demand is approximately the same as in case A and B.

¹⁸ The total gas demand is specified in 'kilo Watts' of gas power for comparison. The subscript 'g' is used to differentiate from other types of energy carriers. The gross calorific value of natural gas is assumed as 41.04MJ/m^3

5.2.3 Energy distribution losses

Figure 5-7 shows the energy distribution losses in different networks. The branch numbering used in Figure 5-7 is given by,

	Electricity network	District heating network	District cooling network
Branch #1	E1-E2	H1-H2	C2-C1
Branch #2	E2-E3	H2-H3	C2-C3
Branch #3	E3-E4	H3-H4	

The friction losses in natural gas distribution are not considered. In the district heating network energy losses in both the supply and return lines are considered. In the district cooling network the heat gains to the supply line branches are considered and the heat losses in return lines are ignored.

The maximum electrical power loss of 19kW_e is observed in case C. In the Reference case the largest electrical power loss is in branch 3 whereas in case C it's in branch 1.

The distribution energy losses in the district heating network are significantly higher compared to other networks. The maximum thermal power loss of 258kW_{th} is in the Reference case. Thermal losses are driven by the large temperature difference in the hot water delivered and the ambient temperature (10°C).

The distribution energy losses in the district cooling network are relatively small compared to the district heating network. This is due to the small temperature difference between the chilled water and the ambient temperature.

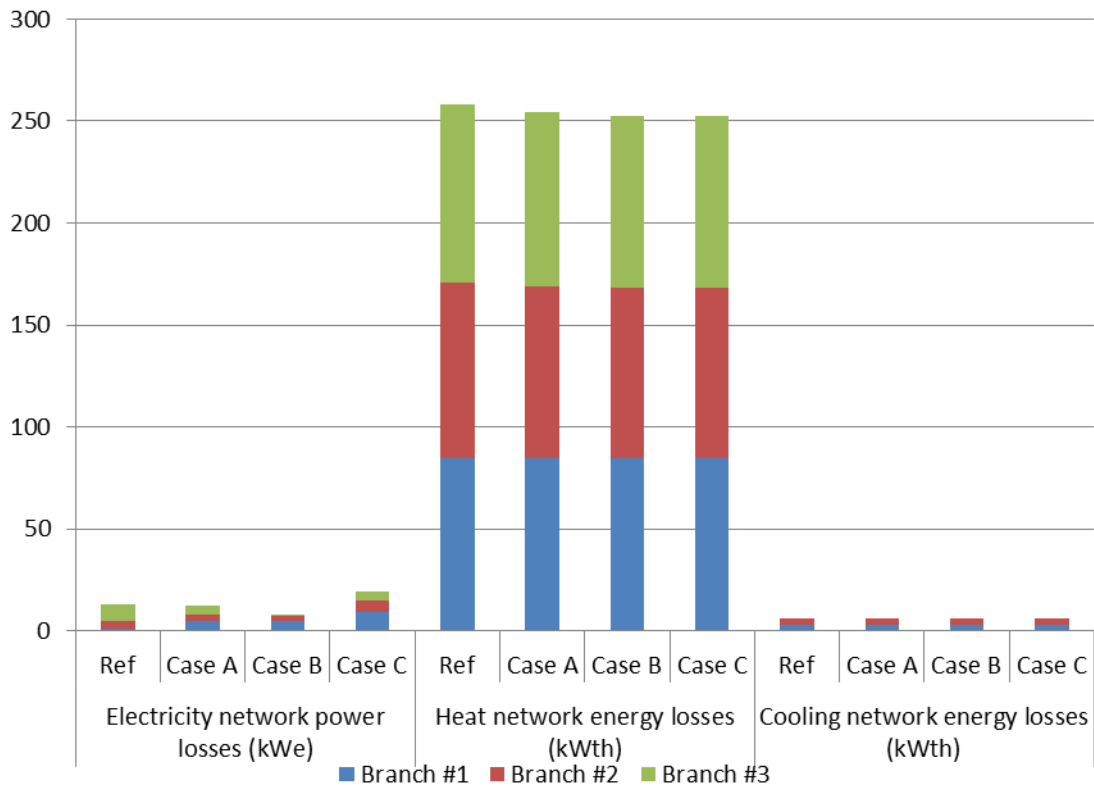


Figure 5-7: Distribution line losses

5.2.4 Convergence characteristics

The number of iterations for convergence and the computation time in each case are shown in Table 5-5.

Table 5-5: Convergence characteristics

	Reference	Case A	Case B	Case C
No of iterations to converge	6	16	9	9
Computation time¹⁹	1.5s	1.8s	1.7s	1.6s

All simulations were completed within 2 seconds. The maximum number of iterations for convergence was in case A with 16 iterations.

The imbalances in network equations (see section 4.3.4) are shown in Figure 5-8.

¹⁹ Simulations performed on MatLab R14 running on an Intel® Core™ i7-3770K CPU @ 3.50GHz (8 CPU's) and 16GB RAM machine

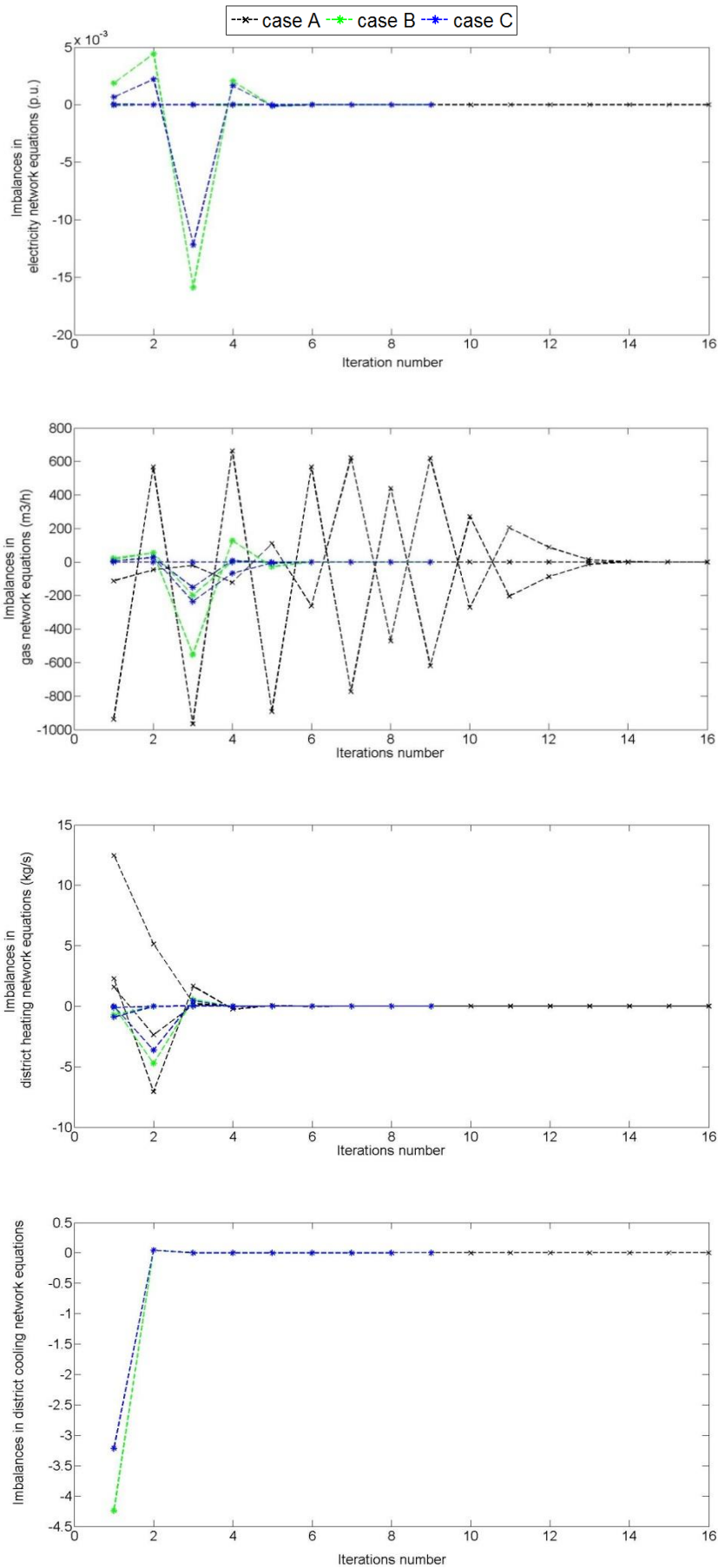


Figure 5-8: Iterations information

The tolerance limit set for electricity network equation imbalances are 0.001p.u. The electricity network equations converge within 5 iterations in all cases.

The tolerance limit set for gas network equation imbalances are $1\text{m}^3/\text{hr}$. The gas network equations in Case A show slower convergence compared to the other case scenarios. The convergences of gas network equations are much slower compared to electricity and thermal network equations.

The tolerance limit set for thermal network equation imbalances are 0.1kg/s. District heating and district cooling network equations converge within 5 and 3 iterations in all cases.

The scale of the equations (e.g. per unit system in electricity network) in different networks vary significantly. This creates a set of equations that are not equally balanced. This can impact convergence when solving networks with a large number of nodes. The method could potentially be improved by developing a per unit system to represent the different networks being analysed.

5.3 Chapter summary

This chapter presents a case study of simultaneous steady state analysis of a coupled energy network system. The analysis provides quantified information of the interactions and inter-dependencies between coupled energy networks.

It shows that the mode of operating the coupling units and the energy demand levels in different networks are important to determine the operational state of each energy network. For example It was shown that the mode of operating the CHP unit (electricity driven or heat driven) and the gas boiler (fixed heat supply, heat balancing) and the heat and cooling demands in the case study impact on the state of the natural gas network and the electricity network.

The relationship between energy supply and conversions in different scenarios were shown in section 5.2.2 . The inter-dependencies between energy networks in different case studies were discussed. For example, a high heat load was shown to have a significant impact on gas demand and therefore on gas pressure delivery. When the CHP unit operates in heat driven mode a high heat load may generate excess electricity and cause a reversal of electrical power flow direction at the grid supply point.

The convergence characteristics of the solution method were analysed. It was shown that the gas network equations converge relatively slower than the electricity and thermal network equations. It was proposed to develop a per unit measurement system to represent all networks being analysed in order to avoid the differences in scales of the equations being solved and thus improve convergence.

Chapter 6: Gas network analysis with distributed injection of alternative gases

This chapter presents a method developed for the steady state analysis of gas networks with injections of alternative gas types. A case study presents the impact of alternative gas injections on pressure delivery and gas quality in the network.

6.1 Introduction

The future role of natural gas in the UK energy mix has become an increasingly debated issue (Cary, 2012, Dodds and McDowall, 2013). It is evident that to meet the statutory carbon emission targets the use of natural gas needs to decline over time (HM Government, December 2011). The UK Government strategy for low carbon heat (DECC, 2013b) identifies opportunities to decarbonize parts of the gas network by using renewable gas. Government incentives are already in place for developers of anaerobic digesters to inject upgraded biogas into the natural gas grid. A number of other new sources of gas are also anticipated to be injected into the gas distribution grid (e.g. shale gas, biomass gasification products, coal bed methane and hydrogen).

The current gas quality standards are based on the quality of gas sourced from the UK continental shelf (UKCS)(HSE, 1996). This has traditionally been the primary source of gas supply for Britain. However, over the next few decades, it may be necessary to assess the feasibility of the gas supply system to utilize a range of gas sources. Variations in the gas composition (molar fractions of different gases) have an impact on the combustion characteristics at the appliance level and also on gas transportation characteristics at the network level (e.g. pressure delivery). Some of these new gas sources (e.g. shale gas) are remotely located which could have significant implications for managing the distribution network operation. For example, shale gas supply from a particular site may exceed the gas demand in the local network necessitating supply interruptions. Tools for modelling and

simulating gas network operation are required to analyse the impact of introducing new supply sources to the gas grid.

Gas network operation is simulated by using mathematical models of gas flow in pipes. Simulations can be carried out in steady and transient states. The scope of this work is on simulating gas networks in steady state. Steady state is a snapshot of the gas network operation where the parameters characterizing gas flow is independent of time. Steady state analysis computes nodal gas pressures and pipe flows for specified source pressures and gas demands in a given gas network (Osiadacz, 1987).

Traditional methods of modelling and simulating gas networks assume a gas mixture with a uniform composition to be transported via the network (Osiadacz, 1987, Segeler, 1965). Newton-nodal, Newton loop and Hardy Cross methods are widely used (Brkić, 2009, Goldfinch, 1984, Osiadacz, 1988b, Osiadacz, 1988a). Previous studies on assessing the impact of alternative gas supply sources has focused on the durability and safety aspects of gas system components to different gas mixtures e.g. hydrogen tolerance levels in components of the gas system (NaturalHy, 2009, De Vries et al., 2007). Several studies have initiated methods for tracking the calorific value of gas in gas distribution grids (Peter Schley, 2011). To the authors best knowledge a method for analysing the impact of alternative gas injections on gas flow in pipes and thereby steady state gas network operation have not been investigated in detail.

This chapter presents a method developed for the steady state analysis of gas networks with injections of alternative gas types. The method extends the Newton-nodal method for steady state analysis to study the impact of injecting alternative gas supplies (e.g. Hydrogen, biogas) at different locations on a given network. The method can support decision making on the allowable amount and content of alternative gas in distribution grids. Two approaches for gas demand formulation are compared. A case study

demonstrates the impact of alternative gas injections on the steady state gas flow parameters.

6.2 Gas interchangeability and the impact of alternative gases in the gas grid

Different components connected to a gas supply system, such as underground and over ground storage, gas turbines and engines, domestic and industrial appliances, compressors, and valves, are designed to operate on natural gas with a standard composition. Tolerance levels of these components to alternative gas types can vary. For example up to 10% Hydrogen (in volume) is tolerated in parts of the natural gas system whereas the limit drops to 2% if a natural gas vehicles refuelling system is connected (NaturalHy, 2009)(due to steel tanks in natural gas vehicles).

Extensive research has been undertaken for ways to predict the interchangeability of one gas mixture with another (Qin and Wu, 2009, Dodds and Demoullin, 2013, Zachariah et al., 2007, NaturalHy, 2009). The Wobbe index (WI) is widely used together with a measured or calculated flame speed factor for assessing gas interchangeability (Weber, 1965, Cagnon et al., 2004, Qin and Wu, 2009). WI is proportional to the heat input to a gas burner at constant pressure and defined as,

$$\text{Wobbe Index (WI)} = \frac{\text{Gross Calorific Value (GCV)}}{\sqrt{\text{Specific Gravity (SG)}}} \quad (6.1)$$

Variations in gas composition has an impact on temperature variations and pressure delivery of gas through a pipeline network (NaturalHy, 2009, Schouten et al., 2004). Several studies have investigated the effect of hydrogen injection on the thermodynamic and transportation properties of natural gas (Öney et al., 1994, Schouten et al., 2004). It has been shown that the condensation behavior, Joule Thomson effect at pressure reduction

stations, energy density and pressure drops in pipelines will need investigation upon injection of an alternative gas (Schouten et al., 2004). The scope of this study is on the analysis of the impact on energy density and pressure drop in pipelines.

6.3 Problem description

A gas network within a single pressure tier consists of one or more natural gas infeed sites, alternative gas supply sites, gas pipelines and gas demands.

The problem of steady state analysis is to compute the nodal gas pressures, molar fraction of gases at nodes and gas flows in individual pipes for a given source pressure, source gas mixture composition that meets the gas demands. A summary of the gas network steady state analysis problem is shown in Table 6-1.

Table 6-1: Summary of the problem

Node type	Quantities specified	State variables to be calculated
Gas infeed node	Nodal Pressure (pr_i) Molar fraction of gases (x_i^j)	-
Alternative gas injection node	Gas injection (Energy) ($E_{s,i}$) Molar fraction gases (x_i^j)	Nodal Pressure (pr_i)
Gas load node	Gas demand (Energy) ($E_{d,i}$)	Nodal Pressure (pr_i), Molar fraction of gases (x_i^j)

6.4 Methodology

6.4.1 Modelling gas demands

The gas demand is modelled as a gas volume flow rate by considering the energy available through combustion. Gas demand at a node i is expressed as,

$$\dot{V}_{d,i} = \frac{E_{d,i}}{GCV_i} \times 3600 \quad (6.2)$$

Where,

- $\dot{V}_{d,i}$ - Gas demand (volume flow rate) at node i [m^3/hr]
- $E_{d,i}$ - Energy demand at node i [kW_g]
- GCV_i - Calorific value of gas mixture at node i [kJ/m^3]

Traditional methods for gas network analysis (Osiađacz, 1987) assume the use of natural gas of a specified molar composition across the network. However, if alternative gases are injected the molar composition of gas in parts of the network may vary. The method presented computes the molar fraction of gas mixture components at each node. The calorific value of gas at a node i (GCV_i) is then calculated as,

$$GCV_i = \sum_{j=1}^N x_i^j \times GCV_i^j \quad (6.3)$$

where,

- x_i^j - molar fraction of component j at node i
- N - number of components in the gas mixture at node i
- GCV_i^j - Molar calorific value of component j as specified in the British Standard EN ISO 6976:2005.

Distributed injection of an alternative gas is modelled as a negative gas load for steady state analysis purposes. The molar composition of the gas and the energy content injected is specified.

6.4.2 Modelling steady state gas flow in pipes

The equation for steady-state gas flow in a horizontal pipe is given by (Osiadacz, 1987),

$$\dot{V} = \sqrt{\frac{\pi^2 R_{air}}{64} \frac{T_n}{pr_n}} \sqrt{\frac{[(pr_i^2 - pr_j^2)] D^5}{fSLTZ}} \quad (6.4)$$

where,

- \dot{V} - gas volume flow at standard temperature and pressure conditions (STP) [m³/s]
- R_{air} - gas constant for air [Nm⁻²]
- pr_i - gas pressure at pipe starting node i [Nm⁻²]
- pr_j - gas pressure at pipe ending node j [Nm⁻²]
- pr_n, T_n - standard pressure [Nm⁻²] and temperature [K]
- S - relative density of gas [-]
- Z - gas compressibility factor [-] typically assumed as 1 for steady state analysis
- T - temperature of gas [K]
- f - friction factor[-]
- L - pipe length [m]
- D - pipe internal diameter [m]

The value of f is determined as (Osiadacz, 1987) given by,

$$\left\{ \begin{array}{l} f = 0.0044 \left(1 + \frac{12}{0.276D} \right) \text{ for low pressure networks (0–100mbar)} \\ \sqrt{\frac{L}{f}} = 5.338 (Re)^{0.076} \text{ for medium pressure networks (0.1–7bar)} \end{array} \right\}$$

where,

- Re - Gas flow Reynolds number

The relative density of a gas mixture S is independent of state and is calculated as,

$$S = \sum_{j=1}^N x^j \times \frac{M^j}{M^{air}} \quad (6.5)$$

where,

- S - relative density of gas mixture
- N - number of components in the gas mixture at node
- M^j - molar mass of component j as specified in the British Standard EN ISO 6976:2005.
- M^{air} - molar mass of dry air of standard composition (28.962 kg/kmol)

6.4.3 Formulating equations for pipe network analysis

To formulate network equations perfect mixing is assumed at gas nodes i.e. the mixing of two or more gas flows create no chemical reaction or state change in the constituent gases.

The gas volume balance at STP conditions at each node i is expressed as,

$$0 = \left(\sum_{k=1}^{n_{pipe}} A_{i,k} \dot{V}_k \right) - \dot{V}_{d,i} \quad (6.6)$$

where,

- n_{pipe} - number of gas pipes
- $A_{i,k}$ - elements of the gas network branch-nodal incidence matrix (A) derived as,

$$A_{i,k} = \begin{cases} -1 & \text{if } V_k \text{ is leaving node } i \\ +1 & \text{if } V_k \text{ is entering node } i \\ 0 & \text{if branch } k \text{ is not connected to node } i \end{cases} ;$$
- \dot{V}_k - gas flow rate in gas pipe k as given by equation (6.4);
- $\dot{V}_{d,i}$ - gas demand at node i ;

From equation (6.4) the gas pipe flow \dot{V}_k is a function of pressure drop ($\Delta p r_k$) and relative density of the gas mixture in pipe k (S_k).

$$\dot{V}_k = \phi(\Delta pr_k, S_k) \quad (6.7)$$

The pressure drop in a branch k (Δpr_k) is given by (Osiadacz, 1987),

$$\Delta pr_k = \sum_{i=1}^{n_{gas}} -(A^t)_{k,i} pr_i \quad (6.8)$$

where,

- n_{gas} -number of gas nodes
- $(A^t)_{k,i}$ - elements of the transpose of branch-nodal incidence matrix (A)
- pr_i -nodal gas pressure at node i

The relative density of a gas mixture is computed using molar fractions of gas mixture components as shown in equation (6.5).

The molar fraction of a component j in the gas mixture at a node i , (x_i^j) is calculated by considering the mixing of gas flows at node i as,

$$(x_i^j) = \frac{\sum_{\dot{V}_k \text{ incoming to node } i} x_k^j \times \dot{V}_k}{\sum_{\dot{V}_k \text{ incoming to node } i} \dot{V}_k} \quad j = 1, \dots, N \quad (6.9)$$

where,

- x_k^j -molar fraction of component j in gas mixture in pipe k
- \dot{V}_k - gas flow rate in pipe k (all incoming to node i)
- N - number of components in the gas mixture at node

Therefore, the relative densities of gas in pipes are a function of gas pipe flows which are in turn dependent on nodal gas pressures. Hence equation (6.10) is expressed as,

$$0 = \left(\sum_{k=1}^{n_{\text{gas pipe}}} A_{i,k} \times \psi(P_r) \right) - \left(\frac{E_{d,i}}{GCV_i} \times 3600 \right) \quad (6.10)$$

where,

- P_r - nodal gas pressure vector

The method solves the set of non-linear equations (6.10) formulated at each gas node with an updated value for relative density and calorific value at each iteration to compute nodal gas pressures.

6.4.4 Solution method

The set of non-linear equations (6.10) are solved using the 'Newton-Raphson' method. The steps of the solution method are described below.

- **Step 1:** Make an initial approximation for gas flows in each branch. The method adopted in the model is to assume that all the demands are supplied via tree branches and a uniform gas composition i.e. composition of natural gas.
- **Step 2:** Compute the gas pressure at each node that provides the assumed gas flow in pipes using equation (6.4) and equation (6.8).
- **Step 3:** Depending on gas flow direction/nodal pressure establish a node analysis sequence as described by the flow diagram in Figure 6-1 such that the composition of incoming gas flows to a node is always known.
- **Step 4:** Calculate the molar fraction of gas components at each node using equation (6.9)
- **Step 5:** Calculate the calorific value and relative density of gas at each node.
- **Step 6:** Calculate the gas flow imbalance at each gas node (f_i) using equation (6.10)

$$f_i = \sum_{k=1}^{n_{\text{gas pipe}}} A_{i,k} \dot{V}_k - \left(\frac{E_i}{GCV_i} \times 3600 \right) \quad i = 1, 2, \dots, N \quad (6.11)$$

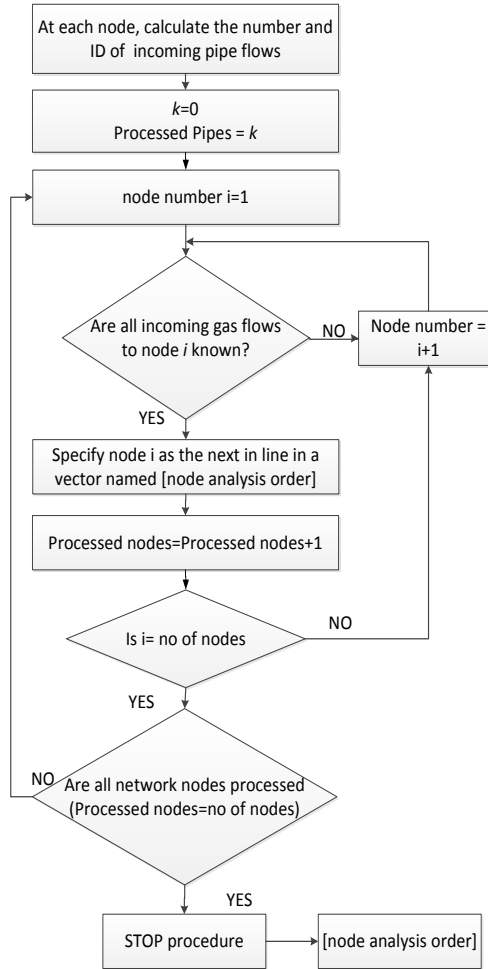


Figure 6-1: Algorithm for establishing a node analysis sequence

- Step 7: Calculate the elements of the nodal Jacobi matrix (J) given by,

$$J^o = \begin{bmatrix} \frac{\partial f_1}{\partial pr_1} & \frac{\partial f_1}{\partial pr_2} & \dots & \frac{\partial f_1}{\partial pr_n} \\ \frac{\partial f_2}{\partial pr_1} & \frac{\partial f_2}{\partial pr_2} & \dots & \frac{\partial f_2}{\partial pr_n} \\ \vdots & \vdots & \ddots & \vdots \\ \frac{\partial f_n}{\partial pr_1} & \frac{\partial f_n}{\partial pr_2} & \dots & \frac{\partial f_n}{\partial pr_n} \end{bmatrix}_{Pr=Pr^0} \quad (6.12)$$

Where, Pr - vector of nodal pressures.

The Jacobian matrix is derived as shown in (Osiadacz, 1987),

$$J^o = -A_1 D (A_1)^t \quad (6.13)$$

where,

- A_1 -Reduced branch nodal incidence matrix for gas network
 - $(A_1)^t$ - transpose of A_1
 - $D = \text{diag}\left(\frac{1}{2} \frac{\dot{V}_{(k)}}{\Delta Pr_{(k)}}\right)$ for $k = 1, \dots, n_{\text{gas pipe}}$
- **Step 8:** Calculate the correction for nodal pressure by solving the following,

$$\Delta Pr^o = -(J^o)^{-1} F(Pr^o) \quad (6.14)$$

where,

$$\Delta Pr^o = \begin{cases} \Delta pr_1 \\ \Delta pr_2 \\ \vdots \\ \Delta pr_{n_{\text{gas}}} \end{cases} : \text{Vector of nodal gas pressure error}$$

$$F(Pr^o) = \begin{cases} f_1(Pr^o) \\ f_2(Pr^o) \\ \vdots \\ f_n(Pr^o) \end{cases} : \text{Nodal imbalances at each node in equation (6.11).}$$

- **Step 9:** Apply the correction and determine the nodal pressures for the next iteration

$$Pr^1 = Pr^0 + \Delta Pr^o \quad (6.15)$$

Repeat the iterations from step 3 until the imbalances $F(P_r^k)$ are less than a specified tolerance. The flow chart of the solution method is shown in Figure 6-2

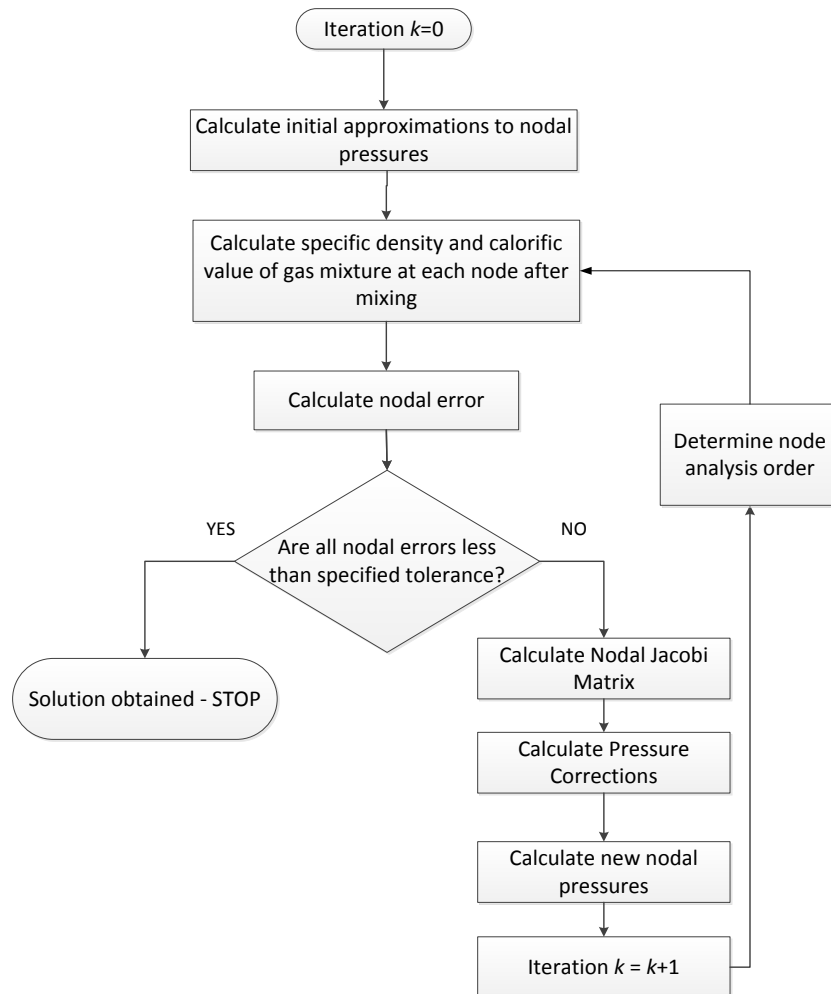


Figure 6-2: Flow chart for the Method

The calculation steps of the method are illustrated using an example shown in Appendix C.1.

6.5 Case study

Figure 6-3 shows the schematic of a gas network used to analyse the impact of alternative gas injections.

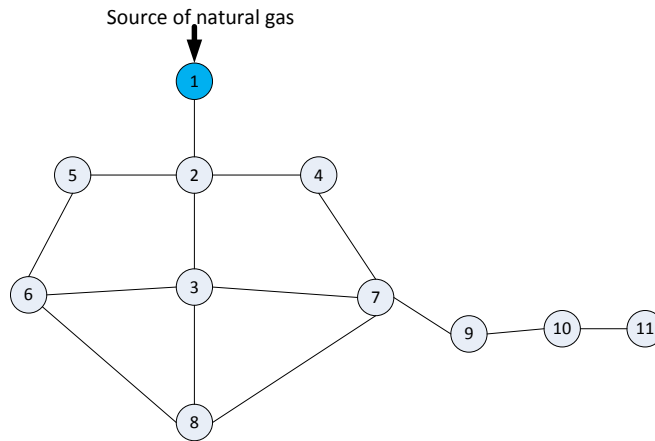


Figure 6-3: Case study network

The meshed network is connected to the main natural gas infeed at node 1. The pressure at Node 1 is 75mbar in all scenarios. The feeder from Node 7 (Node 7 → 9 → 10 → 11) represents an extended branch of the gas network. Nodes 2, 3, 4, 5, 6, 8 are gas load nodes. Pipe parameters i.e. pipe diameter, pipe length and pipe roughness are included in the Appendix C.2. The energy demand at each node is shown in Table 6-2.

The steady state cases analysed are described in Table 6-3. Case 1 establishes a baseline by simulating the network with natural gas as the only source of gas supply at Node 1. The 2nd and 3rd case studies analyse the steady state parameters in the gas network with hydrogen enriched natural gas (10% Hydrogen) and an upgraded biogas mixture as the main source of gas supply at Node 1. The 4th and 5th case studies simulate the network with distributed injection of hydrogen and upgraded biogas at Node 12, while maintaining the infeed of natural gas as the balancing supply at Node 1.

Table 6-2: Gas demand data

Node number	Energy demand (kJ/s)	Natural gas demand (m ³ /hr)
1 (Source Node)	0	0
2	2500	219
3	2200	192
4	2000	175
5	2600	228
6	1800	157
7	500	43.8
8	2350	206
9	550	48
10	475	42
11	350	30

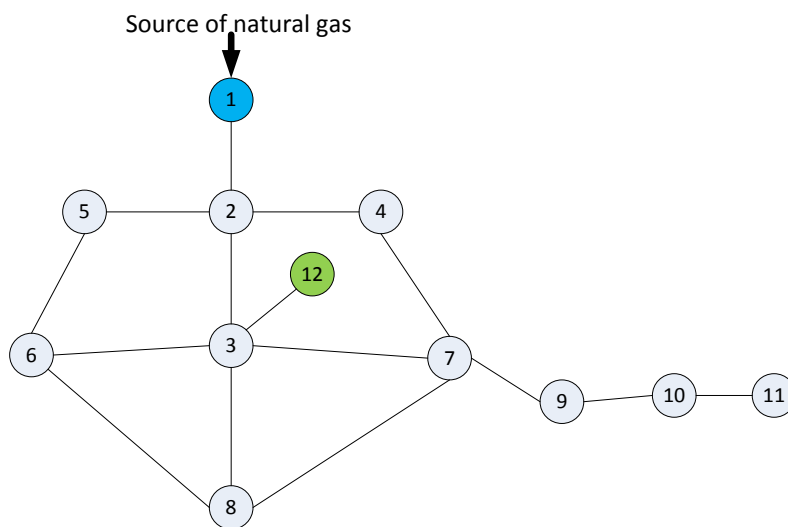


Figure 6-4: Case study network with distributed injection of alternative gases at node 12

The gas demand in case studies is formulated in two different ways,

- Method A - gas demands are calculated assuming the calorific value of natural gas across the network
- Method B - gas demands are calculated considering the calorific value of the gas at each node computed using the proposed method

Table 6-3: Case studies

Case study	Description	Method of gas demand formulation	
		A	B
1	Conventional natural gas supply at Node 1	✓	
2	10% hydrogen in the natural gas blend supplied at Node 1 (Hydrogen enriched natural gas)	✓	✓
3	Upgraded biogas supplied at Node 1	✓	✓
4	200kj/s Hydrogen injected at Node 12	✓	✓
5	200kj/s upgraded Biogas injected at Node 12	✓	✓

The gas mixture compositions in case studies are shown in Table 6-4.

Table 6-4: Molar fractions of gases in mixtures used for case studies

	Natural gas	Hydrogen enriched Natural Gas blend	Upgraded biogas	Hydrogen Injected @ Node 12
CH₄	0.9	0.81	0.94	-
C₂H₆	0.06	0.054	0	-
C₃H₈	0.01	0.009	-	-
C₄H₁₀	0.001	0.009	-	-
CO₂	0.005	0.0045	0.025	-
N₂	0.02	0.018	0.025	-
H₂	-	0.1	0.005	1
Other	-	-	0.005	-
GCV (MJ/m³)	41.04	37.06	37.40	12.75
SG	0.6048	0.545	0.58	0.0696
WI (MJ/m³)	52.77	50.2	49.1	48.33

6.6 Results

6.6.1 Case 1 simulation results – Baseline

Table 6-5 shows the results for Case 1, including the nodal gas pressure, gas flow rate in each branch and the no of iterations for solution. This is the baseline case to which other simulation results are compared. Figure 6-5 illustrates the gas flow pattern in the network.

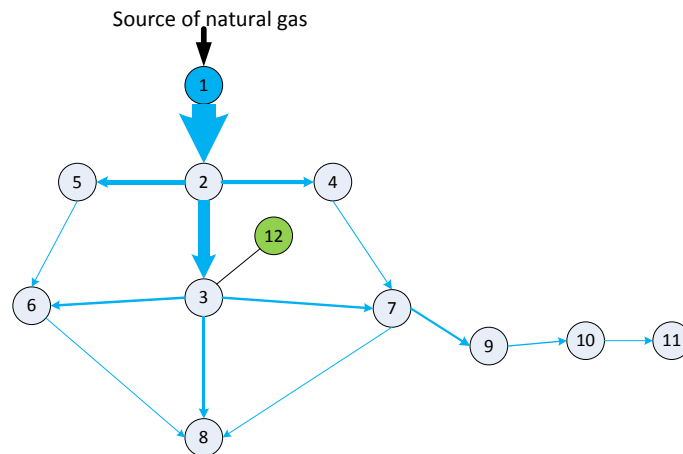


Figure 6-5: Gas flow pattern in case 1 (Width of arrow is proportional to flow rate)

Table 6-5: Steady state simulation results for case 1

Node	Pressure (mbar)	Branch	From - To	Flow rate (m ³ /hr)
1	75	1	1-2	1344
2	66.09	2	2-3	627.37
3	46.68	3	2-4	233.10
4	46.95	4	2-5	264.47
5	41.45	5	3-6	139.91
6	38.40	6	3-7	132.10
7	39.30	7	3-8	162.39
8	37.39	8	5-6	36.41
9	28.15	9	4-7	57.67
10	24.14	10	6-8	18.43
11	23.42	11	7-8	25.31
		12	7-9	120.61
		13	9-10	72.36
		14	10-11	30.70

Minimum pressure observed under steady state is 23.4mbar at Node 11. Minimum flow rate of 18.4m³/hr is observed in the branch connecting Node 6 to Node 8.

6.6.2 Case 2 & 3 simulation results – Impact of an alternative gas mixture

Table 6-6 shows the simulation results of nodal gas pressure for Case 2 and Case 3.

Table 6-6: Results for Case 2 and 3 simulations

Node no.	Pressure (mbar)				
	Ref	Hydrogen enriched natural gas mixture		Upgraded biogas mixture	
		Method A	Method B	Method A	Method B
1	75	75	75	75	75
2	66.09	66.88	65.63	66.41	64.65
3	46.68	49.18	45.22	47.70	42.12
4	46.95	49.43	45.50	47.96	42.43
5	41.45	44.42	39.72	42.66	36.05
6	38.40	41.64	36.52	39.72	32.52
7	39.30	42.46	37.42	40.59	33.53
8	37.39	40.71	35.45	38.74	31.34
9	28.16	32.30	25.74	29.84	20.62
10	24.14	28.64	21.53	25.97	15.96
11	23.42	27.99	20.77	25.28	15.13

Figure 6-6 shows the pressure gradient from node 1 to node 11 in case studies 2 and 3. It shows the effect of an alternative gas mixture and the method used for modelling gas demand on steady state nodal pressure.

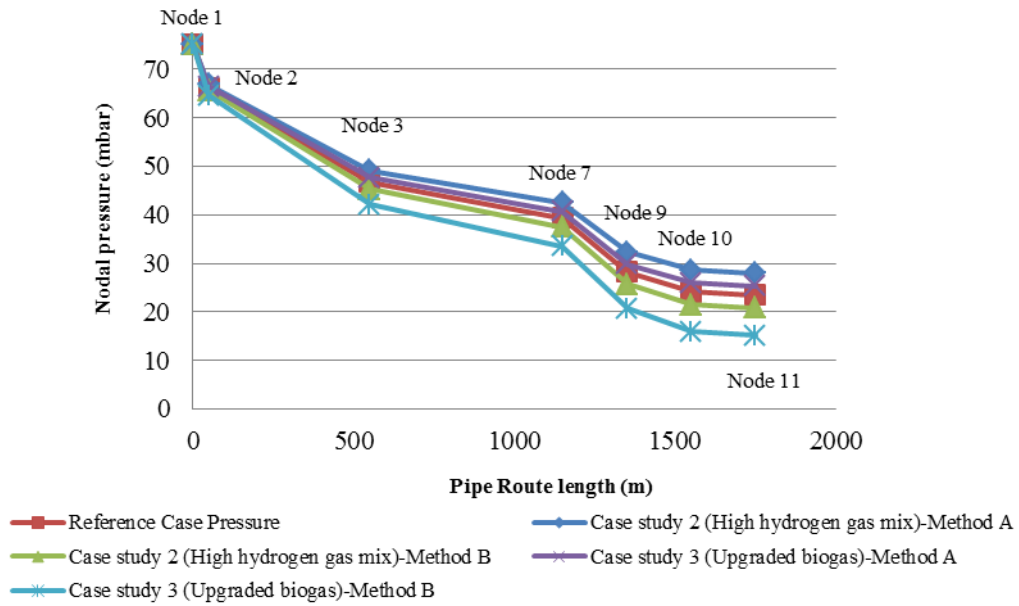


Figure 6-6: Pressure gradient plot from Node 1 to Node 11 -Case studies 2 and 3

When method A is used for modelling the gas demands, gas pressure delivered show an increase (compared to case 1) in both cases 2 and 3. This is due to the lower relative density of both the hydrogen enriched natural gas and upgraded biogas compared to the natural gas mixture in case 1. As the gas demand remains the same as the baseline case in method A, the pressure drop in each branch is reduced due to lower relative density of the gas mixture (see equation (6.4)).

Hydrogen enriched natural gas mixture and upgraded biogas both have a lower calorific value compared to the baseline natural gas mixture (see Table 4). Therefore, the gas demands calculated in method A does not meet the energy requirements at nodes. Table 6-7 shows the energy available at nodes when method-A was used in cases 2 and 3.

Table 6-7: Energy available at nodes in cases 2 & 3 - method A

Node Number	Actual energy demand (kJ/s)	Available energy at nodes	
		Case 2	Case 3
1(Source Node)	0		
2	2500	2257.80	2278.22
3	2200	1986.87	2004.83
4	2000	1806.25	1822.57
5	2600	2348.12	2369.34
6	1800	1625.62	1640.31
7	500	451.56	455.64
8	2350	2122.34	2141.52
9	550	496.72	501.21
10	475	428.98	432.86
11	350	316.09	318.95

When method B is used to model the gas demand, calorific value of the gas mixture delivered at the node is taken into account. The calorific value of hydrogen enriched natural gas and upgraded biogas is both less than the natural gas mixture used in case 1. Therefore, to meet the same energy demand, gas flow rate at each gas load needs to increase. Due to the increase in gas demand, a drop in nodal pressures is observed compared to the baseline case (see Figure 6-6). Two opposing effects on the nodal pressure calculation occur when method B is used in cases 2 and 3. A higher gas flow rate in pipes tends to increase the pressure drop, while the lower relative density of the gas mixture reduces it. The combined effect is an increase in pressure drops resulting in lower nodal pressures across the network. This shows that, the gas mixture composition and the method of modelling the gas demand has an impact on the final solution in steady state analysis.

6.6.3 Case 4 & 5 simulation results – Impact of distributed injection of an alternative gas

Cases 4 and 5 analyses the distributed injection of an alternative gas at node 12. This results in a varied gas composition in different parts of the network. The variations in gas mixture composition depend on the load distribution and the amount of gas injected. Table 6-8 and Table 6-9 show the simulation results including nodal gas pressure, Wobbe Index at gas nodes, branch flow rates for case 4 and 5.

Table 6-8: Simulation results for case study 4

Node	Method A		Method B		Branch	From - To	Method A	Method B
	Pressure (mbar)	Wobbe Index	Pressure (mbar)	Wobbe Index			Flow rate (m ³ /hr)	Flow rate (m ³ /hr)
1	75.0	52.77	75.0	52.77	1	1-2	1288	1292
2	66.8	52.77	66.3	52.77	2	2-3	584.9	588.6
3	49.9	51.63	47.8	51.67	3	2-4	226.8	227.3
4	48.7	52.77	47.4	52.77	4	2-5	256.7	257.3
5	43.6	52.77	41.9	52.77	5	3-6	145.3	144.9
6	41.7	51.82	39.1	51.88	6	3-7	137.1	136.7
7	42.6	51.94	40.0	51.99	7	3-8	166.0	165.8
8	41.0	51.68	38.1	51.73	8	5-6	28.7	29.2
9	32.1	51.94	28.5	51.99	9	4-7	51.4	51.9
10	28.3	51.94	24.4	51.99	10	6-8	16.1	16.2
11	27.6	51.94	23.7	51.99	11	7-8	24.0	24.1
12	50.0	48.33	47.9	48.33	12	7-9	120.6	120.6
					13	9-10	72.4	72.4
					14	10-11	30.7	30.7
					15	12-3	56.5	56.5

Table 6-9: Simulation results for case study 5

Method A		Method B		Method A		Method B		
Node	Pressure (mbar)	Wobbe Index	Pressure (mbar)	Wobbe Index	Branch From - To	Flow rate (m3/hr)	Flow rate (m3/hr)	
1	75.0	52.77	75.0	52.77	1	1-2	1325	1326
2	66.3	52.77	66.3	52.77	2	2-3	612.1	613.3
3	47.8	52.66	47.8	52.66	3	2-4	231.3	231.5
4	47.4	52.77	47.4	52.77	4	2-5	262.3	262.6
5	42.1	52.77	42.0	52.77	5	3-6	141.4	141.6
6	39.3	52.69	39.3	52.69	6	3-7	133.6	133.8
7	40.2	52.70	40.2	52.70	7	3-8	163.4	163.7
8	38.4	52.67	38.3	52.67	8	5-6	34.2	34.5
9	29.1	52.70	29.0	52.70	9	4-7	55.9	56.1
10	25.1	52.70	25.0	52.70	10	6-8	17.8	17.9
11	24.4	52.70	24.3	52.70	11	7-8	25.0	25.1
12	47.8	48.98	47.8	48.98	12	7-9	120.6	120.8
					13	9-10	72.4	72.5
					14	10-11	30.7	30.8
					15	12-3	19.3	19.3

The impact of distributed gas injection on nodal pressure in case studies 4 and 5 is shown in Figure 6-7. Nodal pressure across the network increases (relative to the baseline case) due to the elevated gas pressure at node 12 and reduced gas flow from node 1.

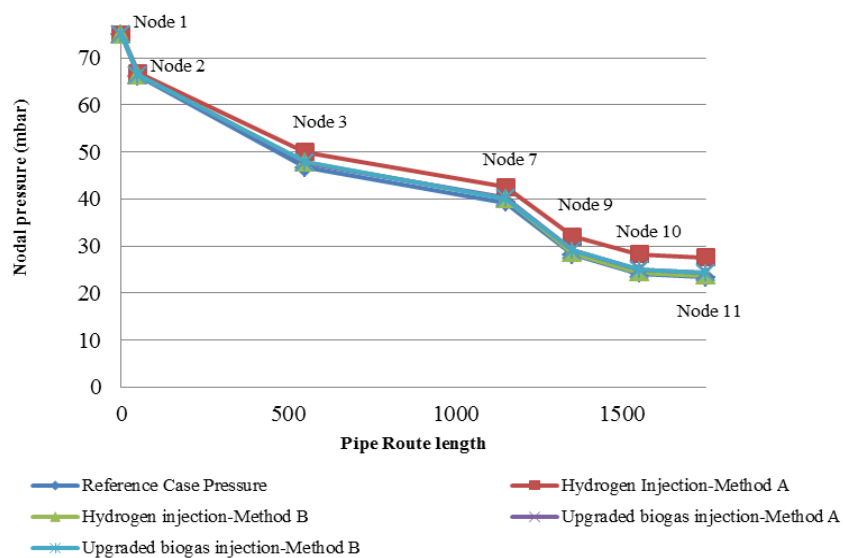


Figure 6-7: Pressure profile plot for case 4 and case 5 (Node 1 to Node 11)

The alternative gas injected at node 12 in case 4 and 5 does not reach gas nodes 1, 2, 4 and 5, due to the flow pattern in the network. However, the gas received at other nodes is a mixture of natural gas from node 1 and the gas injected at node 12. The gas demands calculated using method A does not meet the energy requirements at these nodes. Figure 6-8 shows the unmet energy demand at nodes in cases 4 and 5 when using method A for modelling the gas demand.

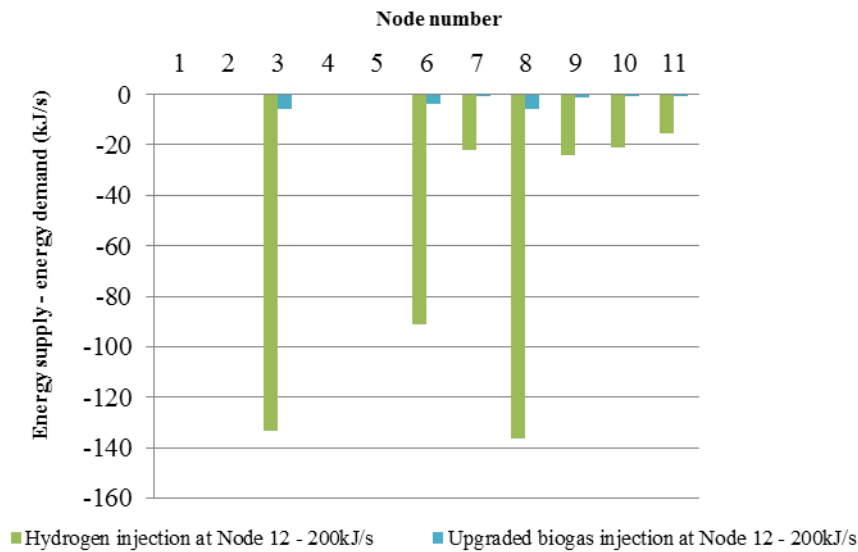


Figure 6-8: Unmet energy demand at gas nodes in case studies 4 and 5 (Method A)

An energy content of 200kJ/s injected at node 12 translates to a gas flow rate of 57 m³/hr and 19.25m³/hr in hydrogen and upgraded biogas. The relatively large unmet energy demand in case 4 is a combined effect of a larger Hydrogen flow rate and the low energy density of Hydrogen (less than 1/3 of natural gas). Upgraded biogas is relatively similar to natural gas in terms of energy density and relative density. Therefore the unmet energy demand in case 5 is comparatively lower.

When method B is used, the gas demand is iteratively calculated depending upon the calorific value of the gas mixture at the particular node. The gas demand increases in nodes where the alternative gas from node 12 is reached due to a reduction in calorific value.

6.7 Discussion

The research work extends the conventional method of steady state simulation of gas networks to a more comprehensive analysis that considers the distributed injection of new gas supply sources. The mathematical model has shown good convergence characteristics. In all case studies, the number of iterations required to reach an error tolerance of 0.01 (m^3/hr) was less than 12. However, real gas network models simulate a much larger number of nodes and branches (Banda and Herty, 2008, Brkić, 2009, Chaudry et al., 2008). Further studies need to be undertaken to test the performance of the numerical solution technique applied to more complex networks.

Conventional gas network analysis methods use natural gas flow rate as a proxy to energy demand at gas load sites. As the case studies show, gas flow rate alone is not sufficient to ensure the supply of energy requirements when the gas composition varies.

The case studies show that the injection of alternative gases in gas mains has an impact on pressure and the gas quality (i.e. Wobbe index, Calorific value, relative density) delivered to final consumers. If managed within limits these changes may be tolerated by the gas appliances. Further theoretical and experimental studies on the impact of alternative gas compositions and varying pressure input on gas appliance performance and network durability is required. If it is found that alternative gas injections can be tolerated by local gas networks without serious concerns, it would improve the economic viability of many projects that would otherwise not be feasible. This is particularly the case for power to gas plants and many anaerobic digester installations where the regulations for gas injections are restrictive. This will allow more renewable gas to be utilised.

6.8 Chapter Summary

Studies of gas networks needs to take account the impact of utilizing a diversity of gas supply sources. This research work presents a method developed for the steady state analysis of gas networks with centralized and decentralized alternative gas sources. Two methods of modelling the gas demand are compared. A case study was carried out to analyse the impact of alternative gas injections on pressure delivery and gas quality in the network. The method of modelling the gas demand is shown to have an impact on the final simulation results. Further work is required to understand the implications of each method of formulating the gas flow problem.

Chapter 7: Conclusions and future work

This chapter provides an overview of the research undertaken, the conclusions and recommendations for future work.

7.1 Conclusions of the work

The overall aim of this research is to develop a comprehensive model for the steady state simulation and optimal operation planning of integrated energy supply systems. As parts of this the following objectives were set out,

- To review the existing literature on the available methods for analysing integrated energy systems
- To analyse the optimal power dispatch in an integrated energy supply system
- To develop a method for the simultaneous steady state analysis of an integrated electricity, gas, district heating and district cooling network system
- To develop a method for the steady state analysis in gas networks with distributed injection of alternative gases

The conclusions of the work are summarised below.

7.1.1 Review of the benefits, analysis methods, research gaps and challenges in integrated energy systems research

A review of the literature on integrated energy systems was undertaken to identify the benefits and the methods used for the analysis of integrated energy systems. The potential benefits were identified as,

- Reduce the use of primary energy
- Increase the generation and utilisation of renewable energy
- Reduce/delay capital expenditure
- Provide cost effective flexibility in the electrical power system

- Enhance opportunities for business innovation
- Increase reliability of the electrical power system (e.g. security of supply)
- Facilitate low carbon sustainable districts and local governance of community projects

It was recognized that further research and development supported by the implementation of live projects are necessary to understand the real challenges of unlocking the potential benefits of integrated energy systems.

Recently, there is a significant interest primarily in the scientific community to develop methods and tools for the analysis of integrated energy systems. These were reviewed in detail in Chapter 2 and are categorised as used for,

- Coupled energy network modelling and simulation
- Operation planning and control (e.g. optimization, demand response)
- Techno-economic and environmental performance analysis
- Design and expansion planning
- Reliability analysis of integrated energy systems

It was recognized that (among others) a modelling tool for the combined steady state simulation and the optimal operation planning of integrated energy systems was not established and its development is explored in this thesis.

7.1.2 Optimal power dispatch in integrated energy systems

The method of mathematical formulation and the analysis of results of optimal power dispatch in a real integrated energy supply system were studied.

The energy supply system at the University of Warwick was used as a case study. The optimization problem was solved using MATLAB software. Real energy demand data was used for the analysis. The data showed significant seasonal variation of the heating demand

from the summer to winter period. The electricity demand showed relatively regular weekly oscillations. An analysis of the frequency of occurrence for electricity and heat demand combinations identified times of common demand. These were used to formulate four load scenarios representing the seasonal demand variations which were analysed in detail. Simulations were also carried out for the complete range of electricity and heat demand combinations in the case system.

The optimal power dispatch analysis shows that valuable insights to the design and optimal operation of an energy supply system are realised through an integrated approach to energy systems analysis. A strategy for the utilisation of energy conversion units and grid energy imports for different load combinations in the case system was recommended.

It was shown that the CHP unit is a key component in the optimal design and operation of the integrated energy supply system. The use of the CHP unit was shown to be cost-effective compared to the use of grid electricity and a gas boiler for the supply of heat. The CHP unit output is fixed by the electricity or the heating demand in the system. The cooling supply system comprising of an electric chiller and an absorption chiller was used as a source of flexibility when operation of the CHP unit was constrained. The electric chiller and the absorption chiller are used to facilitate the maximum utilisation of the CHP unit while meeting the cooling demand.

The marginal costs of different energy outputs were also analysed. The analysis showed that during particular load combinations the system would benefit from additional heat or cooling demands and the use of thermal storage in the system. It was also shown that the system would also benefit from an electricity export contract that would allow the optimal use of the CHP unit. Further studies were suggested for investment analysis considering the costs of implementation and the time varying nature of the energy demands.

This study demonstrates the value of considering the overall energy system and the interactions between different energy systems in design and operation planning to achieve the most economic energy system.

7.1.3 Simultaneous steady state analysis of coupled energy systems

A method for the simultaneous steady state analysis of a coupled electricity, gas, district heating and district cooling system was developed. The method of formulating network analysis equations considering the interactions between different energy carrier systems was presented. The set of non-linear equations was solved using the Newton-Raphson method. The mathematical model was implemented in MATLAB software. An example was used to illustrate the formulation of equations and the steps of the iterative solution method. The results of the steady state simulation were validated using commercial software used for power flow analysis of individual energy networks.

Case studies were carried out to demonstrate the application of the method for integrated energy network analysis. Case studies were designed to analyse the impact of coupling component operation and the varying energy demand levels on the state of energy networks. The converged steady state parameters for the different case studies were analysed. The energy exchanges between networks and the distribution energy losses in different case studies were also discussed.

All simulations showed good convergence characteristics and with considerable speed.

7.1.4 Gas network analysis with distributed injection of alternative gas types

A method for the steady state analysis of gas networks with injection of alternative gas types was developed. The method extends the well-established Newton-nodal method for gas network analysis to analyse networks with injections of alternative gas types. An

example was used to illustrate the formulation of equations and the steps of the iterative solution method.

A case study was carried out to illustrate the impact of alternative gas injections on the steady state gas flow parameters. Two methods of formulating the gas demand were compared. It was shown that the injection of alternatives gases in gas mains has an impact on pressure and the gas quality (i.e. Wobbe index, Calorific value, relative density) delivered to final consumers. It was also shown that the method of modelling the gas demand has an impact on the final simulation results.

The mathematical model has shown good convergence characteristics. In all case studies, the number of iterations required to reach an error tolerance of 0.01 (m³/hr) was less than 12.

7.2 Contributions of the thesis

- The benefits of energy systems integration were identified and qualitatively described with examples.
- A review of the state of the art in analysis methods in integrated energy systems analysis was presented and the research gaps and challenges were identified.
- A real world case study for the optimal power dispatch in an integrated energy system was presented. The potential ways for improving the energy system were identified and possible solutions were discussed.
- A method for simultaneous power flow analysis in a coupled electricity, gas, district heating and district cooling system was developed. A novel method of solving the equations based on the Newton-Raphson method was developed and demonstrated using an example calculation. The model was validated by comparing the results with the outputs from commercial software.

- A method for the steady state analysis of gas networks with centralized and decentralized alternative gas sources was developed. A case study was carried out to demonstrate the impact of alternative gas injections on the pressure delivery and gas quality in the network.

7.3 Future work

The work carried out in the thesis lays the foundation for the development of a model for the combined steady state simulation and operation planning of integrated energy supply systems. A schematic of the proposed model structure shown in section 1.4 is reproduced below.

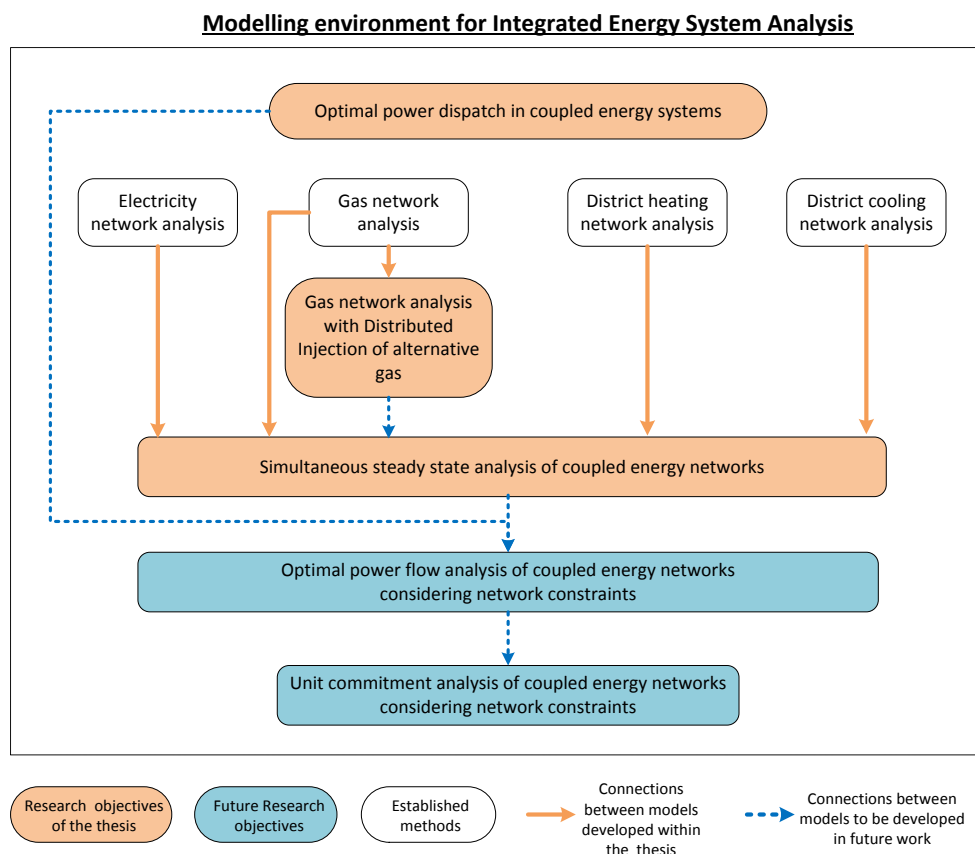


Figure 7-1: Proposed modelling environment for integrated energy systems analysis

The proposed future research works are,

- To incorporate the improved model for gas network analysis with the model for simultaneous steady state analysis of a coupled energy network system. This would allow analysis of the impact of technologies such as power to gas which interconnects electricity and gas networks.
- To extend the optimal power dispatch analysis to incorporate network constraints.
- To extend the optimal power dispatch analysis for multi time period optimization of integrated energy systems. The energy storage elements constitute an important aspect of integrated energy systems and this tool could be developed to incorporate energy storage components in different energy vectors.
- To develop a modelling tool for optimal unit commitment considering transmission system constraints in an integrated energy system.

References

- 21ST CENTURY POWER PARTNERSHIP. 2014. *Flexibility in 21st century power systems* [Online]. Available: <http://www.nrel.gov/docs/fy14osti/61721.pdf> [Accessed 10th April 2016].
- ABEYSEKERA, M. & WU, J. 2015. Method for Simultaneous Power Flow Analysis in Coupled Multi-vector Energy Networks. *Energy Procedia*, 75, 1165-1171.
- ABEYSEKERA, M., WU, J. & JENKINS, N. 2016a. Integrated energy systems: An overview of benefits, analysis methods, research gaps and opportunities. *HubNET position paper series*. HubNET. Available: <http://www.hubnet.org.uk/filebyid/791/InteEnergySystems.pdf>. [Accessed 10th September 2016]
- ABEYSEKERA, M., WU, J., JENKINS, N. & REES, M. 2016b. Steady state analysis of gas networks with distributed injection of alternative gas. *Applied Energy*, 164, 991-1002.
- ACHA, S., GREEN, T. C. & SHAH, N. Techno-economical tradeoffs from embedded technologies with storage capabilities on electric and gas distribution networks. Power and Energy Society General Meeting, 2010 IEEE, 25-29 July 2010 2010. 1-8.
- ACHA, S. & HERNANDEZ-ARAMBURO, C. Integrated modelling of gas and electricity distribution networks with a high penetration of embedded generation. SmartGrids for Distribution, 2008. IET-CIRED. CIRED Seminar, 23-24 June 2008 2008. 1-4.
- ALLEGRI, J., OREHOUNIG, K., MAVROMATIDIS, G., RUESCH, F., DORER, V. & EVINS, R. 2015. A review of modelling approaches and tools for the simulation of district-scale energy systems. *Renewable and Sustainable Energy Reviews*, 52, 1391-1404.
- APPLIED ENERGY. 2015. *Special Issue on "Integrated Energy Systems"* [Online]. ELSEVIER. Available: <http://www.journals.elsevier.com/applied-energy/call-for-papers/special-issue-on-integrated-energy-systems/>.
- ARNOLD, M., KIENZLE, F. & ANDERSSON, G. 2008a. Distributed Control Applied to Multi-Energy Generation Portfolios. *Smart Energy Strategies: Meeting the Climate Change Challenge*. Energy Science Center ETH Zurich.
- ARNOLD, M., NEGENBORN, R. R., ANDERSSON, G. & DE SCHUTTER, B. 2008b Distributed control applied to combined electricity and natural gas infrastructures. Infrastructure Systems and Services: Building Networks for a Brighter Future (INFRA), 2008 First International Conference on, 10-12 Nov.. 1-6.
- ARNOLD, M., NEGENBORN, R. R., ANDERSSON, G. & DE SCHUTTER, B. Model-based predictive control applied to multi-carrier energy systems. Power & Energy Society General Meeting, 2009. PES '09. IEEE, 26-30 July 2009 2009. 1-8.
- ARNOLD, M., NEGENBORN, R. R., ANDERSSON, G. & DE SCHUTTER, B. 2010. Distributed Predictive Control for Energy Hub Coordination in Coupled Electricity and Gas Networks. In: NEGENBORN, R. R., LUKSZO, Z. & HELLENDORF, H. (eds.) *Intelligent Infrastructures*. Springer, Dordrecht, Netherlands.
- ARTECONI, A., HEWITT, N. J. & POLONARA, F. 2012. State of the art of thermal storage for demand-side management. *Applied Energy*, 93, 371-389.
- BAGDANAVICIUS, A., JENKINS, N. & HAMMOND, G. P. 2012. Assessment of community energy supply systems using energy, exergy and exergoeconomic analysis. *Energy*, 45, 247-255.

- BAKKEN, B. H., SKJELBRED, H. I. & WOLFGANG, O. 2007. eTransport: Investment planning in energy supply systems with multiple energy carriers. *Energy*, 32, 1676-1689.
- BANDA, M. K. & HERTY, M. 2008. Multiscale modeling for gas flow in pipe networks. *Mathematical Methods in the Applied Sciences*, 31, 915-936.
- BRKIĆ, D. 2009. An improvement of Hardy Cross method applied on looped spatial natural gas distribution networks. *Applied Energy*, 86, 1290-1300.
- BRODECKI, L., TOMASCHEK, J., FAHL, U. & ALONSO, J. 2014. *Synergies in the integration of energy networks for electricity, gas, heating and cooling* [Online]. INSIGHT_E. Available: http://insightenergy.org/ckeditor_assets/attachments/37/rreb1.pdf [Accessed 20th September 2016].
- CAGNON, F., MEUNIER, P. & MARQUER, O. Gas interchangeability: How Europe deals with it? Natural Gas Technologies II: Ingenuity and Innovation, 8 February 2004 through 11 February 2004 2004 Phoenix, AZ; United States;.
- CARDELL, J. B. Distributed resource participation in local balancing energy markets. 2007 IEEE POWERTECH Lausanne. 510-515.
- CARPANETO, E., CHICCO, G., MANCARELLA, P. & RUSSO, A. 2011a. Cogeneration planning under uncertainty. Part I: Multiple time frame approach. *Applied Energy*, 88, 1059-1067.
- CARPANETO, E., CHICCO, G., MANCARELLA, P. & RUSSO, A. 2011b. Cogeneration planning under uncertainty. Part II: Decision theory-based assessment of planning alternatives. *Applied Energy*, 88, 1075-1083.
- CARY, R. 2012. *The future of gas power: Critical market and technology issues* [Online]. London 2012: Green Alliance. Available: http://www.green-alliance.org.uk/page_46.php [Accessed 14th May 2016].
- CHAUDRY, M., JENKINS, N., QADRAN, M. & WU, J. 2014. Combined gas and electricity network expansion planning. *Applied Energy*, 113, 1171-1187.
- CHAUDRY, M., JENKINS, N. & STRBAC, G. 2008. Multi-time period combined gas and electricity network optimisation. *Electric Power Systems Research*, 78, 1265-1279.
- CHAUDRY, M., WU, J. & JENKINS, N. 2013. A sequential Monte Carlo model of the combined GB gas and electricity network. *Energy Policy*, 62, 473-483.
- CHICCO, G. & MANCARELLA, P. 2009. Matrix modelling of small-scale trigeneration systems and application to operational optimization. *Energy*, 34, 261-273.
- CIPRIANI, G., DI DIO, V., GENDUSO, F., LA CASCIA, D., LIGA, R. & MICELI, R. 2013. Perspective on hydrogen energy carrier and its automotive applications. *International Journal of Hydrogen Energy*, 39, 8482-8494.
- CLEGG, S. & MANCARELLA, P. Integrated electrical and gas network modelling for assessment of different power-and-heat options. Power Systems Computation Conference (PSCC), 18-22 Aug. 2014 2014. 1-7.
- CLEGG, S. & MANCARELLA, P. 2015. Integrated Modeling and Assessment of the Operational Impact of Power-to-Gas (P2G) on Electrical and Gas Transmission Networks. *IEEE Transactions on Sustainable Energy*, 6, 1234-1244.
- CONNOLLY, D., LUND, H., MATHIESEN, B. V. & LEAHY, M. 2010. A review of computer tools for analysing the integration of renewable energy into various energy systems. *Applied Energy*, 87, 1059-1082.

- CONTRERAS, I. & FERNÁNDEZ, E. 2012. General network design: A unified view of combined location and network design problems. *European Journal of Operational Research*, 219, 680-697.
- DE VRIES, H., FLORISSON, O. & TIEKSTRA, G. C. Safe operation of natural gas appliances fueled with hydrogen/natural gas mixtures (progress obtained in the naturalhy-project). International Conference of Hydrogen Safety, 2007 San Sebastian, Spain.
- DECC. 2012a. *Electricity System: Assessment of Future Challenges-Summary* [Online]. Available: <https://www.gov.uk/government/publications/electricity-system-assessment-of-future-challenges> [Accessed 15th June 2016].
- DECC. 2012b. *The Future of Heating: A Strategic Framework for low carbon heat in the UK* [Online]. Available: https://www.gov.uk/government/uploads/system/uploads/attachment_data/file/48574/4805-future-heating-strategic-framework.pdf [Accessed 20th May 2015].
- DECC. 2013a. *The Future of Heating: Meeting the Challenge* [Online]. Available: <https://www.gov.uk/government/publications/the-future-of-heating-meeting-the-challenge> [Accessed 20th June 2016].
- DECC. 2013b. *The Future of Heating: Meeting the Challenge* [Online]. Available: <https://www.gov.uk/government/publications/the-future-of-heating-meeting-the-challenge> [Accessed 28th October 2015].
- DECC. 2014. *Community energy strategy* [Online]. Available: https://www.gov.uk/government/uploads/system/uploads/attachment_data/file/275163/20140126Community_Energy_Strategy.pdf [Accessed 14th June 2016].
- DECC. 2015. *Heat networks delivery funding* [Online]. UK Government. Available: <https://www.gov.uk/government/publications/heat-networks-funding-stream-application-and-guidance-pack> [Accessed 28th October 2015].
- DODDS, P. E. & DEMOULLIN, S. 2013. Conversion of the UK gas system to transport hydrogen. *International Journal of Hydrogen Energy*, 38, 7189-7200.
- DODDS, P. E. & MCDOWALL, W. 2013. The future of the UK gas network. *Energy Policy*, 60, 305-316.
- EERA. 2015. *The EERA Joint Programme in Energy Systems Integration* [Online]. Available: <http://www.eera-set.eu/eera-joint-programmes-jps/energy-systems-integration-2/> [Accessed 20th September 2016].
- ERIKSSON, H. 1994. *Short term operation of district heating system*. PhD thesis, Chalmers University of Technology, Sweden.
- ETI. 2014. *Smart Systems and Heat: Decarbonising heat for UK homes* [Online]. Available: <http://www.eti.co.uk/wp-content/uploads/2015/03/Smart-Systems-and-Heat-Decarbonising-Heat-for-UK-Homes-.pdf> [Accessed 14th September 2016].
- ETI. 2015. *Energy Technologies Institute* [Online]. Available: <http://www.eti.co.uk/> [Accessed 14th August 2016].
- EUROPEAN COMMISSION. 2015a. *Horizon 2020: Work Programme 2016-2017* [Online]. Available: http://ec.europa.eu/research/participants/data/ref/h2020/wp/2016_2017/main/h2020-wp1617-energy_en.pdf [Accessed 14th September 2016].

- EUROPEAN COMMISSION. 2015b. *The Strategic Energy Technology Plan (SET) Plan* [Online]. Available: <https://ec.europa.eu/energy/en/topics/technology-and-innovation/strategic-energy-technology-plan>.
- EUROPEAN POWER TO GAS. 2015. *Power to gas (demonstration) projects in Europe* [Online]. Available: <http://www.europeanpowertogas.com/demonstrations> [Accessed 14th September 2016].
- FAVRE-PERROD, P., GEIDL, M., KLÖCKL, B. & KOEPEL, G. 2005. A vision of future energy networks. *Power Engineering Society Inaugural Conference and Exposition in Africa, 2005 IEEE*.
- FAVRE-PERROD, P., KIENZLE, F. & ANDERSSON, G. 2010. Modeling and design of future multi-energy generation and transmission systems. *European Transactions on Electrical Power*, 20, 994-1008.
- FREDERIKSEN, S. & WERNER, S. 2013. *District heating and cooling*, Lund, Sweden, Studentlitteratur.
- GAHLEITNER, G. 2013. Hydrogen from renewable electricity: An international review of power-to-gas pilot plants for stationary applications. *International Journal of Hydrogen Energy*, 38, 2039-2061.
- GEIDL, M. & ANDERSSON, G. 2006. Operational and structural optimization of multi-carrier energy systems. *European Transactions on Electrical Power*, 16, 463-477.
- GEIDL, M. & ANDERSSON, G. 2007. Optimal Power Flow of Multiple Energy Carriers. *Power Systems, IEEE Transactions on*, 22, 145-155.
- GEIDL, M. & ANDERSSON, G. 2008. Optimal power dispatch and conversion in systems with multiple energy carriers. Available: http://www.eeh.ee.ethz.ch/uploads/tx_ethpublications/pssc_2005_geidl.pdf.
- GEIDL, M., G. KOEPEL, P. FAVRE-PERROD, B. KLÖCKL, G. ANDERSSON, K. FRÖHLICH 2007. Energy hubs for the future. *IEEE Power & Energy Magazine*.
- GOLDFINCH, M. C. 1984. MICROCOMPUTERS SIMULATE NATURAL GAS NETWORKS. *Oil and Gas Journal*, 82.
- GRAINGER, J. J. & STEVENSON JR, W. D. 1994. *Power System Analysis*, McGraw-Hill, Inc.
- GROND, L., SCHULZE, P. & HOLSTEIN, J. 2013. *Systems analyses Power to Gas: A technology review* [Online]. Available: <http://www.northseapowertogas.com/documents>.
- HEATON, C. 2014. *Modelling Low-carbon energy system designs with the ETI ESME Model* [Online]. Available: http://www.eti.co.uk/wp-content/uploads/2014/04/ESME_Modelling_Paper.pdf.
- HELSETH, A. & HOLEN, A. T. Reliability modeling of gas and electric power distribution systems; similarities and differences. Probabilistic Methods Applied to Power Systems, 2006. PMAPS 2006. International Conference on, 11-15 June 2006. 1-5.
- HM GOVERNMENT. December 2011. *Carbon Plan: Delivering our low carbon future* [Online]. Available: <https://www.gov.uk/government/publications/the-carbon-plan-reducing-greenhouse-gas-emissions--2> [Accessed 20th September 2016].
- HORLOCK, J. H. 1987. *Cogeneration-Combined Heat and Power (CHP); Thermodynamics and economics*, Great Britain, A. Wheaton & Co. Ltd., Exeter.
- HOUWING, M., NEGENBORN, R. R. & DE SCHUTTER, B. 2011. Demand Response With Micro-CHP Systems. *Proceedings of the IEEE*, 99, 200-213.

- HSE. 1996. *A guide to the Gas Safety (Management) Regulations 1996* [Online]. Available: <http://www.hse.gov.uk/pubns/priced/l80.pdf> [Accessed 14th June 2015].
- HUBNET. 2015. *HubNet-A Hub for Energy Networks Research* [Online]. Available: <http://www.hubnet.org.uk/> [Accessed 14th July 2016].
- IEA. 2014. *Linking Heat and Electricity Systems* [Online]. Available: <https://www.iea.org/publications/freepublications/publication/LinkingHeatandElectricitySystems.pdf> [Accessed 15th August 2016].
- IEEE 2013. Special Issue on Energy Systems Integration. Energy comes together: The integration of all systems, *IEEE Power and Energy Magazine*, ,11, 5.PP 18-23.
- IET. 2014. *Britains Power System: The case for a system architect* [Online]. Available: <http://www.theiet.org/factfiles/energy/brit-power-page.cfm> [Accessed 13th June 2016].
- IIESI. 2015a. *Educational Opportunities* [Online]. Available: <http://iiesi.org/resources.html> [Accessed 14th August 2016].
- IIESI. 2015b. *Summary of iiESI workshop on energy systems integration research challenges in London* [Online]. Available: <http://iiesi.org/resources.html> [Accessed 15th August 2016].
- INNOVATEUK. 2014. *Localised energy systems - a cross-sector approach* [Online]. Available: <https://interact.innovateuk.org/-/localised-energy-systems-a-cross-sector-approach> [Accessed 14th August 2014].
- INNOVATEUK. 2015a. *Energy Systems Catapult* [Online]. Available: <https://es.catapult.org.uk/> [Accessed 14th August 2016].
- INNOVATEUK. 2015b. *Integrated supply chains for energy systems* [Online]. Available: <https://interact.innovateuk.org/-/integrated-supply-chains-for-energy-systems> [Accessed 14th August 2014].
- ITMPOWER 2013. Power-to-gas: A UK Feasibility study.
- ITRC. 2015. *UK Infrastructure Transitions Research Consortium* [Online]. Available: <http://www.itrc.org.uk/> [Accessed 14th August 2016].
- KEIRSTEAD, J., JENNINGS, M. & SIVAKUMAR, A. 2012. A review of urban energy system models: Approaches, challenges and opportunities. *Renewable and Sustainable Energy Reviews*, 16, 3847-3866.
- KIENZLE, F. & ANDERSSON, G. Location-dependent valuation of energy hubs with storage in multi-carrier energy systems. International Conference on the European Energy Market, 23-25 June 2010 2010.
- KIENZLE, F. & ANDERSSON, G. 2011. Valuing Investments in Multi-Energy Conversion, Storage, and Demand-Side Management Systems Under Uncertainty. *IEEE Transactions on Sustainable Energy*, 2, 194-202.
- KIERSTEAD, J., SAMSATLI, N. & SHAH, N. SYNCITY: An integrated toolkit for urban energy systems modelling. Fifth Urban Research Symposium, 2009.
- KITAPBAYEV, Y., MORIARTY, J. & MANCARELLA, P. 2014. Stochastic control and real options valuation of thermal storage-enabled demand response from flexible district energy systems. *Applied Energy*, 137, 823-831.

- KITAPBAYEV, Y., MORIARTY, J., MANCARELLA, P. & BLOCHLE, M. A real options assessment of operational flexibility in district energy systems. International Conference on the European Energy Market, EEM, 27-31 May 2013 2013.
- KOEPPEL, G. 2007. *Reliability considerations of future energy systems: multi-carrier systems and the effect of energy storage*. PhD, ETH Zurich.
- KOEPPEL, G. & ANDERSSON, G. 2009. Reliability modeling of multi-carrier energy systems. *Energy*, 34, 235-244.
- KRAUSE, T., KIENZLE, F., ART, S. & ANDERSSON, G. Maximizing exergy efficiency in multi-carrier energy systems. Power and Energy Society General Meeting, 2010 IEEE, 25-29 July 2010 2010. 1-8.
- KROPOSKI, B., GARRETT, B., MACMILLAN, S., RICE, B., KOMOMUA, C., O'MALLEY, M. & ZIMMERLE, D. 2012a. Energy Systems Integration: A Convergence of Ideas. NREL.
- KROPOSKI, B., GARRETT, B., MACMILLAN, S., RICE, B., KOMOMUA, C., O'MALLEY, M. & ZIMMERLE, D. 2012b. *Energy Systems Integration: A Convergence of Ideas* [Online]. NREL. Available: <http://www.nrel.gov/docs/fy12osti/55649.pdf>.
- KUSCH, W., SCHMIDLA, T. & STADLER, I. 2012. Consequences for district heating and natural gas grids when aiming towards 100% electricity supply with renewables. *Energy*, 48, 153-159.
- KYRIAKARAKOS, G., DOUNIS, A. I., ROZAKIS, S., ARVANITIS, K. G. & PAPADAKIS, G. 2011. Polygeneration microgrids: A viable solution in remote areas for supplying power, potable water and hydrogen as transportation fuel. *Applied Energy*, 88, 4517-4526.
- KYRIAKARAKOS, G., PIROMALIS, D. D., DOUNIS, A. I., ARVANITIS, K. G. & PAPADAKIS, G. 2013. Intelligent demand side energy management system for autonomous polygeneration microgrids. *Applied Energy*, 103, 39-51.
- LIU, C., SHAHIDEHPOUR, M. & WANG, J. 2011. Coordinated scheduling of electricity and natural gas infrastructures with a transient model for natural gas flow. *Chaos*, 21, 025102.
- LIU, X. 2013. *Combined analysis of electricity and heat networks*. PhD thesis, Cardiff University.
- LIU, X. & MANCARELLA, P. 2015. Modelling, assessment and Sankey diagrams of integrated electricity-heat-gas networks in multi-vector district energy systems. *Applied Energy*.
- LIU, X. & MANCARELLA, P. 2016. Modelling, assessment and Sankey diagrams of integrated electricity-heat-gas networks in multi-vector district energy systems. *Applied Energy*, 167, 336-352.
- MANCARELLA, P., 2012, Distributed multi-generation options to increase environmental efficiency in smart cities, IEEE Power and Energy Society General Meeting. PP 1-8.
- MANCARELLA, P. 2014. MES (multi-energy systems): An overview of concepts and evaluation models. *Energy*, 65, 1-17.
- MANCARELLA, P. & CHICCO, G. 2013a, Integrated energy and ancillary services provision in multi-energy systems. Symposium on Bulk Power System Dynamics and Control (IREP) . August 25-30, 2013, Rethymnon, Greece.
- MANCARELLA, P. & CHICCO, G. 2013b. Real-Time Demand Response From Energy Shifting in Distributed Multi-Generation. *Smart Grid, IEEE Transactions on*, 4, 1928-1938.

- MARTINEZ-MARES, A. & FUERTE-ESQUIVEL, C. R. 2012. A unified gas and power flow analysis in natural gas and electricity coupled networks. *IEEE Transactions on Power Systems*, 27, 2156-2166.
- MEIBOM, P., HILGER, K. B., MADSEN, H. & VINTHER, D. 2013. Energy Comes Together in Denmark: The Key to a Future Fossil-Free Danish Power System. *Power and Energy Magazine, IEEE*, 11, 46-55.
- MENDES, G., IOAKIMIDIS, C. & FERRÃO, P. 2011. On the planning and analysis of Integrated Community Energy Systems: A review and survey of available tools. *Renewable and Sustainable Energy Reviews*, 15, 4836-4854.
- MUNOZ, J., JIMENEZ-REDONDO, N., PEREZ-RUIZ, J. & BARQUIN, J. Natural gas network modeling for power systems reliability studies. Power Tech Conference Proceedings, 2003 IEEE Bologna, 23-26 June 2003 2003. 8 pp. Vol.4.
- NATIONALGRID. 2008. *Gas Transportation Transmission Planning Code* [Online]. Available: <http://www.nationalgrid.com/NR/rdonlyres/4E9A7154-E991-4A51-8219-105817A8E1E3/30742/200810TPCAApprovedv10.pdf> [Accessed 13th September 2016].
- NATURALHY. 2009. *Using the Existing Natural Gas System for Hydrogen* [Online]. Available: <http://www.naturalhy.net/> [Accessed 12th June 2013].
- NESHEIM, S. J. & ERTESVÅG, I. S. 2007. Efficiencies and indicators defined to promote combined heat and power. *Energy Conversion and Management*, 48, 1004-1015.
- NIEMI, R., MIKKOLA, J. & LUND, P. D. 2012. Urban energy systems with smart multi-carrier energy networks and renewable energy generation. *Renewable Energy*, 48, 524-536.
- NREL. 2015a. *Energy Systems Integration* [Online]. Available: <http://www.nrel.gov/esi/> [Accessed 12th June 2016].
- NREL. 2015b. *Energy Systems Integration Facility* [Online]. Available: <http://www.nrel.gov/esif/> [Accessed 10th September 2016].
- OFGEM. 2015. *Network Innovation* [Online]. Available: <https://www.ofgem.gov.uk/network-regulation-riio-model/network-innovation> [Accessed 10th September 2016].
- OLANREWAJU, O. T., CHAUDRY, M., QARDAN, M., WU, J. & JENKINS, N. 2015. Vulnerability assessment of the European natural gas supply. *Proceedings of the Institution of Civil Engineers - Energy*, 168, 5-15.
- ÖNEY, F., VEZIROLU, T. N. & DÜLGER, Z. 1994. Evaluation of pipeline transportation of hydrogen and natural gas mixtures. *International Journal of Hydrogen Energy*, 19, 813-822.
- OSIADACZ, A. J. 1987. *Simulation and analysis of gas networks*, Bristol, J.W. Arrowsmith Ltd.
- OSIADACZ, A. J. 1988a. Comparison of numerical methods for steady state simulation of gas networks. *Civil Engineering Systems*, 5, 25-30.
- OSIADACZ, A. J. 1988b. Method of steady-state simulation of a gas network. *International Journal of Systems Science*, 19, 2395-2405.
- PATEL, S. 2012. Progress for Germany's power-to-gas drive. *Power*, 156.
- PETER SCHLEY, J. S., ANDREAS HIELSCHER. Gas Quality Tracking in Distribution Grids. IGRC, 2011 Seoul.

- PYE, S., SABIO, N. & STRACHAN, N. 2015. An integrated systematic analysis of uncertainties in UK energy transition pathways. *Energy Policy*, 87, 673-684.
- QADRAN, M., ABEYSEKERA, M., CHAUDRY, M., WU, J. & JENKINS, N. 2015. Role of power-to-gas in an integrated gas and electricity system in Great Britain. *International Journal of Hydrogen Energy*, 40, 5763-5775.
- QADRAN, M., CHAUDRY, M., WU, J., JENKINS, N. & EKANAYAKE, J. 2010. Impact of a large penetration of wind generation on the GB gas network. *Energy Policy*, 38, 5684-5695.
- QADRAN, M., WU, J., JENKINS, N. & EKANAYAKE, J. 2014. Operating strategies for a gb integrated gas and electricity network considering the uncertainty in wind power forecasts. *IEEE Transactions on Sustainable Energy*, 5, 128-138.
- QIN, C. K. & WU, Z. J. 2009. Natural gas interchangeability in Chinese urban gas supply system. *Natural Gas Industry*, 29, 90-93.
- RAMIREZ-ELIZONDO, L., VELEZ, V. & PAAP, G. C. A technique for unit commitment in multiple energy carrier systems with storage. Environment and Electrical Engineering (EEEIC), 2010 9th International Conference on, 16-19 May 2010 2010. 106-109.
- RAMIREZ-ELIZONDO, L. M. & PAAP, G. C. Unit commitment in multiple energy carrier systems. North American Power Symposium (NAPS), 2009, 4-6 Oct. 2009 2009. 1-6.
- RAMÍREZ-ELIZONDO, L. M. & PAAP, G. C. 2015. Scheduling and control framework for distribution-level systems containing multiple energy carrier systems: Theoretical approach and illustrative example. *International Journal of Electrical Power & Energy Systems*, 66, 194-215.
- RAMIREZ-ELIZONDO, L. M., PAAP, G. C., AMMERLAAN, R., NEGENBORN, R. R. & TOONSEN, R. 2013. On the energy, exergy and cost optimisation of multi-energy-carrier power systems. *International Journal of Exergy*, 13, 364-386.
- RASTETTER, R. W.-G. A. 2013. Power to Gas: The Final Breakthrough for the Hydrogen Economy? *Green*, Volume 3, Pages 69–78.
- REES, M. T., WU, J., JENKINS, N. & ABEYSEKERA, M. 2014. Carbon constrained design of energy infrastructure for new build schemes. *Applied Energy*, 113, 1220-1234.
- REZAI, B. & ROSEN, M. A. 2012. District heating and cooling: Review of technology and potential enhancements. *Applied Energy*, 93, 2-10.
- RINALDI, S. M., PEERENBOOM, J. P. & KELLY, T. K. 2001. Identifying, understanding, and analyzing critical infrastructure interdependencies. *Control Systems, IEEE*, 21, 11-25.
- SALDARRIAGA, C. A., HINCAPIÉ, R. A. & SALAZAR, H. 2013. A holistic approach for planning natural gas and electricity distribution networks. *IEEE Transactions on Power Systems*, 28, 4052-4063.
- SALGADO, F. & PEDRERO, P. 2008. Short-term operation planning on cogeneration systems: A survey. *Electric Power Systems Research*, 78, 835-848.
- SCHOUTEN, J. A., MICHELS, J. P. J. & JANSSEN-VAN ROSMALEN, R. 2004. Effect of H₂-injection on the thermodynamic and transportation properties of natural gas. *International Journal of Hydrogen Energy*, 29, 1173-1180.
- SEGELER, G. 1965. *Gas Engineers Handbook*, New York, The Industrial Press.
- SEUNGWON, A., QING, L. & GEDRA, T. W. Natural gas and electricity optimal power flow. Transmission and Distribution Conference and Exposition, 2003 IEEE PES, 7-12 Sept. 2003 2003. 138-143 Vol.1.

- SHABANPOUR-HAGHIGHI, A. & SEIFI, A. R. 2015. An Integrated Steady-State Operation Assessment of Electrical, Natural Gas, and District Heating Networks. *IEEE Transactions on Power Systems*, PP, 1-12.
- SHAHIDEHPOUR, M., FU, Y. & WIEDMAN, T. 2005. Impact of Natural Gas Infrastructure on Electric Power Systems. *Proceedings of the IEEE*, 93, 1042-1056.
- STRBAC, G., AUNEDI, M. & AL., P. D. E. 2012. *Strategic assessment of the role and value of energy storage systems in the UK low carbon energy future* [Online]. Report for Carbon Trust: Energy futures lab, Imperial college London. Available: <https://www.carbontrust.com/media/129310/energy-storage-systems-role-value-strategic-assessment.pdf> [Accessed 10th September 2016].
- UKERC. 2014a. *Energy Strategy Under Uncertainty* [Online]. Available: <http://www.ukerc.ac.uk/programmes/flagship-projects/energy-strategies-under-uncertainty.html> [Accessed 14th July 2016].
- UKERC. 2014b. *Energy Supply Theme* [Online]. Available: <http://www.ukerc.ac.uk/programmes/energy-supply.html> [Accessed 14th June 2016].
- VANDEWALLE, J., KEYAERTS, N. & D'HAESELEER, W. The role of thermal storage and natural gas in a smart energy system. 2012a.
- VANDEWALLE, J., KEYAERTS, N. & D'HAESELEER, W. The role of thermal storage and natural gas in a smart energy system. 9th International Conference on the European Energy Market (EEM), 10-12 May 2012 2012b. 1-9.
- VELEZ, V., RAMIREZ-ELIZONDO, L. & PAAP, G. C. Control strategy for an autonomous energy system with electricity and heat flows. Intelligent System Application to Power Systems (ISAP), 2011 16th International Conference on, 25-28 Sept. 2011 2011. 1-6.
- WEBER, E. J. 1965. Interchangeability of Fuel Gases. *Gas Engineering Handbook*. United States of America: The Industrial Press New York.
- WHOLESEM. 2015. *Whole Systems Energy Modelling Consortium* [Online]. Available: <http://www.wholesem.ac.uk/> [Accessed 10th February 2016].
- WOOD, A. J., WOLLENBERG, B. F. & SHEBLÉ, G. B. 2014. *Power Generation, Operation and Control*, Hoboken, New Jersey: John Wiley & Sons, Inc.
- XU, X., JIA, H., CHIANG, H. D., YU, D. C. & WANG, D. 2015a. Dynamic Modeling and Interaction of Hybrid Natural Gas and Electricity Supply System in Microgrid. *Power Systems, IEEE Transactions on*, 30, 1212-1221.
- XU, X., JIA, H., WANG, D., YU, D. C. & CHIANG, H.-D. 2015b. Hierarchical energy management system for multi-source multi-product microgrids. *Renewable Energy*, 78, 621-630.
- XU, X., JIN, X., JIA, H., YU, X. & LI, K. 2015c. Hierarchical management for integrated community energy systems. *Applied Energy*, 160, 231-243.
- ZACHARIAH, J. L., EGYEDI, T. M. & HEMMES, K. 2007. From natural gas to hydrogen via the Wobbe index: The role of standardized gateways in sustainable infrastructure transitions *The International Journal of Hydrogen Energy*, 32, 1235-1245.

Appendix A: Landscape of research activities in integrated energy systems

The benefits of integrating energy systems have attracted interest from academia, industry and policy makers in different parts of the world. For example, the European Commission's Strategic Energy Technology plan (SET plan) (European Commission, 2015b) highlights the importance of interoperability between different energy networks and a holistic approach to energy system optimisation. In 2013, the US Department of Energy's National Renewable Energy Laboratory (NREL) opened an Energy Systems Integration Facility (ESIF) at a cost of US\$135 million (Kroposki et al., 2012b). In 2013, IEEE Power and Energy Magazine published a special issue in energy systems integration (IEEE, 2013). The Journal of Applied Energy has recently commissioned a special issue titled 'Integrated Energy Systems' dedicated to this particular area of research (Applied Energy, 2015).

A number of titles are used to describe the area such as 'energy systems integration', 'multi-energy -carrier networks', 'multi-vector energy systems' and the 'energy internet'.

A.1 UK research landscape

In the UK, early interest in studying interdependencies of different energy systems was due to its interconnected electricity and natural gas systems. However, the challenges of decarbonising heat, cooling and transport have recently fuelled an interest in the interactions between different energy systems (DECC, 2013a).

Contrary to its earlier emphasis on the electrification of heat (DECC, 2012b), recent UK Government strategy promotes heat networks, particularly in urban areas. The Department of Energy and Climate Change (DECC) published the policy papers 'Future of heating' (DECC, 2013b) and the 'Community energy strategy' (DECC, 2014) which emphasise support for district heating. It is now expected that the gas network will continue to play an important role during the transition to a low carbon energy system with an increased

use of renewable gas (e.g. biogas, synthetic methane). The use of hydrogen as an energy vector for industrial heating and transport has also been highlighted.

The UK has a number of funding mechanisms supporting RD&D in integrated multi-energy systems from an early stage through to demonstration. Figure A.1 shows the main funding organisations and their stages of engagement.

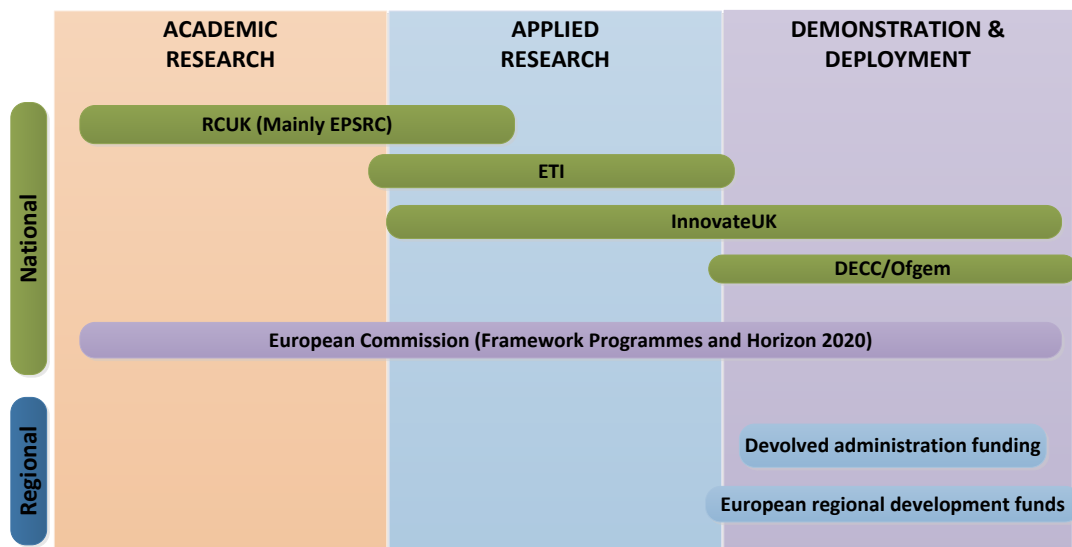


Figure A.1: UK Integrated energy systems research funding programmes from academic research through to demonstration

A.1.1 Academic research in the UK

The Engineering and Physical Sciences Research Council (EPSRC) is the UK’s main agency for funding academic research in engineering and physical sciences. Several of the main projects are listed below.

The UK Energy Research Centre (UKERC) funded by the Research Councils UK (RCUK) Energy programme carried out pioneering work on analysing the interdependencies between GB’s electricity and gas systems (UKERC, 2014b). A modelling tool for the optimisation of GB’s combined gas and electricity network operation (CGEN) was developed through UKERC funding (Chaudry et al., 2008). Ongoing research programmes at

UKERC investigates the interactions, synergies and potential conflicts between electricity, hydrogen and heat vectors at multiple scales of the energy system (i.e. local, national and European).

The HubNet research programme funded by the EPSRC (HubNET, 2015) includes a dedicated research theme for multi-energy systems. The theme aims at developing new modelling and analysis techniques for optimal coordination and planning of integrated energy systems.

The EPSRC Grand Challenge programme Transforming the Top and Tail investigates interactions between different energy vectors at multiple scales of the energy system. For example, the role of European gas supplies in the UK's energy security is being investigated. HubNet and Transforming the Top and Tail projects are collaborations between multiple UK universities and industrial partners.

EPSRC recently funded a research programme titled MY-STORE (Multi-energy storage-social, techno-economic, regulatory and environmental assessment under uncertainty) to investigate the technical, economic, regulatory and environmental performance of multiple forms of energy storage. The project expects to examine opportunities in integrated energy systems to provide energy storage capacity.

Several EPSRC funded whole energy system research consortiums such as ITRC (ITRC, 2015) and WholeSEM (wholeSEM, 2015) are investigating the interaction and interdependencies of national infrastructure such as electricity, gas, transport, water, waste and ICT using detailed models.

A.1.2 Applied Research in the UK

In the UK, the Energy Technologies Institute (ETI) and InnovateUK (previously the Technology Strategy Board) bring together academia, industry and the Government to accelerate the development of low carbon technologies through investment and targeted innovation calls. Integrated energy systems are emerging as a strategic area of interest in both these organizations.

I. Energy Technologies Institute (ETI)

ETI is a public-private partnership between global energy and engineering companies²⁰ and the UK Government (ETI, 2015). Several technology programmes in ETI (Distributed Energy, Smart Systems and Heat, Energy Storage and Distribution) have investigated the role of the electricity, gas and heat sectors in the low carbon transition.

The Smart Systems and Heat programme (SSH) investigates the interactions between different energy vectors and system components in the optimal generation and distribution of heat (ETI, 2014). The SSH programme has recently transitioned to the Innovate UK's Energy Systems Catapult (discussed below). A project under the Energy Storage and Distributed Energy programme titled 'Gas vector pathways development' investigates implications and challenges of transporting novel gases (e.g. hydrogen and synthetic natural gas) through the gas grid.

The Energy System Modelling Environment (ESME) program developed at ETI is a powerful energy system model for the UK (Heaton, 2014). Its whole system scope includes all major flows of energy and interactions between different energy sectors. ESME has been used in a number of research projects including UKERC's 'Energy strategies under uncertainty'(UKERC, 2014a, Pye et al., 2015).

²⁰ The companies part funding ETI are BP, Caterpillar, EDF, Rolls Royce and Shell

II. InnovateUK

InnovateUK brings together academia and industry to realise opportunities in science and technology through targeted funding competitions. It is sponsored by the Department for Business, Innovation and Skills.

The Energy Systems Catapult was set up by InnovateUK to develop a network of specialist companies, and serve as an independent source of specialist knowledge on the transformation of heat, gas and electricity networks (InnovateUK, 2015a). The scope of the Energy Systems Catapult includes system design, interoperability, and integration of ICT, data analytics and storage as well as the integration of electricity, gas and heat networks. The Energy Systems Catapult is to deliver Phase one of the ETI's SSH programme as its first major project for the energy industry. Phase one of the project is to work with three local authorities in the UK (Bridgend, Manchester and Newcastle) to realise local area energy plans.

The following are some of the InnovateUK funding competitions that considered innovation in integrated energy systems within its scope.

- Localised energy systems – a cross sector approach (2014): The competition promoted the integration of different energy systems, at a scale from clusters of buildings up to whole districts. The details of projects funded are available at (InnovateUK, 2014)
- Integrated supply chains for energy systems (2015): The competition invested in innovative projects that addressed the challenges in integration of new energy supply and demand side technologies. The details of projects funded are available at (InnovateUK, 2015b)

- Cities integrated by design – (2015/16): The competition intends to invest in technical feasibility studies that examine integrating new or retrofit infrastructure projects into other urban systems in a beneficial way.
- Energy catalyst – (2015/16): The competition funds projects from early concept stage through to pre-commercial technology validation that incorporates integrated whole-system approaches. The scope of the competition includes electricity and heat networks and their systems integration as a specific theme.

A.1.3 Demonstration projects in the UK

In the UK, demonstration projects traditionally demonstrate the benefits of innovation to an individual energy sector (i.e. electricity, heat or transport). This is largely due to the existing regulatory and market structure that defines clear boundaries between each energy sector. For example, Ofgem's²¹ Network Innovation Competitions (NIC) (Ofgem, 2015) fund electricity and gas network companies independently to deliver innovative projects that can demonstrate benefits to its customers. DECC's Heat Network Delivery Unit (DECC, 2015) provides grant funding and guidance to local authorities to realise heat network schemes.

Nevertheless, a number of demonstration projects that consider multiple energy systems and their interactions have been developed through community initiatives. Support from European regional funding programmes and the Devolved Administrations is evident in the development of demonstration projects.

A.2 European research landscape

The European Commissions' (EC) research and innovation programme Horizon 2020, includes a number of funding calls related to the integration of energy systems. Details of

²¹ Office of gas and electricity markets

the Horizon 2020 work programme for 2016-2017 is available at (European Commission, 2015a). For example, the call for low carbon energy includes a competition to promote technologies, tools and/or services that demonstrate synergies between energy networks (LCE-01-2016-2017).

INSIGHT_E, an energy think tank which informs the EC, published a policy briefing paper in 2014 on the synergies of integrating energy networks for electricity, gas, heating and cooling (Brodecki et al., 2014).

The European Energy Research Alliance (EERA) has initiated the development of a Joint Programme²² focused on energy systems integration (EERA, 2015). The Programme once operational will bring together research organisations in European countries for shared priority setting and collaboration on research projects.

The research programme 'Vision of future energy networks (VoFEN)' led by ETH-Zurich was a pioneering project in developing frameworks and analysis methods in integrated multi-carrier energy systems (Favre-Perrod et al., 2005). The concept of an energy hub was developed and used in methods for economic dispatch, optimal power flow and reliability analysis in integrated energy systems.

Scandinavian countries such as Sweden and Denmark have advanced RD&D in integrated energy systems. They are extensive users of co-generation systems coupled to district heating networks. Denmark for example, has approximately 60% of its heat supplied through district heating systems, a high proportion of wind power (over 30% wind energy on an annual energy balance) and a nationwide natural gas system. The status of RD&D in Denmark is discussed in (Meibom et al., 2013).

²² There are 15 EERA Joint Programmes (JP's) established in a wide range of energy research fields. Joint Programmes are aligned with the priorities defined in the SET-Plan for low carbon technology development.

Germany is undertaking research and development of power-to-gas energy systems. They are driven by the need for balancing high levels of renewable generation and a demand for electricity storage media. A number of power-to-gas demonstration plants are being developed across Germany for various applications as shown in (European Power to Gas, 2015).

A.3 Other activities

The International Institute for Energy Systems Integration (iiESI) was established as a global institute aimed at supporting education, internships and collaboration opportunities in this research area. This was an initiative sponsored by a group of US and European entities including NREL, Pacific Northwest National Laboratory, the Electric Power Research Institute, University College Dublin and Technical University of Denmark. Several educational workshops have been held in the USA and Europe to address concepts of energy systems integration from technical, market and regulatory perspectives. The workshop programmes and presentations from speakers are available at (iiESI, 2015a). The iiESI also organized a workshop on the key research challenges of energy systems integration in March 2015. The workshop brought together an experienced group of international researchers with a diverse range of expertise. Minutes from the workshop are available at (iiESI, 2015b).

NREL's Energy Systems Integration Facility is pursuing research and development that considers interactions between electricity, thermal, fuel, data and information networks (NREL, 2015a). A white paper was published by NREL in 2012 (Kroposki et al., 2012b). The Energy Systems Integration Facility (ESIF) at NREL houses a hardware-in-the-loop system, electrical power system simulator, a thermal distribution system, fuel distribution system, SCADA system and facilities for interconnection and systems integration testing. Details of the facilities at ESIF are available at (NREL, 2015b).

The International Energy Agency (IEA) published a report on the benefits of linking heat and electricity systems through co-generation and district heating and cooling systems. The report is available at (IEA, 2014).

A presentation delivered at the HubNet Smart Grids Symposium 2015, provided an overview of the ongoing research programmes, their objectives and the demonstration activities in integrated energy systems in China. The presentation is available at (HubNET). Integrated energy systems have attracted significant interest in the Chinese government's urban development drive with over £600million R&D funding in 2013.

Appendix B: Steady state analysis of coupled energy networks

B.1 Example of simultaneous steady state analysis of coupled energy networks

An interconnected system of electricity, natural gas, district heat and district cooling networks shown in Figure B-1 is used as an example to illustrate the formulation of equations and the solution method for simultaneous steady state analysis.

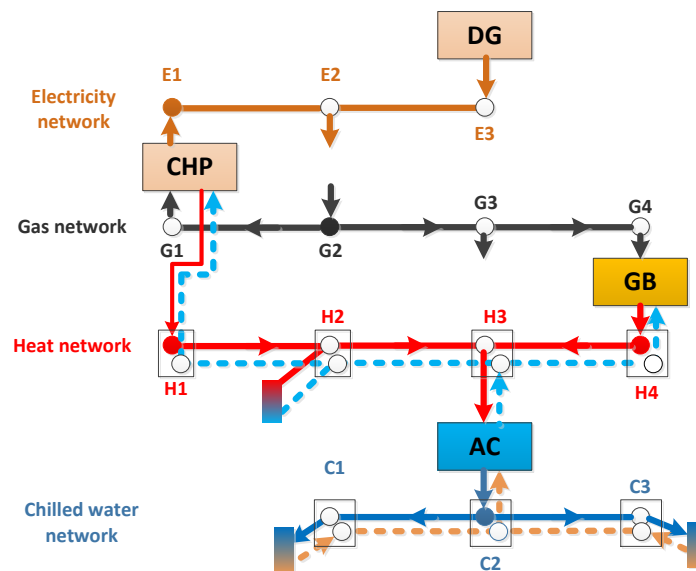


Figure B-1: Schematic of the example system

Data for the network coupling components are shown in Table B-1.

Table B-1: Coupling component data

k	Type	Network Node number				Simulation mode	$C_{C_k,i}^\alpha$	Conversion efficiency
		E	G	DH	DC			
1	CHP	1	1	1	-	Slack node (District Heat)	$C_{C_1,1}^E = +1$ $C_{C_1,1}^G = -1$ $C_{C_1,1}^H = +1$	$\eta_{C_1}^{H/E} = 0.875$ $\eta_{C_1}^{G/E} = 0.35$ $\eta_{C_1}^{G/H} = 0.4$
2	GB	-	4	4	-	Pre-specified heat supply	$C_{C_2,4}^G = -1$ $C_{C_2,4}^H = +1$	$\eta_{C_2}^{G/H} = 0.9$
3	AC	-	-	3	2	Slack node (District Cooling)	$C_{C_3,3}^H = -1$ $C_{C_3,2}^C = +1$	$\eta_{C_3}^{H/C} = 0.65$

The network parameters, the node types and the energy supply and demand data in different networks are shown in Table 5-2 and Table B-3.

Table B-2: Node data for energy networks

Electricity network nodal data							
Node	Type	Local generation		Local demand		Voltage	
		$p_{g,i}^E$ [MW]	$q_{g,i}^E$ [MVar]	$p_{d,i}^E$ [MW]	$q_{d,i}^E$ [MVar]	Magnitude [p.u.]	Angle [deg.]
E1	PV	0	0	0.8	0.1	1.02	-
E2	PQ	0	0	0.8	0.1	-	-
E3	Slack	-	-	0.4	0.25	1.0	0°
Natural gas network nodal data							
Node	Node type	Local supply		Local demand		Nodal pressure (mbar)	
		$\dot{V}_{s,i}^G$ [m3/hr]		$\dot{V}_{d,i}^G$ [m3/hr]			
G1	Gas load	0		200		-	
G2	Gas Infeed	0		50		100	
G3	Gas load	0		100		-	
G4	Gas load	0		180		-	

Table B-2 Contd.

District heating network nodal data							
Node	Node type	Local supply		Local demand		Temperatures	
		$\dot{Q}_{s,i}^H$ [kW]	$\dot{Q}_{d,i}^H$ [kW]	$T_{s,i}^H$ [°C]	$T_{out,i}^H$ [°C]		
H1	Slack_H	-	400	100	-		
H2	Demand_H	0	1200	-	50		
H3	Demand_H	0	0	-	50		
H4	Supply_H	500	0	100	-		

District cooling network nodal data							
Node	Node type	Local supply		Local demand		Temperatures	
		$\dot{Q}_{s,i}^H$ [kW]	$\dot{Q}_{d,i}^H$ [kW]	$T_{s,i}^H$ [°C]	$T_{out,i}^H$ [°C]		
C1	Demand_C	0	400	0	12		
C2	Slack_C	-	0	5	-		
C3	Demand_C	0	400	0	12		

Table B-3: Energy network parameters

Electricity network parameters					
Circuit#	From-to	Series Impedance		Series Admittance	
		R (p.u.)	X (p.u.)	G (p.u.)	B (p.u.)
1	E1-E2	0.02	0.04	10	-20
2	E2-E3	0.01	0.02	20	-40

Natural gas network parameters			
Pipe#	Gas pipe	Pipe diameter (mm)	Pipe length (m)
1	G2-G1	150	680
2	G2-G3	150	500
3	G3-G4	150	420

District heating network parameters				
Pipe#	Pipe	Pipe diameter (mm)	Pipe length (m)	Radial heat transmission coefficient (W/m2K)
1	H1-H2	150	3000	0.9
2	H2-H3	150	3000	0.9
3	H3-H4	150	3000	0.9

Table B-3 Contd.

District cooling network parameters				
Pipe#	pipe	Pipe diameter (mm)	Pipe length (m)	Heat transmission coefficient (W/m2K)
1	C1-C2	160	100	0.9
2	C2-C3	160	100	0.9

The electricity network bus admittance matrix is calculated as,

$$Y_{bus} = \begin{bmatrix} y_{12} & -y_{12} & 0 \\ -y_{21} & y_{21} + y_{23} & -y_{23} \\ 0 & -y_{23} & y_{23} \end{bmatrix} = \begin{bmatrix} 10 - 20j & -10 + 20j & 0 \\ -10 + 20j & 30 - 60j & -20 + 40j \\ 0 & -20 + 40j & 20 - 40j \end{bmatrix}$$

In polar form Y_{bus} is expressed as,

$$Y_{bus} = \begin{bmatrix} 22.36 \angle -63.43^{\circ} & 22.36 \angle 116.56^{\circ} & 0 \\ 22.36 \angle 116.56^{\circ} & 67.08 \angle -63.43^{\circ} & 44.72 \angle 116.56^{\circ} \\ 0 & 44.72 \angle 116.56^{\circ} & 44.72 \angle -63.43^{\circ} \end{bmatrix}$$

The gas network branch-nodal incidence matrix (A^G) is given by,

$$A^G = \begin{bmatrix} +1 & 0 & 0 \\ -1 & -1 & 0 \\ 0 & +1 & -1 \\ 0 & 0 & +1 \end{bmatrix}$$

The reduced branch-nodal incidence matrix (A_r^G) is expressed as,

$$A_r^G = \begin{bmatrix} +1 & 0 & 0 \\ 0 & +1 & -1 \\ 0 & 0 & +1 \end{bmatrix}$$

For low pressure natural gas networks the flow exponent (m) for pipe flow calculation is 2 .

The pipe constants for natural gas flow as described in equation (4.2) are calculated as,

K_1^G	K_2^G	K_3^G
1.047×10^{-4}	7.7×10^{-5}	6.471×10^{-5}

The district heating network branch-nodal incidence matrix (A^H) is given by,

$$A^H = \begin{bmatrix} -1 & 0 & 0 \\ +1 & -1 & 0 \\ 0 & +1 & +1 \\ 0 & 0 & -1 \end{bmatrix}$$

The reduced branch-nodal incidence matrix for the district heating network (A_1^H) is given by,

$$A_1^H = \begin{bmatrix} +1 & -1 & 0 \\ 0 & +1 & +1 \\ 0 & 0 & -1 \end{bmatrix}$$

The district cooling network branch-nodal incidence matrix is given by,

$$A^C = \begin{bmatrix} +1 & 0 \\ -1 & -1 \\ 0 & +1 \end{bmatrix}$$

The reduced branch-nodal incidence matrix for the district cooling network (A_1^C) is given by,

$$A_1^C = \begin{bmatrix} +1 & 0 \\ 0 & +1 \end{bmatrix}$$

The set of imbalance equations for steady state analysis is formulated as follows.

1. Real (electrical) power flow balance at all PV and PQ type nodes in the electricity network is expressed as,

@ Node E1:

$$F_{1,1} = -p_{d,1}^E + \frac{C_{C_1,1}^E}{baseMVA} \left| \frac{(\dot{Q}_1^H)}{\eta_{c_1}^{H-E}} \right| - real \left[\mathbf{v}_1 (\mathbf{Y}_{11} \mathbf{v}_1 + \mathbf{Y}_{12} \mathbf{v}_2)^* \right]$$

$$F_{1,1} = -p_{d,1}^E + \frac{C_{C_1,1}^E}{baseMVA} \left(\left| \frac{\dot{m}_1^H \times c_p \times (T_{sup,1}^H - T_{ret,1}^H)}{\eta_{c_1}^{H-E} \times 1000} \right| \right) + \dots$$

$$- \left[|\mathbf{v}_1|^2 \mathbf{Y}_{11} | \cos(-\theta_{11}) + |\mathbf{v}_1 \mathbf{v}_2 \mathbf{Y}_{12} | \cos(\delta_1 - \delta_2 - \theta_{12}) \right]$$

$$F_{1,1} = -0.008 + \frac{(+1)}{100} \left(\left| \frac{\dot{m}_1^H \times 4.18 \times (100 - T_{ret,1}^H)}{0.875 \times 1000} \right| \right) + \dots$$

$$- \left[|1.02|^2 \times 22.36 | \cos(63.43^\circ) + |1.02 \times \mathbf{v}_2 \times 22.36 | \cos(\delta_1 - \delta_2 - 116.56) \right]$$

$$F_{1,1} = -0.008 + \frac{4.18 \dot{m}_1^H \times (100 - T_{ret,1}^H)}{87.5 \times 1000} - \left[10.4 + 22.8 \times |\mathbf{v}_2| \cos(\delta_1 - \delta_2 - 116.56) \right]$$

@ Node E2:

$$F_{1,2} = -p_{d,1}^E - real \left[\mathbf{v}_2 (\mathbf{Y}_{21} \mathbf{v}_1 + \mathbf{Y}_{22} \mathbf{v}_2 + \mathbf{Y}_{23} \mathbf{v}_3) \right]$$

$$F_{1,2} = -p_{d,1}^E - \left[|\mathbf{v}_2 \mathbf{v}_1 \mathbf{Y}_{21} | \cos(\delta_2 - \delta_1 - \theta_{21}) + |\mathbf{v}_2|^2 \mathbf{Y}_{22} | \cos(-\theta_{22}) + \dots \right]$$

$$+ |\mathbf{v}_2 \mathbf{v}_3 \mathbf{Y}_{23} | \cos(\delta_2 - \delta_3 - \theta_{23}) \left. \right]$$

$$F_{1,2} = -0.008 - \left[|\mathbf{v}_2 \times 1.02 \times 22.36 | \cos(\delta_2 - \delta_1 - 116.56) + |\mathbf{v}_2|^2 \times 67.08 | \cos(63.43) \right]$$

$$+ |\mathbf{v}_2 \times 1 \times 44.72 | \cos(\delta_2 - 0 - 116.56) \left. \right]$$

$$F_{1,2} = -0.008 - \left[|22.8 \mathbf{v}_2 | \cos(\delta_2 - \delta_1 - 116.56) + 30 \times |\mathbf{v}_2|^2 + \dots \right]$$

$$+ 44.72 \times |\mathbf{v}_2 | \cos(\delta_2 - 116.56) \left. \right]$$

2. Reactive (electrical) power flow balance at all *PQ* type nodes in the electricity network is expressed as,

@ *Node E2*:

$$F_{2,2} = -q_{d,2}^E - \text{imag} \left[\mathbf{v}_2 (\mathbf{Y}_{21} \mathbf{v}_1 + \mathbf{Y}_{22} \mathbf{v}_2 + \mathbf{Y}_{23} \mathbf{v}_3)^* \right]$$

$$F_{2,2} = -q_{d,2}^E - \left[\begin{array}{l} |\mathbf{v}_2 \mathbf{v}_1 \mathbf{Y}_{21}| \sin(\delta_2 - \delta_1 - \theta_{21}) + |\mathbf{v}_2^2 \mathbf{Y}_{22}| \sin(-\theta_{22}) \\ + |\mathbf{v}_2 \mathbf{v}_3 \mathbf{Y}_{23}| \sin(\delta_2 - \delta_3 - \theta_{23}) \end{array} \right]$$

$$F_{2,2} = -0.001 - \left[\begin{array}{l} |\mathbf{v}_2 \times 1.02 \times 22.36| \sin(\delta_2 - \delta_1 - 116.56) + 60 \times |\mathbf{v}_2^2| + \dots \\ + 44.72 \times |\mathbf{v}_2| \sin(\delta_2 - 116.56) \end{array} \right]$$

3. Gas volume flow balance at all *gas load* type nodes in the gas network is expressed as,

@ *Node G1*:

$$F_{3,1} = -\dot{V}_{d,2}^G + C_{c1,2}^G \left(\frac{(|\dot{Q}_{c1,1}^H| + \dot{Q}_{d,1}^H)}{\eta_{c1}^{G \rightarrow H}} \text{GCV} \right) \times 3600 + A_{1,1}^G \times S_{2,1} \left(S_{2,1} \frac{(pr_2 - pr_1)}{K_1^G} \right)^{\frac{1}{m}}$$

$$F_{3,1} = -200 + (-1) \left(\frac{(\dot{m}_1^H \times 4.18 \times (100 - T_{ret,1}^H) + 400)}{0.4 \times (41.04 \times 10^3)} \times 3600 \right) + \dots$$

$$+ \left((+1) \times S_{2,1} \left(S_{2,1} \frac{(100 - pr_1)}{1.047 \times 10^{-4}} \right)^{\frac{1}{2}} \right)$$

$$F_{3,1} = -200 - 0.9166 \dot{m}_1^H (100 - T_{ret,1}^H) - 87.72 + S_{2,1} \left(S_{2,1} \frac{(100 - pr_1)}{1.047 \times 10^{-4}} \right)^{\frac{1}{2}}$$

@ *Node G3*:

$$F_{3,3} = -\dot{V}_{d,3}^G + \left(A_{3,2}^G \times S_{2,3} \left(S_{2,3} \frac{(pr_2 - pr_3)}{K_2^G} \right)^{\frac{1}{m}} + A_{3,3}^G \times S_{3,4} \left(S_{3,4} \frac{(pr_3 - pr_4)}{K_3^G} \right)^{\frac{1}{m}} \right)$$

$$F_{3,3} = -100 + \left((+1) \times S_{2,3} \left(S_{2,3} \frac{(100 - pr_3)}{7.7 \times 10^{-5}} \right)^{\frac{1}{m}} + (-1) \times S_{3,4} \left(S_{3,4} \frac{(pr_3 - pr_4)}{6.471 \times 10^{-5}} \right)^{\frac{1}{2}} \right)$$

$$F_{3,3} = -100 + S_{2,3} \left(S_{2,3} \frac{(100 - pr_3)}{7.7 \times 10^{-5}} \right)^{\frac{1}{2}} - S_{3,4} \left(S_{3,4} \frac{(pr_3 - pr_4)}{6.471 \times 10^{-5}} \right)^{\frac{1}{2}}$$

@ Node G4:

$$F_{3,4} = -\dot{V}_{d,4}^G + C_{c1,2}^G \left| \frac{(\dot{Q}_4^H)}{\eta_{c_2}^{G \rightarrow H} GCV} \times 3600 \right| + \left(A_{4,3}^G \times S_{3,4} \left(S_{3,4} \frac{(pr_3 - pr_4)}{K_3^G} \right)^{\frac{1}{2}} \right)$$

$$F_{3,4} = -180 + (-1) \left| \frac{(500)}{0.9 \times 41.04 \times 10^3} \times 3600 \right| + \left((+1) \times S_{3,4} \left(S_{3,4} \frac{(pr_3 - pr_4)}{6.471 \times 10^{-5}} \right)^{\frac{1}{2}} \right)$$

$$F_{3,4} = -228.73 + S_{3,4} \left(S_{3,4} \frac{(pr_3 - pr_4)}{6.471 \times 10^{-5}} \right)^{\frac{1}{2}}$$

4. Mass flow balance at all *Supply_T* and *Demand_T* type nodes in the district heating networks is expressed as,

@ Node H2:

$$F_{4,2} = -\dot{M}_{d,2}^H + (A_{2,1}^H \times \dot{m}_1^H + A_{2,2}^H \times \dot{m}_2^H)$$

$$F_{4,2} = -\dot{M}_{d,2}^H + ((+1)\dot{m}_1^H + (-1)\dot{m}_2^H)$$

$$\text{Where, } \dot{M}_{d,2}^H = \frac{\dot{Q}_{d,2}^H}{c_p \times (T_{sup,2}^T - T_{out,2}^T)} = \frac{1200}{4.18 \times (T_{sup,2}^T - 50)} \text{ [kg / s]}$$

$$F_{4,2} = -\frac{1200}{4.18 \times (T_{sup,2}^T - 50)} + \dot{m}_1^H - \dot{m}_2^H$$

@ Node H3:

$$F_{4,3} = C_{C_3,3}^H \left(\left| \dot{M}_{C_3,3}^H \right| \right) + (A_{3,2}^H \times \dot{m}_2^H + A_{3,3}^H \times \dot{m}_3^H)$$

$$F_{4,3} = (-1) \times \left| \dot{M}_{C_3,3}^H \right| + ((+1)\dot{m}_2^H + (+1)\dot{m}_3^H)$$

Where,

$$\left| \dot{M}_{C_3,3}^H \right| = \left| \frac{\dot{Q}_{d,3}^H}{c_p \times (T_{sup,3}^H - T_{out,3}^H)} \right| = \left| \frac{\dot{Q}_{C_3,Slack}^C / \eta_{C_3}^{C-H}}{c_p \times (T_{sup,3}^H - T_{out,3}^H)} \right|$$

$$\left| \dot{M}_{C_3,3}^H \right| = \frac{\left[\sum_{k=1}^{n_{C_pipe}} A_{i,k}^C \dot{m}_k^C \right] c_p \times (T_{s,2}^C - T_{ret,2}^C) / \eta_{C_3}^{C-H}}{c_p \times (T_{sup,3}^H - T_{out,3}^H)}$$

$$\left| \dot{M}_{C_3,3}^H \right| = \left| \frac{((-1) \times \dot{m}_1^C + (-1) \times \dot{m}_2^C) \times 4.18 \times (5 - T_{ret,1}^H) / 0.65}{4.18 \times (T_{sup,3}^H - 50)} \right| = \left| \frac{(\dot{m}_1^C + \dot{m}_2^C) \times (5 - T_{ret,1}^H)}{0.65 (T_{sup,3}^H - 50)} \right| [kg / s]$$

$$F_{4,3} = - \left| \frac{(\dot{m}_1^C + \dot{m}_2^C) \times (5 - T_{ret,1}^H)}{0.65 (T_{sup,3}^H - 50)} \right| + \dot{m}_2^H + \dot{m}_3^H$$

@ Node H4:

$$F_{4,4} = C_{C_2,4}^H \left| \dot{M}_{C_2,4}^H \right| + (A_{4,3}^H \times \dot{m}_3^H)$$

$$F_{4,4} = (+1) \times \dot{M}_{C_2,4}^H + ((-1)\dot{m}_3^H)$$

$$\text{Where } \dot{M}_{C_2,4}^H = \frac{\dot{Q}_{s,4}^H}{c_p \times (T_{s,4}^H - T_{ret,4}^H)} = \frac{500}{4.2 \times (100 - T_{ret,4}^H)} = \frac{119.05}{(100 - T_{ret,4}^H)} [kg / s]$$

$$F_{4,4} = \frac{119.05}{(100 - T_{ret,4}^H)} - \dot{m}_3^H$$

Mass flow balance at all *Demand_C* type nodes in the district cooling network,

@ Node C1:

$$F_{5,1} = 0 = -\dot{M}_{d,1}^C + (A_{1,1}^C \times \dot{m}_1^C + A_{1,2}^C \times \dot{m}_2^C)$$

$$F_{5,1} = 0 = -\dot{M}_{d,1}^C + \dot{m}_1^C$$

$$\text{Where } \dot{M}_{d,1}^C = \frac{\dot{Q}_{d,1}^C}{c_p \times |T_{sup,1}^C - T_{out,1}^C|} = \frac{400}{4.2 \times |T_{sup,1}^C - 12|}$$

$$F_{5,1} = 0 = -\frac{400}{4.2 \times |T_{sup,1}^C - 12|} + \dot{m}_1^C$$

@ Node C3:

$$F_{5,3} = 0 = -\dot{M}_{d,3}^C + (A_{3,1}^H \times \dot{m}_1^C + A_{3,2}^H \times \dot{m}_2^C)$$

$$F_{5,3} = 0 = -\dot{M}_{d,3}^C + \dot{m}_2^C$$

$$\text{Where } \dot{M}_{d,3}^C = \frac{\dot{Q}_{d,3}^C}{c_p \times |T_{sup,1}^C - T_{out,1}^C|} = \frac{400}{4.2 \times |T_{sup,1}^C - 12|}$$

$$F_{5,3} = 0 = -\frac{400}{4.2 \times |T_{sup,1}^C - 12|} + \dot{m}_2^C$$

The steps of the iterative method for solving the set of equations are as follows.

Step 1: Calculate initial approximations for steady state parameters.

- The initial estimates of the unknown voltages at the PQ node, $E2$ is taken as $1.0 [p.u.] \angle 0^\circ$. The initial estimate for the voltage angle at the PV node $E1$ is taken as $\angle 0^\circ$.

$$(X^E)^o = \begin{bmatrix} (\delta_1^E)^o \\ (\delta_2^E)^o \\ |v_2^{Eo}| \end{bmatrix} = \begin{bmatrix} 0^\circ \\ 0^\circ \\ 1 \end{bmatrix}$$

- The initial estimates for nodal gas pressures are calculated by approximating the gas demand of the coupling units and assuming the gas loads are supplied via branches of an equivalent radial network²³.

The gas demand of the CHP unit is approximated by considering the net heat demand of the district heating network.

$$\dot{V}_{C_1,1}^H = \frac{\dot{Q}_{d,net}^H}{\eta_{c_1}^{G/H} \times GCV} \times 3600$$

$$\text{Where, } \dot{Q}_{d,net}^H = \sum_{i=1}^{n_{heat}} (\dot{Q}_{d,i}^H - \dot{Q}_{s,i}^H)$$

$$\dot{Q}_{d,net}^H = 400 + 1200 - 500 = 1100 \text{ kW}_{th}^H$$

$$\dot{V}_{C_1,1}^H = \frac{1100}{0.4 \times 41.04 \times 1000} \times 3600 = 241.23 [m^3 / hr]$$

²³ This is In the case of meshed networks. The example gas network is a radial network.

The gas demand of the GB unit is calculated by considering the heat supplied to the district heating network.

$$\dot{V}_{C_2,A}^G = \frac{\dot{Q}_{C_2,A}^H}{\eta_{C_2}^{G/H} \times GCV} \times 3600$$

where $\dot{Q}_{C_2,A}^H = 500 \text{ kW}_{th}^H$

$$\dot{V}_{C_2,A}^G = \frac{500}{0.9 \times 41.04 \times 1000} \times 3600 = 48.73 [m^3 / hr]$$

The revised nodal gas demands are,

Node	<i>G1</i>	<i>G2</i>	<i>G3</i>	<i>G4</i>
Initial gas demand [m³/hr]	200	50	100	180
Gas demand from coupling components [m³/hr]	241.23	0	0	48.73
Revised nodal gas demand [m³/hr]	441.23	50	100	228.73

The gas flow rates in the branches are calculated using equation (4.13) as,

$$\dot{V}_i^G = \sum_{k=1}^{n_{\text{gas pipe}}} A_{i,k}^G \times \dot{V}_k$$

$$\begin{bmatrix} \dot{V}_{d,1}^G \\ \dot{V}_{d,3}^G \\ \dot{V}_{d,4}^G \end{bmatrix} = A_l^G \times \begin{bmatrix} \dot{V}_{(1)}^G \\ \dot{V}_{(2)}^G \\ \dot{V}_{(3)}^G \end{bmatrix}$$

$$\begin{bmatrix} 441.23 \\ 100 \\ 228.73 \end{bmatrix} = \begin{bmatrix} +1 & 0 & 0 \\ 0 & +1 & -1 \\ 0 & 0 & +1 \end{bmatrix} \times \begin{bmatrix} \dot{V}_{(1)}^G \\ \dot{V}_{(2)}^G \\ \dot{V}_{(3)}^G \end{bmatrix}$$

$$\begin{bmatrix} \dot{V}_{(1)}^G \\ \dot{V}_{(2)}^G \\ \dot{V}_{(3)}^G \end{bmatrix} = \begin{bmatrix} 441.23 \\ 328.73 \\ 228.73 \end{bmatrix}$$

The pressure drop in each gas pipe is calculated using equation (4.2) and the pipe constants as,

Branch	$G2-G1$ ($k=1$)	$G2-G3$ ($k=2$)	$G3-G4$ ($k=3$)
Initial estimate for Gas flow $(\dot{V})_k$ [m ³ /hr]	441.23	328.73	228.73
Pipe constant	1.047×10^{-4}	7.7×10^{-5}	6.471×10^{-5}
Pressure drop [mbar]	20.38	8.32	3.38

The initial approximations of the nodal gas pressure are calculated as,

$$(X^G)^o = \begin{bmatrix} (pr_1^G)^o \\ (pr_3^G)^o \\ (pr_4^G)^o \end{bmatrix} = \begin{bmatrix} pr_2^G - \Delta (Pr_{k=1}^G)^o \\ pr_2^G - \Delta (Pr_{k=2}^G)^o \\ pr_3^G - \Delta (Pr_{k=3}^G)^o \end{bmatrix} = \begin{bmatrix} 100 - 20.38 \\ 100 - 8.32 \\ pr_3^G - 3.38 \end{bmatrix} = \begin{bmatrix} 79.62 \\ 91.68 \\ 88.3 \end{bmatrix} \text{ [mbar]}$$

- In the district heating network initial estimate for the branch mass flow rates are taken as 1.0 kg / s . The unknown temperature at supply line nodes is assumed as 100° C and in the return line is taken as 50° C .

$$(X^H)^o = \begin{bmatrix} (\dot{m}_1^H)^o \\ (\dot{m}_2^H)^o \\ (\dot{m}_3^H)^o \end{bmatrix} = \begin{bmatrix} 1 \\ 1 \\ 1 \end{bmatrix}$$

$$\begin{bmatrix} (T_{sup,2}^H)^o \\ (T_{sup,3}^H)^o \end{bmatrix} = \begin{bmatrix} 100 \\ 100 \end{bmatrix}$$

$$\begin{bmatrix} (T_{ret,1}^H)^o \\ (T_{ret,4}^H)^o \end{bmatrix} = \begin{bmatrix} 50 \\ 50 \end{bmatrix}$$

- In the district cooling network initial estimate of the branch mass flow rates are taken as 5.0 kg / s . The unknown temperature at supply line nodes is taken as 5° C and in the return line is taken as 12° C .

$$(X^C)^o = \begin{bmatrix} (\dot{m}_1^C)^o \\ (\dot{m}_2^C)^o \end{bmatrix} = \begin{bmatrix} 1 \\ 1 \end{bmatrix}$$

$$\begin{bmatrix} (T_{sup,1}^C)^o \\ (T_{sup,3}^C)^o \end{bmatrix} = \begin{bmatrix} 5 \\ 5 \end{bmatrix} \text{ [}^\circ \text{ C]}$$

$$\begin{bmatrix} (T_{ret,2}^C)^o \end{bmatrix} = \begin{bmatrix} 12 \end{bmatrix}$$

Step 3: Calculate the imbalances in equations for the first estimate of steady state variables

The imbalances in the set of equations for the first iteration are calculated by substituting the first estimates for state variables.

$$\begin{bmatrix} F_{1,1} \\ F_{1,2} \\ F_{2,1} \\ F_{3,1} \\ F_{3,3} \\ F_{3,4} \\ F_{4,2} \\ F_{4,3} \\ F_{4,4} \\ F_{5,1} \\ F_{5,3} \end{bmatrix} = \begin{bmatrix} -0.2132 [p.u.] \\ 0.1815 [p.u.] \\ 0.4042 [p.u.] \\ -195.36 [m^3 / hr] \\ 0.1671 [m^3 / hr] \\ -0.1875 [m^3 / hr] \\ -5.742 [kg / s] \\ -0.1538 [kg / s] \\ 1.381 [kg / s] \\ -8.6054 [kg / s] \\ -8.6054 [kg / s] \end{bmatrix}$$

Step 4: Calculate elements of the Jacobian matrix

The Jacobian matrix for the example is expressed as,

$$J = \begin{bmatrix} \frac{\partial F_{1,1}}{\partial \delta_1} & \frac{\partial F_{1,1}}{\partial \delta_2} & \frac{\partial F_{1,1}}{\partial |V_2|} & & & \frac{\partial F_{1,1}}{\partial m_1^H} & \frac{\partial F_{1,1}}{\partial m_2^H} & \frac{\partial F_{1,1}}{\partial m_3^H} \\ \frac{\partial F_{1,2}}{\partial \delta_1} & \frac{\partial F_{1,2}}{\partial \delta_2} & \frac{\partial F_{1,2}}{\partial |V_2|} & & & & & & \\ \frac{\partial F_{2,1}}{\partial \delta_1} & \frac{\partial F_{2,1}}{\partial \delta_2} & \frac{\partial F_{2,1}}{\partial |V_2|} & & & & & & \\ & & & \frac{\partial F_{3,1}}{\partial Pr_1} & \dots & \frac{\partial F_{3,1}}{\partial Pr_4} & \frac{\partial F_{3,1}}{\partial m_1^H} & \dots & \frac{\partial F_{3,1}}{\partial m_3^H} \\ & & & \vdots & & \vdots & & & \\ & & & \frac{\partial F_{3,3}}{\partial Pr_1} & \dots & \frac{\partial F_{3,3}}{\partial Pr_4} & & & \\ & & & & & & \frac{\partial F_{4,1}}{\partial m_1^H} & \dots & \frac{\partial F_{4,1}}{\partial m_3^H} \\ & & & & & & \vdots & & \vdots \\ & & & & & & \frac{\partial F_{4,3}}{\partial m_1^H} & \dots & \frac{\partial F_{4,3}}{\partial m_3^H} \\ & & & & & & & \frac{\partial F_{4,2}}{\partial m_1^C} & \frac{\partial F_{4,2}}{\partial m_2^C} \\ & & & & & & & \frac{\partial F_{5,1}}{\partial m_1^C} & \frac{\partial F_{5,1}}{\partial m_2^C} \\ & & & & & & & \frac{\partial F_{5,2}}{\partial m_1^C} & \frac{\partial F_{5,2}}{\partial m_2^C} \end{bmatrix}$$

The elements of the Jacobian matrix for the first iteration are computed as follows.

- Elements $\left. \frac{\partial F_{1,i}}{\partial \delta_n} \right|_{X=X^0}$ are computed as,

$$\frac{\partial F_{1,1}}{\partial \delta_1} = \left[\sum_{\substack{n=1 \\ n \neq i}}^{n_{elec}} |\mathbf{v}_1 \mathbf{Y}_{1n} \mathbf{v}_n| \sin(\delta_1 - \theta_{1n} - \delta_n) \right] = \left[|\mathbf{v}_1 \mathbf{Y}_{12} \mathbf{v}_2| \sin(\delta_1 - \theta_{12} - \delta_2) \right] = -20.4$$

$$\frac{\partial F_{1,1}}{\partial \delta_2} = -\left(|\mathbf{v}_1 \mathbf{Y}_{12} \mathbf{v}_2| \sin(\delta_1 - \theta_{12} - \delta_2) \right) = 20.4$$

$$\frac{\partial F_{1,2}}{\partial \delta_1} = -\left(|\mathbf{v}_2 \mathbf{Y}_{21} \mathbf{v}_1| \sin(\delta_2 - \theta_{21} - \delta_1) \right) = 20.4$$

$$\frac{\partial F_{1,2}}{\partial \delta_2} = \left[\sum_{\substack{n=1 \\ n \neq i}}^{n_{elec}} |\mathbf{v}_2 \mathbf{Y}_{2n} \mathbf{v}_n| \sin(\delta_2 - \theta_{2n} - \delta_n) \right] = \left[|\mathbf{v}_2 \mathbf{Y}_{21} \mathbf{v}_1| \sin(\delta_2 - \theta_{21} - \delta_1) + \dots \right] = -60.4$$

- Elements $\frac{\partial F_{1,i}}{\partial |\mathbf{v}_n|}$ are computed as,

$$\frac{\partial F_{1,1}}{\partial |\mathbf{v}_2|} = -(|\mathbf{v}_1 \mathbf{Y}_{12}| \cos(\delta_1 - \theta_{12} - \delta_2)) = -10.20$$

$$\frac{\partial F_{1,2}}{\partial |\mathbf{v}_2|} = \left[-2|\mathbf{v}_2 \mathbf{Y}_{22}| \cos(-\theta_{ii}) - \sum_{\substack{n=1 \\ n \neq i}}^{n_{elec}} |\mathbf{Y}_{2n} \mathbf{v}_n| \cos(\delta_2 - \theta_{2n} - \delta_n) \right]$$

$$\frac{\partial F_{1,2}}{\partial |\mathbf{v}_2|} = \left[-2|\mathbf{v}_2 \mathbf{Y}_{22}| \cos(-\theta_{ii}) - |\mathbf{Y}_{21} \mathbf{v}_1| \cos(\delta_2 - \theta_{21} - \delta_1) + \dots \right. \\ \left. - |\mathbf{Y}_{23} \mathbf{v}_3| \cos(\delta_2 - \theta_{23} - \delta_3) \right] = -29.81$$

- Elements of $\frac{\partial F_{2,i}}{\partial \delta_n}$ are computed as,

$$\frac{\partial F_{2,1}}{\partial \delta_1} = (|\mathbf{v}_2 \mathbf{Y}_{21} \mathbf{v}_1| \cos(\delta_2 - \theta_{21} - \delta_1)) = -10.20$$

$$\frac{\partial F_{2,1}}{\partial \delta_2} = - \left[\sum_{\substack{n=1 \\ n \neq i}}^{n_{elec}} |\mathbf{v}_2 \mathbf{Y}_{2n} \mathbf{v}_n| \cos(\delta_2 - \theta_{2n} - \delta_n) \right]$$

$$\frac{\partial F_{2,1}}{\partial \delta_2} = \left[- \left(|\mathbf{v}_2 \mathbf{Y}_{21} \mathbf{v}_1| \cos(\delta_2 - \theta_{21} - \delta_1) + \dots \right) \right. \\ \left. + |\mathbf{v}_2 \mathbf{Y}_{23} \mathbf{v}_3| \cos(\delta_2 - \theta_{23} - \delta_3) \right] = 30.19$$

- Elements $\frac{\partial F_{2,i}}{\partial |\mathbf{v}_n|}$ are computed as,

$$\frac{\partial F_{2,1}}{\partial |\mathbf{v}_2|} = -2|\mathbf{v}_2 \mathbf{Y}_{22}| \sin(-\theta_{ii}) - (|\mathbf{v}_1 \mathbf{Y}_{21}| \sin(\delta_2 - \theta_{21} - \delta_1)) - (|\mathbf{v}_3 \mathbf{Y}_{23}| \sin(\delta_2 - \theta_{23} - \delta_3))$$

$$\frac{\partial F_{2,1}}{\partial |\mathbf{v}_2|} = -59.59$$

- Elements in $\frac{\partial F_3}{\partial \text{Pr}}$ are computed as,

$$\frac{\partial F_3}{\partial \text{Pr}} = -A_1^G D (A_1^G)^T$$

Where,

$$A_1^G = \begin{bmatrix} +1 & 0 & 0 \\ 0 & +1 & -1 \\ 0 & 0 & +1 \end{bmatrix}$$

$$D = \frac{1}{m_1} \begin{bmatrix} \frac{\dot{V}_{(1)}^G}{\Delta \text{Pr}_{(1)}^G} & 0 & 0 \\ 0 & \frac{\dot{V}_{(2)}^G}{\Delta \text{Pr}_{(2)}^G} & 0 \\ 0 & 0 & \frac{\dot{V}_{(3)}^G}{\Delta \text{Pr}_{(3)}^G} \end{bmatrix}$$

$$\frac{\partial F_3}{\partial \text{Pr}} = - \begin{bmatrix} +1 & 0 & 0 \\ 0 & +1 & -1 \\ 0 & 0 & +1 \end{bmatrix} \times \frac{1}{2} \begin{bmatrix} \frac{441.19}{20.38} & 0 & 0 \\ 0 & \frac{328.7}{8.32} & 0 \\ 0 & 0 & \frac{228.55}{3.38} \end{bmatrix} \times \begin{bmatrix} +1 & 0 & 0 \\ 0 & +1 & 0 \\ 0 & -1 & +1 \end{bmatrix}$$

$$\frac{\partial F_3}{\partial \text{Pr}} = - \begin{bmatrix} -10.82 & 0 & 0 \\ 0 & -53.56 & 33.81 \\ 0 & 33.81 & -33.81 \end{bmatrix}$$

- Elements in $\frac{\partial F_4}{\partial \dot{m}^H}$ are computed as,

$$\frac{\partial F_4}{\partial \dot{m}^H} = A_1^H = \begin{bmatrix} +1 & -1 & 0 \\ 0 & +1 & +1 \\ 0 & 0 & -1 \end{bmatrix}$$

- Elements in $\frac{\partial F_5}{\partial \dot{m}^C}$ are computed as,

$$\frac{\partial F_5}{\partial \dot{m}^C} = A_1^C = \begin{bmatrix} +1 & 0 \\ 0 & +1 \end{bmatrix}$$

- Elements in $\frac{\partial F_{1,i}}{\partial \dot{m}^H}$ are computed as,

$$\frac{\partial F_{1,i}}{\partial \dot{m}^H} = \frac{C_{C_k,i}^E}{baseMVA \times \eta_{C_i}^{H/E}} \left| A^H_{slack} c_p \times (T^H_{sup,slack} - T^H_{ret,slack}) \right|$$

$$\frac{\partial F_{1,1}}{\partial \dot{m}^H} = \frac{+1}{100 \times 0.875} \left| [-1 \ 0 \ 0] \times 4.18 \times (100 - 50) \right|$$

$$\frac{\partial F_{1,1}}{\partial \dot{m}_1^H} = \frac{+1}{100 \times 0.875} \left| (-1) \times 4.18 \times (100 - 50) \right| = 2.388$$

$$\frac{\partial F_{1,1}}{\partial \dot{m}_2^H} = 0$$

$$\frac{\partial F_{1,1}}{\partial \dot{m}_3^H} = 0$$

- Elements in $\frac{\partial F_{3,i}}{\partial \dot{m}^H}$ are computed as

$$\frac{\partial F_{3,i}}{\partial \dot{m}^H} = \frac{C_{c_k,i}^G \times \left| A^H_{slack,n} \times c_p \times (T^{th}_{sup,slack} - T^{th}_{ret,slack}) \right|}{\eta_{C_k}^{G-H} \times GCV}$$

$$\frac{\partial F_{3,i}}{\partial \dot{m}^H} = \frac{(-1) \times \left| [-1 \ 0 \ 0] \times 4.18 \times (100 - 50) \right|}{0.4 \times 1000 \times 41.04}$$

$$\frac{\partial F_{3,1}}{\partial \dot{m}_1^H} = \frac{(-1) \times \left| (-1) \times 4.18 \times (100 - 50) \right|}{0.4 \times 1000 \times 41.04} = -0.01273$$

$$\frac{\partial F_{3,1}}{\partial \dot{m}_2^H} = 0$$

$$\frac{\partial F_{3,1}}{\partial \dot{m}_3^H} = 0$$

Step 6: Determine the value of X for the next iteration

$$X^1 = X^0 + \Delta X^0$$

$$\begin{bmatrix} (\delta_1^E)^I \\ (\delta_2^E)^I \\ |V_2^E|^I \\ (pr_1^G)^I \\ (pr_3^G)^I \\ (pr_4^G)^I \\ (\dot{m}_1^H)^I \\ (\dot{m}_2^H)^I \\ (\dot{m}_3^H)^I \\ (\dot{m}_1^C)^I \\ (\dot{m}_2^C)^I \end{bmatrix} = \begin{bmatrix} (\delta_1^E)^I \\ (\delta_2^E)^I \\ |V_2^E|^I \\ (pr_1^G)^I \\ (pr_3^G)^I \\ (pr_4^G)^I \\ (\dot{m}_1^H)^I \\ (\dot{m}_2^H)^I \\ (\dot{m}_3^H)^I \\ (\dot{m}_1^C)^I \\ (\dot{m}_2^C)^I \end{bmatrix} + \begin{bmatrix} \Delta(\delta_1^E)^O \\ \Delta(\delta_2^E)^O \\ \Delta|V_2^{Eo}| \\ \Delta(pr_1^G)^O \\ \Delta(pr_3^G)^O \\ \Delta(pr_4^G)^O \\ \Delta(\dot{m}_1^H)^O \\ \Delta(\dot{m}_2^H)^O \\ \Delta(\dot{m}_3^H)^O \\ \Delta(\dot{m}_1^C)^O \\ \Delta(\dot{m}_2^C)^O \end{bmatrix} = \begin{bmatrix} 0 \\ 0 \\ 1 \\ 79.62 \\ 91.68 \\ 88.3 \\ 1 \\ 1 \\ 1 \\ 5 \\ 5 \end{bmatrix} + \begin{bmatrix} 1.4323 \\ 0.4835 \\ 0.0066 \\ 18.0388 \\ -0.001 \\ -0.0066 \\ 8.2215 \\ 2.4798 \\ 1.3810 \\ 8.6054 \\ 8.6054 \end{bmatrix} = \begin{bmatrix} 1.4323 \\ 0.4835 \\ 1.0066 \\ 97.6588 \\ 91.6790 \\ 88.2934 \\ 9.2215 \\ 3.4799 \\ 2.3810 \\ 13.6054 \\ 13.6054 \end{bmatrix}$$

Step 7: Compute the supply and return line temperatures at thermal network nodes for the new branch flow rate estimates.

The equations for computing the unknown supply and return line temperatures at thermal networks nodes are formulated considering the direction of branch flow rates.

In the district heating network,

Supply line temperatures

@Node H2;

$$T_{sup,2}^H = T_{sup,1}^H - \Delta T_{sup,12}^H$$

$$\text{where } \Delta T_{sup,(l)}^H = \frac{\pi \chi_{(l)}^H L_{(l)}^H D_{(l)}^H (T_{start,(l)}^H - T_{amb})}{\dot{m}_l^H c_p} = \frac{3.14 \times 0.9 \times 3000 \times 0.15 \times (100 - 10)}{9.2214 \times 4.18 \times 1000} = 2.96$$

$$T_{sup,2}^H = 100 - 2.96 = 97.03$$

@Node H3

$$T_{sup,3}^H = \frac{\left(\dot{m}_2^H (T_{sup,2}^H - \Delta T_{sup,(2)}^H) + \dot{m}_3^H (T_{sup,4}^H - \Delta T_{sup,(3)}^H) \right)}{\dot{m}_2^H + \dot{m}_3^H}$$

$$\Delta T_{sup,(2)}^H = \frac{\pi \chi_{(2)} L_{(2)} D_{(2)} (T_{start,(2)}^H - T_{amb})}{\dot{m}_2^H c_p} = -\frac{3.14 \times 0.9 \times 3000 \times 0.15 \times (97.03 - 10)}{3.4798 \times 4.18 \times 1000} = -7.61$$

Where;

$$\Delta T_{sup,(3)}^H = \frac{\pi \chi_{(3)} L_{(3)} D_{(3)} (T_{start,(3)}^H - T_{amb})}{\dot{m}_3^H c_p} = -\frac{3.14 \times 0.9 \times 3000 \times 0.15 \times (100 - 10)}{2.3810 \times 4.18 \times 1000} = -11.5$$

$$T_{sup,3}^H = \frac{(3.4798(97.03 - 7.61) + 2.3810(100 - 11.5))}{3.4798 + 2.3810} = 89^\circ C$$

Return line temperatures

@Node H3;

$$T_{ret,3}^H = T_{out,3}^H = 50;$$

@Node H4;

$$T_{ret,4}^H = T_{ret,3}^H - \Delta T_{ret,43}^H$$

$$\text{Where, } \Delta T_{ret,43}^H = \frac{\pi \chi_{(3)} L_{(3)} D_{(3)} (T_{ret,3}^H - T_{amb})}{\dot{m}_3^H c_p} = \frac{3.14 \times 0.9 \times 3000 \times 0.15 \times (50 - 10)}{2.3810 \times 4.18 \times 1000} = 5.11$$

$$T_{ret,4}^H = 50 - 5.11 = 44.89$$

@Node H2

$$T_{ret,2}^H = \frac{\dot{m}_2^H (T_{ret,3}^H - \Delta T_{ret,(2)}^H) + \dot{M}_{d,2} T_{out,2}^H}{\dot{m}_2^H + \dot{M}_{d,2}}$$

$$\text{Where, } \Delta T_{ret,(2)}^H = -\frac{\pi \chi_{(2)} L_{(2)} D_{(2)} (T_{ret,3}^H - T_{amb})}{\dot{m}_2^H c_p} = -\frac{3.14 \times 0.9 \times 3000 \times 0.15 \times (50 - 10)}{3.4798 \times 4.18 \times 1000} = 3.50$$

$$\dot{M}_{d,2} = \frac{1200}{4.18 \times (T_{sup,2}^T - 50)} = \frac{1200}{4.18 \times (97.03 - 50)} = 6.104$$

$$T_{ret,2}^H = \frac{3.4798(50 - 3.5) + 6.104 \times 50}{3.4798 + 6.104} = 48.73$$

@Node H1

$$T_{ret,1}^H = T_{ret,2}^H - \Delta T_{ret,12}^H$$

$$\text{Where, } \Delta T_{ret,(2)}^H = \frac{\pi \chi_{(1)} L_{(1)} D_{(1)} (T_{ret,2}^H - T_{amb})}{\dot{m}_1^H c_p} = \frac{3.14 \times 0.9 \times 3000 \times 0.15 \times (48.73 - 10)}{9.2214 \times 4.18 \times 1000} = 1.278$$

$$T_{ret,1}^H = 48.73 - 1.278 = 47.4$$

District cooling network nodal temperatures for the updated mass flow rates are computed as,

Supply line temperatures

@Node C1;

$$T_{sup,1}^C = T_{sup,2}^C - \Delta T_{sup,12}^C$$

$$\text{Where, } \Delta T_{sup,(1)}^C = \frac{\pi \chi_{(1)}^C L_{(1)}^C D_{(1)}^C (T_{start,(1)}^C - T_{amb})}{\dot{m}_1^C c_p} = \frac{3.14 \times 0.9 \times 100 \times 0.16 \times (5 - 10)}{13.6054 \times 4.18 \times 1000} = -0.004$$

$$T_{sup,1}^C = 5 - (-0.004) = 5.004$$

@Node C3;

$$T_{sup,3}^C = T_{sup,2}^C - \Delta T_{sup,(2)}^C$$

$$\text{Where, } \Delta T_{sup,(2)}^C = \frac{\pi \chi_{(2)}^C L_{(2)}^C D_{(2)}^C (T_{start,(2)}^C - T_{amb})}{\dot{m}_2^C c_p} = \frac{3.14 \times 0.9 \times 100 \times 0.16 \times (5 - 10)}{13.6054 \times 4.18 \times 1000} = -0.004$$

$$T_{sup,3}^C = T_{sup,2}^C - (-0.004) = 5.004$$

Return line temperatures

@Node C2;

$$T_{ret,2}^C = \frac{\dot{m}_1^C (T_{ret,1}^C - \Delta T_{ret,(1)}^C) + \dot{m}_3^C (T_{ret,3}^C - \Delta T_{ret,(2)}^C)}{\dot{m}_1^C + \dot{m}_2^C}$$

$$\Delta T_{ret,(1)}^C = \frac{\pi \chi_{(l)}^C L_{(l)}^C D_{(l)}^C (T_{start,(l)}^C - T_{amb})}{\dot{m}_1^C c_p} = \frac{3.14 \times 0.9 \times 100 \times 0.16 \times (12 - 10)}{13.6054 \times 4.18 \times 1000}$$

Where,

$$\Delta T_{ret,(2)}^C = \frac{\pi \chi_{(l)}^C L_{(l)}^C D_{(l)}^C (T_{start,(l)}^C - T_{amb})}{\dot{m}_1^C c_p} = \frac{3.14 \times 0.9 \times 100 \times 0.16 \times (12 - 10)}{13.6054 \times 4.18 \times 1000}$$

$$T_{ret,2}^C = \frac{13.6054 \times (12 - 1.59e-3) + 13.6054 \times (12 - 1.59e-3)}{13.6054 + 13.6054} = 11.99$$

Step 9: Repeat from step 3 until the imbalances in equations are less than specified tolerance limits for the different equations.

The tolerance of the imbalance equations are taken as,

- The real and reactive power imbalance tolerance set as 0.01 p.u.
- The gas volume flow imbalance set as 1 m³/hr
- The nodal mass flow imbalance tolerance in thermal networks set as 0.1 kg/s

The results of the iterations are shown in Table B-4

Table B-4: Iterations information

	Iteration number							Iteration number					
	2	3	4	5	6	7		2	3	4	5	6	7
δ_1	1.4323	0.3969	-0.0052	0.0387	-0.0113	-0.0093	$F_{1,1}$	-21.10	-4.4781	0.2072	-0.65	0.0303	-0.0137
δ_2	0.4835	0.1776	-0.0003	0.0128	-0.0041	-0.0034	$F_{1,2}$	-8.6383	-5.4934	-0.7896	-0.0229	-0.0086	0
$ v_2 $	1.0066	1.0708	1.0288	1.0071	1.0069	1.0066	$F_{2,2}$	-12.1669	-3.9027	-1.3149	-0.0402	-0.0170	-0.0001
pr_1^G	97.66	51.9564	45.5285	44.9714	44.3915	29.8991	$F_{3,1}$	-494.66	-69.6122	-5.999	-6.2767	-1.7145	-0.8276
pr_3^G	91.68	91.6790	91.6790	91.6790	91.6790	91.6790	$F_{3,3}$	-0.0001	0	0	0	0	0
pr_4^G	88.29	88.2934	88.2934	88.2934	88.2934	88.2934	$F_{3,4}$	-0.0001	0	0	0	0	0
\dot{m}_1^H	9.2215	11.4527	11.0249	11.1105	11.0941	11.0969	$F_{4,2}$	-0.3627	0.0742	-0.0118	0.0024	0	0.0001
\dot{m}_2^H	3.48	5.3484	4.9948	5.0686	5.0547	5.0570	$F_{4,3}$	-1.6423	0.3739	-0.0717	0.0141	-0.0028	0.0005
\dot{m}_3^H	2.38	2.16	2.1397	2.1377	2.1375	2.1374	$F_{4,4}$	-0.2209	-0.0203	-0.0021	-0.0002	0	0
\dot{m}_1^C	13.60	13.6178	13.6178	13.6178	13.6178	13.6178	$F_{5,1}$	-0.0124	0	0	0	0	0
\dot{m}_2^C	13.60	13.6178	13.6178	13.6178	13.6178	13.6178	$F_{5,3}$	-0.0124	0	0	0	0	0
$T_{sup,2}^H$	97.03	97.608	97.5152	97.5343	97.5307	97.5314							
$T_{sup,3}^H$	89.04	61.0959	90.6869	90.7668	90.7510	90.7536							
$T_{ret,1}^H$	47.45	47.8953	47.8229	47.8381	47.8352	47.8358							
$T_{ret,2}^H$	48.73	48.9299	48.8968	48.9038	48.9026	48.9028							
$T_{ret,3}^H$	50	50	50	50	50	50							
$T_{ret,4}^H$	44.89	44.3633	44.3098	44.3043	44.3037	44.3037							
$T_{sup,1}^C$	5.0064	5.0064	5.0064	5.0064	5.0064	5.0064							
$T_{sup,3}^C$	5.0064	5.0064	5.0064	5.0064	5.0064	5.0064							
$T_{ret,2}^C$	11.99	11.99	11.99	11.99	11.99	11.99							

B.2 Validation of results using commercial software

The results are validated using established commercial software used for load flow analysis of individual energy networks. Simulation of each network was carried out using the following software packages.

Electricity network	IPSA version 2.4
Gas network	PSS SINCAL 7.0
District heating network	Bentley sisHyd V8i
District cooling network	Bentley sisHyd V8i

The energy flows at the network interfaces are computed using converged state parameters in section 4.5 and specified as an input for the simulations.

The energy flows at the network interfaces are computed as follows.

The heat supply from the CHP unit at node H1 ($\dot{Q}_{C_1,l}^H$) is computed as,

$$\dot{Q}_{C_1,l}^H = \dot{m}_{(l)}^H \times c_p \times (T_{s,l}^H - T_{ret,l}^H) + \dot{Q}_{d,l}^H \quad [kW_{th}]$$

$$\dot{Q}_{C_1,l}^H = 11.1 \times 4.12 \times (100 - 47.84) + 400 = 2785.4 [kW_{th}]$$

The electricity supply injected at node E1 from the CHP unit ($p_{g,l}^E$) is computed as,

$$p_{g,l}^E = \dot{Q}_{C_1,l}^H \times \eta_{C_1}^{H/E} \quad [kW_e]$$

$$p_{g,l}^E = 2785.4 \times 0.875 = 2437.23 [kW_e]$$

The gas demand at node G1 from the CHP unit ($\dot{V}_{C_1,l}^G$) is computed as,

$$\dot{V}_{C_{1,1}}^G = \frac{\dot{Q}_{C_{1,1}}^H}{\eta_{C_1}^{G/H}} \times \frac{3600}{GCV} \left[m^3 / hr \right]$$

$$\dot{V}_{C_{1,1}}^G = \frac{2785.4}{0.4} \times \frac{3600}{41.04 \times 1000} = 610.83 \left[m^3 / hr \right]$$

The gas demand at node G4 from the gas boiler unit ($\dot{V}_{C_{2,4}}^G$) is computed as,

$$\dot{V}_{C_{2,4}}^G = \frac{\dot{Q}_{C_{2,4}}^H}{\eta_{C_2}^{G/H}} \times \frac{3600}{GCV} \left[m^3 / hr \right]$$

$$\dot{V}_{C_{2,4}}^G = \frac{500}{0.9} \times \frac{3600}{41.04 \times 1000} = 48.73 \left[m^3 / hr \right]$$

The cooling from the absorption chiller unit ($\dot{Q}_{C_{3,2}}^C$) is computed as,

$$\dot{Q}_{C_{3,2}}^C = (\dot{m}_{(1)}^C + \dot{m}_{(2)}^C) \times c_p \times |(T_{s,2}^C - T_{ret,2}^C)| \left[kW_{th} \right]$$

$$\dot{Q}_{C_{3,2}}^C = (13.62 + 13.62) \times 4.18 \times |(5 - 11.99)| = 795.9 \left[kW_{th} \right]$$

The heat demand at node H3 from the absorption chiller ($\dot{Q}_{C_{3,3}}^H$) is computed as,

$$\dot{Q}_{C_{3,3}}^H = \frac{\dot{Q}_{s,2}^C}{\eta_{C_3}^{H/C}} \left[kW_{th} \right]$$

$$\dot{Q}_{C_{3,3}}^H = \frac{795.9}{0.65} = 1224.46 \left[kW_{th} \right]$$

B.2.1 Electricity network results validation

At node E1 a real power generation of 2.437 MW_e is specified for the load flow analysis. All other parameters are as specified in Table 5-2 and Table B-3. Results from the load flow simulation in IPSA's graphical user interface are shown in Figure B-2.

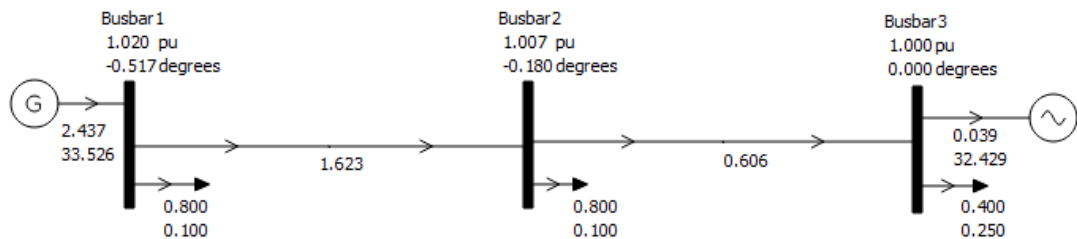


Figure B-2: Load flow analysis results as seen in IPSA's graphical user interface

A comparison of the electricity network analysis results from the combined network analysis tool and the IPSA simulation are shown below. The results agree closely with each other.

Table B-5: Electricity network results validation using IPSA

	Tool	IPSA
δ_1	-0.533 deg	-0.517 deg
δ_2	-0.194 deg	-0.180 deg
$ v_2 $	1.007 p.u.	1.007 p.u.

B.2.2 Gas network results validation

The gas demand at nodes with coupling components is calculated as follows.

At node G1 the total gas demand is calculated as,

$$\dot{V}_1^G = \dot{V}_{C_1,1}^G + \dot{V}_{d,1}^G \left[m^3 / h \right]$$

$$\dot{V}_1^G = 610.83 + 200 = 810.83 \left[m^3 / h \right]$$

At node G2 the total gas demand is calculated as,

$$\dot{V}_4^G = \dot{V}_{C_2,1}^G + \dot{V}_{d,4}^G \left[m^3 / h \right]$$

$$\dot{V}_4^G = 48.73 + 180 = 228.73 \left[m^3 / h \right]$$

All other parameters for the load flow simulation are as specified in Table 5-2 and Table B-3. The network schematic and results from the load flow simulation of the gas network in SINICAL graphical user interface are shown in Figure B-3.

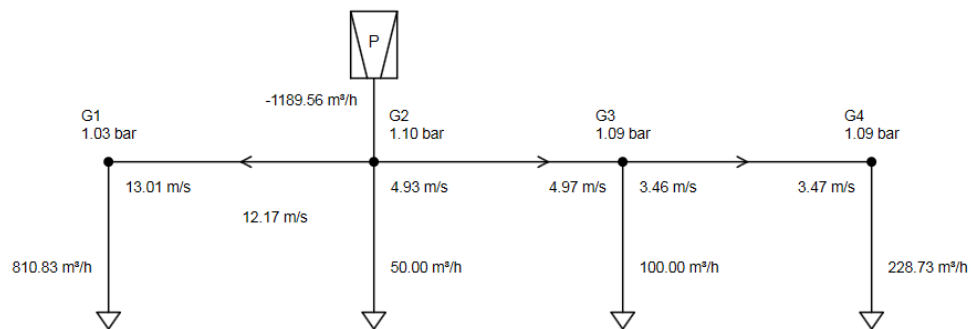


Figure B-3: Load flow analysis results as seen in SINICAL’s graphical user interface
Note: Natural gas density is specified as 0.8 kg/m³; the roughness in pipes specified as 0.25mm. The absolute gas pressure value is shown in the figure

A comparison of the gas network analysis results from the combined network analysis tool and the SINICAL simulation are shown below. The results show close agreement with each other.

Table B-6: Gas network results validation using SINICAL

	Tool	SINICAL (gas)
pr_1^G	29.89	29
pr_3^G	91.67	92
pr_4^G	88.29	89

B.2.3 District heating network results validation

A heat demand of 1224.46 kW_{th} at node H1 and a heat supply of 500kW_{th} at node H4 are specified for the district heating network simulation. All other parameters are as specified in Table 5-2 and Table B-3.

A comparison of the results from the combined network analysis tool and the *Bentley sisHyd* simulation are shown below. The results show close agreement with each other.

Table B-7: District heating network results validation using Bentley sisHyd

	Tool	Bentley sisHyd
\dot{m}_1^H	11.09	10.93
\dot{m}_2^H	5.06	4.92
\dot{m}_3^H	2.14	2.16
$T_{sup,2}^H$	97.53	97.5
$T_{sup,3}^H$	90.75	91.0
$T_{ret,1}^H$	47.84	48.1
$T_{ret,2}^H$	48.90	48.9
$T_{ret,3}^H$	50	50
$T_{ret,4}^H$	44.30	44.7

B.2.4 District cooling network results validation

Steady state simulation of the district cooling network was carried out using Bentley sisHyd.

All parameters are as specified in Table 5-2 and Table B-3. A comparison of the results from the combined network analysis tool and the Bentley sisHyd simulation are shown below.

The results show close agreement with each other.

Table B-8: District cooling network results validation using Bentley sisHyd

	Tool	Bentley sisHyd
\dot{m}_1^C	13.62	13.66
\dot{m}_2^C	13.62	13.66
$T_{sup,1}^C$	5.01	5
$T_{sup,3}^C$	5.01	5
$T_{ret,2}^C$	11.99	12

B.3 Case study network data (Chapter 5)

Table B-9: Energy network parameters

Electricity network parameters					
Circuit		Series Impedance		Series Admittance	
#	From-to	R (p.u.)	X (p.u.)	G (p.u.)	B (p.u.)
1	E1-E2	0.02	0.04	10	-20
2	E2-E3	0.01	0.02	20	-40
3	E3-E4	0.01	0.02	20	-40
Natural gas network parameters					
Pipe#	Gas pipe	Pipe diameter (mm)	Pipe length (m)		
1	G2-G1	150	680		
2	G2-G3	150	500		
3	G3-G4	150	420		
District heating network parameters					
Pipe#	Pipe	Pipe diameter (mm)	Pipe length (m)	Radial heat transmission coefficient (W/mK)	Pipe roughness (m)
1	H1-H2	150	3000	0.43	0.15×10^{-3}
2	H2-H3	150	3000	0.43	0.15×10^{-3}
3	H3-H4	150	3000	0.28	0.15×10^{-3}
District cooling network parameters					
Pipe#	pipe	Pipe diameter (mm)	Pipe length (m)	Radial heat transmission coefficient (W/mK)	Pipe roughness(m)
1	C1-C2	160	100	0.43	0.15×10^{-3}
2	C2-C3	160	100	0.43	0.15×10^{-3}

Appendix C: Gas network analysis with distributed injection of alternative gases

C.1 Example calculation

The network schematic of the example system is shown below. It is used to illustrate the formulation of equations and the solution method for gas network steady state analysis with distributed injection of alternative gas.

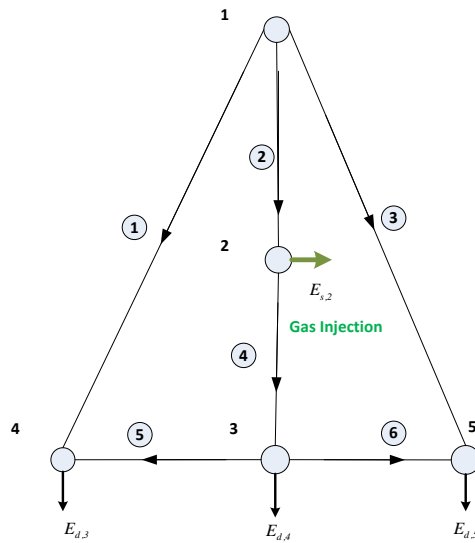


Figure C-1: Schematic of the example gas network

The energy demand and injections are shown in Table C-1.

Table C-1: Gas demand data

Node number	Gas Pressure (mbar)	Energy supply (kJ/s)	Energy demand (kJ/s)
1 (Source Node)	75		0
2	-	1000	0
3	-		1140
4	-		2850
5	-		2052

The pipe parameters are shown in Table C-2

Table C-2: Pipe data for example gas network

Branch	From - To	Pipe Length (m)	Pipe Diameter (mm)
1	1-4	680	150
2	1-2	250	100
3	1-5	420	150
4	2-3	250	100
5	3-4	600	100
6	3-5	340	100

The molar fractions of gas components at the main gas infeed node 1 and the gas injected at node 2 are shown in Table C-3.

Table C-3: Molar fractions of gases in mixtures used for case studies

	Natural gas	Upgraded biogas
(x_2^i)	0.9	0.94
$(x_2^{CH_4})$	0.06	0
$(x_2^{C_3H_8})$	0.015	0
$(x_2^{CO_2})$	0.005	0.03
$(x_2^{N_2})$	0.02	0.02
$(x_2^{H_2})$		0.01
GCV (MJ/m3)	41.41	37.46
SG	0.6104	0.5861

The gas network branch-nodal incidence matrix (A^G) is given by,

$$A = \begin{bmatrix} -I & -I & -I & & & \\ & +I & -I & & & \\ & & & +I & -I & -I \\ +I & & & & +I & \\ & & & +I & & +I \end{bmatrix}$$

For low pressure natural gas networks the friction factor in pipes (f) is calculated using the equation,

$$f = 0.0044 \left(1 + \frac{12}{0.276D} \right)$$

The friction factor for the pipes are computed as,

$f_{(1)}$	$f_{(2)}$	$f_{(3)}$	$f_{(4)}$	$f_{(5)}$	$f_{(6)}$
5.675×10^{-3}	6.313×10^{-3}	5.675×10^{-3}	6.313×10^{-3}	6.313×10^{-3}	6.313×10^{-3}

The steps of the steady state analysis are demonstrated below.

- **Step 1: Compute an initial approximation for gas flows in each branch. The method adopted is to assume all gas demands are supplied via tree branches and a uniform gas composition i.e. composition of natural gas.**

Assuming natural gas composition throughout the network (i.e. GCV=41.05 MJ/m³) the volume flow rate at gas loads are calculated as,

Node number	Energy demand (kJ/s)	Natural gas demand (m ³ /hr)
1 (Source Node)	0	0
2	-1000	-87.72
3	1140	100
4	2850	250
5	2052	180

Assuming all the demands are supplied via the tree branches e.g. pipe 1,2,3 and 4 only (the flows in pipe 5 and 6 are zero). The gas flows in the tree branches are computed as,

$\dot{V}_{(1)}$	$\dot{V}_{(2)}$	$\dot{V}_{(3)}$	$\dot{V}_{(4)}$	$\dot{V}_{(5)}$	$\dot{V}_{(6)}$
250	12.28	180	100	0	0

- **Step 2: Compute the pressure drop at each pipe that provides the assumed gas flow in pipes using equation (6.4) shown below.**

$$\dot{V} = \sqrt{\frac{\pi^2 R_{air}}{64}} \frac{T_n}{pr_n} \sqrt{\frac{[2pr_n (pr_i - pr_j)] D^5}{fSLTZ}}$$

The values for parameters used in the calculation are,

$$R_{air} = 286.9 \text{ Jkg}^{-1} \text{ K}^{-1}$$

$$T_n = 288 \text{ K}$$

$$pr_n = 1.013 \text{ Pa}$$

$$T = 288 \text{ K}$$

$$Z = 1$$

The pressure drop in pipes ($pr_i - pr_j$) are calculated as,

	$\Delta pr_{(1)}$	$\Delta pr_{(2)}$	$\Delta pr_{(3)}$	$\Delta pr_{(4)}$	$\Delta pr_{(5)}$	$\Delta pr_{(6)}$
In mbar	5.8276	0.0437	1.8659	2.8958	-	-

The nodal gas pressures are calculated using equation (6.8) shown below as,

$$\Delta pr_k = \sum_{i=1}^{n_{gas}} - (A^T)_{k,i} pr_i$$

pr_1	pr_2	pr_3	pr_4	pr_5
--------	--------	--------	--------	--------

In	75	74.95	72.06	69.17	73.14
<i>mbar</i>					

- **Step 3: Calculate gas flow rates in pipe 5 and 6 for the computed nodal pressures assuming natural gas flow using equation (6.4) as,**

The pressure drop in each branch is calculated as,

	$\Delta pr_{(1)}$	$\Delta pr_{(2)}$	$\Delta pr_{(3)}$	$\Delta pr_{(4)}$	$\Delta pr_{(5)}$	$\Delta pr_{(6)}$
In	5.8276	0.0437	1.8659	2.8958	2.8882	-1.0735
<i>mbar</i>						

The gas volume flow is calculated as,

	$\dot{V}_{(1)}$	$\dot{V}_{(2)}$	$\dot{V}_{(3)}$	$\dot{V}_{(4)}$	$\dot{V}_{(5)}$	$\dot{V}_{(6)}$
<i>m³ / hr</i>	250	12.28	180	100	64.46	-52.21

- **Step 4: Depending on gas flow direction/nodal pressure magnitude, establish a node analysis sequence such that the composition of incoming gas flows to a node is always known.**

Due to the negative flow in pipe number 6, node analysis sequence for the first iteration of the example is,

Node 2→Node 5→Node 3→Node4

- **Step 5: Calculate the molar fraction of gas components at each node following the node analysis sequence.**

For example, the gas volume flow injected at node 2 is calculated as,

$$\dot{V}_{s,2} = \frac{E_{s,2}}{GCV} \times 3.6 [m^3 / hr]$$

$$\dot{V}_{s,2} = \frac{1000}{37.46} \times 3.6 = 96.1 m^3 / hr$$

The molar fractions of gas components at Node 2 are calculated as,

$$(x_2^i) = \frac{\sum_{\dot{V}_k \text{ incoming to node 2}} x_k^i \times \dot{V}_k}{\sum_{\dot{V}_k \text{ incoming to node 2}} \dot{V}_k}$$

$$(x_2^{CH_4}) = \frac{0.9 \times 12.28 + 0.94 \times 96.1}{12.28 + 96.1} = 0.935$$

$$(x_2^{C_2H_6}) = \frac{0.06 \times 12.28 + 0 \times 96.1}{12.28 + 96.1} = 0.0068$$

$$(x_2^{C_3H_8}) = \frac{0.015 \times 12.28 + 0 \times 96.1}{12.28 + 96.1} = 0.0017$$

$$(x_2^{CO_2}) = \frac{0.005 \times 12.28 + 0.03 \times 96.1}{12.28 + 96.1} = 0.027$$

$$(x_2^{N_2}) = \frac{0.02 \times 12.28 + 0.02 \times 96.1}{12.28 + 96.1} = 0.02$$

$$(x_2^{H_2}) = \frac{0 \times 12.28 + 0.01 \times 96.1}{12.28 + 96.1} = 0.0089$$

Similarly the molar fractions at all gas nodes are calculated.

	Node1	Node2	Node 3	Node 4	Node 5
(x_2^i)	0.9	0.935	0.923	0.905	0.9
$(x_2^{CH_4})$	0.06	0.0068	0.025	0.0528	0.06
$(x_2^{C_3H_8})$	0.015	0.0017	0.0063	0.0132	0.015
$(x_2^{CO_2})$	0.005	0.027	0.0196	0.008	0.005
$(x_2^{N_2})$	0.02	0.02	0.02	0.02	0.02
$(x_2^{H_2})$	0	0.0089	0.0058	0.0012	0
GCV (MJ/m3)	41.41	37.91	39.11	40.9381	41.4092
SG	0.6104	0.5888	0.5962	0.6075	0.6104

- **Step 5: Calculate the revised gas flow demand at nodes and the pipe flow rate of gas in each pipe.**

	$\dot{V}_{d,1}$	$\dot{V}_{d,2}$	$\dot{V}_{d,3}$	$\dot{V}_{d,4}$	$\dot{V}_{d,5}$	
m^3 / hr	0	-96.1	104.93	250.62	178.40	
	$\dot{V}_{(1)}$	$\dot{V}_{(2)}$	$\dot{V}_{(3)}$	$\dot{V}_{(4)}$	$\dot{V}_{(5)}$	$\dot{V}_{(6)}$
m^3 / hr	247.87	12.18	178.47	100.94	64.67	-51.77

- **Step 6: Calculate the gas flow imbalance at each gas node (other than the gas infeed node) (f_i)**

$$f_i = \sum_{k=1}^{n_{\text{gas pipe}}} A_{i,k}^G \dot{V}_k - \left(\frac{E_i}{GCV_i} \times 3600 \right) \quad i = 1, 2, \dots, N$$

$$f_2 = \dot{V}_{(2)} - \dot{V}_{(4)} - (-\dot{V}_{s,2}) = 12.18 - 100.94 - (-96.1) = 7.34$$

$$f_3 = \dot{V}_{(4)} - \dot{V}_{(5)} - \dot{V}_{(6)} - \dot{V}_{d,3} = 100.94 - 64.67 - (-51.77) - 104.93 = -16.89$$

$$f_4 = \dot{V}_{(1)} + \dot{V}_{(5)} - \dot{V}_{d,4} = 247.87 + 64.67 - 250.62 = 61.92$$

$$f_5 = \dot{V}_{(3)} - \dot{V}_{(6)} - \dot{V}_{d,5} = 178.47 + (-51.77) - 178.4 = -51.7$$

- **Step 7: Calculate the elements of the nodal Jacobi matrix (J) given by**

$$J^o = -A_i^G D (A_i^G)^t$$

$$\text{where } D = \text{diag} \left(\frac{1}{2} \frac{\dot{V}_{(k)}}{\Delta p r_{(k)}} \right) \text{ for } k = 1, \dots, n_{\text{pipe}}$$

- **Step 9: Apply the correction and determine the nodal pressures for the next iteration**

The nodal gas pressure values for next iteration are calculated as,

$$Pr^1 = Pr^0 + \Delta Pr^0$$

$$\begin{bmatrix} pr_2 \\ pr_3 \\ pr_4 \\ pr_5 \end{bmatrix} = \begin{bmatrix} 74.95 \\ 72.06 \\ 69.17 \\ 73.14 \end{bmatrix} + \begin{bmatrix} 0.0123 \\ -0.3101 \\ 1.8004 \\ -0.8226 \end{bmatrix} = \begin{bmatrix} 74.9686 \\ 71.7504 \\ 70.9727 \\ 72.3114 \end{bmatrix}$$

- **Repeat the iterations from step 3 until the imbalances f_i are less than a specified tolerance.**

The iteration results for the example are shown below.

	Iteration 1	Iteration 2	Iteration 3	Iteration 4
Nodal pressure				
pr_2	74.9686	74.96	74.96	74.96
pr_3	71.7504	74.7263	71.7278	71.7279
pr_4	70.9727	70.7435	70.7326	70.7326
pr_5	72.3114	72.2787	72.2794	72.2794
Nodal error				
f_2	7.3313	-1.0143	-0.1497	-0.0077
f_3	-16.89	4.4534	0.3015	0.0057
f_4	61.91	-10.2970	-0.5	-0.0091
f_5	-51.69	-1.5950	-0.0028	0

C.2 Case study network data

Table A: Network pipe data

Branch	From - To	Pipe Length (m)	Pipe Diameter (mm)
1	1-2	50	160
2	2-3	500	160
3	2-4	500	110
4	2-5	500	110
5	3-6	600	110
6	3-7	600	110
7	3-8	500	110
8	5-6	600	80
9	4-7	600	80
10	6-8	780	80
11	7-8	780	80
12	7-9	200	80
13	9-10	200	80
14	10-11	200	80